Circular 176 1981

Pennsylvanian stratigraphy, petrography, and petroleum geology of Big Hatchet Peak section, Hidalgo County, New Mexico

by
Sam Thompson III
and
Alonzo D. Jacka

New Mexico Bureau of Mines & Mineral Resources

A DIVISION OF
NEW MEXICO INSTITUTE OF MINING & TECHNOLOGY

Circular 176

New Mexico Bureau of Mines & Mineral Resources

A DIVISION OF
NEW MEXICO INSTITUTE OF MINING & TECHNOLOGY

Pennsylvanian stratigraphy, petrography, and petroleum geology of Big Hatchet Peak section, Hidalgo County, New Mexico

by Sam Thompson III and Alonzo D. Jacka

COVER SKETCH—CLIFFS OF LIMESTONE AND DOLOSTONE IN THE HORQUILLA FORMATION (PENNSYLVANIAN–PERMIAN) ON NORTH SIDE OF BIG HATCHET PEAK; top is at elevation of 8,356 ft. View is southward from Chaney Canyon at an elevation of about 5,400 ft. For further detail, see figs. 5, 12, and 23.

SOCORRO 1981

First Printing, 1981

Published by Authority of State of New Mexico, NMSA 1953 Sec. 63-1-4
Printed by University of New Mexico Printing Plant, March, 1981

Available from New Mexico Bureau of Mines & Mineral Resources, Socorro, NM 87801 Price $10.00

Preface

This report documents an occurrence of the best petroleum-reservoir objective that has been observed so far in Hidalgo County, New Mexico. It is the second in a series of published reports evaluating the petroleum source and reservoir quality of surface and subsurface stratigraphic sections in the Pedregosa Basin. The first in this series is New Mexico Bureau of Mines and Mineral Resources Circular 152 on the KCM No. 1 Forest Federal well.

At the beginning of an exploration boom in the middle 1950's, Pennsylvanian reefs were considered to be a major objective in southwestern New Mexico; however, no observations of definite reservoir facies had been reported. In 1958, the Humble Oil & Refining Company No. 1 State BA well was drilled southwest of the Big Hatchet Mountains. The deep-marine basin facies of the upper Pennsylvanian to lower Permian section that was encountered in this well prompted R.A. Zeller (1960, 1965) to postulate a reef margin in the Big Hatchet Peak area.

As an employee of Humble, I measured a reconnaissance section in the Big Hatchet Peak area during the summer of 1961 in order to evaluate the reservoir quality of the inferred reef margin. Zeller suggested that a base of the section could be reached in Chaney Canyon to the north of the peak. Several thick units of dolostone were seen to have significant porosity; however, the even bedforms appeared more like those of banks instead of reefs. That brief work did not reach the highest cliffs on Big Hatchet Peak, and the top of the Pennsylvanian was not documented. That summer I was assisted in the field by D.G. Griggs.

After joining the Bureau in 1974, I obtained permission from Exxon Company, U.S.A. (formerly Humble) to use the description in my 1961 report as a guide for a more comprehensive study of the stratigraphic succession. I am grateful to Exxon for the loan of that description. However, the section was completely reworked and extended such that none of the original description is used in this circular.

From June 1976 to July 1979, I spent a total of 74 field days reconnoitering, measuring, describing, and sampling the Big Hatchet Peak section. Several delays were caused by inclement weather and the logistical problems of working this remote area. I am grateful to the ranchers listed in the appendix for their permission and encouragement to work this section. Especially I am grateful to W.J. Everhart of the Hatchet Ranch for supervising the transportation by horseback of the camping gear, food, and water that I needed to do the work from the campsite on Big Hatchet Peak.

To document the development of the dolostone reservoirs, I asked A.D. Jacka, professor of geology at Texas Tech University (Lubbock), to join me as co-author of this circular. His wide experience with petrographic analyses of carbonate reservoir rocks enables him to decipher the complex depositional and diagenetic history of the dolostones, limestones, cherts, and sulfates. He joined me on a reconnaissance trip to study the dolostones in the first cliff, analyzed the thin sections of all the samples, prepared the text and appendix sections on petrography, and assisted in the preparation of the text on petroleum geology and the summary plot in the appendix. I am grateful to him for the large amount of research time spent on this project and for his many helpful suggestions.

To place the section in a biostratigraphic framework, I asked G.L. Wilde of Exxon Company, U.S.A. in Midland, Texas, to identify the fusulinids and other microfossils collected. He not only is a recognized authority in this field but also has the experience of identifying fusulinids from my 1961 Big Hatchet Peak section and the several sections measured by Zeller (1965) in other parts of the Big Hatchet Mountains. I am grateful to him for donating much time and thought to this project and for continuing to identify microfossils in hand specimens and thin sections until the series boundaries were determined as closely as possible. Moreover, both Jacka and I are grateful to him for reviewing our manuscript and suggesting improvements in its clarity.

Samples of the dark limestones were sent to P.J. Cernock at GeoChem Laboratories, Inc. in Houston, Texas, for analyses of petroleum-source quality. Samples of the porous dolostones were sent to K.W. Andrews at Core Laboratories, Inc. in Dallas, Texas, for analyses of porosity and permeability. Funds for these and other analyses as well as for part of the field work were provided by a grant (Project No. 2-66-3306) from the New Mexico Energy Institute at New Mexico Institute of Mining and Technology, C.C. Nathan, Director.

Information in this circular should be useful to petroleum geologists who are exploring the Hidalgo County area in southwestern New Mexico, to stratigraphers and sedimentologists who are interested in depositional and diagenetic relationships in the Horquilla Formation (Pennsylvanian-Permian) of the Pedregosa Basin, to carbonate petrographers who are interested in the evidence for fresh-water diagenesis with occlusion of porosity in the limestones and for salt-water diagenesis with preservation of porosity in the dolostones, and to any geologists who wish to examine the Big Hatchet Peak section in the field.

Sam Thompson III
Petroleum Geologist
New Mexico Bureau of Mines
and Mineral Resources

Alonzo D. Jacka
Professor of Geology
Geosciences Department
Texas Tech University

Socorro, New Mexico, and
Lubbock, Texas
June 1, 1980

Contents

TABLES

FIGURES

Abstract

Big Hatchet Peak section includes the uppermost 78 ft of Paradise Formation (Mississippian/Chesterian) and 3,230 ft of Horquilla Formation (Pennsylvanian-Permian/Morrowan to Wolfcampian). About 200 ft of uppermost Horquilla have been removed from the peak by erosion. Nearly all of the section consists of shallow-marine shelf carbonates. Paradise contains skeletal-oolitic limestones; cross-laminae indicate paleocurrents toward the southeast and southwest. In the Horquilla, the lower member (Morrowan to Desmoinesian) is 1,363 ft thick and consists of limestone with abundant chert in some beds. A disconformity may be present at the top. The upper member (Desmoinesian to Wolfcampian) is at least 1,867 ft thick and consists of alternating limestone and dolostone; chert is rare. Limestones contain biostromes of phylloid algae and a few ancient solution cavities. Dolostones range in thickness from 54 to 148 ft, are laterally extensive, and exhibit vuggy porosity. Petrographic evidence shows that limestones were stabilized within fresh-water diagenetic environments and that they contained much primary or secondary porosity; practically all of the porosity was occluded by marine- or fresh-water cements. Dolostones also contained much secondary intercrystalline and moldic porosity that was partially occluded by epitaxial cements and coarse recrystallization of initial neomorphic rhombs. Anhydrite porphyroblasts were emplaced by hypersaline waters and dissolved later by fresh ground waters to form molds with distinctive stairstep outlines; this tertiary (third-stage) porosity in dolostones was partially filled by gravitational cements, and some microstalactite tips were dolomitized paramorphically. Darker limestones in the Horquilla are rated as fair petroleum-source units. Land-derived kerogens indicate sources of gas, and alteration indices of 3 to 3 + indicate a moderate thermal history. Porous dolostones in the upper member are rated as fair to good reservoir units. Matrix porosity and permeability are poor, but they should improve farther south along the shelf edge and on the slope. The net thickness of 484 ft of dolostones with vuggy porosity supports the ranking of this facies as the best petroleum-reservoir objective in the Pedregosa Basin area.

Introduction

The purpose of this report is to describe, analyze, and evaluate an exposure of the best petroleum objective found to date in Hidalgo County, New Mexico. One of the advantages of petroleum exploration in the Basin and Range Province is that source and reservoir units can be studied where they are exposed in the uplifts. This critical yet inexpensive surface control can be used in combination with available well data to extrapolate the objectives into the subsurface of the adjacent structural depressions, where the potential is greater for the preservation of oil and gas in commercial quantities.

Fig. 1 shows the regional setting of the Pedregosa Basin, an area of subsidence in Pennsylvanian time where over 2,000 ft of sedimentary rocks were deposited; fig. 1 also shows the position of the Big Hatchet Peak section along the shelf margin adjacent to the Alamo Hueco Basin, an area where subsidence so exceeded sedimentation that deep-marine facies were deposited in Desmoinesian to Wolfcampian time. Additional background information on these basins and on the surface and subsurface control is presented in Greenwood and others (1977) and in Thompson and others (1978).

Fig. 2 shows the location of the Big Hatchet Peak area in the present topographic setting of the Big Hatchet Mountains in Hidalgo County, New Mexico. This map shows the general access routes from the village of Hachita to Chaney Canyon on the west side of the mountains, where the base of the Big Hatchet Peak section is reached and most of the section is worked, and to Thompson Canyon on the east side, where the trail begins to the peak from where the upper part of the section is worked. Before attempting to study this section in the field, one should consider the hazards of

FIGURE 1—REGIONAL SETTING OF BIG HATCHET PEAK SECTION ALONG OUTER-SHELF MARGIN OF ALAMO HUECO BASIN; boundaries of Pedregosa and Orogrande Basins are drawn where thickness of Pennsylvanian is 2,000 ft; boundaries of uplifts are drawn where Pennsylvanian rocks have been removed by erosion. Boundary of Alamo Hueco Basin is drawn between shallow- and deep-marine deposits of Pennsylvanian age (modified from Thompson and others, 1978).

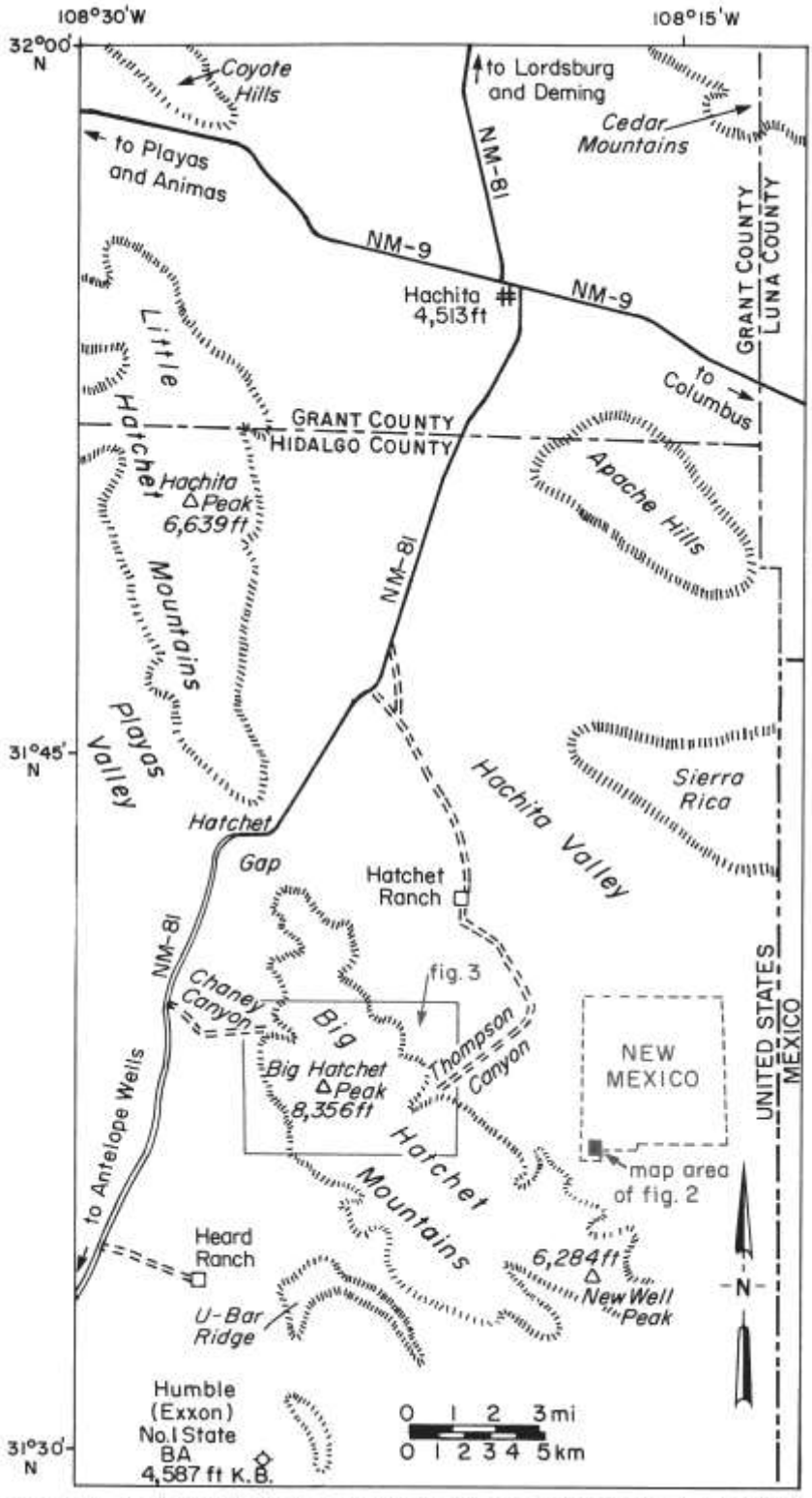

FIGURE 2—Location of Big Hatchet Peak area in Hidalgo County, New Mexico (modified from Douglas 1° × 2° quadrangle).

climbing the cliffs. If only the Pennsylvanian succession needs to be studied and not this particular facies, the New Well Peak section of Zeller (1965, p. 84-88) is much more accessible and far less hazardous.

In the main body of the text, the general aspects of the Big Hatchet Peak section are discussed in the chapters on 1) the local geologic setting covering the stratigraphic and structural framework, 2) the stratigraphic succession, 3) the petrographic evidence of the depositional/diagenetic history, and 4) the petroleum geology, including documentation of source and reservoir evaluations with geochemical analyses and porosity/permeability measurements. In the appendices, more specific information is presented on field data (including detailed directions to the measured section and discussion of the hazards), petrographic data, and the columnar stratigraphic section.

Geologic setting

Fig. 3 is a geologic map of the Big Hatchet Peak area. The stratigraphic framework in the Big Hatchet Mountains is based on Zeller (1965) and the structural framework is based on Zeller (1975).

Pre-Mississippian rocks consist generally of Precambrian granite, Cambrian sandstone, Ordovician carbonates, and Devonian mudstone. Mississippian, Pennsylvanian, and Permian rocks are dominantly carbonates. This Paleozoic section is about 11,500 ft thick and was deposited mainly under shallow-marine, stable-shelf conditions.

South of the map area, the Permian is overlain unconformably by a Lower Cretaceous sequence, about 10,000 ft thick, of conglomerates and redbeds, limestones with rudists in the upper part, and shallow-marine to deltaic sandstones. In other parts of the region, the Lower Cretaceous rocks are overlain unconformably by Upper Cretaceous nonmarine conglomerates that indicate the onset of the Laramide orogeny.

Laramide low-angle thrust faults with vergence toward the southwest are shown in the southern part of the map area; displacements appear to be less than a few

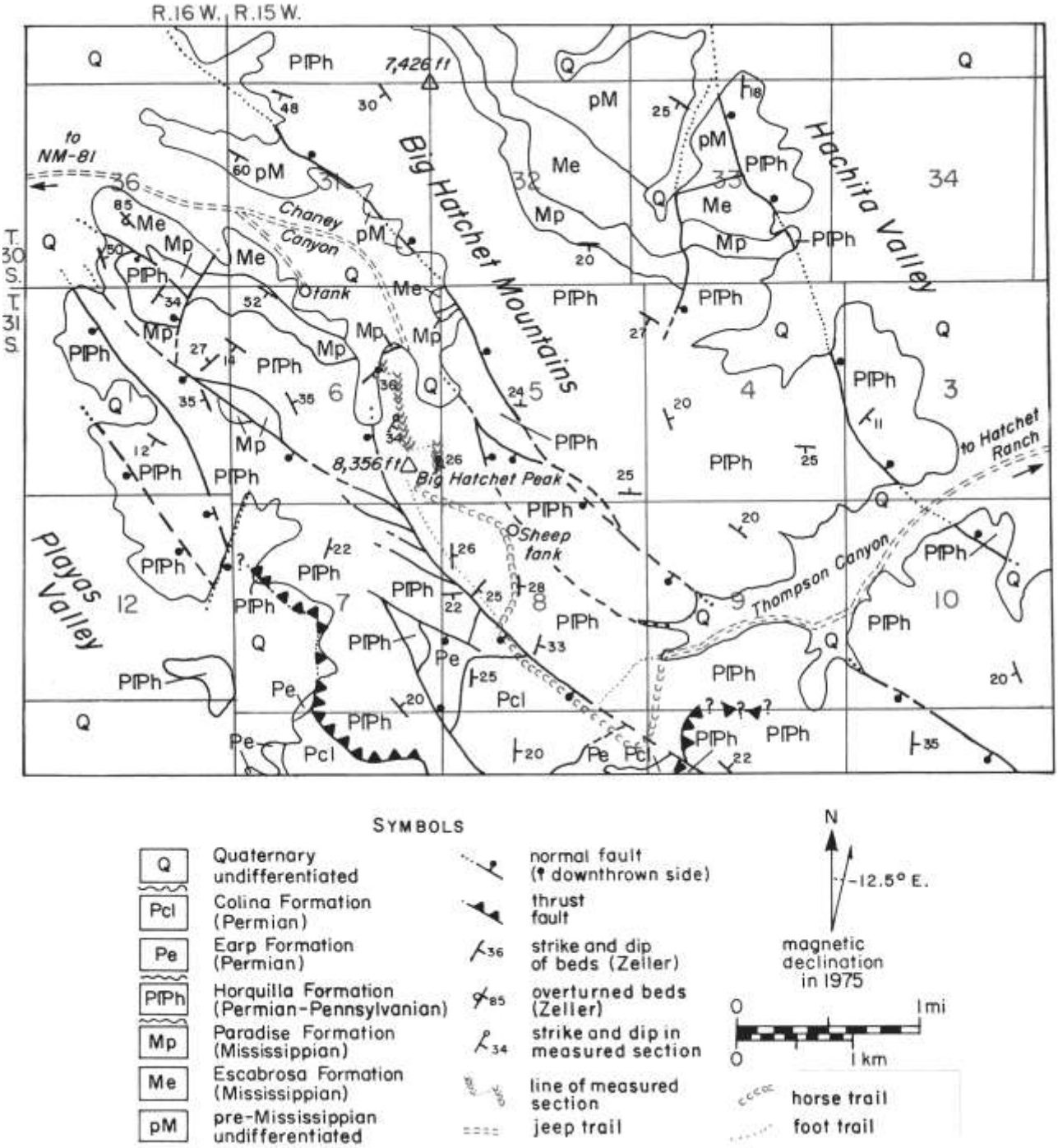

FIGURE 3—Geologic map of Big Hatchet Peak area (modified from Zeller, 1975, sheet 1); some offsets in the line of measured section are not shown at this scale.

thousand feet. In the main part of the thrust belt to the north, the vergence is generally toward the northeast and displacements are greater. Lower to middle Tertiary volcanic rocks and plutonic intrusives seen in surrounding ranges are absent in the Big Hatchet Mountains. High-angle normal and reverse faults of the middle Tertiary Basin and Range deformation trend northwest-southeast in this area and have maximum displacements up to a few thousands of feet. Minor strike-slip movement is indicated (Zeller, 1975, sheet 2, cross sections D-D E-E G-G ', and H-H ').

Most of the structural data shown on fig. 3 is taken directly from Zeller (1975, sheet 1), although many details are omitted. Some fault patterns were developed using the new aerial photographs. With the new topographic bases that are being prepared by the U.S. Geological Survey, the entire Big Hatchet Mountains can be remapped more accurately. Along the line of the measured stratigraphic section and in adjacent areas that were checked by tracing beds, the structure is generally simple. In the limestone cliffs of the upper part of the section, vertical fracturing locally is intense and a few small normal faults are seen to have less than 100 ft of stratigraphic throw. In a few of the cliffs, fractures parallel to bedding appear to have no stratigraphic throw, but they may be low-angle thrusts with minor displacements.

Stratigraphy

Fig. 4 is a generalized stratigraphic column of the Big Hatchet Peak section. The entire section is 3,308 ft thick, including the uppermost 78 ft of Mississippian (Chesterian), 2,511 ft of Pennsylvanian (Morrowan through Virgilian), and the lowermost 719 ft of Permian (Wolfcampian).

Table 1 shows the identifications of fusulinids and other fossils and the age determinations made by G.L. Wilde. Sample notations include the lithostratigraphic unit number and the footage above the base of the unit where the collection was made. For paleontological analyses, at least one sample was collected from each unit in which fusulinids were found in the field. After the initial identifications were made, additional samples were taken to determine the series boundaries more closely. Some small microfossils were identified from the petrographic thin sections.

Thicknesses of the series in the Pennsylvanian are 247 ft of Morrowan, 378 ft of Derryan (Atokan), 1,001 ft of Desmoinesian, 466 ft of Missourian, and 419 ft of Virgilian. The intervals between the highest determination in each series and the lowest determination in the overlying series are 52 ft, 55 ft, 58 ft, 18 ft, and 173 ft, respectively. The latter interval includes a 148-ft dolostone unit between the highest Virgilian and lowest Wolfcampian dates; any fusulinids in that unit probably have been so altered by dolomitization that they could not be identified. Conodonts may be present in the dolostones and may be useful in determining that series boundary more closely.

The Paradise and the Horquilla Formations are the only two formal lithostratigraphic map units recognized in the section. Both are defined in accordance with the stratigraphic framework of Zeller (1965), who correlated these units from their type sections in southeastern Arizona. The Horquilla is designated here as a formation, instead of as a limestone as in the conventional designation, because it contains many thick dolostone units in this shelf-margin facies and contains much mudstone in the basin facies to the south.

As shown on fig. 4, the Horquilla is subdivided into informal lower and upper members. The lower member is 1,383 ft thick and consists mainly of limestone and chert. The upper member is at least 1,867 ft thick and consists mainly of limestone and dolostone; chert is minor. A disconformity is inferred at the contact between the members. These units have been recognized in other parts of the Big Hatchet Mountains, but they have not been mapped. If later work shows that they should be elevated to formal status, the lower and upper members may be named the Chaney Canyon Member and the Big Hatchet Peak Member, respectively, based on the prominent topographic features where they are exposed, and the Big Hatchet Peak section may be designated as the type section for these units.

Fig. 5 is a panoramic photograph of the Big Hatchet Peak section showing the general traverse of the measured section. Some segments and offsets cannot be shown because they are blocked from view by protuberances along the cliffs or by the fanglomerates. The north-facing slope below the peak retains more moisture than other parts of the mountains because it lies in shadow much of the year, and thus this slope supports more grass and piñon/juniper trees, especially in the lower part of the section below the cliffs.

In the following subdivisions of the text, the Paradise and the lower and upper Horquilla are discussed generally regarding their sedimentary features, depositional and diagenetic environments, and petroleum source and reservoir characteristics. Documentation of the petroleum evaluation is given in a later section. Details of the field data are provided in appendix 1, including complete descriptions of the individual column units (unit 1-unit 78), discussions of basic concepts and methods used in the description, traverse data used to construct the stratigraphic column, and a list of samples collected. Appendix 3 contains a columnar stratigraphic section plotted on the standard scale of 1 inch:100 ft that summarizes the stratigraphic and petrographic information as well as the petroleum evaluation.

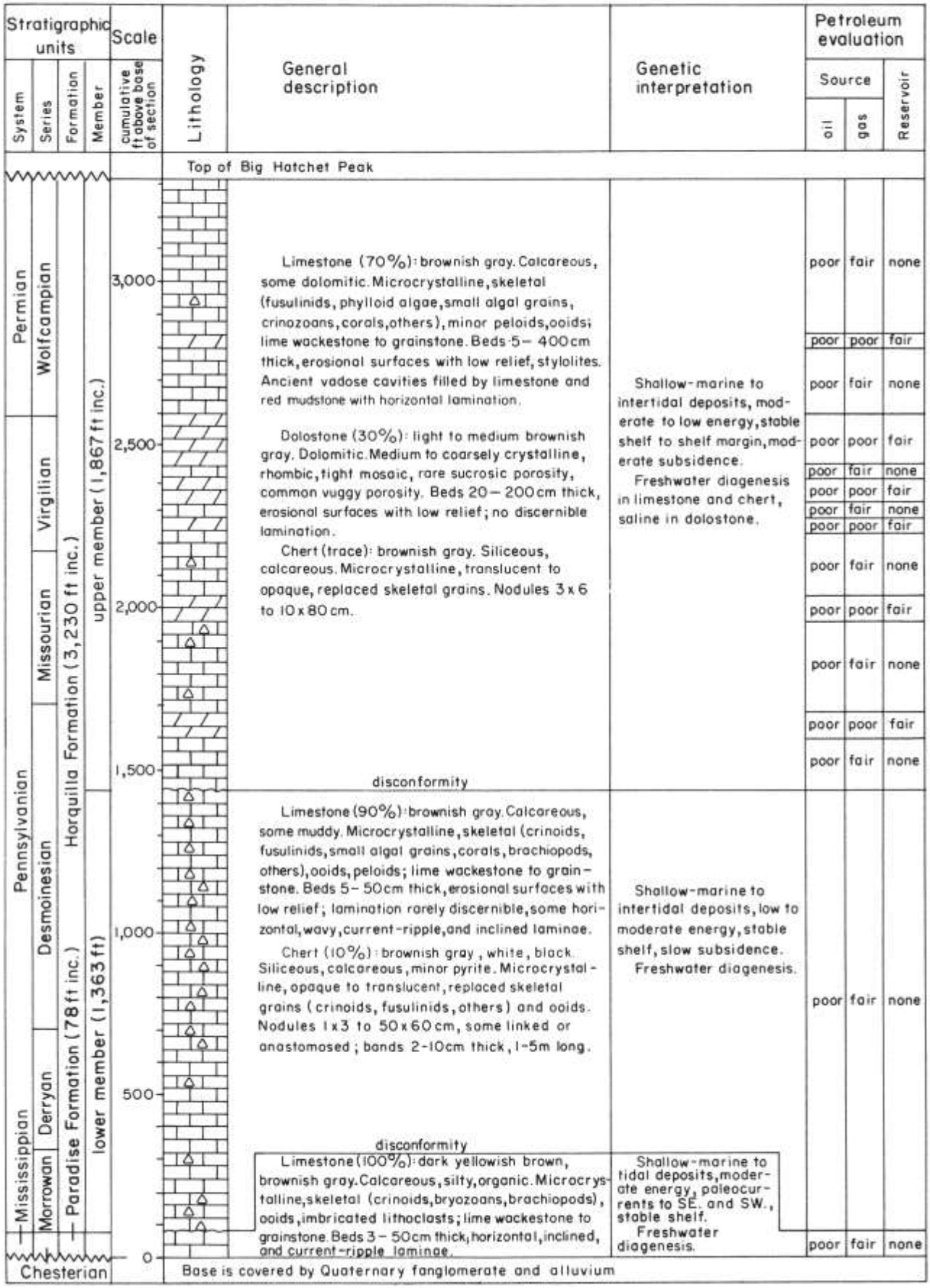

FIGURE 4—GENERALIZED STRATIGRAPHIC COLUMN OF BIG HATCHET PEAK SECTION.

TABLE 1—AGE DETERMINATIONS IN THE BIG HATCHET PEAK SECTION based on identifications of fusulinids and other fossils by G.L. Wilde. Sample notation indicates BHP unit number and footage above base of unit.

Sample Notation (BHP-)	Fossils	Age
top peak	*Triticites* ex. gr. *T. pinguis, Schwagerina?* sp.	Early Wolfcampian
78-42	*Triticites* cf. *T. pinguis, Pseudofusulina?* sp.	Early Wolfcampian
78-4	*Triticites* cf. *T. pinguis, T.*cf. *T. ventricosus* and *T. meeki*	Early Wolfcampian
77-41	*Triticites pinguis*	Early Wolfcampian
76-8	*Triticites* ex.gr. *T. pinguis, T.*ex.gr. *T. ventricosus, Schwagerina* sp. (or *Pseudofusulina* sp.), *Tubiphytes* sp.	Early Wolfcampian
76-3	*Triticites* spp., *Schwagerina* sp., *Schubertella* sp.	Early Wolfcampian
75-7	*Triticites* sp., *Schwagerina* sp., algae including *Tubiphytes?* sp.	Early Wolfcampian
74-54	*Triticites* ex.gr. *T. pinguis, T.*sp., *Schwagerina* sp., *Leptotriticites?* sp., *Schubertella* sp.	Early Wolfcampian
74-0	*Triticites* ex.gr. *T. pinguis*	Early Wolfcampian
72-2	*Triticites* sp., *Leptotriticites* sp.	Early Wolfcampian
71-2	*Triticites* sp.	Early Wolfcampian
69-85	Oncolitic, encrusting algae and foraminifers	Early Wolfcampian
69-24	*Triticites* spp.	Early Wolfcampian
69-3	*Triticites* spp.	Early Wolfcampian
68-70	*Triticites* ex.gr. *T. pinguis*	Early Wolfcampian
68-4	*Triticites* sp., *Schwagerina* sp.	Early Wolfcampian
66-9	*Triticites* spp.	Virgilian
64-1	*Triticites* spp.	Virgilian
62-5	*Triticites* spp.	Virgilian
61-2	*Triticites* spp.	Missourian
58-1	*Triticites* sp.	Missourian
57-23	*Triticites* spp.	Missourian
57-10	*Triticites* ex.gr. *T. ohioensis,* tubiform foraminifers	Missourian
55-2	*Triticites* sp.	Missourian
54-2	*Eowaeringella* sp., *Triticites* sp.	Missourian
53-3	*Eowaeringella* sp.	Missourian
52-5	*Eowaeringella* sp., *Triticites* sp.	Missourian
50-1	*Fusulina* sp., *Bartramella?* sp.	Desmoinesian
48-2	*Bartramella?* or *Frumentella?* sp., *Plectofusulina* sp., *Fusulina?* sp.	Desmoinesian
46-1	Phylloid algae	
45-17	*Fusulina?* sp.	Desmoinesian
45-3	*Chaetetes* sp. and other corals	
43-7	Algae	
42-12	Sample lost	
40-1	*Fusulina* sp.	Desmoinesian
39-1	*Fusulina* sp., *Komia* and/or *Ungdarella* sp.	Desmoinesian
38-3	*Fusulina* sp.	Desmoinesian
36-2	*Fusulina* sp., *Wedekindellina* sp.	Desmoinesian
34-6	*Fusulina* sp., *Wedekindellina* sp.	Desmoinesian
33-6	*Fusulina* sp., *Wedekindellina* sp., *Eowaeringella* of the group of *E. matura,* crinoids	Desmoinesian
31-10	*Fusulina* sp.	Desmoinesian
30-0	*Plectofusulina* sp., tubiform foraminifers	Desmoinesian
28-5	*Fusulina* sp., abundant crinoids	Desmoinesian
26-0	No identifiable fusulinids or algae	
25-3	*Fusulina* sp.	Desmoinesian
24-1	*Plectofusulina* sp., *Komia* sp.	Desmoinesian
22-1	*Fusulinella?* sp., *Millerella?* sp., endothyrids, *Komia* sp.	Derryan
20-2	*Fusulinella* sp.	Derryan
18-0	*Fusulinella* sp.	Derryan
17-4	*Profusulinella* sp.	Derryan
16-4	*Profusulinella* sp.	Derryan
14-3	*"Profusulinella" copiosa, Staffella* sp., *Eostaffella* sp., *Millerella* sp., *Donezella* sp., *Cuneiphycus?* sp.	Derryan
13-75	*"Profusulinella" copiosa, Millerella* sp.	Derryan
13-23	*Eostaffella* sp., endothyrids, *Donezella* sp.	Morrowan
13-7	*Eostaffella* sp., *Cuneiphycus* sp.	Morrowan
12-1	*Eostaffella?* sp.	Morrowan
11-1	*Eostaffella* sp., *Millerella* sp.	Morrowan
9-6	*Eostaffella* sp., endothyrids, kamaenids	Morrowan
9-5	*Millerella* sp.	Morrowan
8-1a	*Millerella* sp., *Asphaltina* sp.	Morrowan
5-0	*Millerella* spp.	Morrowan
3-2	Crinoids (with points)	Chesterian?
2-1	Endothyrids	Chesterian?
1-0	Fenestrate bryozoans, crinoids	Chesterian?

FIGURE 5—PANORAMIC PHOTOGRAPH OF BIG HATCHET PEAK SECTION SHOWING THE GENERAL TRAVERSE OF THE MEASURED SECTION WITH A CHEVRON PATTERN; view is southward from Chaney Canyon at an elevation of about 5,400 ft; peak is at 8,356 ft. **Mp** = Paradise Formation (hidden by ridge of fanglomerate), **Phl** = lower member of Horquilla Formation, **Phu** = upper member of Horquilla Formation, **Qf** = Quaternary fanglomerate. Major normal faults disrupt the stratigraphic succession in adjacent areas, but not in the Big Hatchet Peak area.

Paradise Formation (Mississippian)

Only the uppermost 78 ft of the Paradise Formation are exposed in the Big Hatchet Peak section (units 1-4). Figs. 6-11 are photographs of the general outcrop and selected exposures. Quaternary fanglomerates and alluvial deposits of the Chaney Canyon drainage cover the base. Exposures are limited to a small arroyo (fig. 6). A complete section of Paradise is fairly well exposed about 0.7 mi to the northwest (fig. 3), but the main reference section in the Big Hatchet area is in the Mescal Canyon section of Zeller (1965, p. 76-77), where he measured 318 ft of this formation.

The upper part of the Paradise is Chesterian and the lower part is Meramecian in age (Zeller, 1965, p. 30). None of the microfossils from the Big Hatchet Peak section that were studied by Wilde (table 1) could be dated definitely as Chesterian; however, additional samples and thin sections may provide adequate material for dating purposes. The endothyrids and the crinoid stems with points are probably Mississippian and support the correlation with the Paradise. In the field, the distinctive cryptostome bryozoan *Archimedes* sp. is recognized with spiral axes and attached fronds (unit 1, 0-11 ft; fig. 7). This fossil is generally of Mississippian age and is abundant in other sections of the Paradise.

Limestone constitutes nearly 100 percent of the upper Paradise in this section. Fresh color ranges from dark yellowish brown, to brownish gray, to olive black. Composition is dominantly (over 90 percent) calcareous with a trace (less than 10 percent) of quartz silt and organic material. Textural constituents include microcrystalline calcite, skeletal grains (crinozoans, bryozoans, brachiopods, and rare gastropods), ooids, and limestone lithoclasts that are imbricated with an initial inclination to the northeast (upcurrent, fig. 10). Grain tangency (percentage of grains in depositional contact) ranges from poor (0-10 percent) to good (50-90 percent) in different beds. According to the subclassification of limestones given by Dunham (1962), the designations range from lime wackestone to lime grainstone.

Thicknesses of the limestone beds range from 3 to 50 cm, with an estimated mode around 20 cm (fig. 8). Bedding surfaces generally are sharp and initially horizontal, although some are slightly uneven. In one interval (unit 2, 1-3 ft; fig. 9), laminasets are 5-10 cm thick, with tabular to wedge shapes, and contain convex-up, inclined laminae that lap out downward with 15 ° initial dip to N. 77 ° E. (determined after simple rotation about present structural dip). These laminasets are incised by a channel 50 cm wide and 5 cm deep, with an initial alignment of the axis about N. 20° W.-S. 20° E., and are filled by horizontal and current-ripple laminae. In a higher interval (unit 2, 13-15 ft), trough laminae show an initial plunge direction about S. 20 ° E.

Siltstone constitutes less than 2 percent of this section (unit 4, 12-13 ft). Color is olive brown. Composition is mostly (over 50 percent) quartz silt with minor (less than 50 percent) calcareous material. Textural constituents are mostly silt grains with minor microcrystalline calcite and chonetid brachiopod shells. This rock type occurs as a single bed, 1 ft thick, and appears to grade into the overlying black limestone near the top of the Paradise (fig. 11).

These sedimentary properties indicate a depositional environment on a shallow-marine, relatively stable shelf with moderate energy occasionally strong enough to transport limestone pebbles, but generally not strong enough to winnow away finer matrix material. The few channels may have been eroded by tidal currents; however, only ebb-current deposits appear to have been preserved as indicated by the trough laminae plunging southeast and the imbricate pebbles dipping northeast (paleocurrent to southwest). The convex-up, downlapping laminae, with an initial dip direction to the east-northeast may be lateral accretion deposits associated with the tidal currents. The limestones probably were stabilized in a fresh-water diagenetic environment.

The limestones, especially the black organic ones at the top, probably are at least fair source rocks for gas and poor to possibly fair source rocks for oil. No porosity was observed, and no reservoir quality is inferred. Petroleum source and reservoir properties will be documented at the more complete reference section in Mescal Canyon.

Horquilla Formation, lower member (Pennsylvanian)

The lower member of the Horquilla Formation is 1,363 ft thick in the Big Hatchet Peak section, which is designated here as the type section of this informal member (units 5-42). Figs. 12-22 are photographs of

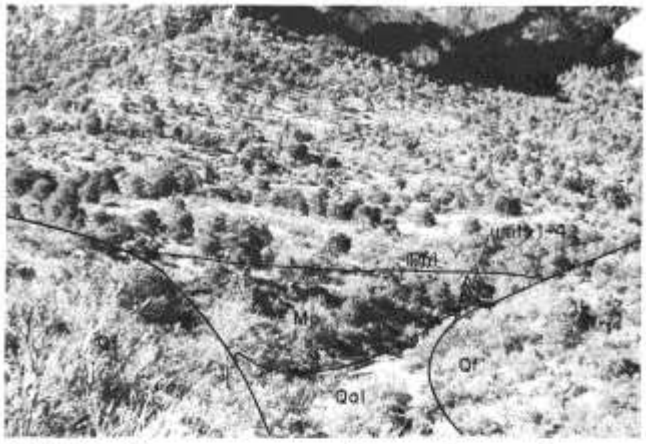

FIGURE 6—OUTCROP OF UPPERMOST 75 FT OF PARADISE FORMATION (**Mp**), with line of measured section (units 1–4). Base is covered by Quaternary fanglomerate (**Qf**) and alluvial (**Qal**) deposits; view is south-southeast, downhill from jeep trail.

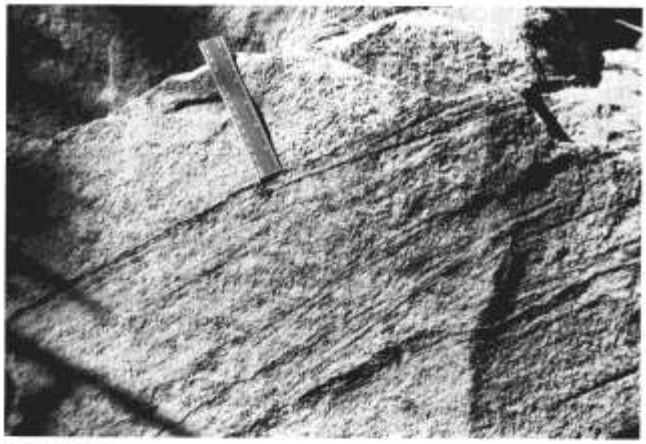

FIGURE 9—CROSS-LAMINAE WITHIN LIMESTONE BEDS OF PARADISE (unit 2, about 2 ft above base); view is south-southeast. Present dip is 45° SE.; initial inclination is 15° ENE. after simple rotation about present structural dip; cross-laminae may be lateral accretion deposits associated with tidal currents.

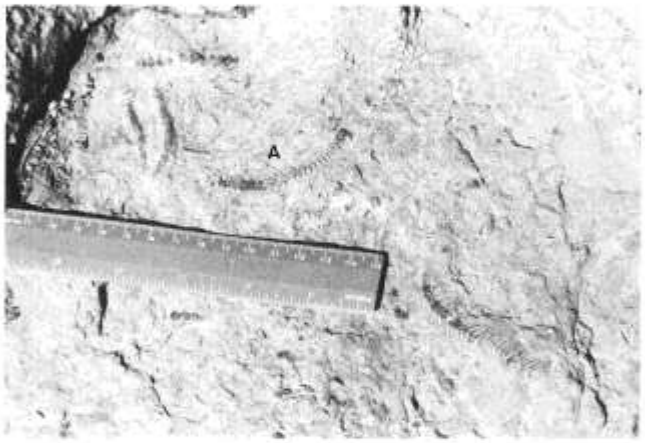

FIGURE 7—*ARCHIMEDES* SP. (**A**), A CRYPTOSTOME BRYOZOAN WITH SPIRAL AXES AND ATTACHED FRONDS—a characteristic fossil of the Paradise; stratigraphic position is in unit 1 of measured section, about 10 ft above the base of the unit (near top). View is southwest (down) on top of bedding surface; scale 15 cm = 6 inches long and is used in subsequent closeups.

FIGURE 10—IMBRICATED (**i**) LIMESTONE LITHOCLASTS IN PARADISE (UNIT 3, NEAR BASE); VIEW IS SOUTHEAST. Pebbles dip upcurrent to northeast, indicating a paleocurrent to southwest.

FIGURE 8—LIMESTONE BEDS IN PARADISE FORMATION (units 1 and 2), striking N. 50° E. and dipping 36° SE.; view is southwest.

FIGURE 11—SILTSTONE (**zs**) GRADING TO BLACK LIMESTONE (**blk ls**) NEAR TOP OF PARADISE (unit 4, 12–13 ft, 13–14 ft). Disconformable contact with overlying Horquilla (unit 5) in limestone (**ls**) ledges; view is east-southeast.

the general outcrop and selected exposures of sedimentary features. Several offsets were made in the line of section to follow the locus of best exposures in arroyos or on spurs (fig. 12). This member can be correlated at least to the New Well Peak section of Zeller (1965, p. 86-88), where his equivalent units (1-68) have a total thickness of 1,346 ft.

Based on the fusulinid determinations by Wilde (table 1), the age of the lower Horquilla ranges from Morrowan, through Derryan (Atokan), into Desmoinesian. The Morrowan-Derryan boundary in the Big Hatchet Peak section lies approximately at the top of the generally treeless strip, which probably was produced by a logging operation that cut piñon/juniper trees many years ago (fig. 12; unit 13, 35 ft above base; also obvious on fig. 6). The Derryan-Desmoinesian boundary lies at the base of a limestone and chert unit (unit 23). Very small fusulinids (less than 1 mm long) in most of the Morrowan part are hard to recognize in the field with a 10 x hand lens. Those in the upper MorrowanDerryan-Desmoinesian part can be recognized although they generally are relatively small (1-2 or rarely 3 mm in transverse diameter, and 2-4 or rarely 6 mm long). With experience, tentative generic identifications can be made in the field; however, best results are obtained by sending samples to fusulinid specialists.

The contact with the underlying Paradise is fairly well exposed in the Big Hatchet Peak section (fig. 11). This contact appears to be a sharp, low-relief disconformity as seen at other localities. The hiatus is probably short because no foraminiferal zones are missing (Armstrong and Mamet, 1978, p. 184).

Limestone constitutes over 90 percent of the lower Horquilla (although 25 percent of the member is covered in this section and may conceal some mudstone). Fresh color is mostly in the brownish gray range, with darker shades grading to brownish black in the lower part and lighter shades more common in the upper part. Based on field estimates, the composition is dominantly calcareous; some units appear to be muddy, especially in the lower part. Silicification is minor and glauconite is rare.

Textural constituents of the limestones are diverse. Microcrystalline calcite is the most abundant overall, ranging from a trace of intergranular matrix, to patches, to nearly 100 percent of many beds (fig. 20).

Skeletal constituents are the most abundant types of grains, although they are absent in some beds. Crinozoans dominate; they constitute nearly 100 percent of a few beds (for example, unit 28). Fusulinids are present in nearly every unit of the lower member, but they seldom are abundant. Scattered rugose corals are present in many units, but generally are not found in growth position. Tabulate corals are rare; chaetetid types are the largest, with diameters up to 10 cm, in colonies 30 x 40 cm (unit 12, 11-17 ft; see also fig. 17). Small algal grains are present (see identifications by Wilde, table 1) and may be abundant where indistinguishable in the field from other small grains, especially in the lower part. Brachiopods generally are rare, but they occur in thin beds made almost entirely of broken shells (for example, unit 9, 7-9 ft). Bryozoans and conispiral foraminifers are very rare.

Other grain types are important constituents of some limestones. Coated grains, including ooids and elongate types, are abundant in many beds, especially in the lower part of the member (fig. 15); grapestone grains are rare. Peloids generally are scarce, but they are abundant in a few beds (for example, unit 13, 55-65 ft). Grain tangency generally is fair to good, although the range is from none to perfect. According to Dunham's subclassification, these limestones range from lime wackestone to lime grainstone based on petrographic analyses. The only lime boundstones are the small colonies of tabulate corals. All of the limestones are well indurated, and no porosity was observed.

In fair to good exposures, limestone bodies contain beds averaging 30 cm in thickness and generally not more than 50 cm. Where separated by chert bands, limestone beds are as thin as 5-10 cm (fig. 19). Some successions are alternating beds of matrix material and carbonate grains; within other beds, the percentage of grains decreases upward or downward, and in rare cases grains are concentrated into lenses (unit 38, 0-4 ft). Most beds contain heterogeneous mixtures of carbonate grains, but in some cases alternating beds contain segregated skeletal and coated grains (for example, unit 9). On the other hand, some alternating layers of muddy and purer limestones do not appear to be differentiated into separate beds (unit 10, 3-4 ft). Initial orientations of beds are nearly all horizontal in this member; in one case beds lap out downward to the northeast (unit 15, 0-2 ft). Bedding surfaces are fairly sharp and mostly flat. Stylolites are less common than in the upper member. Possible mudcracks were observed on one bedding surface (unit 7, 17-19 ft; fig. 14). Measurable erosional relief was found in two cases to be 1-2 cm (unit 20, 0-1 ft) and 30 cm (unit 12, 0-3 ft). One channel 20 cm deep and 40 cm wide contains shells and limestone lithoclasts (unit 18, 4-5 ft). Within most beds, even in those that are well exposed, no lamination is discernible. Horizontal to wavy lamination is barely to moderately discernible in some beds (fig. 13), and current-ripple lamination is evident in a few (unit 27, 4-25 ft). Inclined laminae, observed in only one bed (unit 6, 12-14 ft), have an initial dip of 40° to N. 17 ° W. (after simple rotation).

Chert constitutes less than 10 percent of the total volume of the lower Horquilla; however, it constitutes 30 percent of several individual units (fig. 19). All of the chert occurs within limestone host rock. Color is generally brownish gray; lighter shades are more common in the upper part and darker shades in the lower part, paralleling color changes in the associated limestones. Many colors have a light bluish tinge. Some cherts are nearly white; others are black or brownish black (fig. 18). Alternating black and white stripes produce a distinctive zebralike pattern with concentric layers in nodules and parallel layers in bands of chert. This zebra-patterned chert constitutes a possible stratigraphic marker at the top of the Morrowan (unit 13, 34-35 ft; fig. 16). Composition of the cherts is dominantly siliceous. Calcareous material ranges from 0 to 10 percent in most cases but may be as high as 40 percent, especially where unreplaced carbonate grains are abundant and where white calcareous layers alternate with black siliceous ones in the zebra-patterned chert. Traces of pyrite are present in a few cherts. Black cherts may contain carbonaceous material. Texture is dominantly

microcrystalline (crystals smaller than 1/16 mm) and probably is extremely finely crystalline (smaller than 1/256 mm). Diaphaneity of the microcrystalline material is opaque to translucent. Original carbonate grains include crinozoans, fusulinids, and less common brachiopods, corals, and ooids; they may be completely to selectively replaced or completely unreplaced. Rhombic porphyrotopes may be replaced dolomite crystals (unit 31, 10-20 ft).

Chert mostly occurs in nodules, ranging from 1 x 3 cm up to 50 x 60 cm, averaging about 5 x 10 cm to 10 x 50 cm (figs. 18-22). Contacts with limestone host rocks generally are sharp but may be smooth or irregular. Orientations of long axes commonly are parallel to bedding of the limestones. Many nodules are linked laterally parallel to bedding or are anastomosed by connections normal or oblique to bedding. Some chert occurs in bands (length/width ratio is 10:1 or greater) 2-10 cm thick and 1 to about 5 m long that generally are parallel to bedding.

Nearly the entire lower member of the Horquilla appears to have been deposited in a shallow-marine environment with open circulation that was generally free of terrigenous influx. This interpretation is supported by the lithologic properties, the stratification, the few colonies of tabulate corals in growth position, the locally abundant algal material, and the scattered occur

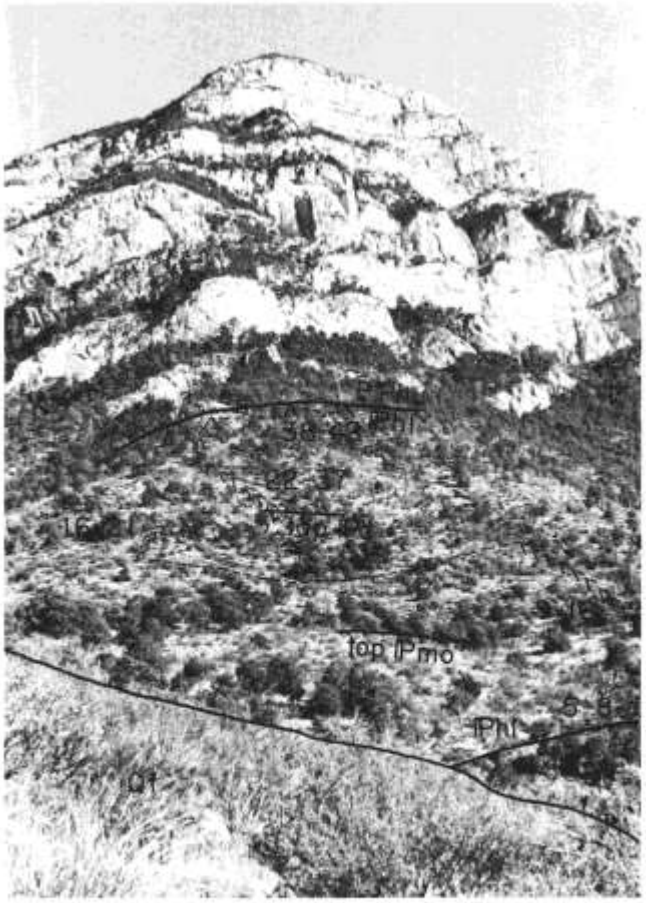

FIGURE 12—Outcrop of lower member of Horquilla (Phl), 1,363 ft thick, with line of measured section (units 5–42); several lateral offsets were needed to follow the locus of best exposures. Approximate tops of Morrowan (Pmo) and Derryan (Pd) Series are shown within the lower Horquilla; view is south-southeast, downhill from jeep trail.

rences of rugose corals that probably were transported only short distances. The dominant microcrystalline-limestone lithology indicates low energy in the depositional environment. Ooids and other completely coated grains suggest agitation, and concentrations of fragmental skeletal grains indicate at least moderate turbulence. Such fluctuations from lower to higher energy may have been produced by slight relative falls of sea level, increases in sediment supply, approaches of migrating tidal channels, and/or other mechanisms.

The Pennsylvanian shoreline generally was many miles north or northwest of the Big Hatchet area, although the occurrence of possible mudcracks indicates minor regression. The north-northwest initial inclination of the cross laminae is opposite to the inferred paleoslope and may be a result of flood-tide deposition or lateral accretion in a meandering tidal channel. The shelf probably subsided slowly but continuously over about 25 m.y. of early Pennsylvanian time to accommodate the 1,363 ft of shallow-marine limestone in the lower Horquilla. The gross sedimentation rate of 54.5 ft (16.6 m) per m.y. is below the maximum of 40 m per m.y. estimated by Wilson (1975, p. 15, table I-1) for ancient shallow-marine carbonates. Judging by the wide distribution of similar correlative facies in the region, the shelf probably was very broad. The nearest known deep-marine facies is in the Marathon area of western Texas, about 300 mi to the southeast; those deposits were thrust several miles to the northwest in Wolfcampian time.

As the petrographic evidence will show, the limestones probably were stabilized in a fresh-water environment during diagenesis. The cherts are diagenetic replacements of the limestones, as indicated by the replaced carbonate grains and matrix material; the silica probably was brought in during the fresh-water incursions.

Many limestones contain sufficient organic matter to be classified as fair sources of petroleum (see documentation in the chapter on petroleum geology). Kerogens are of the herbaceous-woody-coaly types and indicate sources of gas. Fresh-water diagenesis may have caused some oxidation of the source material at an early stage. No porosity was observed, and no reservoir quality is inferred.

FIGURE 13—Horizontal and wavy laminae in limestone beds near base of Horquilla (unit 5, 0–5 ft); view is southeast.

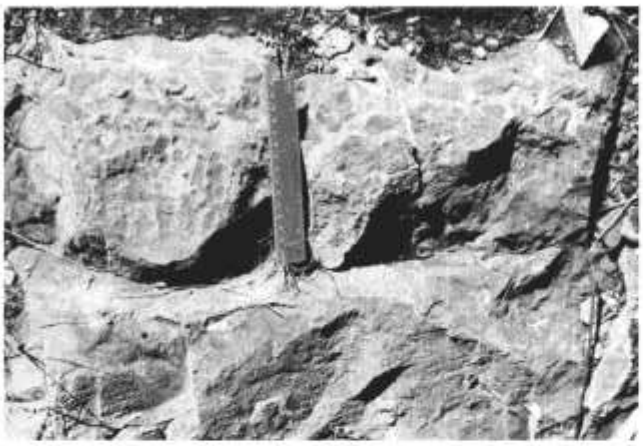

FIGURE 14—POSSIBLE MUDCRACKS ON BEDDING SURFACE OF MICROCRYSTALLINE LIMESTONE IN LOWER HORQUILLA (unit 7, 17–19 ft); mudcracks are filled by sparry calcite and extend only a few cm below bedding surface; view is southeast (obliquely down).

FIGURE 17—*CHAETETES* SP. (C), A TABULATE CORAL, LOWER HORQUILLA (unit 13, about 60 ft above base); generally restricted to Derryan–Desmoinesian in Big Hatchet area; view is southeast (down) on main foot trail to east of line of section.

FIGURE 15—OOLITIC, SKELETAL LIMESTONE (UNIT 11, 0–6 FT), UNDERLAIN BY MICROCRYSTALLINE LIMESTONE AND CHERT (UNIT 10) IN LOWER HORQUILLA; view is south-southeast.

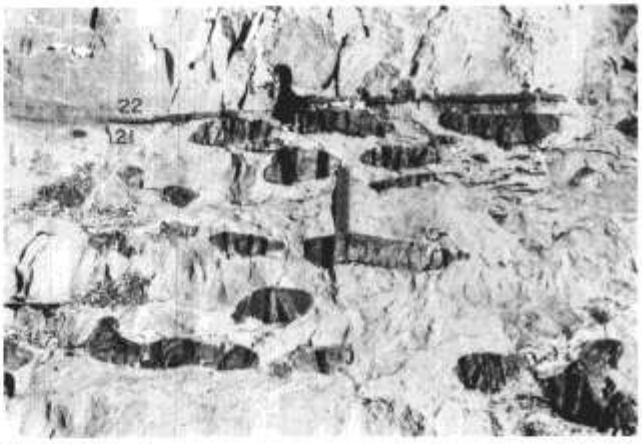

FIGURE 18—NODULES OF BLACK CHERT IN MICROCRYSTALLINE LIMESTONE (unit 21, 1–6 ft); above erosion surface is 2-cm-thick bed (dark layer) of crinoid hash and a thicker bed of microcrystalline limestone (unit 22, 0–2 ft). All in lower Horquilla; view is southeast.

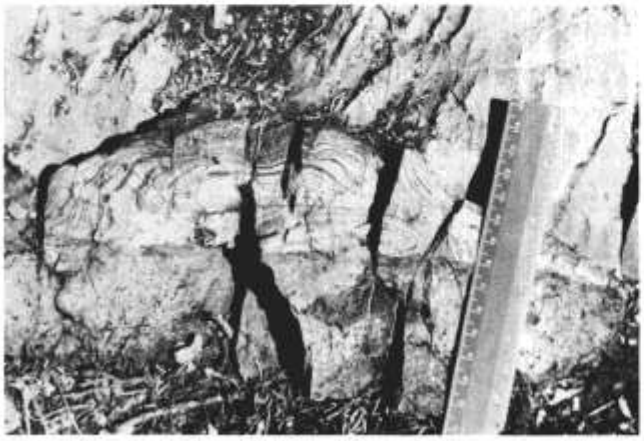

FIGURE 16—ZEBRALIKE STRIPES IN CHERT NODULE OF DARK SILICEOUS MATERIAL AND LIGHT CALCAREOUS MATERIAL (unit 13, 34–35 ft); possible stratigraphic marker at top of Morrowan, within lower Horquilla; view is southeast.

FIGURE 19—NODULES AND BANDS OF BROWN CHERT, SOME LINKED, SOME ANASTOMOSED, IN MICROCRYSTALLINE LIMESTONE OF LOWER HORQUILLA (unit 25, 0–7 ft); view is southeast.

FIGURE 20—MICROCRYSTALLINE LIMESTONE IN BEDS 50 CM OR MORE THICK (UNIT 32, 0–10 FT) OVERLYING LIMESTONE AND CHERT (UNIT 31, 10–20 FT), ALL IN LOWER HORQUILLA; view is southwest.

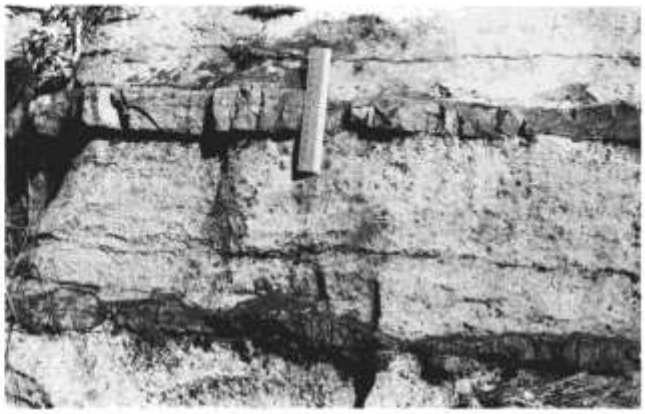

FIGURE 21—CHERT BAND 5 CM THICK, AND LAYER BELOW OF LINKED CHERT NODULES, IN MICROCRYSTALLINE TO SKELETAL LIMESTONE OF LOWER HORQUILLA (unit 39, 0–13 ft); view is southeast.

FIGURE 22—LARGE CHERT NODULES, SOME LINKED, SOME ANASTOMOSED, IN MICROCRYSTALLINE LIMESTONE, NEAR TOP OF LOWER HORQUILLA (unit 42, 0–28 ft); view is southeast.

Horquilla Formation, upper member (Pennsylvanian-Permian)

In the Big Hatchet Peak section, a total of 1,867 ft of the upper member of the Horquilla Formation was measured up to the present erosion surface on the top of the peak. The contact with the overlying Earp Formation is not seen in this fault block but is seen in the downthrown block to the west, about 1 mi south of Big Hatchet Peak (fig. 3). R.A. Zeller, Jr. (personal communication, 1961) estimated that over 200 ft of upper Horquilla have been eroded from the top of the peak. The total measured section of the Horquilla here is 3,230 ft, so the total estimated thickness is about 3,500 ft. Zeller (1965, p. 37) measured nearly complete sections in the New Well Peak area (3,245 ft) and Bugle Ridge area (3,530 ft) and estimated that the total thickness of the Horquilla in the Big Hatchet Mountains is no greater than 3,600 ft. The Big Hatchet Peak section (units 43-78) is designated as the type section of this informal upper member of the Horquilla, unless a complete section or a tie to an exposure of the uppermost part and the overlying Earp can be found in later work.

Figs. 23-39 are photographs of the general outcrop and selected exposures. Several offsets were made in the line of section, mainly to connect segments measured in the places where the cliffs could be climbed and worked with a minimum of hazards (fig. 23). Exposures generally are better than those in the lower member, and only 10 percent of the succession is concealed by major covered intervals of talus, soil, and/or vegetation. Some parts of the cliffs are locally fractured and deeply weathered or are covered by modern carbonate crusts, but these parts generally can be bypassed with offsets to better exposed intervals.

A small normal fault was crossed at the prominent spur in the first cliff (fig. 23). The main line of section (units 43-47) goes up to the top of the cliff west of the spur, ending at a stratigraphic marker (unit 48) near the fault on the upthrown side. The fault trends N. 20° E. parallel to that part of the cliff, dips steeply to the southeast, and is downthrown to the southeast with about 50 ft of stratigraphic throw. A short section (units 48-49) was measured on the downthrown side in the reentrant to the east of the spur. A fair stratigraphic marker (base of unit 50) was traced back to the west where the next main part of the section was measured. Other small faults may be present; however, units can be traced without major disruption across each of the cliff faces within the large horst block of the Big Hatchet Peak area. The field evidence of the stratigraphic succession is supported by the normal sequence of fusulinid zones.

The age of the upper Horquilla ranges from Des-

moinesian, through Missourian and Virgilian, into Wolfcampian, based on Wilde's fusulinid identifications (table 1). The Desmoinesian-Missourian boundary determined in the Big Hatchet Peak section lies in the lower part of the second cliff (fig. 23, top unit 50). The Missourian-Virgilian boundary lies in the upper part of the third cliff (top unit 61). The Virgilian-Wolfcampian boundary lies at the base of the fifth cliff (base of unit 68, above major lateral offset to west, traceable along top of tree line). Fusulinids in the Pennsylvanian part of the member are the same relatively small size (1-2 or rarely 3 mm in diameter, and 2-4 or rarely 6 mm long) as those in the lower member (above the basal part). Many fusulinids in the Wolfcampian part are noticeably larger (3-4 or rarely 2 mm in diameter, and 5-6 or rarely 4 mm long). Fusulinids were not found in several limestone units and, where found, generally are less abundant in the Pennsylvanian part of the upper member, as compared to the lower member; however, they were found in all but one limestone unit of the Wolfcampian part and are abundant in several beds.

The contact between the lower and upper Horquilla is not well exposed in the Big Hatchet Peak section, but it appears to be a low-relief disconformity (fig. 24). The hiatus is probably short because Desmoinesian fusulinids are found below and above.

Limestone constitutes 70 percent of the upper Horquilla. Fresh color is generally medium to light brownish gray, and darker shades are less common than in the lower member. Composition is dominantly calcareous, with only a few traces of muddy impurities. In some beds minor silicification is indicated, but it may be a result of superficial weathering because chert is relatively rare in the upper member. Of the textural constituents, microcrystalline material generally is dominant, although most beds contain at least a trace of skeletal material.

In addition to fusulinids, the more abundant skeletal types in the limestones are algae and crinozoans. Phylloid algae intermittently are abundant in the Pennsylvanian part (units 45-64). They form laterally extensive biostromal accumulations of disarticulated plates, but mounds were not observed in this section. A thin basal zone of tabulate corals underlies the oldest biostrome of phylloid algae (unit 45). In the overlying sequence (unit 46), phylloid algal plates are most abundant in the basal part (fig. 27), are separated by patches of microcrystalline material in the middle (fig. 28), and are in clusters or dispersed within microcrystalline material in the upper part (fig. 29). Low-relief erosional surfaces form the boundaries at the base and top. In hand specimen, the individual thalli range in width from 1 to 4 mm. Small skeletal grains, probably disarticulated fragments of other algal types, are abundant in many beds, especially in the upper part of the member. In the Wolfcampian part, algal oncoids (7 mm wide, 10 mm long, with encrustations 3 mm thick) are formed by *Tubiphytes* sp. (units 76-77). Crinozoans appear to be dominant on the surface in only one unit (unit 60) in contrast to the lower Horquilla, but are abundant in many petrographic thin sections. Corals are rare, consisting of favositid and chaetetid tabulate types in the Desmoinesian (unit 45, 0-3 ft, fig. 26) and rugose types in the Missourian (unit 52). Other sparse or rare fossils include brachiopods, sponge spicules, and biserial foraminifers.

Peloids, ooids, and other coated grains are much less common than in the limestones of the lower member. Grain tangency mostly is poor, although the range is from none to excellent. According to Dunham's (1962) classification, these limestones mostly are lime wackestone, with a range from lime mudstone to lime grainstone; lime boundstone is recognized in the small colonies of tabulate corals and in the algal oncoids. All of the limestones are well indurated. No significant porosity was observed, although some small vugs and thin fractures are filled with calcite, and some traces of vuggy porosity are present only on the weathered surface (unit 74, 34-54 ft). No reservoir quality is indicated.

A few ancient cavities are present locally. The best exposed one is in Missourian limestone, is 2 ft high and 3 ft wide, and is filled with horizontally laminated, microcrystalline limestone and thinly interlayered red mud-stone (unit 54, 95-97 ft; figs. 32-34). The limestone is reddish because of oxidation of pyrite inclusions. Partial dolomitization of the fill indicates a diagenetic relationship with the next dolostone 68 ft above (unit 56). Modern caves up to 10 ft high indicate Quaternary solution of the limestones in this uplifted fault block (unit 54, 105-120 ft, and unit 76, 0-7 ft).

Composite thicknesses of limestone units range from several hundred feet to 26 ft where separated by dolostones. Thicknesses of beds within the limestones generally are 10-50 cm, with a range from 5 to 400 cm where discernible. Patterns of successively thinner beds indicate filling of a broad channel in the Missourian (unit 60), and successively thicker beds indicate progradation in the Wolfcampian (unit 76, 7-44 ft; fig. 38). Generally the bedding surfaces are horizontal, but a few are slightly wavy; many are erosional with low relief. Stylolites are developed along many surfaces, especially in the microcrystalline limestones (fig. 24). Lamination was observed rarely. Beds at the base of the member contain irregular laminae (unit 43, fig. 25), and the fill of the ancient cavities contains horizontal laminae (unit 54, fig. 34).

Dolostone constitutes 30 percent of the upper member. Fresh color is light to medium brownish gray. Composition is dominantly dolomitic, with minor silicification that probably is a result of superficial weathering. Textural constituents are dominantly medium to coarsely crystalline, rhombic, and tightly fitted into a mosaic. Ghosts of replaced crinoids, and a few which escaped replacement during dolomitization, are present in trace amounts. In one interval (unit 49, 0-9 ft, at base), poorly preserved intraclasts appear to be imbricated to dip southwest. Sucrosic, intercrystalline porosity is evident in only a few dolostones. Nearly all have traces to 10 percent of vuggy porosity. On fresh surfaces, the vugs generally are 1-3 cm in diameter; on weathered surfaces, vugs generally are 10-20 cm and range up to 100 mm in diameter where they constitute 30 percent of the surface (unit 49, 9-19 ft; unit 63, 0-15 ft; figs. 31 and 36). The enlargement of vugs on the weathered surface may be attributed to Quaternary solution.

The six laterally extensive dolostone units range in

thickness from 54 to 148 ft and total 484 ft. Thicknesses of beds within the dolostones range from 20 cm to 200 cm, although in many cases bedding is not discernible. Many bedding surfaces appear to be erosional with low relief. No lamination is discernible in the dolostones.

Some contacts between limestones and dolostones are sharp where they coincide with bedding surfaces (figs. 30 and 35), others are transitional and irregular with relief up to 1 ft. In one case (unit 48, 2-5 ft) a lateral transition from limestone to dolostone takes place in only 2 ft, within 20 ft of a fault zone; in another case (unit 46, 4-10 ft) a similar transition takes place within a few yards laterally, but no nearby faulting is evident. Small masses of dolostone (30-50 cm in diameter) appear to have been formed by selective replacement of favositid corals, possibly before silicification of chaetetid corals in the host limestone (unit 45, 0-3 ft; fig. 26).

Chert constitutes only a trace of the upper member, but amounts in individual units range up to 40 percent. Chert only occurs in limestone hosts. Fresh colors overall are lighter than those of the cherts in the lower member; they generally are light to medium brownish gray and are brownish black in only one unit (unit 73). Composition is dominantly siliceous, with a trace to 20 percent of calcareous material and a rare trace of carbonaceous flakes. Texture is dominantly microcrystalline (probably extremely finely crystalline), translucent to opaque, with a trace to 10 percent of skeletal forms including sponge spicules, fusulinids, and crinozoans (some of which are not replaced). Nodules range in size from 3 x 6 cm to 10 x 80 cm, and a few are linked to form masses 100 cm long. Long axes generally are parallel to bedding, and shapes are fairly regular. Bands are rare and small (5 x 70 cm).

Similar to the lower member, nearly all of the upper member of the Horquilla in the Big Hatchet Peak section probably was deposited in a shallow-marine environment. The basal unit of limestone with irregular laminations may be an intertidal deposit. The poorly preserved intraclasts in dolostone, imbricated to dip southwest, may indicate a flood-tide current to the northeast in an intertidal channel. However, most of the member consists of subtidal deposits.

The abundance of phylloid algae in the upper Desmoinesian-Virgilian indicates shelf-margin deposition during much of that time. However, individual biostromes generally are less than 20 ft thick, and upbuilding appears to have been terminated in most cases by surf-base erosion in the shoaling waters. Algal plates served as baffles to trap finer sediment. The upward increase in matrix material observed in some biostromes may indicate that burial in finer sediment was another factor in the termination or retardation of the phylloid algal accumulations.

The 1,867 ft of shallow-marine carbonates were deposited during a time span of about 20 m.y. from late Desmoinesian into early Wolfcampian. The gross sedimentation rate of 93.3 ft (28.4 m) per m.y. is nearly double that of the lower member but is also less than the maximum estimated by Wilson for ancient shallow-marine carbonates. The inferred increase in subsidence may be attributed to the proximity to the basin margin.

As in the lower member, the limestones and cherts probably were stabilized in a fresh-water diagenetic setting. The ancient cavities in the limestones indicate dissolution in a vadose environment and a relative fall of sea level of about 68 ft. The laminated cavity fill probably was deposited under phreatic conditions. The thick, laterally extensive dolostones probably were stabilized penecontemporaneously in a saline diagenetic environment. Small occurrences limited to areas around fault zones may have been formed by solutions migrating along fractures, dissolving Pennsylvanian dolostones and replacing adjacent limestones. Such restricted replacement most likely occurred early, possibly during fracturing associated with middle Wolfcampian uplift. By late Cretaceous to Tertiary time, during Laramide or Basin and Range uplift, the Pennsylvanian carbonates probably were too thoroughly lithified to be subjected to such local dolomitization.

The thick dolostones with vuggy porosity constitute at least a fair petroleum-reservoir objective. Some communication between vugs may be provided by fractures and solution channels. Although the matrix porosity-permeability is poor, it may improve toward the shelf edge where dolomitization may have ceased before the development of tight mosaic textures, in which case sucrosic, intercrystalline porosity would be extensive. The limestones separating the dolostones provide adequate seals to the individual reservoirs and, similar to the limestones in the lower member, these also qualify as fair petroleum-source rocks, especially for gas.

Fig. 40 shows the southeast-to-south panorama from Big Hatchet Peak and the view of several key control sections to be worked in the evaluation of petroleum-source and reservoir relationships along the northwest-southeast trending shelf-basin margin in the upper Horquilla. Fig. 41 shows the reconstructed stratigraphic cross section between the Big Hatchet Peak section on the shelf margin and the Humble No. 1 State BA well drilled in the Alamo Hueco Basin. Although the Wolfcampian shelf has prograded southwestward over the upper Pennsylvanian margin and conceals those rela-

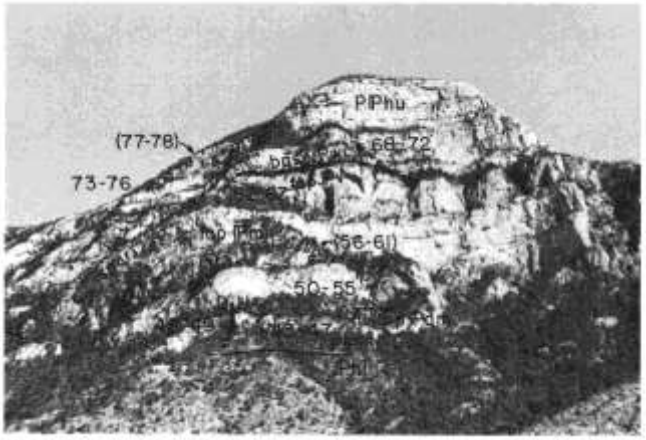

FIGURE 23—OUTCROP OF UPPER MEMBER OF HORQUILLA (**PPhu**), 1,867 FT THICK (TOP ERODED), WITH LINE OF MEASURED SECTION (UNITS 43–78); several lateral offsets were needed to connect segments measured where the cliffs could be climbed and worked. Projecting spurs block the view of some segments (units 56–61, 77–78) and offsets. Approximate tops of Desmoinesian (**P dm**), Missourian (**P mi**), Virgilian (**P v**), the base of the Wolfcampian (**Pwc**) are shown within the upper Horquilla; view is south from Chaney Canyon (enlarged from fig. 5).

tionships over much of the surface exposure, the features along the Wolfcampian margin will provide significant control for projections along the older margins. Based on reconnaissance study of sections described by Zeller (1965) and Wilson (1975, and his students C.F. Jordan and M.A. Schupbach), dolostone reservoirs appear to be absent along the Wolfcampian shelf margin. Debris flows, with some clasts derived from phylloid algal mounds, and terrigeneous clastics were deposited on the clinoform slopes exposed in the Borrego area. Thick units of dark mudstone are tongues from the deep-marine deposits of the Alamo Hueco Basin and may be excellent source rocks that were in a favorable position for updip migration of oil and gas into the shelf-margin reservoirs, especially those in the Pennsylvanian dolostones.

FIGURE 24—DISCONFORMABLE CONTACT BETWEEN LIMESTONE AND CHERT (UNIT 42) OF LOWER HORQUILLA AND LIMESTONE (UNITS 43 AND 44) OF UPPER HORQUILLA; note stylolites along bedding surfaces in microcrystalline limestone (unit 44); view is northeast.

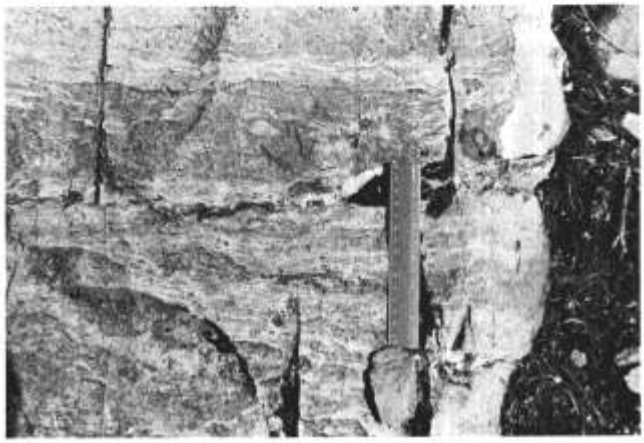

FIGURE 25—IRREGULAR LAMINATIONS IN DOLOMITIC, MICROCRYSTALLINE LIMESTONE (UNIT 43); view is southeast.

FIGURE 26—SELECTIVE DOLOMITIZATION OF FAVOSITID CORALS (F, LIGHT-COLORED) IN LIMESTONE WITH SILICIFIED CHAETETID CORALS (C) IN UPPER HORQUILLA (unit 45, 0–3 ft).

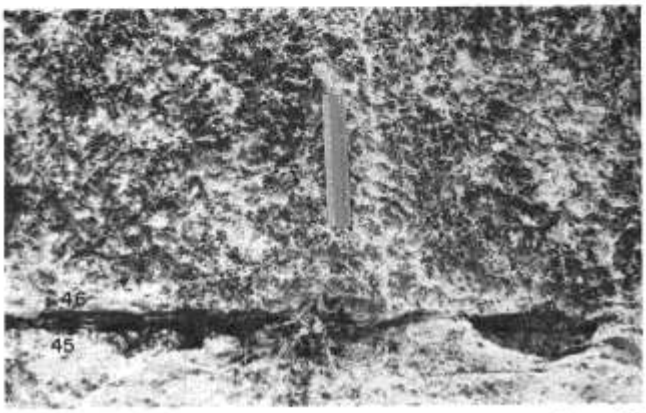

FIGURE 27—ABUNDANT PHYLLOID ALGAE IN LIMESTONE BED (UNIT 46, 0–4 FT) WITH EROSION SURFACE AT BASE, AND MICROCRYSTALLINE LIMESTONE BELOW (UNIT 45, 57–61 FT), BOTH IN UPPER HORQUILLA; view is east-southeast.

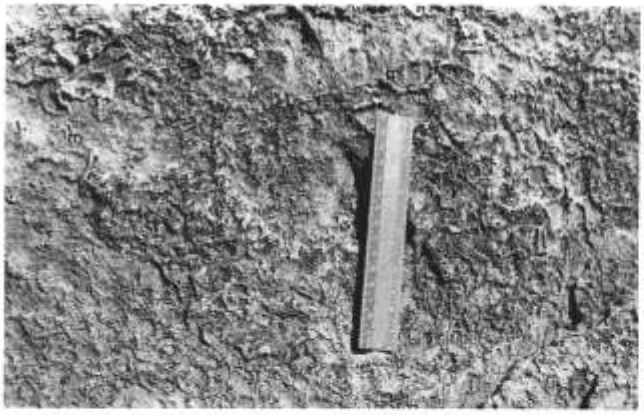

FIGURE 28—PHYLLOID ALGAE WITH PATCHES OF MICROCRYSTALLINE (**m**) LIMESTONE (unit 46, 10–16 ft); view is southeast.

FIGURE 29—CLUSTERS OF PHYLLOID ALGAL PLATES, SOME DISPERSED, IN MICROCRYSTALLINE LIMESTONE, WITH EROSION SURFACE AT TOP (unit 46); view is east-southeast on main foot trail to west of line of section (below unit 50).

FIGURE 30—LIMESTONE WITH MINOR PHYLLOID ALGAE (UNIT 47, UPPER PART), THINNER BEDDED MICROCRYSTALLINE LIMESTONE (**ls**) (UNIT 48, 5 FT THICK), AND DOLOSTONE (**dol**) (UNIT 49, 0–9 FT, 9–19 FT), IN UPPER HORQUILLA; view is east-northeast, taken from line of section in first cliff.

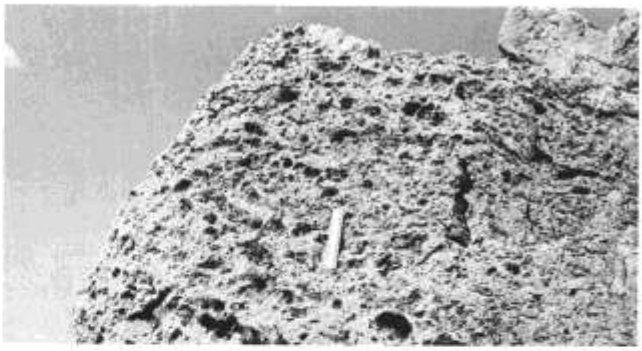

FIGURE 31—DOLOSTONE WITH ABOUT 30 PERCENT VUGGY POROSITY ON WEATHERED SURFACE; average diameter of vugs is 10–20 mm, maximum is 100 mm (unit 49, 9–19 ft). View is northeast, at top of cliff shown in fig. 30.

FIGURE 32—LIMESTONE CLIFF (UNIT 54, 25–120 FT) WITH LIMESTONE AND CHERT IN UPPER PART (UNIT 55, 0–35 FT) AND OVERLYING DOLOSTONE (UNIT 56) IN UPPER HORQUILLA. Note position of ancient cavity (**ac**); view east at breach in second cliff; note climbing ropes (**r**) for scale.

FIGURE 33—ANCIENT CAVITY, PARTIALLY EXHUMED, 2 FT HIGH AND 3 FT WIDE (JACOB STAFF IS 5 FT LONG) IN UPPER HORQUILLA LIMESTONE (unit 54, 95–97 ft); view is southeast.

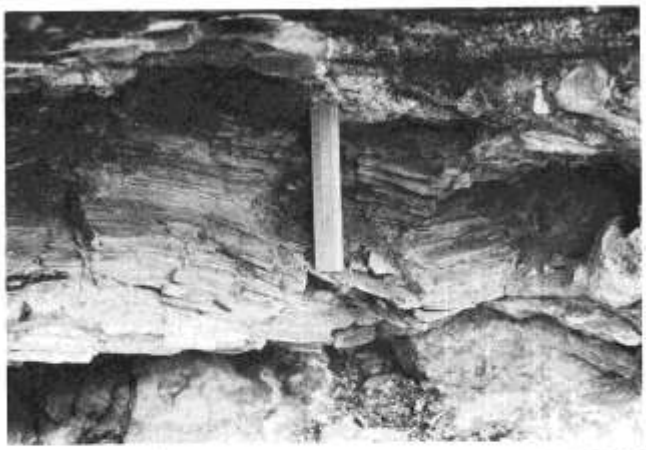

FIGURE 34—HORIZONTAL LAMINATION IN REDDISH-WEATHERING MICROCRYSTALLINE LIMESTONE AND THINLY INTERLAYERED RED MUDSTONE THAT FILL ANCIENT CAVITY SEEN IN FIG. 33; view is S. 60° E.

FIGURE 37—TREES CONCEAL SLOPE (BELOW CLIFFS) WHERE LIMESTONES WITH MINOR CHERT WERE MEASURED ALONG SKYLINE (units 71 and 72; highest units worked from Chaney Canyon campsite about 2,000 ft below); marker unit of limestone and chert (unit 73) was traced toward observer where rest of section was measured (worked from campsite on Big Hatchet Peak about 300 ft above). Limestones form sheer cliffs below the peak—equivalents to units 74 (115 ft thick) and 75 (54 ft thick); view is southwest.

FIGURE 35—SHARP CONTACT BETWEEN MICROCRYSTALLINE LIMESTONE **(ls)** WITH SOME PHYLLOID ALGAE (UNIT 62, 75–95 FT) AND DOLOSTONE **(dol)** (UNIT 63, 0–15 FT); view is south-southeast.

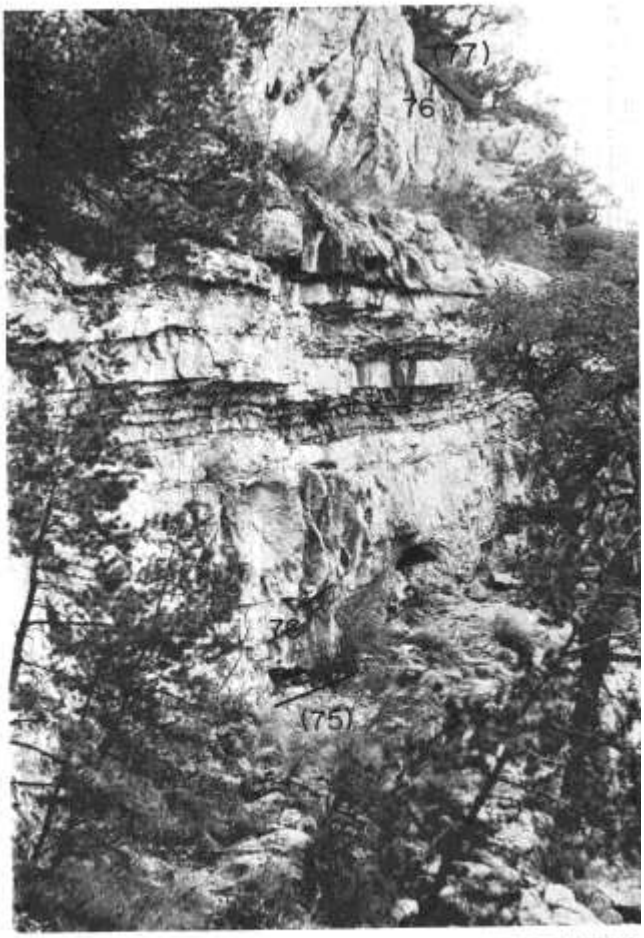

FIGURE 38—LIMESTONE BEDS SHOW THICKENING-UPWARD CYCLES INDICATING PROGRADATION, IN HIGHEST CLIFF OF THE UPPER HORQUILLA (unit 76, 0–44 ft); distinctive thin beds (7–10 ft above base of unit) are 5–10 cm thick. View is southwest, taken from line of section.

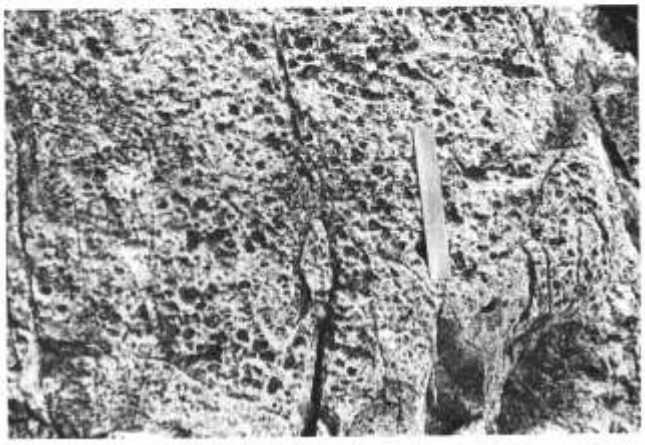

FIGURE 36—DOLOSTONE WITH ABOUT 30 PERCENT VUGGY POROSITY ON WEATHERED SURFACE, diameter of vugs about 10 mm maximum (unit 63, 0–15 ft); view is southeast.

FIGURE 39—LIMESTONES WITH ABUNDANT FUSULINIDS (WOLFCAMPIAN) AT TOP OF BIG HATCHET PEAK (to west of line of section, equivalent to top of unit 78). Cairn marks triangulation station of U.S. Coast and Geodetic Survey (elevation 8,356 ft), Jacob staffs are 5 ft long; solar-powered antenna is used by U.S. Customs Service; view is east.

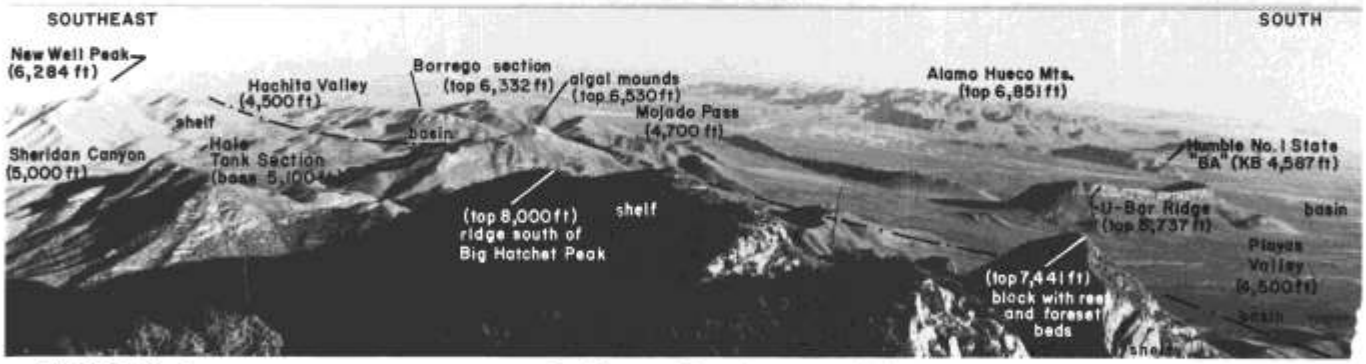

FIGURE 40—PANORAMA SOUTHEAST TO SOUTH, FROM BIG HATCHET PEAK (ELEVATION 8,356 FT) SHOWING KEY CONTROL OF SHELF-TO-BASIN FACIES TRANSITION IN THE UPPER MEMBER OF THE HORQUILLA.

The approximate facies boundary is drawn as a dash-dot line, where exposed or buried, and fault disruptions are ignored. New Well Peak, near the southeast end of the Big Hatchet Mountains (8 mi from observer), is composed of shelf limestones in the upper Horquilla, as described by Zeller (1965, p. 84–86). In Sheridan Canyon, at the base of the Hale tank section, the unconformity is exposed between upper Horquilla limestones and Earp conglomerates, sandstones, and red mudstones, as described by Zeller (1965, p. 95–96); younger Permian rocks crop out to the southwest. In the Borrego section, the upper Horquilla is in a deep-marine basin facies with thick dark mudstones as described by Zeller (1965, p. 93–95); also present are debris-flow conglomerates. Phylloid algal mounds are present along the shelf margin, and clasts derived from them are found in the debris on the relatively steep basin-margin slope to the southwest, as determined by Schüpbach (in Wilson, 1975, p. 179). Shelf limestones are found along the ridge extending south-southeast from Big Hatchet Peak (scrub brush covers eastern side; note mescal stalks about 10–20 ft high); on the downfaulted block to the south, composed mostly of shelf limestone, Zeller (1965, p. 44, fig. 11) shows a reef with foreset beds dipping basinward on the west face. Off the right side of the photograph, in Cement Tank Canyon on the west side of the Big Hatchet Mountains, Schüpbach (in Wilson, 1975, p. 185, fig. VI-13) documents a cyclic alternation of phylloid algal mounds and slope deposits at the shelf margin. U-Bar Ridge, south of Big Hatchet Peak, is composed of massive Lower Cretaceous limestones with rudists, and forms a southeast-plunging syncline; the adjacent anticline was drilled by the Humble No. 1 State BA well (kelly bushing elevation 4,587 ft, total depth 14,585 ft; 10 mi from observer) and the deep-marine basin facies of the upper Horquilla in that well consists of dark mudstone and limestone (6,285–9,400 ft; Zeller, 1965, p. 116–117). South of Mojado Pass are the Alamo Hueco Mountains composed mainly of Tertiary volcanic rocks; they also lie on the Big Hatchet uplift. The uplift is bounded by Basin and Range faults with the Playas Valley graben on the west and the Hachita Valley graben on the east.

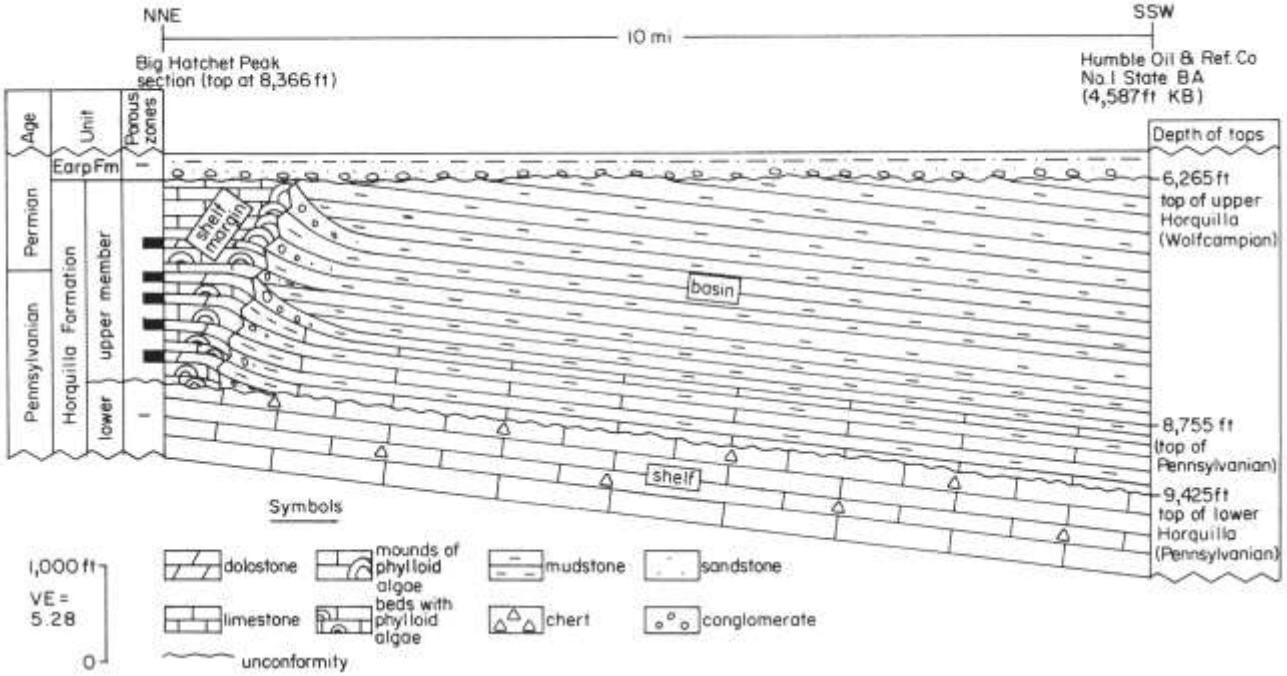

FIGURE 41—NORTH-NORTHEAST-SOUTH-SOUTHWEST STRATIGRAPHIC CROSS SECTION FROM THE BIG HATCHET PEAK SECTION TO THE HUMBLE NO. 1 STATE BA WELL.

In the Horquilla Formation, the lower member (Pennsylvanian/Morrowan–Desmoinesian) consists of shallow-marine shelf deposits over the area of the cross section and beyond. An unconformity is inferred between the lower and upper members. In the upper member (Pennsylvanian–Permian/Desmoinesian–Wolfcampian), an abrupt lateral change from shelf-margin to basin-slope deposits is evident in the Big Hatchet Mountains, and basin-floor deposits are indicated in the Humble well. Porous dolostones are observed in the Big Hatchet Peak section where interbedded limestones contain phylloid algal material; dolostones appear to be absent in exposures of the younger (Wolfcampian) part of the progradational shelf margin where mounds of phylloid algae are observed in the limestones. Limestone conglomerates, including debris from the algal buildups, were deposited on the steep clinoform slopes; the basin was filled with deep-marine mudstone and limestone. After subaerial erosion, nonmarine red beds of the Earp Formation (Wolfcampian) covered the area; cross section is restored with base of Earp as datum. Relationships in the younger part of the shelf margin and on the clinoform slopes are based partly on unpublished work by J. L. Wilson and M. A. Schüpbach; tops in the Humble well are from Zeller (1965, p. 116).

Petrography

The first part of this chapter deals with the basic concepts of diagenesis in carbonate sediments and their stabilization to become limestones and dolostones. The second part applies these concepts to the Horquilla limestones, cherts, and dolostones of the Big Hatchet Peak section, based on the evidence from petrographic analyses. Developments of porosity in carbonate rocks and their preservation in dolostones are documented. Plates 1-19 at the end of this chapter show selected photomicrographs of petrographic features. Appendix 2 includes definitions of terms, a discussion of methods, and a table with detailed petrographic descriptions of all thin sections.

General discussion of carbonate diagenesis

Diagenesis in marine environment

In areas where rates of carbonate sedimentation are not excessively high, micritization of thin-walled crystalline shells and ooids is a widespread phenomenon. Micritization results in a loss of original crystalline fabric as endolithic blue-green algae bore into grains, and the tiny borings become infilled by micritic carbonate (Bathurst, 1975).

Endolithic algae are unable to penetrate completely the relatively thick-shelled bioclasts or large ooids. Consequently, micrite envelopes are formed. Rims similar to micrite envelopes may be formed by precipitation of micritic cement films around grains in meteoric vadose or marine environments (Jacka, 1974a). Peloids may be formed by complete micritization of ooids or by mechanical breakdown and rounding of micritized shells.

Formation of relatively thick algal or algal-foraminiferal encrustations also is widely recorded in shallow subtidal environments. Modern examples have been described from the Bahama platform by Winland and Matthews (1974).

Cementation commonly occurs in peritidal marine environments. Intertidal beachrock cements have been described by Taylor and Illing (1971), Muller (1971), and Jacka (1974a). Modern subtidal cementation has been described by Shinn (1969), Friedman and others (1974), Ginsburg and James (1976), and James and others (1976).

In general, peritidal marine cements consist of films or crusts which form around grains or in primary voids. The films consist of micritic aragonite or high-magnesium calcite, of fibrous aragonite, or of bladed magnesium calcite. In intertidal environments, grains commonly have inner micrite films and outer fibrous or bladed rims. In large voids, the outer fibrous or bladed films commonly exhibit pendulous downward elongation, which represents microstalactitic gravitational cement.

Carbonate mineralogy and stabilization

Newly deposited carbonates consist predominantly of the unstable polymorphs aragonite and high-magnesium calcite (Friedman, 1964; Matthews, 1968; Bathurst, 1975). Only small amounts of calcite (low-magnesium calcite) and traces of dolomite occur in recent carbonates. Ancient carbonates consist almost wholly of the stable polymorphs calcite or dolomite. Thus all ancient carbonates represent diagenetic lithofacies that have stabilized in waters ranging from strictly fresh to highly saline, and with a wide range of Ca/Mg and Mg/Ca ratios. Aragonite stabilizes by becoming calcitized or dolomitized, or dissolves, as in the case of aragonitic shells in a fresh-water diagenetic environment. In such an environment, high-magnesium calcite rapidly stabilizes to low-magnesium calcite through incongruent dissolution of magnesium (Land, 1967). The conversion of low- or high-magnesium calcite to calcite occurs at a much greater rate than calcitization of aragonite (Gavish and Friedman, 1969).

One of the most important factors that controls stabilization of unstable carbonates appears to be the Ca/Mg ratio of diagenetic fluids. Contact with fresh (meteoric) ground waters, having relatively high Ca/Mg ratios, results in calcitization of aragonite and high-magnesium calcite to form limestones. Discharge of waters with high or relatively high Mg/Ca ratios through an unstable carbonate results in dolomitization and formation of dolostones.

Diagenesis of limestones

Most limestones reflect stabilization within freshwater diagenetic environments. Matthews (1968) has established the main diagenetic format for carbonates that stabilize in fresh-water environments. A brief review of Matthew's format follows. Aragonitic lime muds become calcitized, with calcitization initiating on available calcite nuclei (skeletal material consisting of high- or low-magnesium calcite). Aragonitic shell material tends to dissolve because it contains no calcite nuclei. When aragonitic lime mud is replaced by calcite, an 8.3 percent excess of calcium and carbonate ions becomes available for local precipitation as calcite cement because aragonite is denser than calcite (Pingatore, 1970). Calcium and carbonate ions, when released from dissolution of aragonitic shells, may also be precipitated locally as calcite cement. Thus, three processes, calcitization of lime mud, solution of aragonitic shells, and calcite cementation, commonly take place concurrently. Most limestones contain secondary solution molds and/or solution channels and vugs that subsequently become filled to varying degrees by calcite cements.

Jacka and Brand (1977) have shown that vadose/phreatic ground-water dynamics exert an important control over carbonate diagenesis. Meteoric-phreatic zones tend to stabilize rapidly owing to continuous discharge of fresh ground waters, while superjacent vadose zones stabilize much more slowly because they are alternately wet and dry. After stabilization within a phreatic zone has been completed, the overlying, predominantly unstable carbonate in the vadose zone is diagenetically poised to serve as a donor of Ca^{2+} and $C0_3^{2-}$ ions to the subjacent phreatic zone. As the vadose zone finally does stabilize incrementally, Ca^{2+} and $C0_3^{2-}$, which are released by dissolution of aragonitic shells and by conversion of aragonitic lime mud to cal-

cite, are transported downward to the phreatic zone and precipitated within secondary solution cavities; massive occlusion of porosity in the phreatic zone commonly results. Porosity in vadose-diagenetic zones tends to be preserved, particularly if a shale should become deposited above it. If another carbonate unit should be deposited on a porous vadose zone, it may later serve as a massive donor of Ca^{2+} and CO_3^{2-} and occlude all porosity in the subjacent carbonate.

When original aragonitic lime muds become calcitized, the calcite crystals form compromise boundaries with a tight jig-saw-puzzle fit, and the result is a dense matrix. In many instances, aragonitic shells are dissolved before lithification of the matrix is completed. The molds partially collapse and crumbly nontectonic fractures are formed (Jacka and Brand, 1977). Continued discharge of fresh water through the system results in enlargement of shell molds and fractures to form interconnected vugs and solution channels. Most limestone reservoirs have secondary porosity that consists of relatively large, secondary solution molds, vugs, and channels which are interconnected within a dense matrix.

Dolomitization and dedolomitization

When aragonitic lime mud becomes dolomitized, rhombic-dolomite crystals initially form a loose idiotopic fabric with excellent intercrystalline porosity. In many cases, dolomitization is accompanied by selective dissolution of calcitic shells, and thus moldic porosity may enhance intercrystalline porosity. If dolomitizing fluid continues to discharge through a dolostone after dolomitization has been completed, epitaxial cementation on rhombs occurs and porosity becomes occluded by formation of compromise boundaries. Thus, residence time and flux of dolomitizing fluids may determine whether intercrystalline porosity is formed, occluded, or preserved in dolostones.

From study of middle Permian carbonates of the Permian Basin, Jacka (1975) has identified petrographically distinct varieties of dolostone. Neomorphic dolostones initially consist of euhedral to subhedral rhombic-crystal fabrics and were formed by replacement of aragonitic precursors. Paramorphic dolostones are formed by replacement of calcitic limestones, which had been extensively leached and stabilized within fresh-water diagenetic environments. Stabilization occurred during lowstands of sea level when the climate was characterized by greater amounts of rainfall than during highstands. Later, at shallow depths of burial, these limestones became paramorphically dolomitized with petrographically perfect preservation of calcitic textures and fabrics. Only neomorphic dolostones develop intercrystalline porosity.

Dedolomitization—replacement of dolomite by calcite—is a relatively common phenomenon. Dedolomitization takes place near the surface when ground waters with high Ca/Mg ratios discharge through a dolostone (DeGroot, 1967). Dedolomitization represents a paramorphic replacement of rhombic-dolomite crystals by calcite. Apparently, calcite and dolomite replace one another paramorphically; however, aragonite generally becomes neomorphically replaced by calcite and dolomite. Paramorphic replacement of calcite by dolomite, and dolomite by calcite, may in some way reflect the fact that both are hexagonal and have the same unit cell. Neomorphic replacement of aragonite by both calcite and dolomite may reflect the fact that aragonite is orthorhombic and thus has a different unit cell than calcite or dolomite. Transformation of orthorhombic aragonite to hexagonal calcite or dolomite probably requires complete dissolution of aragonite followed by precipitation of the other phase, with a resultant change in crystal fabric. Replacement of calcite by dolomite, and of dolomite by calcite, may represent an ionic substitution with no change in crystal form.

Discussion of dolomitization models

SABKHA MODEL —The only dolomitization mechanism that has been substantiated with documentary evidence from modern environments is the coastalsabkha (supratidal) model. This mechanism of dolomitization was first discovered along the southwestern margin of the Persian Gulf (Curtis and others, 1963; Illing and others, 1965; Kinsman, 1969; Butler, 1969).

The sabkha (or Persian Gulf) model provides only for thin-skin dolomitization. Dolomitization occurs above the salt-water table to the sabkha surface, where the water table lies within 1 m of the surface. Sabkhas represent areas where carbonates produced in subtidal-lagoonal environments are deposited in intertidal and supratidal areas by normal diurnal tides, spring tides, and storm tides.

After a supratidal zone has been recharged by a storm or spring tide, evaporation of pore waters occurs and gypsum is interstitially precipitated. Precipitation of gypsum removes Ca^{2+} ions from pore waters, which become progressively enriched in Mg^{2+} . Ultimately the Mg/Ca ratio may increase from that of normal sea water to as much as 35/1 (Butler, 1969). These magnesium-enriched pore fluids react with predominantly aragonitic carbonates by dolomitizing them. Thus gypsum precipitation is followed by dolomitization. If the shoreline position were to remain stable for prolonged time intervals, and subsidence were continuous, sabkha-dolostone thicknesses could exceed the normal 1 m. Such conditions are rare because rates of progradation in shallow lagoons or epeiric seas are normally high, and rapid progradation forms thin, widespread, dolomitized sabkha deposits. Kinsman (1969) infers that sabkhas along the southwestern margin of the Persian Gulf are presently prograding seaward at rates of 1-2 m per year. Thin sabkha dolostones generally do not represent significant hydrocarbon reservoirs.

SEEPAGE-REFLUX ION AND DORAG MODELS — Two mechanisms have been proposed to explain dolomitization of relatively thick sequences of subtidally deposited carbonates: the seepage-refluxion mechanism (Adams and Rhodes, 1960; Deffeyes and others, 1965), and the fresh-water lens or dorag model (Hanshaw and others, 1971; Land, 1973; Badiozumani, 1973). Neither of these mechanisms adequately explains the relatively thick dolostones so commonly found in the geologic record.

The seepage-refluxion hypothesis was first mentioned as a possible dolomitization mechanism by Newell and others (1953). This mechanism was first proposed for-

mally by Adams and Rhodes (1960) based upon relationships manifested in middle Permian carbonates of the Permian Basin, including the San Andres Formation.

Adams and Rhodes (1960) postulated that the Permian shelves were restricted by a continuous barrier-reef tract. A hydraulic surface current was induced to flow from the Delaware Basin across the broad lagoon of the Northwest shelf by evaporative drawdown of shelf waters. As the surface current flowed shelfward, progressive evaporation and concentration first caused precipitation of gypsum (or anhydrite?); in more landward areas, halite and bittern salts were deposited. Precipitation of calcium sulfates enriched lagoonal brines in Mg^{2+} ions, and a dense magnesium-enriched current sank to the floor of the shelf lagoon; this current refluxed or discharged seaward and also percolated downward through previously deposited shelf carbonates, displacing original pore waters and dolomitizing the sediments.

Jacka and Franco (1974) cited the following objections to the seepage-refluxion hypothesis as proposed by Adams and Rhodes (1960). The reef tract was broken by large submarine canyons and smaller tidal and surge channels; thus the shelf area was not sealed or restricted by a continuous barrier. The sulfates and halite were not precipitated within a restricted shelf lagoon. Anhydrite, which occurs in lagoonal sediments, was diagenetically emplaced after deposition at shallow depths of burial. The remaining sulfates were precipitated landward from the shelf lagoon in coastal sabkhas, brine pans, and inland sabkhas. Therefore, no magnesium-enriched brines could have been generated in broad-shelf lagoons.

Another obstacle to accepting seepage-refluxion mechanisms, as outlined by Adams and Rhodes (1960) and Deffeyes and others (1965), is that massive precipitation of calcium sulfate on a lagoon or lake floor is required to generate a magnesium-enriched brine which could then reflux laterally or downward. Such precipitation would probably form an occlusive seal which would then prevent downward refluxion from occurring. E.A. Shinn (personal communication, 1978) has voiced the same objection.

Except for formation of thin sabkha deposits, the mechanism (or mechanisms) responsible for massive, wholesale dolomitization in the Permian Basin (and elsewhere) remains enigmatic. No clear example of seepage refluxion has been documented in modern carbonate provinces.

Hanshaw and others (1971) proposed a mechanism of dolomitization that was inferred to occur at the base of a coastal fresh-water lens in the zone of mixing of fresh water and sea water. Magnesium for dolomitization was presumed to have been derived from sea water in the zone of diffusion. The mechanism was inferred from study of subsurface Eocene carbonates of Florida. The same mechanism was championed by Land (1973) from study of middle Pleistocene carbonates of Jamaica and by Badiozamani (1973) from study of Middle Ordovician carbonates of Wisconsin. Badiozamani (1973) coined the term "dorag dolomitization" for this mechanism; *dorag* is a Persian word for mixed blood.

Steinen (1974) analyzed borehole data taken through a coastal fresh-water lens that is superimposed on modern metastable carbonates on the island of Barbados. The cores transected the meteoric-vadose, meteoric-phreatic, and marine-phreatic zones. He found that metastable carbonates were rapidly being transformed into limestone within the fresh-water lens, but that no dolomite was found at the base of the lens in the zone of mixing. Thus, the dorag model failed to pass its first test.

Other objections to the dorag mechanism cast doubt on its viability and general applicability. The dorag mechanism should operate at optimal rates under humid climates with heavy rainfall. Under such climates, coastal fresh-water lenses would be developed to maximal degrees. Ancient carbonates accumulated under ambient humid climates in many areas. One such example is Pennsylvanian carbonates of the Permian Basin area. Many if not most of the newly deposited carbonates must have been subjected to the influence of fresh-water lenses that migrated seaward; however, dolostones are very sparsely represented in these carbonates. The same relationship characterized Upper Mississippian and Pennsylvanian carbonates of the Illinois Basin, but only limestones are represented there. Another objection is that the dorag mechanism should be expected to form lenticular dolostone units, rather than stratal dolostones such as occur in most areas. Thus, the dorag model is not well supported by evidence from the geologic record.

As of now, no fully acceptable mechanism has been proposed to explain formation of relatively thick dolostone sequences. At the present time, we do not know where dolomitizing fluids originate or the manner in which they discharge through metastable carbonates.

Petrographic analysis of Horquilla carbonates and cherts

Lithofacies and biofacies relationships

The Horquilla exhibits intercalation of grainstones, packstones, and grain-rich wackestones. The overall proportion of wackestones to packstones and grainstones increases upward in the Horquilla, and they predominate in the upper Horquilla. This upward increase in wackestones may reflect progressive progradation of the shelf margin, so that the Big Hatchet Peak locality became positioned increasingly farther behind the margin. The predominance of wackestones in the upper Horquilla could possibly reflect protected environments behind outer-shelf islands.

In the lower Horquilla, oobiograinstones (pls. 13C, 16C, 17C, 18D) and biograinstones (pls. 13B, D; 15A) are abundantly represented. They are sparsely represented in the upper Horquilla.

The following biotic components, listed in order of decreasing abundance, are represented in Horquilla limestones: crinozoans, bryozoans, *Tubiphytes*, fusulinids, small foraminifers, phylloid algae, pelecypods, brachiopods, ostracods, gastropods, siliceous sponge spicules, *Komia*, and trilobites.

Three examples of nine-component fossil systems were noted (see petrographic descriptions of thin sections in appendix 2; sample notations in the BHP section include the lithostratigraphic unit number and the

footage above the base of the unit): BHP-77-41—*Tubiphytes*, crinozoans, phylloid algae, small foraminifers, pelecypods, brachiopods, bryozoans, fusulinids, and ostracods; BHP-75-1—*Tubiphytes*, phylloid algae, bryozoans, crinozoans, gastropods, pelecypods, ostracods, small foraminifers, and fusulinids; and BHP62-5—crinozoans, bryozoans, fusulinids, brachiopods, phylloid algae, pelecypods, small foraminifers, trilobites, and *Tubiphytes*. Eight-, seven-, six-, and five-component systems are abundantly represented, but four-, three-, and two-component systems are rare and may in part reflect sampling vagaries.

Oolitic grainstones commonly form just inward from outer-shelf margins, as on the present Bahama platform complex, where they form just inward from the reefs and coralgal (backreef) facies (Purdy, 1963). The alga, *Tubiphytes*, also represents an excellent indicator of outer-shelf facies from middle or late Pennsylvanian to middle Permian time. The alga(?), *Komia*, is also associated with carbonate buildups and outer-shelf facies. Phylloid algae also seem to be most abundantly represented in carbonate mounds and in outer-shelf deposits. Phylloid algae are represented by cement-filled molds. Ooids, *Tubiphytes*, and *Komia* can be identified from tiny cuttings samples.

Tubiphytes first appears in BHP-41-20 and is abundantly represented throughout the remainder of the Horquilla to the top of the peak. Like *Komia*, *Tubiphytes* is a problematical creature that is generally considered to be an alga. Wilson (1975) suggests that *Komia* may be a stromatoporoid. *Tubiphytes* is abundantly represented within the Capitan reef complex (middle Permian/Guadalupian).

Diagenesis of Horquilla limestones

FRESH-WATER DIAGENESIS—Nearly all limestones within the Horquilla bear evidence of having stabilized within fresh-water diagenetic environments, according to the format established by Matthews (1968) and Jacka and Brand (1977).

In carbonates with original lime-mud matrix (wackestones and packstones), the matrix became converted to a dense limestone. In wackestones, packstones, and grainstones, aragonitic shells and many ooids were dissolved to form molds (pls. 1C, 2D, 4A, 7B, 9A, 12D, 15C, 16C, 17B) and hollow micrite envelopes (pls. 3D, 18D), while calcitic shells were unaffected by the fresh-water diagenesis. Many aragonitic shells were dissolved before lithification of the matrix had been completed, and the molds partially collapsed to form nontectonic fractures (pls. 1B; 5D; 8B, C). Continued discharge of fresh ground water caused molds to become enlarged into vugs and fractures into solution channels (pls. 2C; 3A, B; 5D).

Phylloid algae, pelecypods, and some gastropods possessed aragonitic shells; these are now represented by molds and vugs. Micritization of these shells or bioclasts precluded dissolution during fresh-water diagenesis.

Intensive recrystallization of original lime-mud matrix is abundantly represented in Horquilla mud-supported limestones (pls. 7A, B; 8B). Jacka and Brand (1977) have shown that intensive recrystallization of original lime-mud matrix represents an overprint of prolonged meteoric-phreatic diagenesis. During recrystallization, syntaxial rims (in optical continuity) commonly are formed on crinozoan components (pl. 6D).

Numerous examples of vadose internal sediment were noted in Horquilla limestones (pls. 2C, 8A, 18D); these record episodes of subaerial exposure.

Much silica was emplaced in Horquilla limestones by fresh ground waters. As shown by Jacka (1974b and 1978a), silica nucleates in organic-rich materials such as fossils, peloids, ooids, burrows, and stromatolites. Exclusive of cherts (which will be discussed in a following section), most silica observed in thin sections has partially to completely replaced shells, peloids, or ooids (pls. 6D, 15A, 16C, 17C). Shells and ooids were replaced by megaquartz and length-slow or length-fast chalcedony. Peloids and micritized shells were replaced by microquartz. Some silica was emplaced as doubly terminated quartz porphyroblasts (pl. 12).

Most cement in Horquilla limestones was emplaced by meteoric ground waters. Drusy cement fabrics (crystals increase in size inward toward centers of voids) are abundantly represented in primary and secondary voids (pls. 3B, D; 7B; 9A; I IC; 15C). Blocky-equant mosaics of calcite cement are also abundantly recorded in secondary and tertiary voids (pls. 1A, B, D; 2A, C, D; 3D; 4A; 6C; 8B; 11D).

Monocrystalline crinozoan components are abundant in biograinstones. The most rapid rate of calcite cement precipitation occurs on monocrystalline components (Jacka, 1974a), and relatively large, optically continuous (epitaxial) aureoles of cement have been precipitated on most of them (pls. 13D, 17C). In instances where fractures transect crinozoan components, drusy or blocky-equant cement fabrics occur where the fracture transects the micritic matrix; epitaxial cement occurs where the fracture transects a monocrystalline crinozoan grain (pl. 8C). Several examples of ferroan-calcite cements were observed in Horquilla limestones (pls. 1A, D; 2A). These cements were precipitated in reducing phreatic-diagenetic environments. One example of zoned ferroan and nonferroan calcite cements was noted (pl. 8B). This reflects an alternation of oxidizing and reducing environments during cementation. Ferroan-calcite cement always occurs as relatively coarse, blocky-equant crystal fabrics.

After secondary voids were filled predominantly with calcite cement, relatively small volumes of anhydrite were emplaced in Horquilla limestones as porphyroblasts. These were emplaced by sulfate-enriched brines and were dissolved by fresh ground waters to form tertiary (third-stage) voids (pls. 3A; 6C; 11D; 12B, C). These tertiary anhydrite molds, with their distinctive stairstep outline, were first discovered by Jacka (1978a, b).

Several examples of dolomitization along stylolites were noted. Whether or not such occurrences were associated with fresh-water diagenesis is uncertain. Dead oil is concentrated along one stylolite with dolomite (pl. 6B).

POROSITY RELATIONSHIPS—During two different stages, large volumes of primary (intergranular and intrabiotic) and secondary (molds, fractures, vugs, and solution channels) porosity existed within Horquilla limestones. Subsequently, the porosity became almost

completely occluded by precipitation of meteoric calcite cements.

Numerous episodes of subaerial exposure and fresh-water diagenesis are recorded in the Horquilla limestones. Under these conditions, mineralogic stabilization of carbonate sediment to form limestone was followed by submergence, rapid transgression, and deposition of another unstable carbonate unit over the subjacent, lithified, stabilized interval. During the next episode of subaerial exposure, the mineralogically unstable unit entered into a donor/receptor relationship with subjacent previously stabilized and lithified carbonates (Jacka and Brand, 1977).

A few Horquilla limestones once had relatively large volumes of tertiary anhydrite-mold porosity. This porosity has been filled predominantly by dolomite cements.

Diagenesis of Horquilla cherts

Cherts in the Horquilla are associated exclusively with limestones. This relationship is to be expected because the fresh ground water that causes mineralogic stabilization of the unstable carbonate to limestone also emplaces the silica.

As indicated under the discussion of limestone diagenesis, silica nucleates in organic-rich components. If silica-bearing meteoric ground water discharges through the carbonate for a sufficient time, silica will replace the matrix beyond the organic-rich nuclei and will form nodules, laminoid-nodular bodies, or irregular layers.

Siliceous sponge spicules also served as nuclei for silicification (pls. 11B; 15B, D). In rare instances some siliceous spicules became replaced by calcite (pl. 15D).

One common by-product of silicification is exsolution of dolomite rhombs (pls. 14A, C; 15B). This phenomenon was first reported by Jacka (1974b). The magnesium required for dolomite exsolution was locally derived from constituents in the carbonate sediment that are composed of high-magnesium calcite (crinozoans, bryozoans, fusulinids, and some of the lime mud). In many instances, dolomite cement was precipitated in intrabiotic cavities of fusulinids and bryozoans during silicification (pl. 14A). Paramorphic dolomitization of crinozoan components commonly accompanied silicification (pl. 13B). In some instances, crinozoans were only partially replaced by an aureole (outer rim) of discrete dolomite rhombs, which are syntaxial with the calcite monocrystals (pls. 14B, C). In many instances, dolomite porphyroblasts and dolomite cements became dedolomitized by normal calcite or ferroan calcite (pls. 8D; 14D; 16B; 17A; 18B, C).

Crystalline shell materials became replaced by megaquartz (pl. 17D) and chalcedony (pls. 8D; 14A, D). Former micrite matrix, micritized shells, and peloids became replaced by microquartz (pls. 11B, 14B, 17D). Drusy quartz and chalcedony also occur as cements.

Diagenesis and porosity relationships of Horquilla dolostones

All dolostone intervals occur in the upper Horquilla. They contain the most coarsely crystalline dolostones ever reported in the available literature for dolomitized matrix; crystals range in diameter up to 4.76 mm. Much of the material appears to be recrystallized (pl. 10B is the best example). All dolostones are neomorphic (pls. 3C; 4C, D; 5A, B, C; 6A; 7C, D; 9C, D; 10A, B, C, D; 11A; 12A) and appear to have been formed by replacement of predominantly aragonitic carbonate. Except for paramorphic replacement of monocrystalline crinozoan components (pls. 7D, 10D), all original textures have been obliterated by coarse neomorphic dolomitization. Most dolostones are inferred to represent biowackestones, but this interpretation cannot be established with certainty.

Paragenesis of Horquilla dolostones is remarkably similar to that described by Jacka and others (1980) in dolostones of the San Andres Formation (middle Permian) in the Permian Basin. Each dolostone interval records a well-developed fluid-invasion sequence of: 1) dolomitizing fluid, 2) anhydritizing fluid, 3) fresh ground water, and, in some instances, 4) a second dolomitizing fluid. First, a dolomitizing fluid discharged through the metastable carbonates and converted them into dolostones. Second, a hypersaline-anhydritizing fluid discharged through the dolostones, forming porphyroblasts and nodules of replacement anhydrite. Third, fresh ground water dissolved the anhydrite to form tertiary stairstep molds (pls. 4C, D; 5A, B, C; 6A; 7D; 10C, D; 13A). Large molds of dissolved nodular anhydrite are seen in an outcrop photo of a porous dolostone (fig. 31). Later during this fresh-water stage, gravitational microstalactitic calcite cements were emplaced in larger anhydrite molds (pls. 4C; 5A, C; 6A) or in solution-enlarged fractures (pl. 12A), both within vadose-diagenetic environments. The gravitational cement is inferred to have consisted originally of aragonite, which was recrystallized to radial-fibrous calcite. Fourth, in some intervals, paramorphic dolomitization of calcitic gravitational cement records discharge of a second dolomitizing fluid.

None of the conventional models of dolomitization can be applied to the Horquilla. No supratidal (coastal sabkha) deposits were noted. All Horquilla dolostones represent thick, subtidally deposited carbonates, which were dolomitized after deposition at shallow depths. The absence of overlying evaporites in this section precludes seepage refluxion as a possible mechanism. The dorag model is rejected for reasons cited in the general discussion, and because the process would tend to form lenticular dolostone bodies rather than the stratal dolostones that are generally seen in the Horquilla. Dolomitizing and anhydritizing fluids are inferred to have discharged laterally through initially unstable-carbonate intervals and to have originated to the north beneath the coastal plain.

One example of a dedolostone was noted in the lower Horquilla (BHP-10-3). This sample contains calcitic fossils (crinozoans and brachiopods) which had not been dolomitized.

Immediately after dolomitization, Horquilla dolostones contained large volumes of secondary intercrystalline porosity. Continued discharge of dolomitizing fluid through the carbonate after dolomitization resulted in precipitation of epitaxial-dolomite cement on original rhombic crystals. Compromise boundaries formed, and intercrystalline porosity was reduced to varying degrees in different intervals (pls. 3C, 5B, 7C).

Most preserved porosity in Horquilla dolostones represents tertiary molds of anhydrite porphyroblasts (pls. 4C, D; 5A, B, C; 6A; 7D; 9D; 10C, D) and nodules (fig. 31). Tertiary porosity was partially occluded by precipitation of calcitic gravitational (microstalactitic) cements (pls. 4C; 5A, C; 6A).

All Horquilla dolostones contain some preserved porosity, which locally ranges from poor (pls. 7D, 10B, 12A) to fair (pls. 4C, D; 5B; 7C; 10A) to good (pls. 3C; 5A, C; 9C, D; 10C, D; 11A). These dolostones would have definite reservoir potential, given the proper geologic history.

Geologic history of Horquilla carbonates

In the Big Hatchet Peak section, the Horquilla appears to consist almost wholly of subtidal deposits that accumulated on the outer-shelf margin of the Alamo Hueco Basin during times when the shelf was broadly submerged. No indications of supratidal or intertidal facies were noted in the petrographic analysis, and only a few intertidal deposits were inferred in field observations (see chapter on stratigraphy).

One question about the history of the Horquilla carbonates concerns this apparent paucity (or absence) of intertidal-supratidal deposits; it may be explained by erosion or nondepositon. Because progradational cycles are so common in shelf carbonates with subtidal, intertidal, and supratidal deposits occurring in ascending order, one possibility is that the intertidal-supratidal parts were deposited and eroded before the next subtidal units were laid down. Nearly every depositional unit in the Horquilla appears to be bounded by a minor disconformity as seen where exposed in the field and as supported by petrographic evidence. A few surfaces show a small amount of erosional relief. However, some erosional remnants of the intertidal-supratidal units should be preserved, so the recurrent-erosion hypothesis is considered unlikely.

Eustatic falls of sea level may have been so rapid that the shorelines did not regress slowly enough across the area for the intertidal-supratidal units to accumulate. Relatively rapid eustatic falls are evident in the subtidal carbonates that were stabilized to limestones during fresh-water vadose diagenesis as indicated by petrographic analyses. Moreover, the stillstand parts of the eustatic cycles may not have been long enough, and the carbonate-sediment supply may not have been great enough to fill the shelf depositional site and prograde intertidal-supratidal deposits from the distant northern shoreline or from possible outer-shelf islands. In future studies, limited occurrences of intertidal-supratidal deposits may be found around the fringes of the land or island areas.

A second question concerning the history of Horquilla carbonates is how alternating thick units became dolomitized. Although both were deposited as subtidal carbonates, the limestones were stabilized mineralogically in fresh-water, vadose-diagenetic environments and the dolostones were stabilized in salt-water, phreatic-diagenetic environments, as shown by petrography. Subtidal carbonates, which later stabilized to limestones and dolostones, probably were deposited during the rise-to-stillstand parts of eustatic cycles. In the case of limestones, stillstands may have been of short duration, because limestones were stabilized on subaerially exposed shelves. In the case of dolostones, stillstands may have been of greater duration, because the dolostones probably were stabilized while the shelves were submerged.

The saline dolomitizing fluids probably developed beneath the coastal plain to the north where anhydrite (or gypsum) was precipitated in an ambient arid climate, and the fluids became relatively enriched in magnesium. As the fluids discharged southward down depositional dip through the initially unstable carbonate layers at shallow depths of burial, these diagenetic fluids probably were perched on subjacent, impermeable limestones that had been stabilized previously. The climate remained arid long enough for the diagenetic fluids to become hypersaline and enriched in calcium sulfate, because, in each dolostone, anhydrite was emplaced as porphyroblasts.

The alternating episodes of fresh- and salt-water diagenesis may be related to glacio-eustatic cycles. During glaciation, sea level fell to a eustatic lowstand, the climate became more humid, and pluvial runoff supplied fresh water to the exposed shelf where carbonate sediment stabilized to form limestone. During interglacial times, sea level rose to a eustatic highstand, the climate became more arid, and evaporation in coastal areas produced the saline and hypersaline fluids for dolomitization and anhydritization.

Because the average thicknesses of the alternating limestones and dolostones are in tens of feet, the corresponding time intervals of eustatic fluctuations appear to be on the scale of glacially controlled changes. Glacio-eustatic cyclothems in the Pennsylvanian of the midcontinent area show the same magnitude of thickness.

The third question concerns the lateral extent of the dolostones. Although thick sections of limestones are present in the Pennsylvanian over a wide shelf extending to the west, north, and east, no thick dolostones have been described outside of the Big Hatchet Peak area. Petrographic analyses may show that some of these limestones represent dedolostones. If such units are correlatives of the dolostones of the Big Hatchet Peak area, the glacio-eustatic model of dolomitization would be supported. However, if the thick dolostones are confined to the outer-shelf margin, the hypothesis would need to be modified or discarded. This question is important in the regional history of carbonate diagenesis and may have implications regarding general models of dolomitization. Moreover, the question is of practical importance in exploration for reservoirs in the Horquilla dolostones.

Conclusions based on petrography

Conclusions concerning the petrographic analyses of Horquilla carbonates and cherts are:

1)—Horquilla carbonates were deposited along the outer-shelf margin of the Alamo Hueco Basin and they predominantly record deposition in subtidal environments.

2)—Grainstones, packstones, and wackestones are all abundantly represented in the Horquilla. The propor-

tion of wackestones to packstones and grainstones increases upward in the Horquilla, and wackestones predominate in the upper Horquilla.

3)—The following biotic components, listed in order of decreasing abundance, are represented in Horquilla limestones: crinozoans, bryozoans, *Tubiphytes,* fusulinids, small foraminifers, phylloid algae, pelecypods, brachiopods, ostracods, siliceous sponge spicules, *Komia,* and trilobites.

4)—All Horquilla limestones bear abundant evidence of having undergone mineralogic stabilization in fresh-water diagenetic environments, such as the following: a) selective dissolution of aragonitic shells, b) calcitization of aragonitic lime mud and high-magnesium calcite, c) precipitation of meteoric cements, d) formation of nontectonic fractures by partial collapse of molds, e) enlargement of molds into vugs and nontectonic fractures into solution channels, f) recrystallization of former lime-mud matrix, and g) silicification.

5)—Large volumes of primary and secondary porosity once existed in Horquilla limestones. This porosity has essentially all been occluded by calcite cements.

6)—Cherts were emplaced in Horquilla limestones by meteoric ground waters. Silica nucleated in organic-rich components such as shells, ooids, peloids, and burrows, as well as on siliceous sponge spicules.

7)—Horquilla dolostones record dolomitization of subtidally deposited carbonates at shallow depths of burial. These dolostones cannot be explained in relation to any of the conventional mechanisms of dolomitization: the sabkha, seepage-refluxion, or dorag models.

8)—The following fluid-invasion sequence is recorded in each Horquilla dolostone interval: a) dolomitizing fluid completely replaced the original metastable carbonate; b) a hypersaline anhydritizing fluid diagenetically emplaced porphyroblasts and nodules of anhydrite; and c) a low-salinity fluid (fresh ground water) dissolved anhydrite, formed tertiary porosity, and precipitated gravitational calcite cement in larger anhydrite molds.

9)—Much secondary intercrystalline and tertiary anhydrite-mold porosity has been preserved in dolostones.

10)—Although Horquilla carbonates were deposited almost exclusively in subtidal environments, numerous internal disconformities record episodes of subaerial exposure and fresh-water diagenesis. A complex series of eustatic fluctuations of sea level and climatic changes is recorded.

Plates of photomicrographs

(1-19)

Plates 1-19 show photomicrographs of petrographic features that were selected to characterize: 1) depositional features including rock types, textures, and fossils; 2) diagenetic features including replacement, cementation, solution, internal sediment, and fracturing; and 3) the resultant porosity relationships that were observed in thin sections of samples from the Big Hatchet Peak section. The plates are in order from the youngest to the oldest parts of the stratigraphic section. Plates 1-13A are of upper Horquilla limestones, dolostones, and cherts; pls. 13B-18 are of lower Horquilla limestones and cherts; and pl. 19 is of Paradise carbonates. At the heading of each caption is the sample notation (BHP-) giving the unit number and the footage above the base of the unit. More complete petrographic descriptions of all samples are given in appendix 2.

Each photomicrograph was taken with a reticle that produces a micrometer grid across the center of the field. The scale of each photo is specified according to the smallest division of the grid, d, which ranges from 10 to 90 microns; a micron, m, is equal to 0.001 mm.

Most photomicrographs were taken in plane-transmitted light; those taken with crossed polarizers are so specified. Because all thin sections were stained with potassium ferricyanide and alizarin red-S, the micritic calcites appear darker in transmitted light than sparry calcites, dolomites, and silica minerals.

Key features are labelled with letter symbols explained in the captions. Arrows are placed to show upward directions determined with gravitational cements.

PLATE 1

Depositional and diagenetic features of upper Horquilla limestones (A, B, C, D).

A Top of peak; biowackestone. Fusulinid chambers were lined by thin crusts of nonferroan calcite crystals (barely visible) and were completely filled by large, blocky-equant crystals of ferroan calcite **(F).** In two chambers, siderite (S) was precipitated after the nonferroan calcite and before the ferroan calcite. The ferroan calcite and siderite were precipitated in reducing phreatic environments; d = 90m.

B Top of peak; biowackestone. Relatively large, solution-enlarged nontectonic fractures cut smaller, nontectonic fractures caused by partial collapse of fusulinid. Fusulinid chambers and all fractures are filled by blocky-equant calcite cement, d = 90m.

C BHP-78-42; biowackestone. Micritized bryozoans **(Br)** are abundantly represented. Aragonitic phylloid-algal bioclasts **(P)** were dissolved by fresh ground waters, and molds became filled by sparry-calcite cement; d = 90m.

D BHP-78-4; biowackestone. Fusulinid chambers are filled by blocky-equant crystals of nonferroan calcite (white) and ferroan-calcite crystals (gray, **F); d =** 90m.

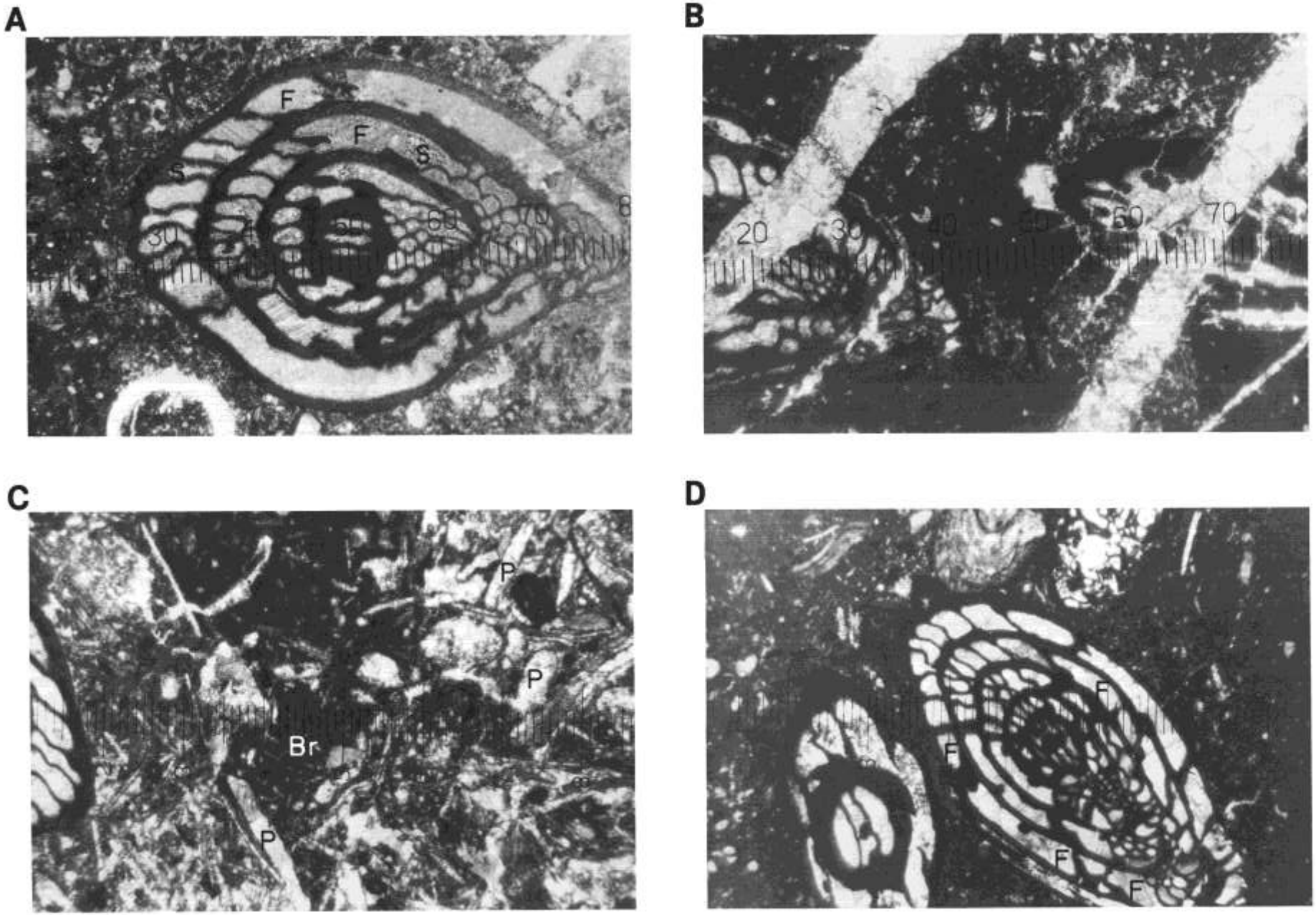
A
F
F
S
S
B
20
30
40
50
60
70
C
P
P
Br
P
D
F
F
F
F

PLATE 2

Depositional and diagenetic features of upper Horquilla limestones (A, B, C, D).

A BHP-77-41; biowackestone. Micritized bryozoans (Br) are abundant. Aragonitic phylloid-algal molds are filled by blocky-equant, ferroan-calcite cement (F); d = 90m.

B BHP-76-8; biowackestone. A thick algal encrustation consists of *Tubiphytes* (dark) and interlayered, crustose red algae (light); d = 90m.

C BHP-76-3; biowackestone. A relatively large solution cavity is floored by micritic, vadose internal sediment (V) and is filled by blocky-equant calcite cement; d = 90m.

D BHP-75-1; oobiopackstone. Dissolution of aragonitic ooids and phylloid algae produced molds, which were subsequently filled by blocky-equant calcite cement; d = 90m.

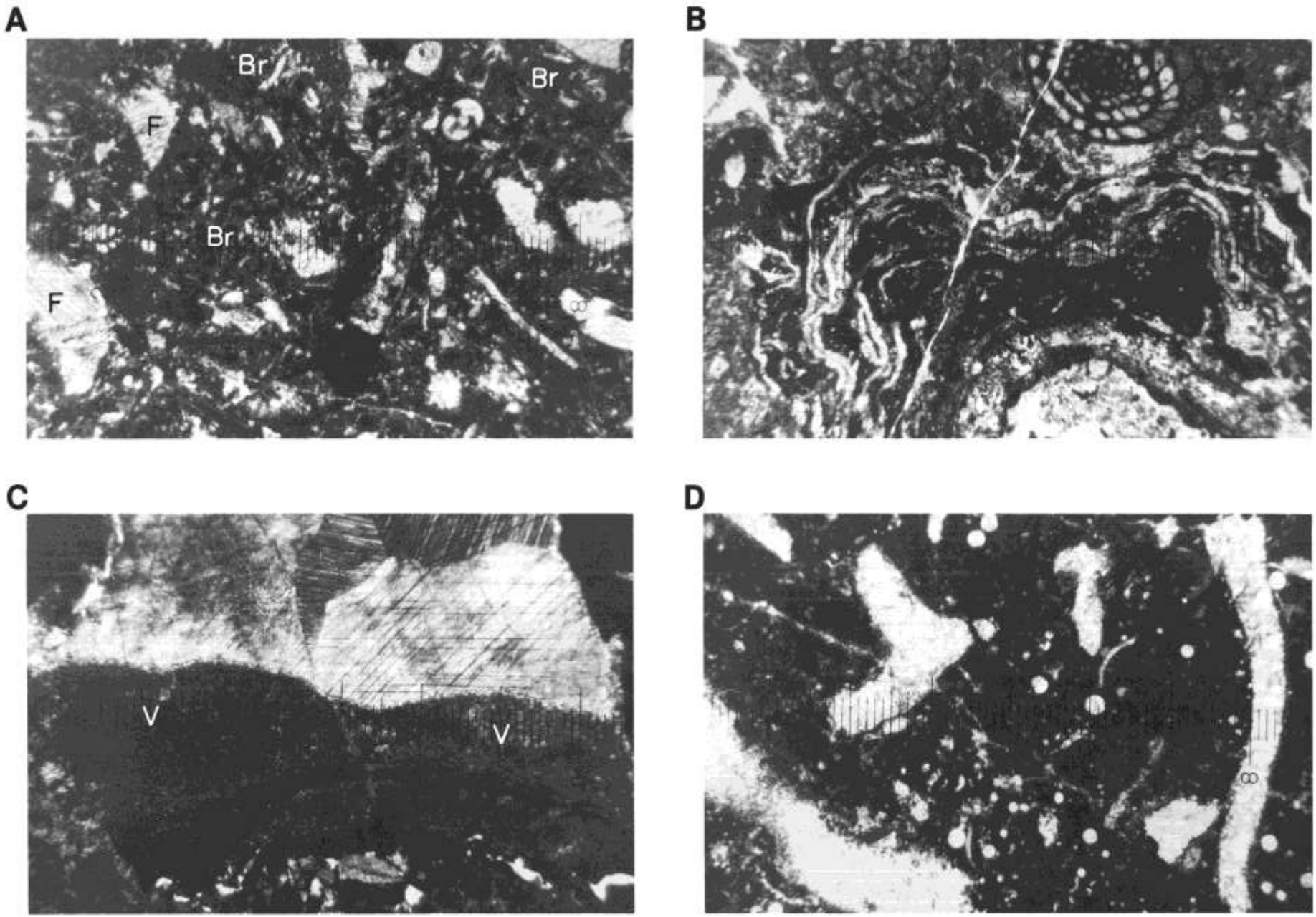
A
Br
Br
F
Br
F
B
C
V
V
D

PLATE 3

Depositional and diagenetic features and porosity relationships in upper Horquilla limestones (A, B, D) and dolostone (C).

A BHP-74-54; biowackestone. Dolomite cement (light) fills a stairstep anhydrite mold (A), which transects sparry-calcite cement (C). The following paragenesis is recorded: 1) a first episode of fresh-water diagenesis formed solution cavities, which became filled with meteoric calcite cement; 2), anhydrite porphyroblasts were emplaced by hypersaline ground water and replaced calcite cement; 3) anhydrite was dissolved by a second influx of fresh ground waters to form a tertiary void; and 4) dolomite cement was precipitated in anhydrite molds; d = 10 m.

B BHP-71-2; biowackestone. Large solution cavity resulted from fresh-water diagenesis. Partial collapse formed brecciated clasts, which were deposited along the floor of the cavity. Cavity subsequently became filled by drusy calcite cement; d = 90p.

C BHP-70-3; porous dolostone. Medium to very coarse neomorphic dolomitization of matrix. Compromise boundaries of many adjacent dolomite crystals have occluded part of the intercrystalline porosity, but both relatively large and small intercrystalline pores are preserved; d = 56m.

D BHP-69-85; biowackestone. Micrite envelopes were formed around most skeletal grains. Aragonitic phylloid-algal bioclasts were dissolved leaving hollow micrite envelopes, which later became filled by drusy, blocky-equant calcite cement (white); d = 56m.

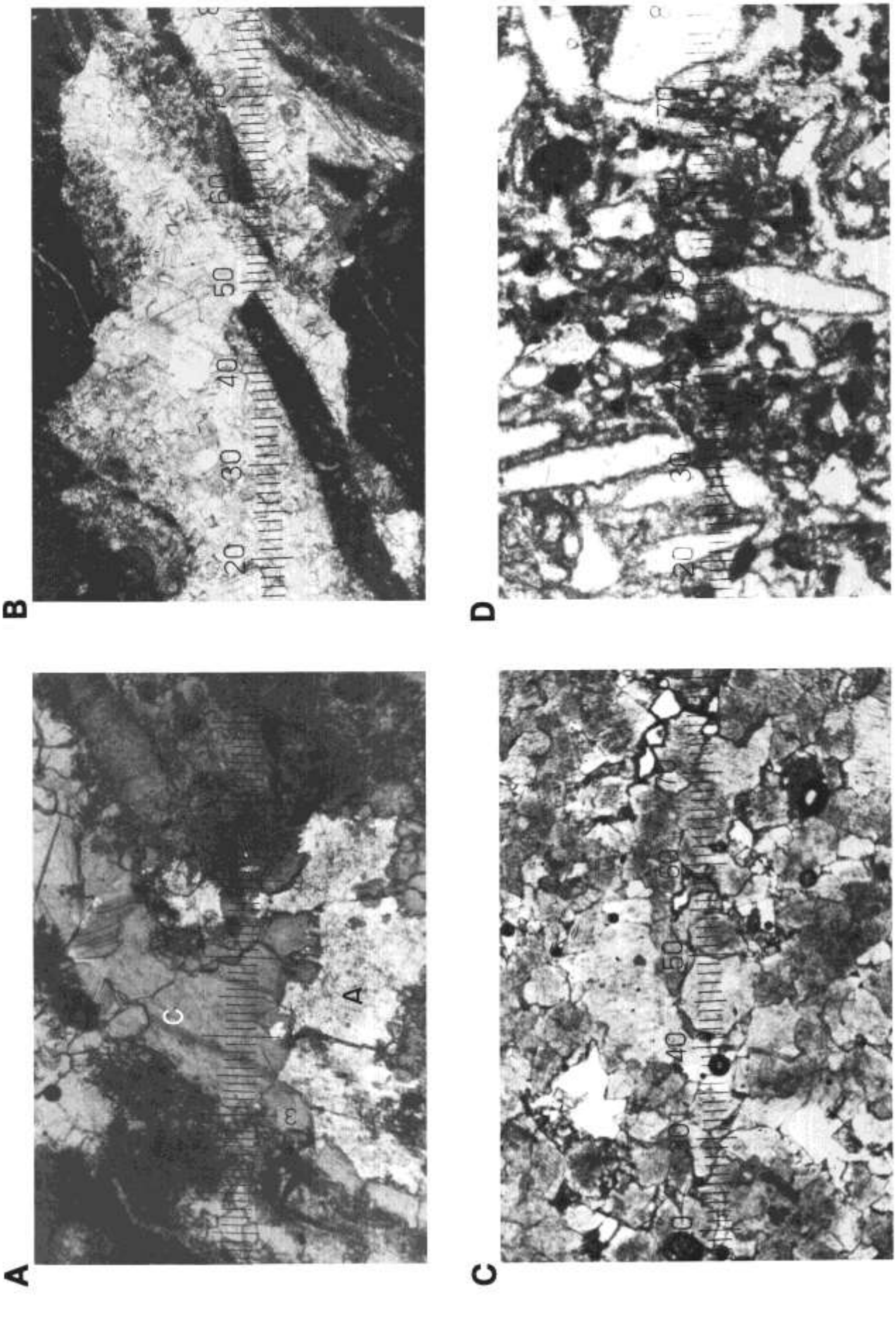
A
B
C
D
C
A
20
30
40
50
60
70
80

PLATE 4

Depositional and diagenetic features and porosity relationships in upper Horquilla limestones (A, B) and dolostones (C, D).

A BHP-68-70; biopelwackestone. Aragonitic phylloid-algal bioclasts were dissolved, and molds were filled by blocky-equant calcite cement (light); d = 90m.

B BHP-68-4; oobiopelwackestone. An aragonitic phylloid-algal bioclast was encrusted by a thick algal coating. Later the bioclast was dissolved by meteoric ground water, and the mold became filled by sparry-calcite cement (white); d = 56m.

C BHP-67-114; porous dolostone. Coarse neomorphic dolomitization of matrix. Relatively large, probable tertiary anhydrite molds became partially filled by calcitic, gravitational, microstalactitic cement (G). Arrow indicates orientation; d = 56m.

D BHP-67-68; porous dolostone. Coarse neomorphic dolomitization of matrix. Small intercrystalline voids and tertiary anhydrite molds (note stairstep outlines) are preserved. Small microstalactites of calcitic gravitational cement (G) partially occlude porosity in large voids. Vertical orientation is indicated by arrow; d = 56m.

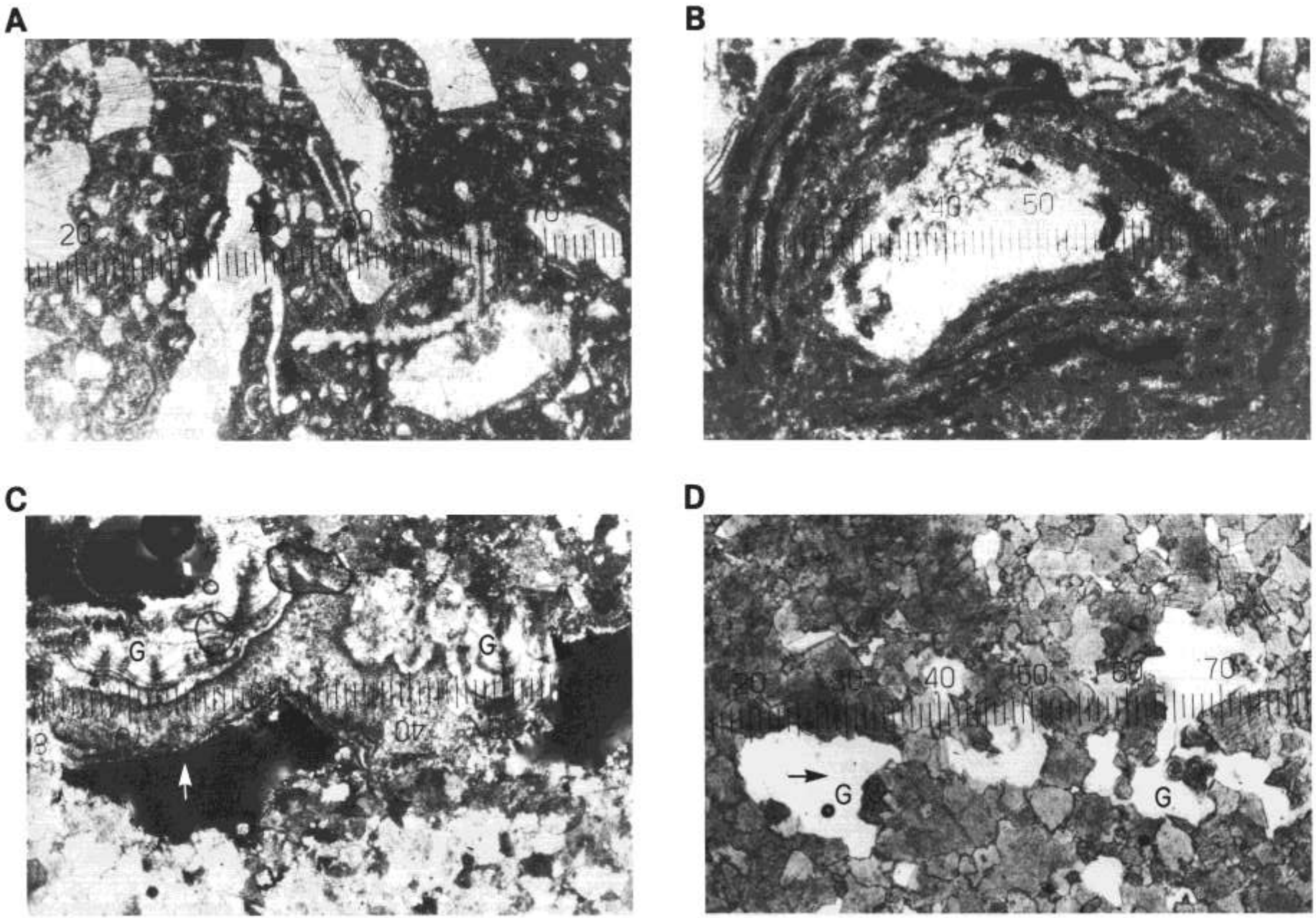
A
B
C
D
G
G
G
G

PLATE 5

Depositional and diagenetic features and porosity relationships in upper Horquilla dolostones (A, B, C) and limestone (D).

A BHP-67-22; porous dolostone. Coarse to very coarse neomorphic dolomitization of matrix. Relatively large, tertiary anhydrite mold has been partially filled by botryoidal, calcitic gravitational cement (G). Vertical orientation is indicated by arrow; d = 56m.

B BHP-67-10; porous dolostone. Medium neomorphic dolomitization of matrix. Compromise boundaries of adjacent dolomite crystals have occluded most of the intercrystalline porosity. Preserved porosity consists of relatively large, tertiary anhydrite molds (note stairstep outlines) and small intercrystalline voids; d = 56m.

C BHP-65-22; porous dolostone. Coarse neomorphic dolomitization of matrix. Small intercrystalline voids and relatively large, tertiary anhydrite molds have been preserved. Anhydrite molds have been partially filled by botryoidal, calcitic gravitational cement (G); d = 56m.

D BHP-64-1; oobiowackestone. *Tubiphytes* bioclasts are transected by tiny nontectonic fractures, which in turn were cut by a larger fracture that became enlarged into a solution channel. Ooids were dissolved to form molds. All voids were filled by sparry-calcite cement; d = 90m.

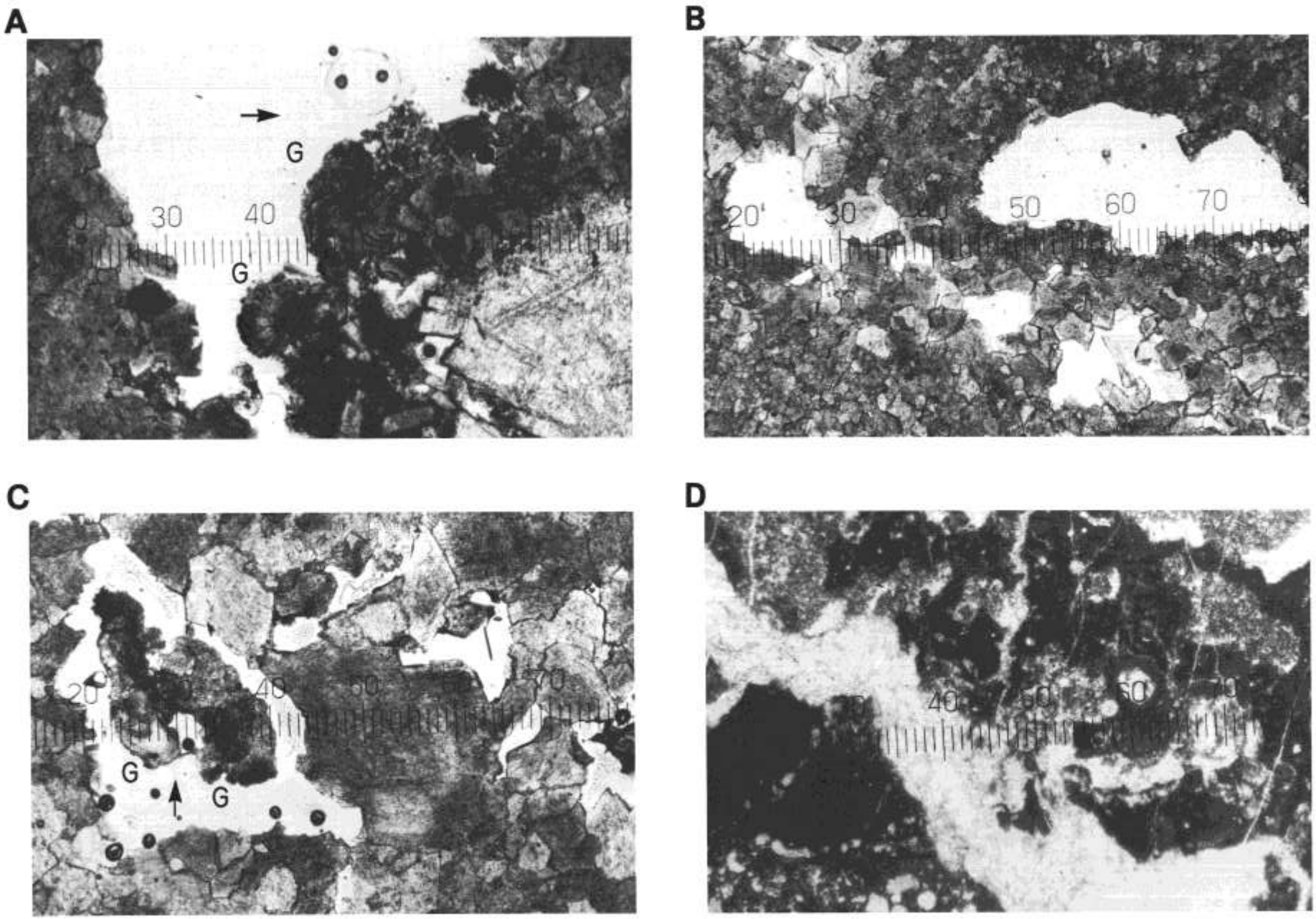
A
G
30
40
G
B
20
30
50
60
70
C
G
G
D

PLATE 6

Depositional and diagenetic features and porosity relationships in upper Horquilla dolostone (A) and limestones (B, C, D).

A BHP-63-2; porous dolostone. Coarse to very coarse neomorphic dolomitization of matrix. Relatively large, tertiary anhydrite mold has been partially filled by botryoidal, calcitic gravitational cement **(G).** Vertical orientation is indicated by arrow; d = 56m.

B BHP-62-5; biowackestone. Both matrix and fusulinid have been transected by a stylolite (St). Dolomitization has occurred along the stylolite seam, and dead oil **(DO)** is present; d = 56m.

C BHP-61-2; biopelwackestone. Several tertiary (third-stage) molds of anhydrite porphyroblasts **(A)** with stairstep outlines became filled by blocky-equant calcite cement; d = 56m.

D BHP-60-2; biopackstone. Most bryozoans **(Br)** have been intensively micritized. Many monocrystalline crinozoan components have syntaxial rims of recrystallization around them; note cleavage continuity. Several crinozoan components have been partially replaced by silica (white); d = 90m.

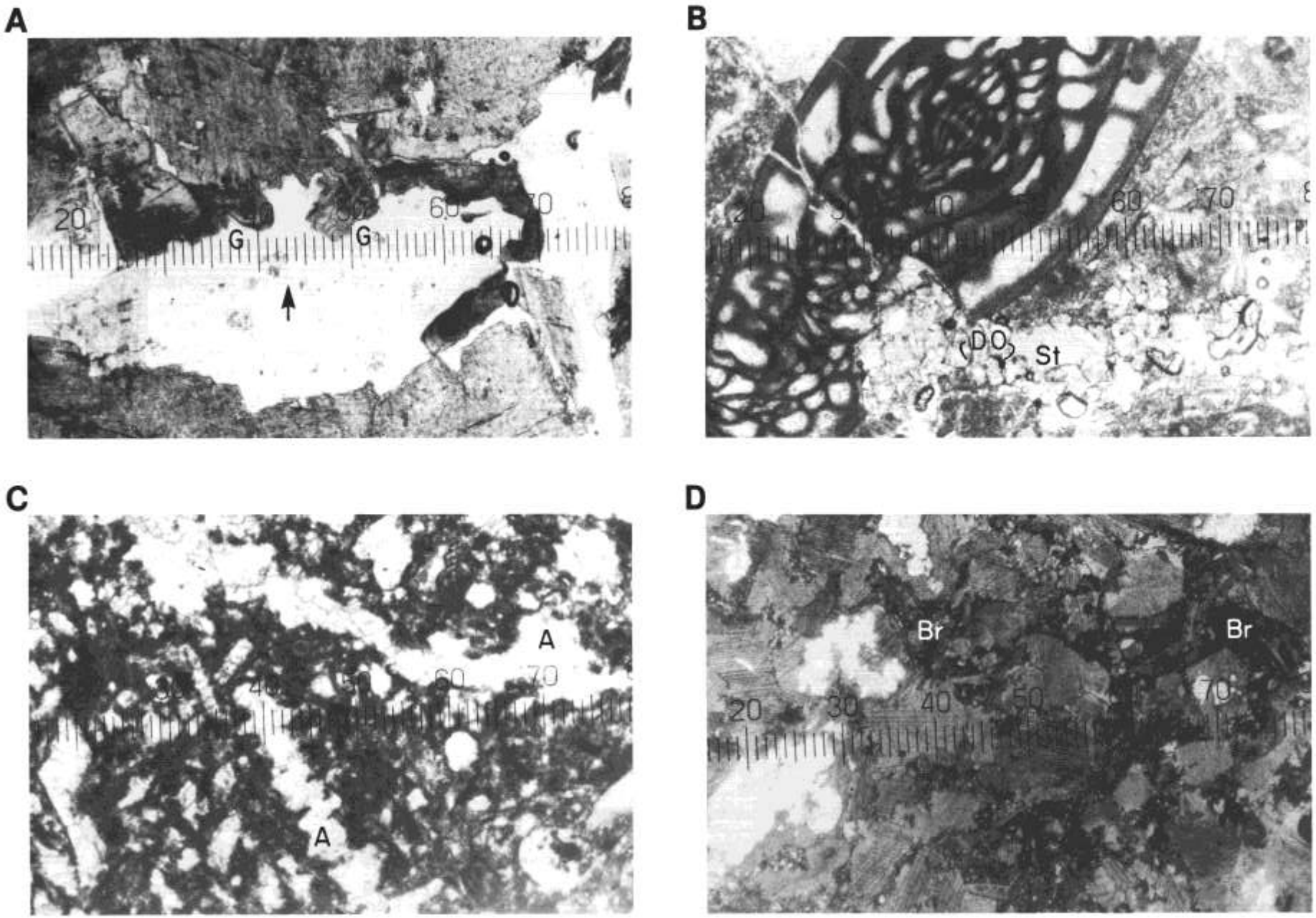
A
G
G
B
DO
St
C
A
A
D
Br
Br

PLATE 7

Depositional and diagenetic features and porosity relationships in upper Horquilla limestones (A, B) and dolostones (C, D).

A BHP-59-1; biowackestone. Matrix has been recrystallized to microspar and pseudospar. Micritized bioclasts (dark) have not been recrystallized; d = 32m.

B BHP-58-1; biowackestone. Aragonitic phylloid-algal bioclasts were dissolved by fresh ground water, and molds became filled by drusy, blocky-equant, meteoric calcite cement. Some recrystallization of matrix. Crossed polarizers; d = 90m.

C BHP-56-92; porous dolostone. Coarse neomorphic dolomitization of matrix. Compromise boundaries of adjacent dolomite crystals have occluded most of the intercrystalline porosity, but part has been preserved; d = 56m.

D BHP-56-7; porous dolostone. Coarse neomorphic dolomitization of matrix. Monocrystalline crinozoan columnal was paramorphically dolomitized and subsequently was replaced partially by anhydrite. Dissolution by fresh ground waters formed a tertiary anhydrite mold **(A),** which has been preserved. Crossed polarizers; d = 32m.

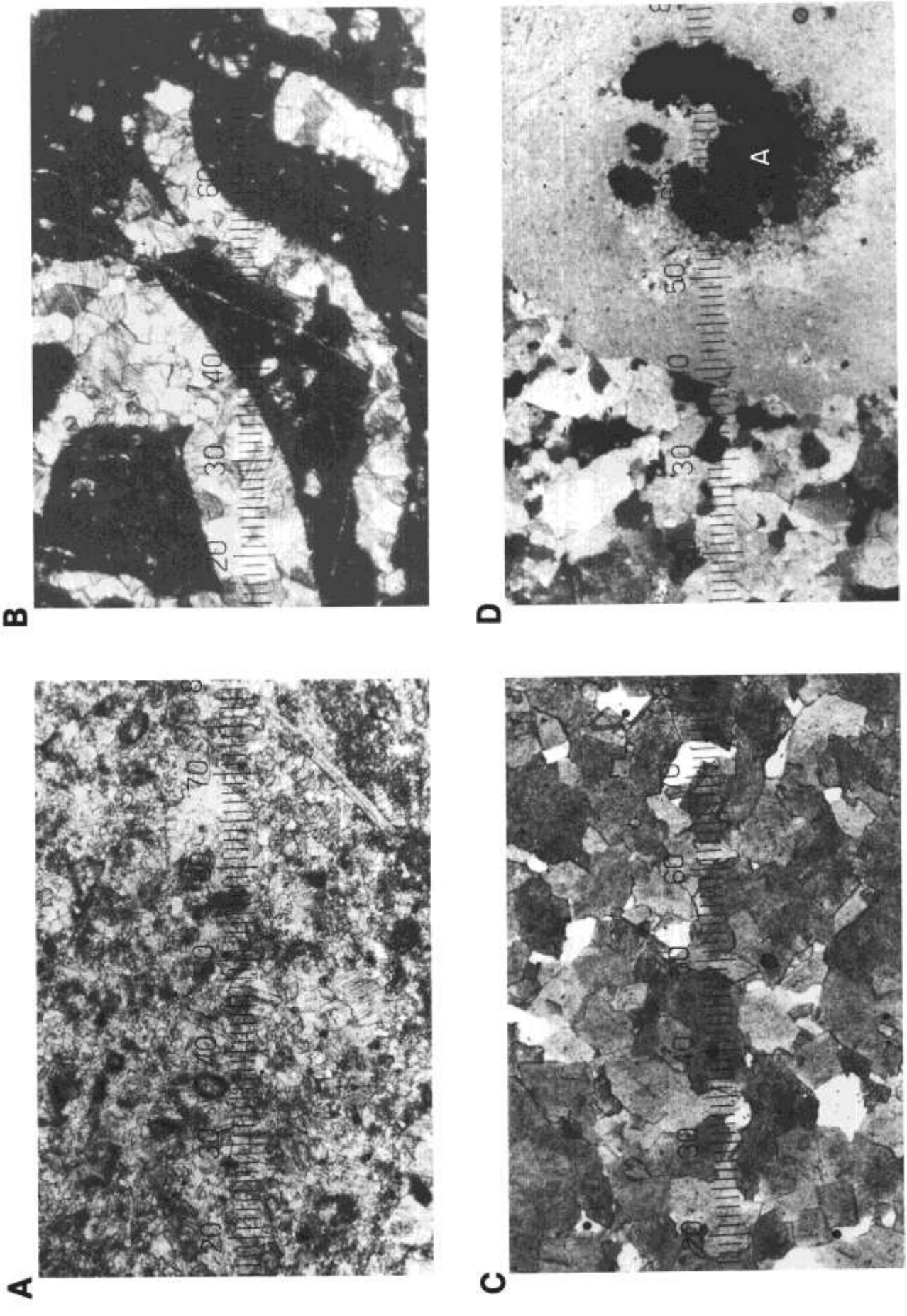
A
B
C
D
A

PLATE 8

Depositional and diagenetic features of upper Horquilla limestones (A, B, C) and chert (D).

A BHP-54-96; red, micritic, distinctly layered, vadose internal sediment. The carbonate was dolomitized then partially replaced by anhydrite. Quartz porphyroblasts (white) were emplaced in the anhydrite and contain anhydrite inclusions. Many tiny pyrite porphyroblasts were emplaced. Later, anhydrite and dolomite were both replaced by calcite, and some recrystallization of calcite took place. The red coloration results from oxidation of the abundant pyrite porphyroblasts to hematite; d = 90m.

B BHP-54-2; biopelwackestone. Aragonitic shells were dissolved and nontectonic fractures were formed; subsequently, the fractures became filled by zoned ferroan- and nonferroan-calcite cement **(Z)** in a blocky-equant mosaic. Recrystallization of matrix; d = 56m.

C BHP-53-1; biowackestone. Nontectonic fracture (F) transects matrix and a crinozoan columnal. Where the fracture cuts the matrix, it is filled by a mosaic of equant calcite crystals. Within the crinozoan columnal, the fracture is filled by epitaxial cement **(E),** which is optically continuous with the monocrystal; note twin-plane continuity. Crossed polarizers; d = 56m.

D BHP-52-3; chert. Micrite matrix has been replaced by microquartz. Bryozoan has been replaced by length-fast chalcedony (chalcedonite). Bryozoan zooecia (chambers) were lined by rhombic-dolomite crystals (dark gray), which were subsequently dedolomitized. Later, zooecia were completely filled by chalcedonite cement (white). The microquartz matrix contains abundant dolomite porphyroblasts, which were not dedolomitized. Crossed polarizers; d = 56m.

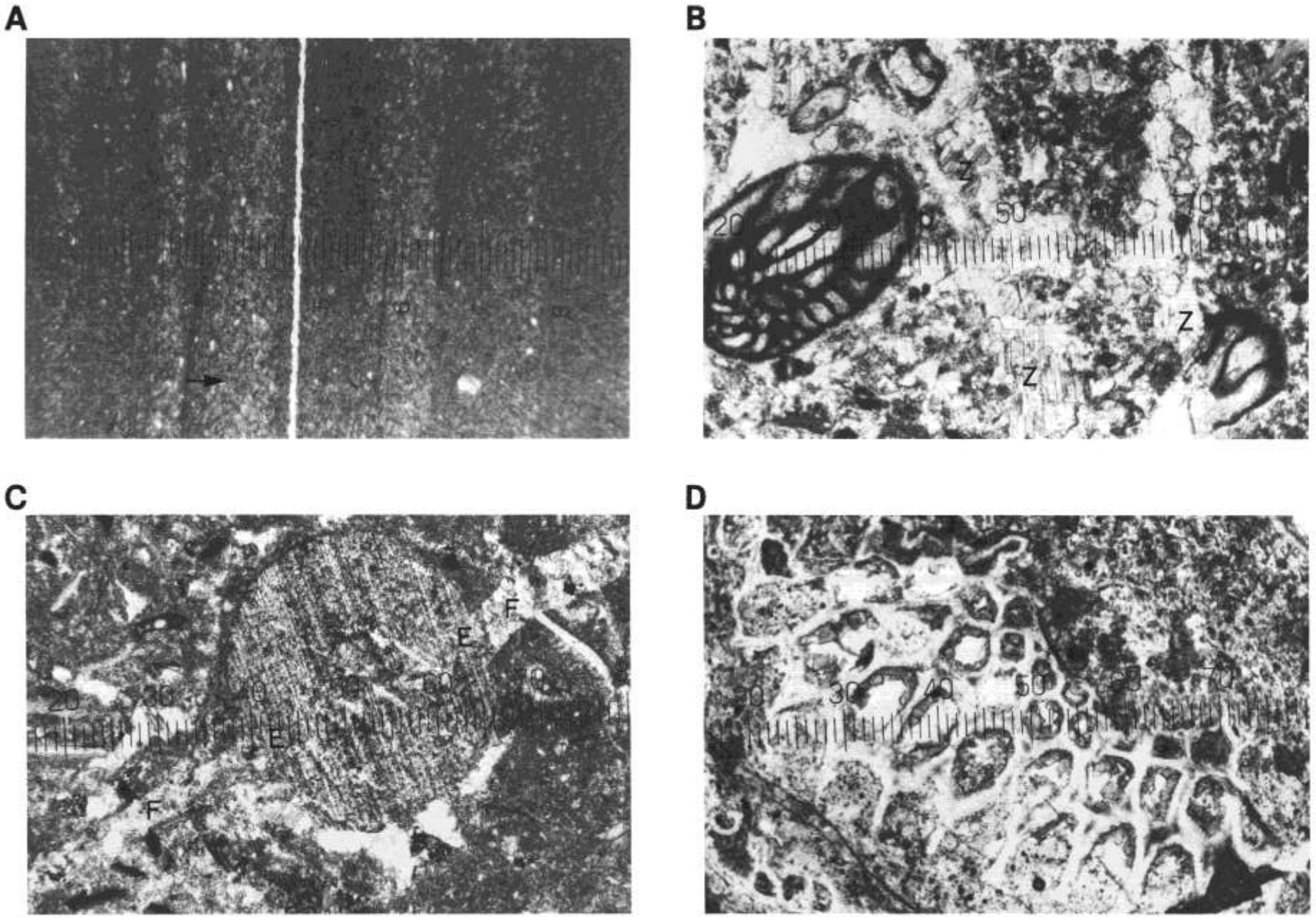
A
B
C
D
Z
Z
Z
F
E
E
F

PLATE 9

Depositional and diagenetic features and porosity relationships in upper Horquilla limestones (A, B) and dolostones (C, D).

A BHP-51-2; biowackestone. Phylloid algae and pelecypod bioclasts were dissolved, and molds became filled by drusy calcite cement (light); d = 90m.

B BHP-50-1; biopelwackestone. During fresh-water diagenesis, hollow micrite envelopes were formed, and the former micrite matrix became highly recrystallized. The hollow envelopes later became filled by sparry-calcite cement. Notice that micrite envelopes and micritized bioclasts were not recrystallized. Most crinozoan columnals (C) have recrystallized syntaxial rims (S) (surrounding matrix is now optically continuous with monocrystals), which are commonly marked by continuity of cleavage and twin planes; d = 42m.

C BHP-49-45; porous dolostone. Fine to very coarse neomorphic dolomitization of matrix. Preserved porosity consists of small intercrystalline voids and larger anhydrite molds (white); d = 90m.

D BHP-49-30; porous dolostone. Fine to extremely coarse neomorphic dolomitization of matrix. Preserved porosity includes tiny intercrystalline voids and larger anhydrite molds. Calcitic, microstalactitic gravitational (dripstone) cement (G) occurs in two anhydrite molds. Vertical orientation is indicated by arrow; d = 42m.

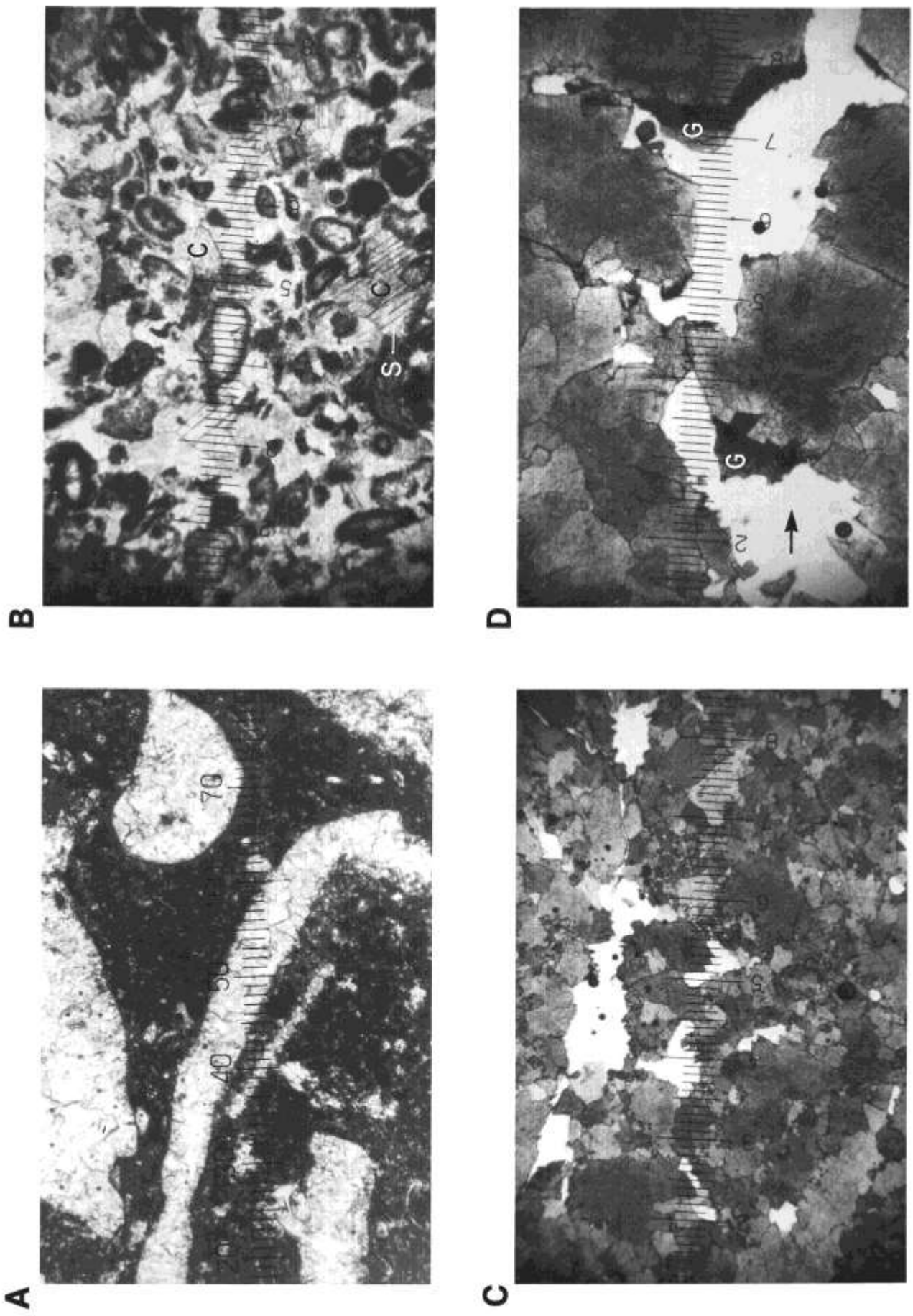
A
B
C
D
C
S
G
G

PLATE 10

Depositional and diagenetic features and porosity relationships in upper Horquilla dolostones (A, B, C, D).

A BHP-49-19; porous dolostone. Fine to very coarse neomorphic dolomitization of matrix. Preserved porosity consists of tiny intercrystalline voids and larger anhydrite molds. Both are interconnected by nontectonic fractures; d = 90m.

B BHP-49-14; slightly porous dolostone. Fine to very coarse neomorphic dolomitization of matrix. With the sutured boundaries of the crystals, the dolostone matrix appears to have been recrystallized to very coarse dolo-pseudospar crystals, which range up to 3.75 mm in diameter; d = 90m.

C BHP-49-4; porous dolostone. Fine to coarse neomorphic dolomitization of matrix. Preserved porosity consists of tiny intercrystalline voids and relatively large, tertiary anhydrite molds **(A).** Some calcitic gravitational cement **(G)** was precipitated in large voids. Vertical orientation is indicated by the arrow; d = 90m.

D BHP-49-1; porous dolostone. Fine to coarse neomorphic dolomitization of matrix. The central portion of a paramorphically dolomitized crinozoan columnal (C) was replaced by anhydrite. Later, the anhydrite was dissolved by fresh ground water, and botryoidal, calcitic gravitational cement **(G)** was precipitated on the upper portion of the tertiary mold. Vertical orientation is indicated by the arrow. Crossed polarizers; d = 90m.

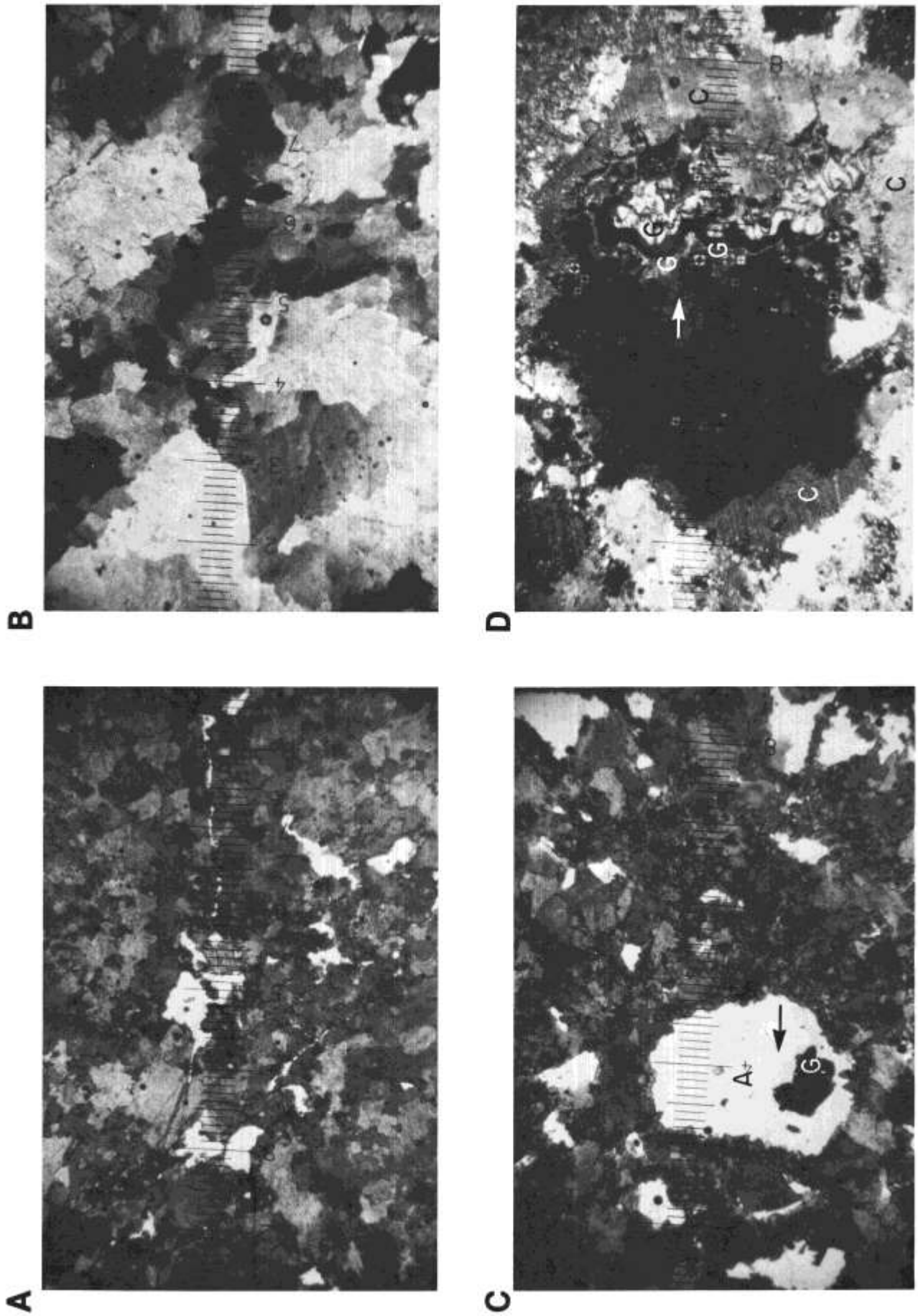
A
B
C
D

PLATE 11

Depositional and diagenetic features and porosity relationships in upper Horquilla dolostone (A), chert (B), and limestones (C, D).

A BHP-49-1; porous dolostone. More highly magnified view of gravitational cement shown in pl. 10D. Lower tip of calcitic dripstone cement has been paramorphically dolomitized **(P).** Crossed polarizers; d = 42m.

B BHP-47-2; chert. Micrite matrix has been replaced by microquartz. Many siliceous sponge spicules (S) have altered to chalcedonite. Two fractures **(F)** were filled by calcite cement. Crossed polarizers; d = 56m.

C BHP-46-17. The cyclostome bryozoan, *Fistulipora*, is illustrated. Zooecia are filled with drusy calcite cement; d = 56m.

D BHP-46-17. A tertiary anhydrite mold has been filled by blocky-equant calcite cement (light); d = 56m.

A

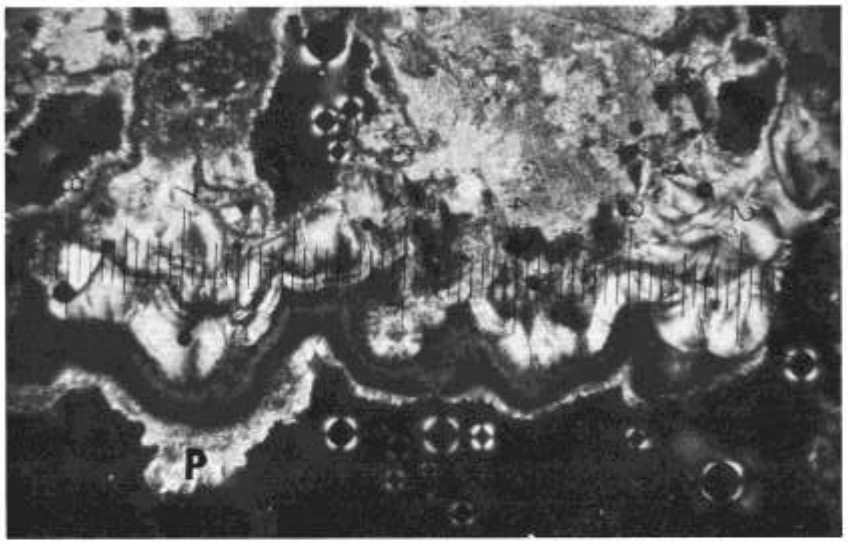

B

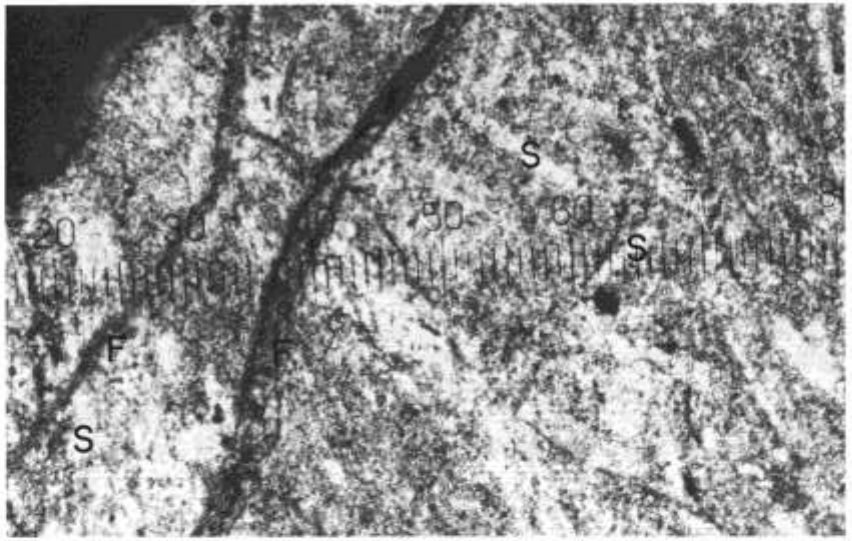

C

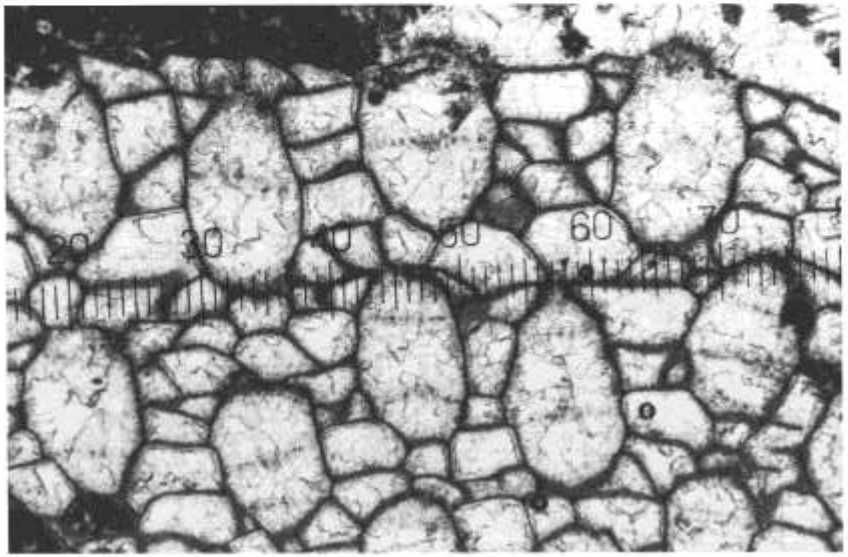

D

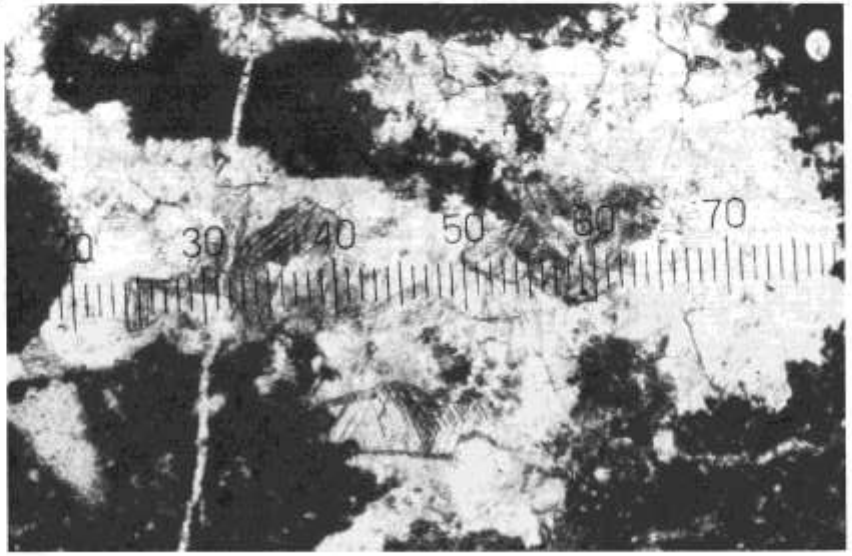

PLATE 12

Depositional and diagenetic features and porosity relationships in upper Horquilla dolostone (A) and limestones (B, C, D).

A BHP-46-5; porous dolostone. Very coarse neomorphic dolomitization of matrix. A relatively large, solution-enlarged horizontal fracture contains calcitic dripstone (gravitational) cement. Vertical orientation is indicated by arrow; d = 56m.

B BHP-46-1; limestone. Dolomite occurs in part as a replacement of anhydrite and as a cement filling anhydrite molds (A). Note stairstep outline of tertiary molds of anhydrite porphyroblasts; d = 56m.

C BHP-45-17; biopelwackestone. Stairstep anhydrite molds have been filled by dolomite cement (D); d = 32m.

D BHP-45-2; intrabiograpestone packstone. Aragonitic phylloid algae (P) were dissolved, and the molds were filled by sparry-calcite cement. Quartz porphyroblasts (white; some doubly terminated) partially replaced grapestone grains; d = 38m.

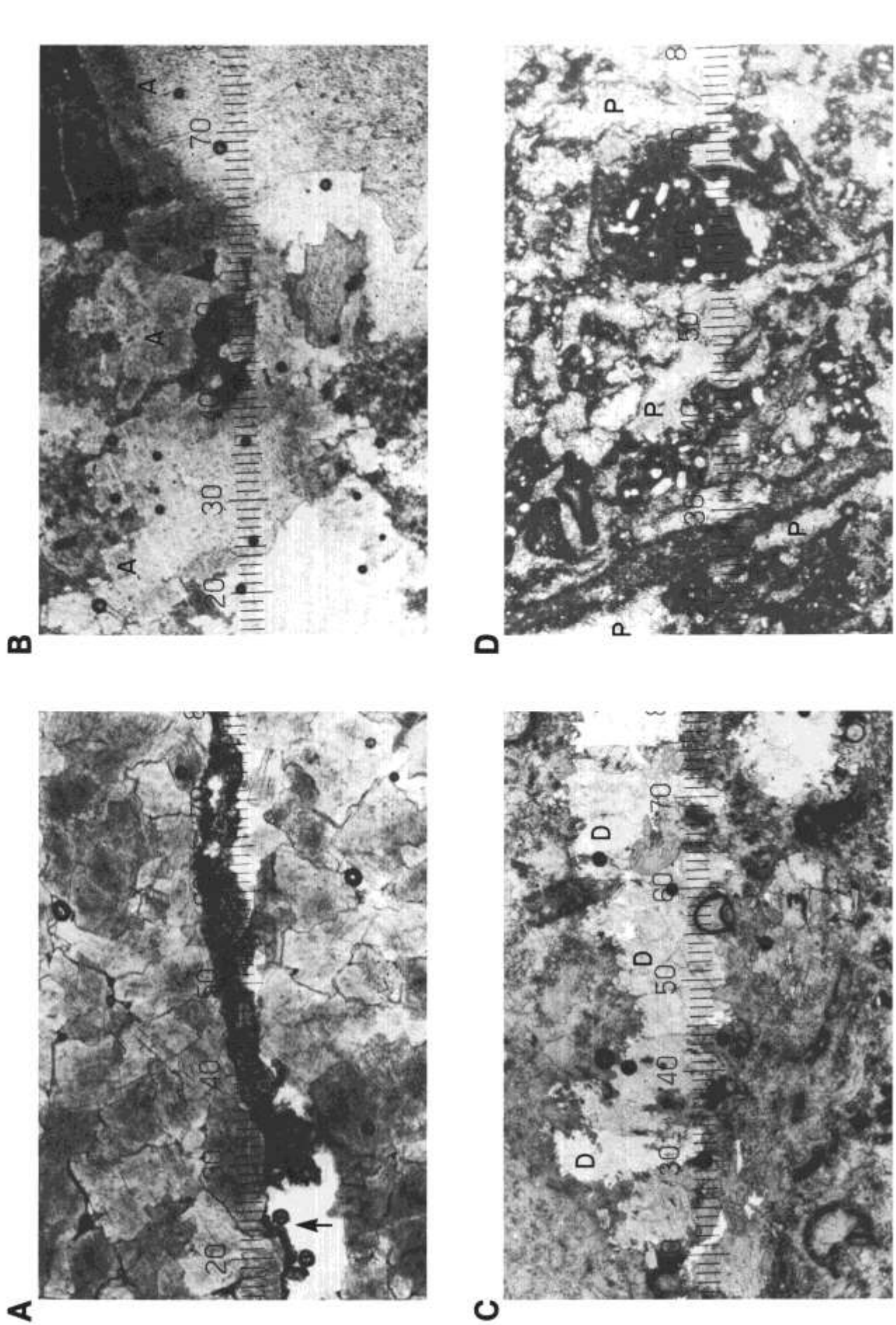
A
B
C
D
A
A
A
D
D
D
P
P
P
R

PLATE 13

Depositional and diagenetic features of upper Horquilla limestone (A), lower Horquilla limestones (C, D), and chert (B).

A BHP-45-1; limestone. A large anhydrite porphyroblast was partially replaced by calcite (C). The remainder of the anhydrite was dissolved, and the tertiary mold was filled by dolomite cement (D); d = 32m.

B BHP-39-4; chert. A Komia-crinozoan-bryozoan grainstone was replaced by silica (chalcedonite). Primary voids were lined by chalcedonite (C) and completely filled by drusy quartz (Dr). Many crinozoan columnals were centripetally replaced by silica, and the remainder was paramorphically dolomitized (P); d = 38m.

C BHP-39-1; oobiograinstone. Relatively large bioclasts represent the alga (or stromatoporoid?), *Komia* (K); d = 90m.

D BHP-38-0; biograinstone. Large aureoles of epitaxial cement (E) were precipitated as optically continuous overgrowths of monocrystalline crinozoan components (Cr). Note cleavage continuity. After cementation, some crinozoan columnals and epitaxial cement were replaced by silica (white); d = 42m.

A

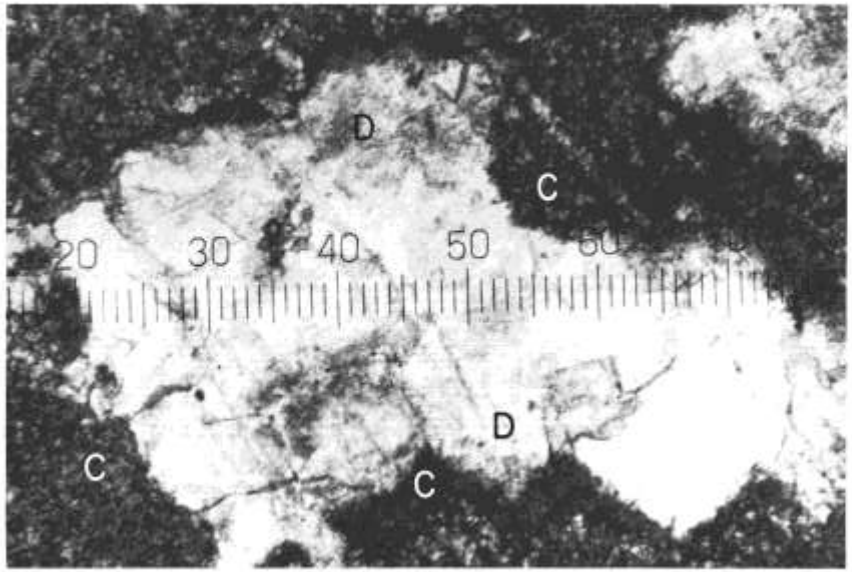
D
C
20
30
40
50
60
D
C
C

B

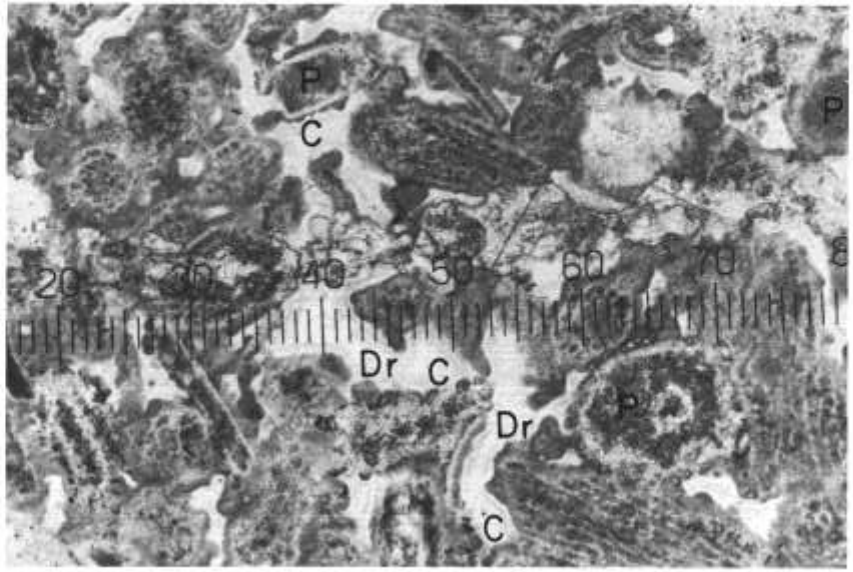
P
C
P
20
30
40
50
60
70
Dr
C
Dr
P
C

C

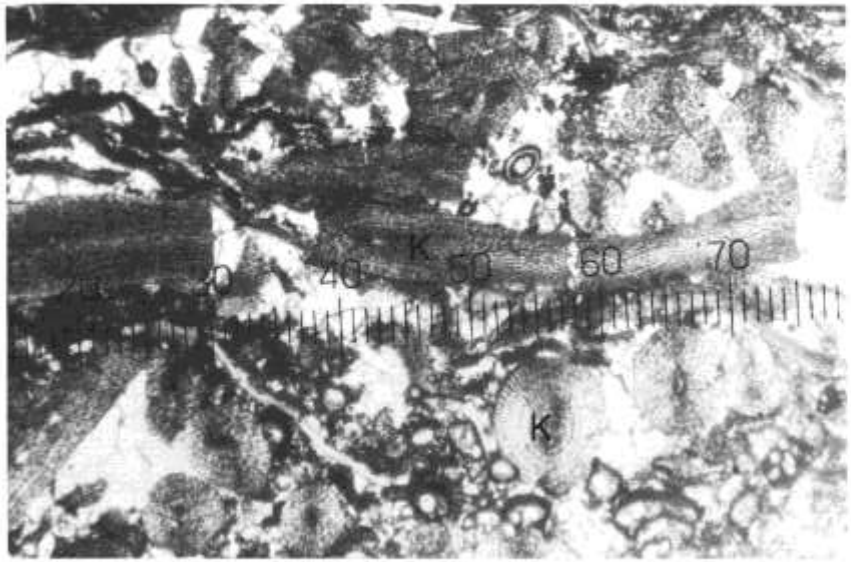
K
40
50
60
70
K

D

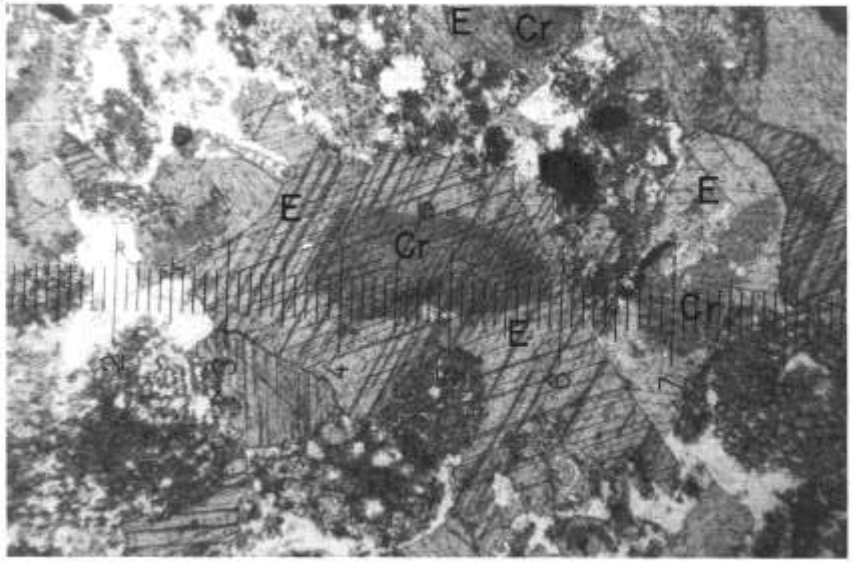
E
Cr
E
E
Cr
E
Cr

PLATE 14

Depositional and diagenetic features of lower Horquilla cherts (A, B, C, D).

A BHP-36-4. Micrite matrix was replaced by microquartz that is studded with dolomite porphyroblasts. Exsolution of dolomite rhombs occurred during silicification. The fusulinid was replaced by chalcedonite. Fusulinid chambers were lined by crusts of rhombic-dolomite crystals and were filled by chalcedonite; d = 38m.

B BHP-33-7. Former micrite matrix was replaced by microquartz **(M).** A calcitic crinozoan component was largely replaced by a rhombic-crystal mosaic of dolomite crystals **(D,** to right), which are syntaxial (exhibit single-crystal extinction) with the unreplaced monocrystal (C). The outer periphery contains a crust of rhombic-dolomite crystals (white **D,** to left), which are also syntaxial with the unreplaced calcite monocrystal **(C).** Crossed polarizers; d = 38m.

C BHP-33-7. Crinozoan components **(Cr)** are surrounded by aureoles of discrete dolomite crystals **(D),** which are syntaxial with the calcitic monocrystals and were exsolved during silicification; d = 38m.

D BHP-33-7. Fusulinid has been replaced by chalcedonite, which also fills chambers. Fusulinid chambers are coated by rhombic-dolomite crystals, which subsequently became dedolomitized. Many dolomite porphyroblasts in the chert matrix have also been dedolomitized; d = 38m.

A

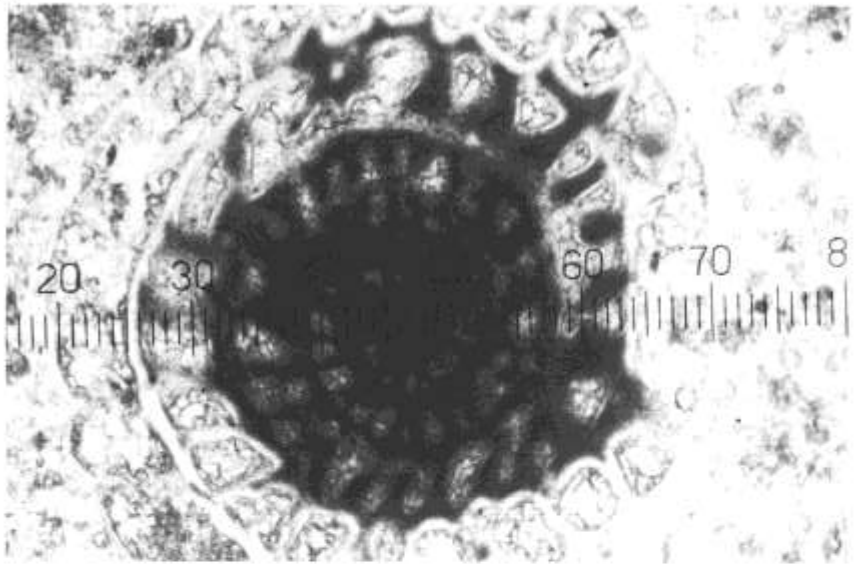

B

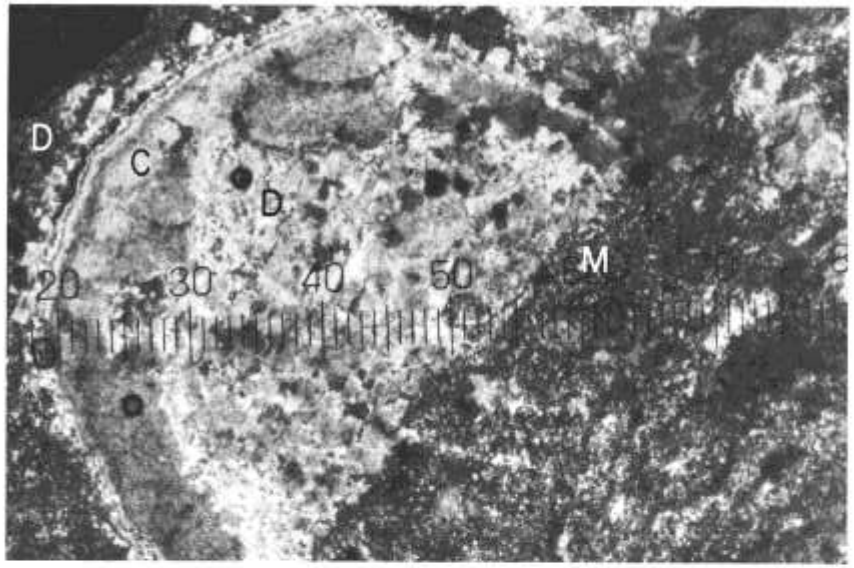

C

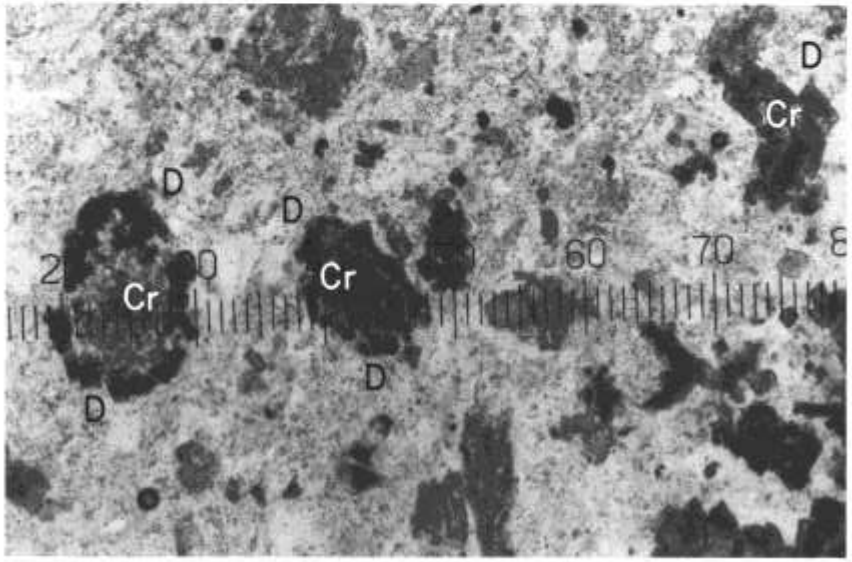

D

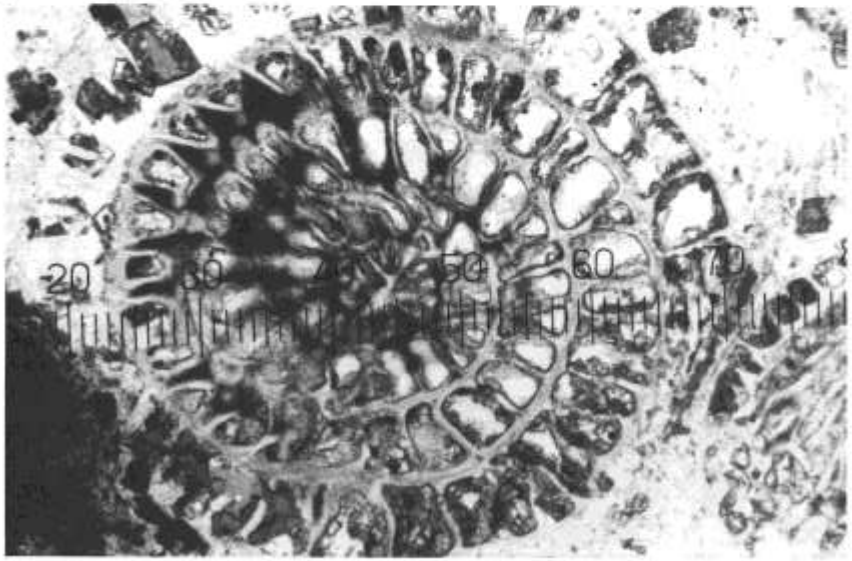

PLATE 15

Depositional and diagenetic features of lower Horquilla limestones (A, C) and cherts (B, D).

A BHP-33-6; biograinstone. Crinozoans (Cr), fusulinids (F), and bryozoan bioclasts **(Br)** are abundantly represented. Some crinozoans have been partially silicified (S); d = 90m.

B BHP-31-15; chert. Large, rhombic-dolomite porphyroblasts exsolved during silicification, and they transect siliceous sponge spicules (S). Siliceous spicules extend from the chert matrix into the dolomite crystals where they appear as light-colored ghosts; d = 38m.

C BHP-30-0; biopelpackstone. Aragonitic pelecypod shells were dissolved, and molds became filled by drusy calcite cement; d = 90m.

D BHP-29-3; chert. Siliceous sponge spicules are abundantly represented, and many have been replaced by calcite (C). The chert matrix contains many dolomite porphyroblasts, which exsolved from the carbonate during silicification; d = 38m.

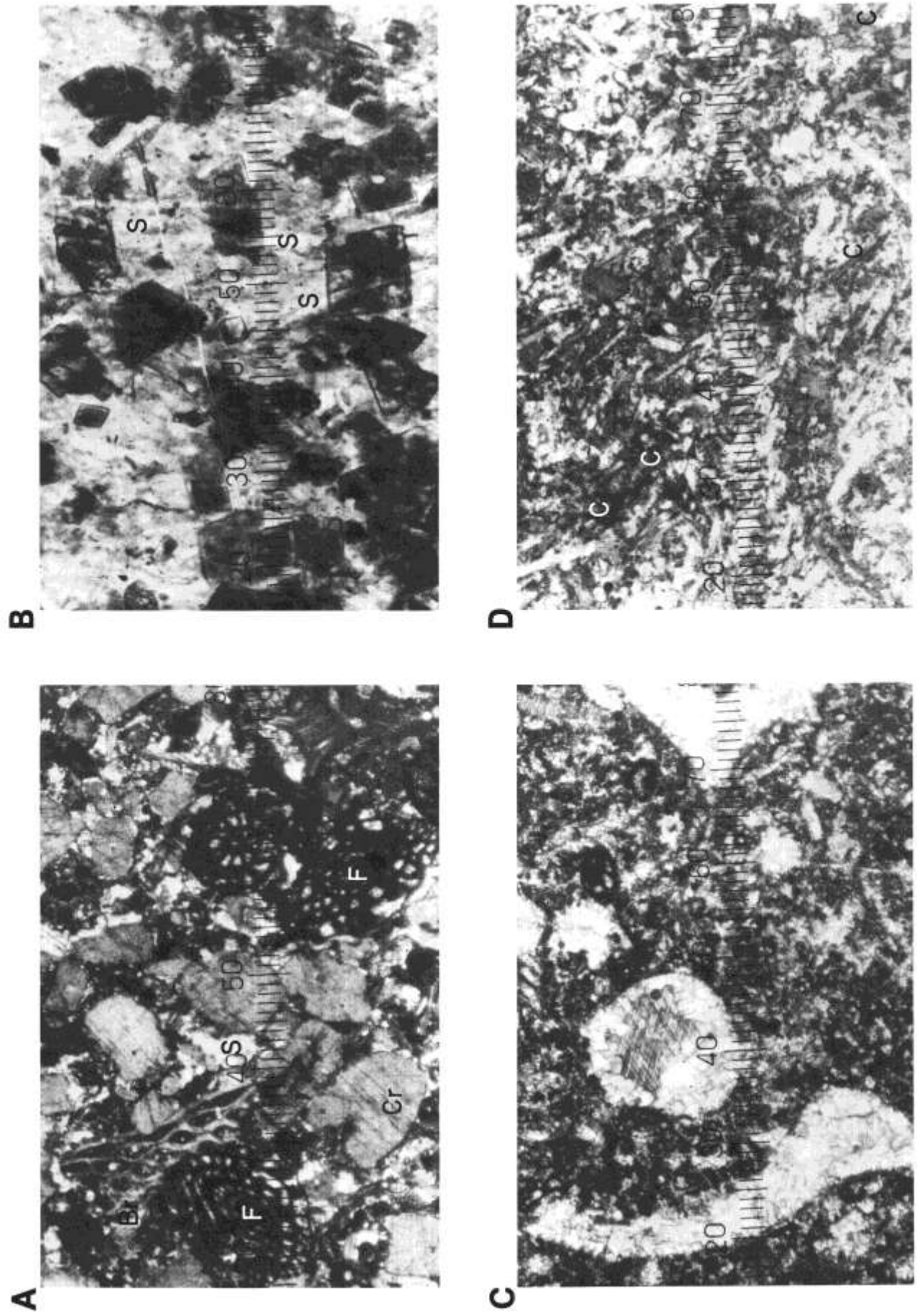
A
B
C
D
F
Cr
S
C

PLATE 16

Depositional and diagenetic features of lower Horquilla limestones (A, C) and cherts (B, D).

A BHP-24-1; Komia-crinozoan-bryozoan grainstone. The largest skeletal grains represent longitudinal and transverse cross sections through the alga (or stromatoporoid?), *Komia.* Notice that in transverse cross sections *Komia* exhibits circular outlines with concentric structures that closely resemble ooids; d = 90m.

B BHP-19-4b; chert. Microquartz matrix contains abundant rhombic-dolomite porphyroblasts, which later became paramorphically replaced by calcite (dedolomitized); d = 56m.

C BHP-18-0; oobiograinstone. Ooids, crinozoans, and bryozoans predominate. Most bryozoans were micritized. Aragonitic pelecypod shells **(P)** were dissolved, and molds were filled by sparry-calcite cement. One crinozoan component (upper right) became silicified (S); d = 90m.

D BHP-16-10; chert. Fusulinids and bryozoans were replaced by chalcedonite. The original micrite matrix was replaced by microquartz. Dolomite porphyroblasts, which were exsolved during silicification, became dedolomitized (De); d = 56m.

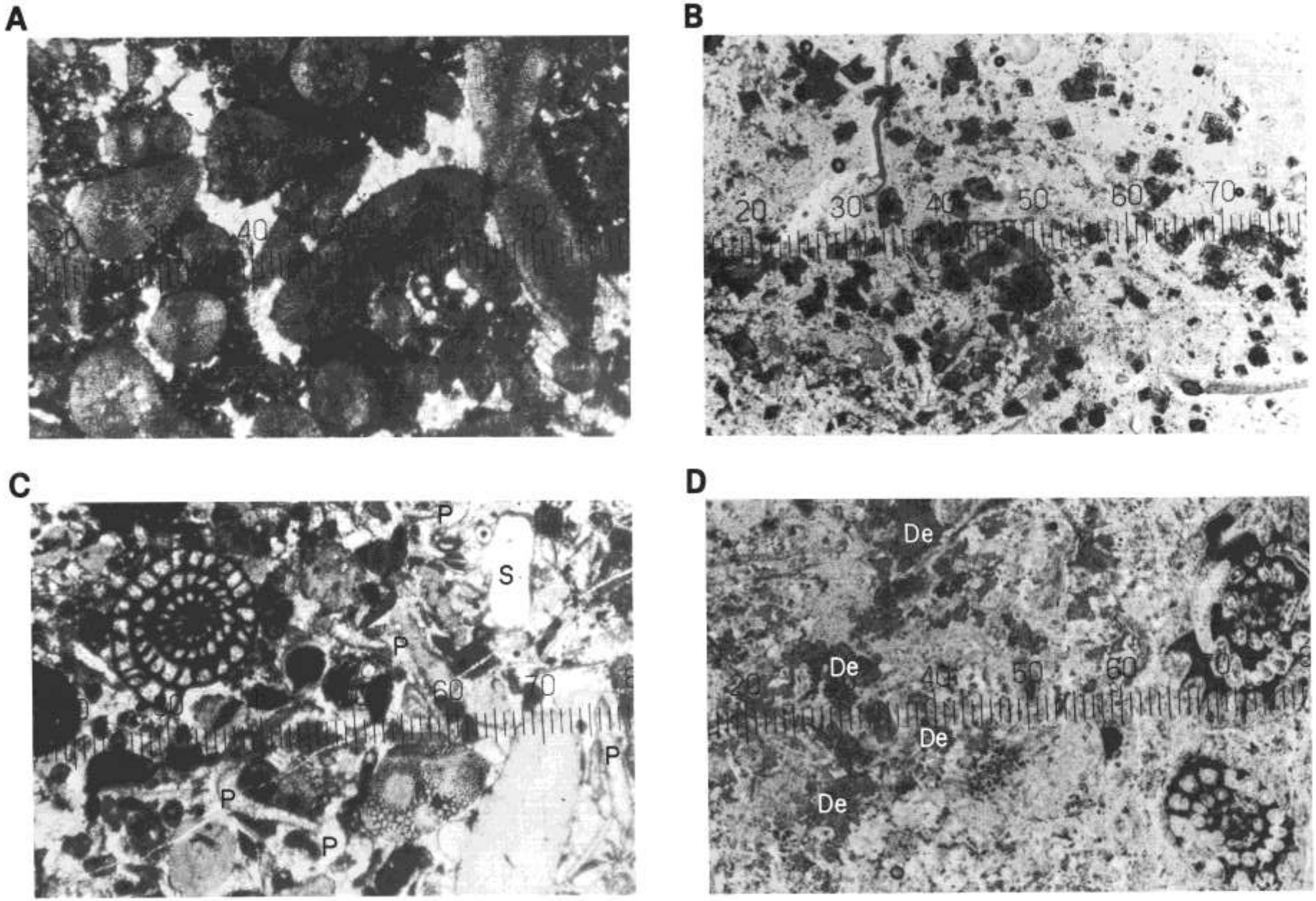
A
B
C
D
P
S
De

PLATE 17

Depositional and diagenetic features of lower Horquilla cherts (A, D) and limestones **(B,** C).

A BHP-13-35; zebra chert. The banding represents alternating layers of chert (Ch) and calcite-rich chert **(CaCh).** The calcite has replaced dolomite and is dedolomite; in some layers, dedolomite predominates over chert. Vertical orientation is indicated by arrow. Crossed polarizers; d = 90 m.

B BHP-12-1; biopackstone. Most bryozoan bioclasts **(Br)** have been intensively micritized. Aragonitic pelecypod shells **(P)** were dissolved, and molds became filled by sparry-calcite cement; d = 90m.

C BHP-9-5; oobiograinstone. Many bioclasts are enveloped by superficial oolitic coatings. Epitaxial cement occurs on monocrystalline crinozoan components, which lack superficial oolitic coatings. Silicification of shells; d = 32 m.

D BHP-8-1b; chert. The original matrix was replaced by microquartz (dark). In center of field, the outer portion of a crinozoan columnal has been replaced by megaquartz (coarsely crystalline quartz). Crossed polarizers; d = 12m.

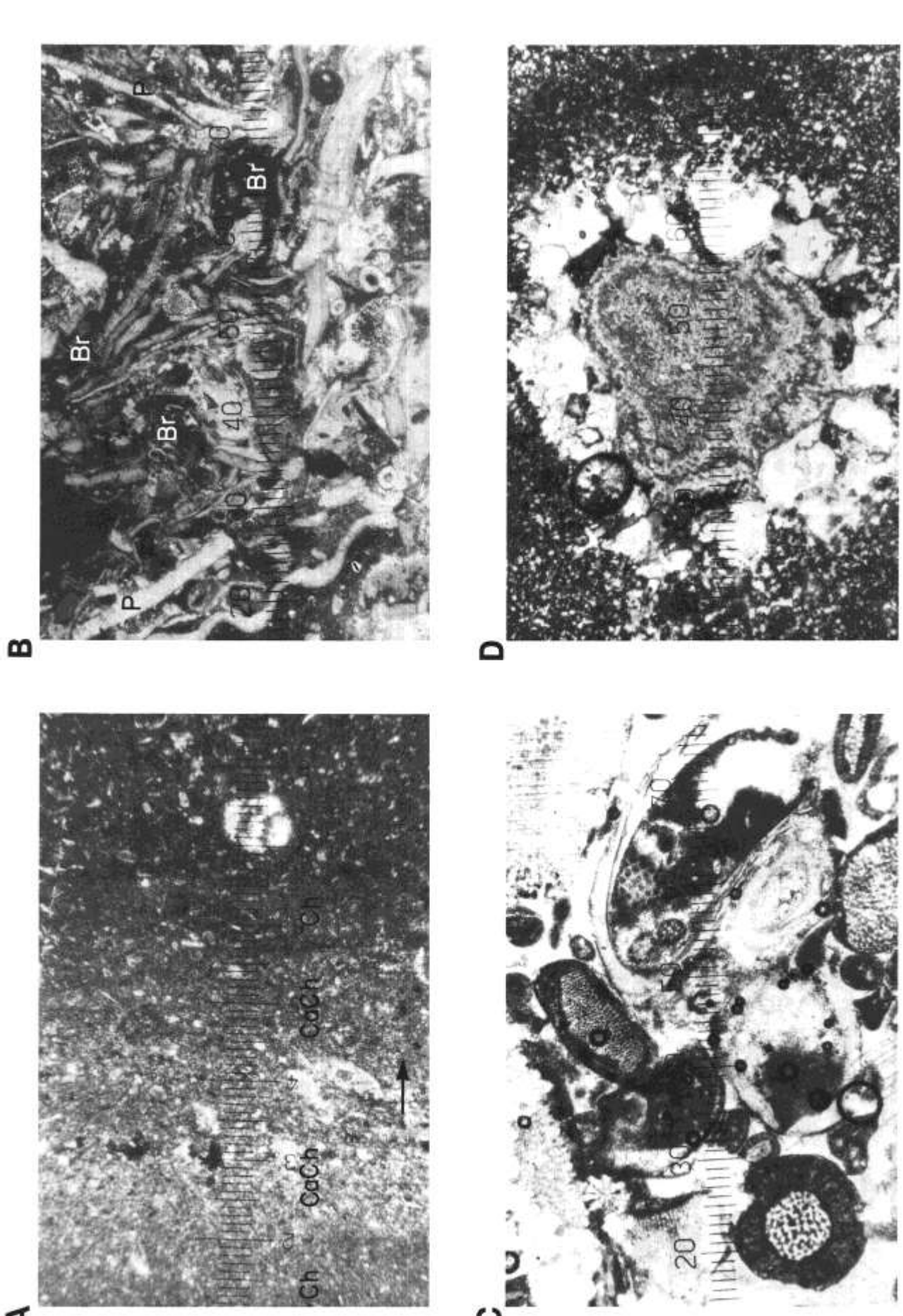
A
B
C
D
Ch
CaCh
Br
P
20
30
40
50

PLATE 18

Depositional and diagenetic features of lower Horquilla cherts (A, B, C) and limestone (D).

A BHP-8-1b; chert. The concentric internal structure of an ooid has been preserved after the carbonate grain was replaced by silica (chalcedonite); d = 12m.

B BHP-8-1b; chert. Ferroan-calcite cement (dark) filled a fracture and replaced the matrix outward from the fracture. The microquartz matrix contains countless tiny porphyroblasts of dedolomite and ferroan dedolomite (small dark rhombs); d = 56m.

C BHP-6-1b; chert. Original dolomite porphyroblasts have been replaced by ferroan calcite (ferroan dedolomite); d = 12m.

D BHP-5-0; oobiograinstone. Micrite envelopes were formed around most bioclasts. Micritic, vadose internal sediment (I) was deposited in many voids. Vertical orientation is indicated by arrow. Beachrock-cement rims formed around the bioclasts after the internal sediment was deposited. Aragonitic pelecypod shells were dissolved to form hollow micrite envelopes, which, along with primary voids, became filled by drusy calcite cement; d = 90m.

A

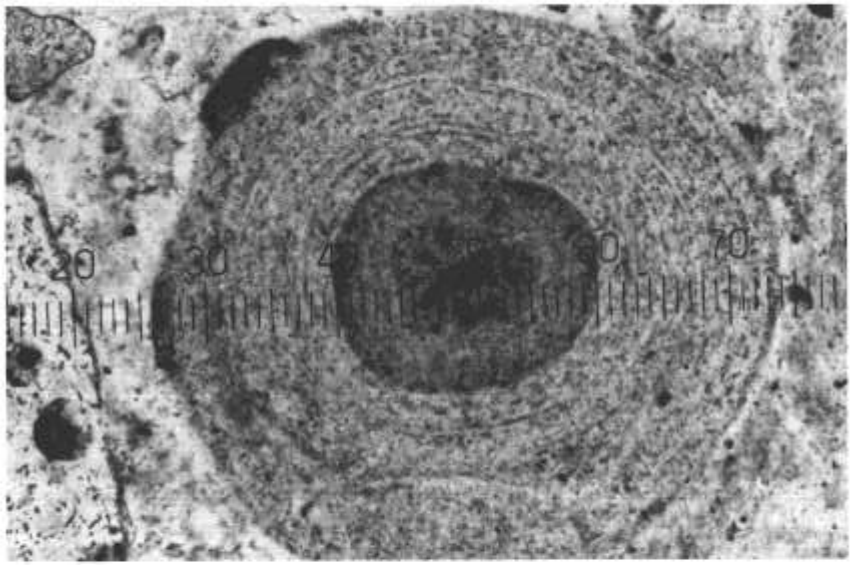

B

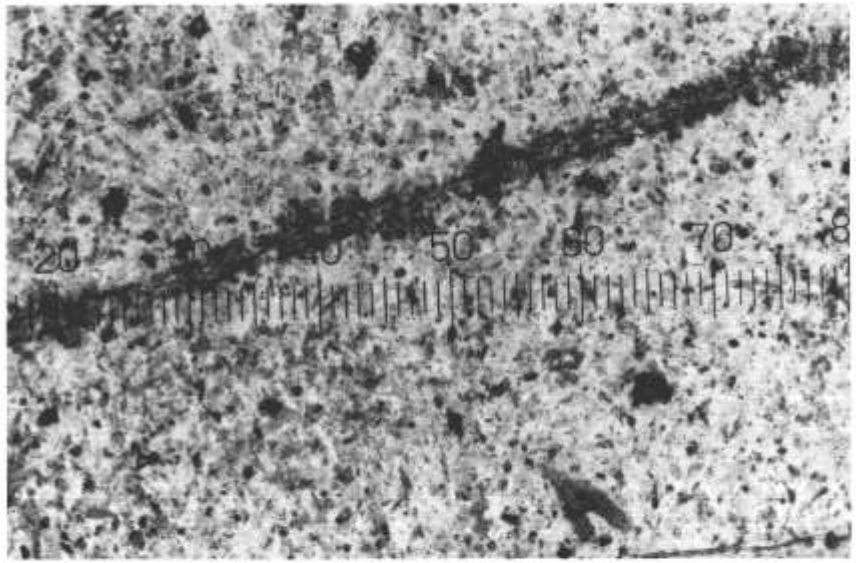

C

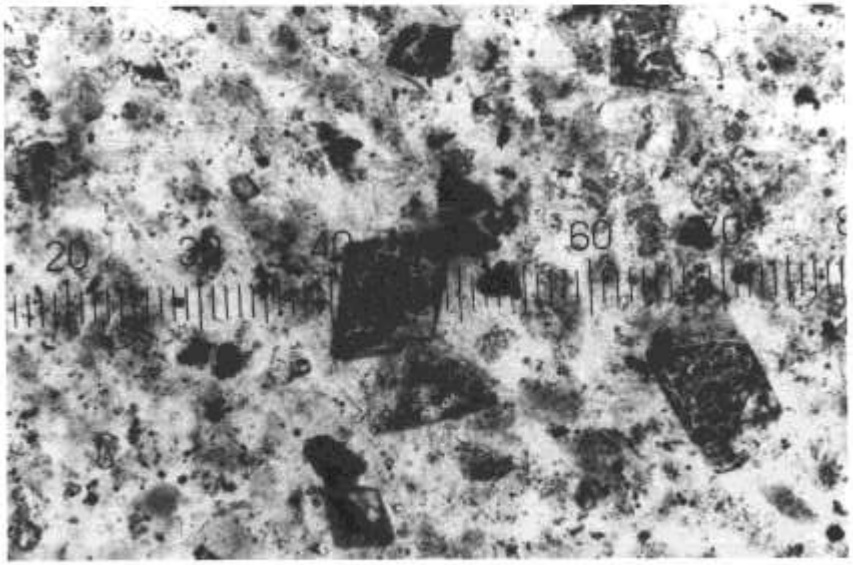

D

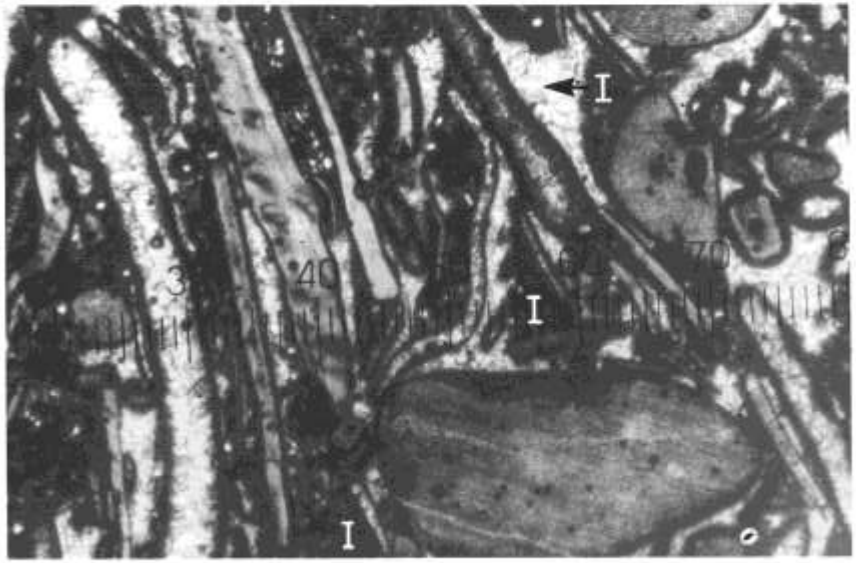

PLATE 19

Depositional and diagenetic features of Paradise (Mississippian) dolostone (A) and limestones (B, C, D).

A BHP-4-13; limy dolostone. The original aragonitic lime-mud matrix was dolomitized to a degree greater than 50 percent; subsequently, the remainder was calcitized as dolomitizing fluid was replaced by fresh ground water. The crinozoan brachial plate was not dolomitized; d = 32m.

B BHP-2-1; oobiograpestone grainstone. Ooids **(0)** exhibit a bimodal size distribution. The smallest grains average 64 microns, while the largest grains range up to 400 microns in diameter. A large grapestone grain **(Gp)** is seen in the upper right; d = 32m.

C BHP-2-0; sandy, silty oobiowackestone. Thick algal coatings (dark) formed around bryozoan bioclasts. Innumerable tiny pyrite porphyroblasts were emplaced within the algal coatings; these later became oxidized. Bryozoan zooecia became filled by ferroan-calcite cement; d = 90m.

D BHP-1-0; crinozoan-bryozoan grainstone. The bryozoans **(Br)** were intensively micritized. Micritic, vadose internal sediment **(I)** has been deposited within large primary voids; d = 90m.

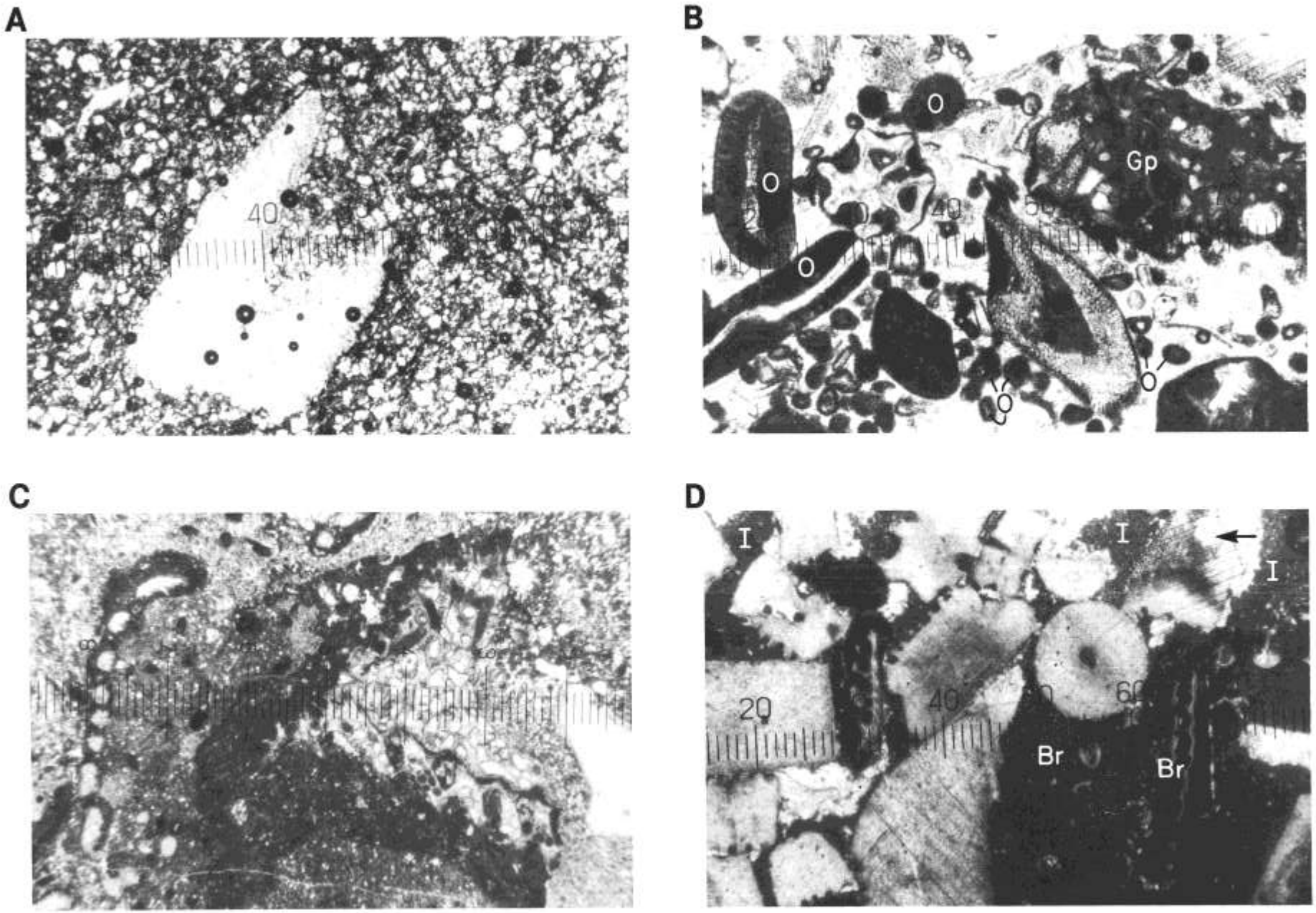
A
40
B
O
O
O
Gp
40
O
O
C
D
I
I
I
20
40
Br
Br

Petroleum geology

In addition to the general evaluation in the field given in the chapter on stratigraphy and more specific evaluation with thin sections given in the chapter on petrography, the petroleum source and reservoir rocks in the Big Hatchet Peak section were evaluated with commercial laboratory analyses of selected samples. Results are discussed in this chapter and are plotted with respect to the stratigraphic column in appendix 3.

Source rocks

Table 2 shows the determinations of percentage of organic carbon, type and amount of kerogen, and the thermal-alteration index on 11 samples that were made by P.J. Cernock and others at GeoChem Laboratories, Inc., Houston, Texas. These samples were selected from dark Horquilla limestones that appeared to have fair to good source ratings in the field and to represent source units of 50 ft or more in thickness. Several additional units with probable source potential were not sampled during this study.

At least six of the samples contain more than 0.3 percent organic carbon that is determined empirically to be the minimum amount in limestones to qualify as a source rock for petroleum (Tissot and Welte, 1978, p. 431; Hunt, 1979, p. 270). Kerogen analyses show that the organic matter was derived exclusively from land-plant material. Most of this material is of the degraded herbaceous type and lesser amounts are of the woody and coaly types.

Because no algal or amorphous kerogens were found, the source rocks probably did not generate much oil. Degraded (partially amorphous), herbaceous kerogen may have been a source for oil (A.B. Reaugh, GeoChem, personal communication, 1980); however, the woody and coaly types would have been sources for gas (Tissot and Welte, 1978, p. 433; Hunt, 1979, p. 274277).

Dominance of land-derived kerogens in these shallow-marine limestones is curious considering the exclusively marine biota described in the field and in the thin sections. The extremely fine land-plant material probably was derived from coastal or inland areas to the north or northwest, and the absence of sand or coarser terrigenous detritus suggests the possibility of light-to-moderate winds being the agent that transported these land-plant remains into the marine environment.

Absence of algal (or amorphous) kerogens is also curious considering the high percentages of algal remains in the limestones. In calcareous algae, the cortical layer is carbonate, but the vegetative material may have produced favorable kerogens. Several processes may account for the selective removal of algal kerogens. Within the original marine environment, algal vegetation is devoured near the beginning of the food chain. After shallow burial, burrowing organisms may feed preferentially on vegetative algal remains. Oxidation in the well-aereated shallow-marine environment and during fresh-water diagenesis of the limestones may have volatilized the algal kerogens (Hunt, 1979, p. 100-101; Cluff and others, 1980; and A.B. Reaugh, personal communication, 1980).

The thermal-alteration index, based on the color of the kerogens, ranges from 2 + to 4 — and generally is 3. Such strongly altered material indicates a paleotemperature of about 150°C (300°F) that is above the optimum for oil generation but is in the range of gas generation, possibly with condensate (Hunt, 1979, p. 324, table 7-10). Thus any oil generated by the degraded herbaceous kerogens is likely to have been altered to condensate or gas by cracking processes.

No plutonic rocks intrude the Paleozoic-Mesozoic sedimentary section of the Big Hatchet Mountains, in contrast to the Cretaceous-Tertiary intrusives that thermally metamorphosed the section locally in other ranges to the north and west. These slightly high paleotemperatures in the Big Hatchet Peak section probably are a result of burial beneath 15,000 ft or more of younger Permian and Lower Cretaceous rocks rather than a result of regional plutonic heating.

Deep-marine limestones and mudstones in the Alamo Hueco Basin to the south are considered to be the main source for petroleum that would have migrated updip into the porous dolostones of the outer-shelf margin. With the added source units below, between, and above the dolostones in the outer-shelf facies of the Big Hatchet Peak section, the probability of petroleum generation is even greater, especially for gas.

TABLE 2—PERCENTAGE OF ORGANIC CARBON, TYPE OF KEROGEN, AND THERMAL-ALTERATION INDEX OF SELECTED DARK LIMESTONES IN THE BIG HATCHET PEAK SECTION. **R** = repeat sample, **H** = herbaceous (degraded), **W** = woody, **C** = coaly, **P** = predominant (60–100 percent), **S** = secondary (20–40 percent), **T** = trace (1–20 percent); alteration index ranges from 1 to 5. Determinations by P.J. Cernock and others, GeoChem Laboratories, Inc., Houston, Texas. Sample notation indicates BHP unit number and footage above base of unit.

Sample notation (BHP-)	Organic carbon (percent of rock)	Kerogen type and amount			Thermal-alteration index
		P	S	T	
76-8	0.24, 0.13R	H	W	C	3
71-2	0.35	H	W-C	—	3 to 3+
68-4	0.53	H	W	C	3− to 3
66-9	0.48	H	—	W	3
52-2	0.15	H	W	—	3 to 3+
41-20	0.24, 0.14R	H	—	—	3 to 3+
31-10	0.28	—	H-W-C	—	3 to 3+
21-2	0.51	H	W	C	3 to 3+
15-2	0.54	H	—	W	2+ to 3−
10-3	0.71, 0.79R	H	W	—	3 to 3+
7-1	0.12	H	—	W	3+ to 4−

Reservoir rocks

Table 3 shows measurements of porosity and permeability on 13 samples from the upper Horquilla that were made by K.W. Andrews and others at Core Laboratories Inc., Dallas, Texas. Samples were selected from all six units of porous dolostones, which range in thickness from 54 to 148 ft. In the field, all the dolostones exhibit vuggy porosity, with individual vugs generally 1-3 cm in diameter in fresh rock and 10-20 cm on weathered surfaces. Vuggy porosity is estimated to range from a trace to 10 percent in most units and up to 30 percent in a few cases where the diameters of the vugs reach 10 cm.

TABLE 3—POROSITY AND PERMEABILITY DATA ON PLUGS OF SELECTED POROUS DOLOSTONES IN THE BIG HATCHET PEAK SECTION; measurements by K.W. Andrews and others, Core Laboratories, Inc., Dallas, Texas. Sample notation indicates BHP unit number and footage above base of unit.

Sample notation (BHP–)	Porosity percent	Permeability to air (millidarcies)
70–3	2.7	0.071
67–68	2.7	0.12
67–22	1.1	0.16
65–94	4.4	0.40
65–22	2.3	0.35
65–2	4.0	0.034
63–2	5.1	0.18
56–92	1.1	0.054
56–7	4.9	42
49–19	2.4	0.78
49–14	2.9	0.06
49–9	1.9	0.09
49–4	5.5	0.31

Sucrosic intercrystalline porosity is rarely seen, and matrix permeability appears to be generally low, judging by water-imbibition tests in the field.

Laboratory analyses were made on plugs 1 inch in diameter that were cut from the outcrop samples, so only matrix characteristics were evaluated. Porosities were determined using helium as the injection medium, and the percentages were calculated according to Boyle's law. The range from 1.1 to 5.5 percent is considered very poor to poor for matrix porosities (Levorsen, 1967, p. 102). Permeabilities were determined with air as the injection medium, and the values were calculated according to Darcy's law. Twelve samples showed a range from 0.034 to 0.78 millidarcies which is considered very poor to poor for matrix permeabilities (Levorsen, 1967, p. 105). The one good permeability of 42 millidarcies was measured on a plug that contained a solution channel. Better evaluations of whole reservoir quality (matrix and vuggy porosity) could have been made with larger samples, preferably with cores 5 inches in diameter and 10 inches long.

Petrographic analyses show that the dolomitization process continued until compromise boundaries were formed between adjacent dolomite crystals and that this process occluded most of the intercrystalline porosity in the dolostones. On the other hand, the following anhydritization process emplaced large porphyroblasts and nodules of anhydrite, which were leached during a later stage of fresh-water diagenesis to form large vugs. Jacka (1978b) observed that much of the porosity in the Permian dolostone reservoirs of the Permian Basin is in such tertiary anhydrite molds. The dolostones of the Big Hatchet Peak section also have porosity in some preserved intercrystalline voids, fossil molds, nontectonic fractures, and solution channels.

Questions have been raised about the reliability of reservoir evaluations using outcrop samples, especially where the effects of surface weathering may be great. In the field, every effort was made to collect fresh material. The thin sections show that depositional and diagenetic features are well preserved and that weathering effects are minimal. Petrographic evidence illustrates that the diagenetic history of neomorphic dolomitization, anhydritization, and subsequent fresh-water leaching produced most of the resulting porosity. This leaching took place during Pennsylvanian-Permian diagenesis as evidenced by the fact that some voids are filled with dolomite cements and that some are partially filled with microstalactitic calcite that has been paramorphically dolomitized; these dolomitizing fluids are unlikely to be of post-Paleozoic age. Some of the vugs in the dolostones have been enlarged by modern surface weathering, and some superficial vugs are seen on the weathered surfaces of limestones but not in the fresh rock a few millimeters below the surface.

The Horquilla limestones had high percentages of porosity in primary voids such as intergranular and intrabiotic cavities and in secondary voids such as leached aragonitic shells, hollow micrite envelopes, nontectonic fractures produced by collapse of the molds, and solution channels. Primary and secondary voids were filled by calcite cements during fresh-water diagenesis, and much of the calcite probably was derived from leaching of these voids or of carbonate sediment in the overlying unit. In a few limestones, tertiary porosity in anhydrite molds is filled with dolomite cement. Thus limestone porosity was occluded diagenetically long before sufficient overburden was available to begin thermal maturation of the hydrocarbons in the penecontemporaneous source rocks; also, such porosity would have been too near the surface to have served as an effective reservoir for oil and gas migrating from older sources.

In contrast, significant porosity has been preserved in upper Horquilla dolostones after diagenesis. These rocks probably retained sufficient permeability to have served as reservoirs for hydrocarbons generated from intercalated shelf limestones and for the greater volumes of oil and gas that likely were generated from the limestones and mudstones of the deep-marine basin facies to the south. Because the dolomitizing fluids are believed to have been developed on the coastal plain to the north, the inner-shelf facies may have been the most highly dolomitized with practically all intercrystalline porosity occluded by compromise boundaries of adjacent dolomite crystals. In the part of the outer-shelf facies where the Big Hatchet Peak section was measured, some inter-crystalline porosity is preserved, indicating that dolomitization was arrested before complete occlusion by compromise boundaries. Perhaps farther south along the shelf edge and on the slope the process was arrested before compromise boundaries began to form. If so, that part of the outer-shelf to slope facies may have excellent intercrystalline porosity and permeability and would be in an optimum reservoir position between adjacent source facies in the basin and a partial seal updip in the inner-shelf facies.

In any case, the upper Horquilla dolostones of the Big Hatchet Peak section constitute an important exploration target in spite of the poor matrix permeability. If only the observed vuggy porosity and some inferred permeability through solution channels and fractures are considered, the net reservoir thickness of 484 ft constitutes sufficient grounds to rank this unit as the best petroleum reservoir objective in the region and the most likely to contain commercial quantities of oil or gas in the subsurface of the adjacent valleys.

Recommendations

With the basic construction, description, sampling, analysis, and evaluation of the Big Hatchet Peak section completed, surface work may proceed with similar studies of other well-exposed sections in the Big Hatchet Mountains. Zeller (1965) has established a fundamental stratigraphic framework for the Paleozoic-Mesozoic of this area; many of his measured sections have already been reconstructed in the field. Plans include redescription, sampling, analysis, and evaluation of his entire sequence from Precambrian basement up through the Lower Cretaceous, with the main objective being the identification of petroleum source and reservoir units. This work will include two sections of the Horquilla that he measured at New Well Peak and Borrego Canyon.

After the key sections have been completed, detailed field study of observed source and reservoir units may be undertaken to determine their vertical and lateral relationships more precisely. With such information, more accurate projections to subsurface prospects may be made.

In the Big Hatchet Peak section, a more detailed lithostratigraphic and biostratigraphic framework with fusulinids and other guide fossils may be established to help in tracing the dolostone reservoir units and the limestone source units. Well-exposed units may be described in a bed-by-bed manner, slab samples may be taken to determine internal lamination and other sedimentary structures, thin sections may be made to provide petrographic analyses of textural features, and the combined results may be used to document depositional sequences and diagenetic history more rigorously. To supplement such sedimentological analyses, paleoecological studies of the algae, corals, and other environmentally sensitive biota would provide critical data on depositional conditions. Samples of light-colored, algal-rich beds may be submitted for organic-geochemical analyses to see if oil-generating, amorphous-sapropelic kerogens are present. Detailed description and sampling across and along the limestone/dolostone boundaries would give important clues to the nature of the dolomitization process. If an adequate drill could be transported up the cliffs, full-diameter cores of the dolostones may be taken to evaluate their reservoir quality more completely.

Lateral tracing of the Horquilla dolostone reservoir units and limestone source units, from the Big Hatchet Peak section to other parts of the mountains, may be possible by detailed field mapping on the new aerial photographs and topographic quadrangles being prepared by the U.S. Geological Survey. Because of the steep cliffs and many structural complications, a series of oblique aerial photographs and a plane-table survey may be needed.

Between field seasons, work should continue on the description, analysis, and evaluation of subsurface sections using cuttings and logs; unfortunately, only a few cores have been taken on the exploration wells drilled so far in the Hidalgo County area. With the combined framework of surface and subsurface sections, the best projections of petroleum source and reservoir units can be made to favorable subsurface prospects, where future exploration wells will provide the decisive tests of the oil and gas potential.

References

Adams, J.E., and Rhodes, M.L., 1960, Dolomitization by seepage refluxion: American Association of Petroleum Geologists, Bull., v. 44, p. 1,912-1,920

Armstrong, A.K., and Mamet, B.L., 1978, The Mississippian system of southwestern New Mexico and southeastern Arizona: New Mexico Geological Society, Guidebook 29th field conference, p. 183192

Badiozamani, K., 1973, The dorag dolomitization model-application to the Middle Ordovician of Wisconsin: Journal of Sedimentary Petrology, v. 43, p. 965-984

Bathurst, R.G.C., 1975, Carbonate sediments and their diagenesis: Amsterdam, Elsevier Scientific Publishing Company, 2nd ed., 658 p.

Bissell, H.J., and Chilingar, G.V., 1967, Classification of sedimentary carbonate rocks, *in* Carbonate rocks, origin, occurrence, and classification, G.V. Chilingar, H.J. Bissell, and R.W. Fairbridge, eds.: Amsterdam, Elsevier Publishing Company, p. 87-168

Butler, G.P., 1969, Modern evaporite deposition and geochemistry of co-existing brines, the sabkha, Trucial Coast, Arabian Gulf: Journal of Sedimentary Petrology, v. 39, p. 70-89

Campbell, C.V., 1967, Lamina, laminaset, bed, and bedset: Sedimentology, v. 8, p. 7-26

Cluff, R.M., Barrows, M.H., and Reinbold, M.L., 1980, Relation of depositional facies and history to hydrocarbon generation in New Albany Shale Group (Devonian-Mississippian) of Illinois (abs): American Association of Petroleum Geologists, Bull., v. 64, no. 5, p. 692-693

Curtis, R., Evans, G., Kinsman, D.J.J., and Shearman, D.J., 1963, Association of dolomite and anhydrite in the recent sediments of the Persian Gulf: Nature, v. 197, p. 679-680

Deffeyes, K.S., Lucia, F.J., and Weyl, P.K., 1965, Dolomitization of Recent and Plio-Pleistocene sediments by marine evaporite waters on Bonaire, Netherland Antilles, *in* Dolomitization and limestone diagenesis-a symposium: L.C. Pray and R.C. Murray, eds.: Society of Economic Paleontologists and Mineralogists, Spec. Pub. 13, p. 71-85

DeGroot, K., 1967, Experimental dedolomitization: Journal of Sedimentary Petrology, v. 37, p. 1,216-1,220

Dunham, R.J., 1962, Classification of carbonate rocks according to depositional texture, *in* Classification of carbonate rocks, W.E. Ham, ed.: American Association of Petroleum Geologists, Mem. 1, p. 108-121

Folk, R.L., 1962, Spectral subdivision of limestone types, *in* Classification of carbonate rocks, W.E. Ham, ed.: American Association of Petroleum Geologists, Mem. 1, p. 62-84

Friedman, G.M., 1964, Early diagenesis and lithification in carbonate sediments: Journal of Sedimentary Petrology, v. 34, p. 777-813

Friedman, G.M., Amid, A.J., and Schneiderman, N., 1974, Submarine cementation in reefs-example from the Red Sea: Journal of Sedimentary Petrology, v. 44, p. 816-825

Friedman, G.M., and Sanders, J.E., 1978, Principles of sedimentology: New York, John Wiley and Sons, 792 p.

Gavish, E., and Friedman, G.M., 1969, Progressive diagenesis in Quaternary to late Tertiary carbonate sediments-sequence and time scale: Journal of Sedimentary Petrology, v. 39, p. 980-1,006

Ginsburg, R.N., and James, N.P., 1976, Submarine botryoidal aragonite in Holocene reef limestones, Belize: Geology, v. 4, p. 431-436

Goddard, E.N., Trask, P.D., DeFord, R.K., Rove, 0.N., Singewald, J.T., Jr., and Overbeck, R.M., 1951, Rock-color chart: Geological Society of America, 11 p.

Greenwood, E., Kottlowski, F.E., and Thompson, S., III, 1977, Petroleum potential and stratigraphy of Pedregosa Basin-comparison with Permian and Orogrande Basins: American Association of Petroleum Geologists, Bull., v. 61, no. 9, p. 1,448-1,469

Hanshaw, B.B., Back, W., and Deike, R.C., 1971, A geochemical hypothesis for dolomitization by groundwater: Economic Geology, v. 66, p. 710-724

Hunt, J.M., 1979, Petroleum geochemistry and geology: San Francisco, W.H. Freeman and Company, 617 p.

Illing, L.V., Wells, A.J., and Wells, J.C.M., 1965, Penecontemporary dolomite in the Persian Gulf, *in* Dolomitization and limestone diagenesis-a symposium: L.C. Pray and R.C. Murray, eds.: Society of Economic Paleontologists and Mineralogists, Spec. Pub. 13, p. 89-111

Jacka, A.D., 1974a, Differential cementation of a Pleistocene carbonate fanglomerate, Guadalupe Mountains: Journal of Sedimentary Petrology, v. 44, p. 85-92

, 1974b, Replacement of fossils by length-slow chalcedony and associated dolomitization: Journal of Sedimentary Petrology, v. 44, p. 421-427

, 1975, Observations on paramorphic and neomorphic dolostones and associated porosity relationships (abs.): American Association of Petroleum Geologists, Annual Convention Book of Abstracts, p. 38-39

_____, 1978a, Deposition and diagenesis of the Fort Terrett Formation (Edwards Group) in the vicinity of Junction, Texas, *in* Cretaceous carbonates of Texas and Mexico, applications to subsurface exploration, D.G. Bebout and R.G. Loucks, eds.: Bureau of Economic Geology, University of Texas (Austin), Inv. Rept. No. 89, p. 182-200

, 1978b, Occurrences of tertiary porosity in carbonate rocks (abs.): American Association of Petroleum Geologists, Bull., v. 62, no. 3, p. 525

Jacka, A.D., Barone, W.E., Muir, N.J., Foley, D.C., Tully, T., and Worthen, J.A., 1980, Cyclic hydrologic and diagenetic events in the San Andres Formation-geologic implications (abs.): American Association of Petroleum Geologists, Southwest Section, Annual Convention Book of Abstracts, p. 37, 27

Jacka, A.D., and Brand, J.P., 1977, Biofacies and development and differential occlusion of porosity in a Lower Cretaceous (Edwards) reef: Journal of Sedimentary Petrology, v. 47, p. 366-381

Jacka, A.D., and Franco, L.A., 1974, Deposition and diagenesis of Permian evaporites and associated carbonates and clastics on shelf areas of the Permian Basin, A.H. Coogan, ed.: Northern Ohio Geological Society, Fourth International Symposium on Salt, p. 67-89

Jacka, A.D., and Stevenson, J.C., 1977, The JFS field, Dimmit County, Texas-some unique aspects of Edwards-McKnight diagenesis: Gulf Coast Association of Geological Societies, Trans., v. 27, p. 45-60

James, N.P., Ginsburg, R.N., Marszalek, D.S., and Choquette, P.W., 1976, Facies and specificity of early subsea cements in shallow Belize (British Honduras) reefs: Journal of Sedimentary Petrology, v. 46, p. 523-544

Kinsman, D.J.J., 1969, Modes of formation, sedimentary associations, and diagnostic features of shallow water and supratidal evaporites: American Association of Petroleum Geologists, Bull., v. 53, p. 830-840

Kottlowski, F.E., 1965, Measuring stratigraphic sections: New York, Holt, Rinehart, and Winston, 253 p.

Land, L.S., 1967, Diagenesis of skeletal carbonates: Journal of Sedimentary Petrology, v. 37, p. 914-930

, 1973, Holocene meteoric dolomitization of Pleistocene limestones, north Jamaica: Sedimentology, v. 20, p. 411-424

Leighton, M.W., and Pendexter, C., 1962, Carbonate rock types, *in* Classification of carbonate rocks, W.E. Ham, ed.: American Association of Petroleum Geologists, Mem. 1, p. 33-60

Levorsen, A.I., 1967, Geology of petroleum: San Francisco, W.H. Freeman and Company, 2nd ed., 724 p.

Lindholm, R.C., and Finkelman, R.B., 1972, Calcite staining-semiquantitative determination of ferrous iron: Journal of Sedimentary Petrology, v. 42, no. 1, p. 239-242

Matthews, R.K., 1968, Carbonate diagenesis-equilibration of sedimentary mineralogy to the subaerial environment, coral cap of Barbados, West Indies: Journal of Sedimentary Petrology, v. 38, p. 1,110-1,119

Muller, G., 1971, Gravitational cement-an indicator of subaerial diagenetic environment, *in* Carbonate cements, O.P. Bricker, ed.: Baltimore, Johns Hopkins Press, p. 301-302

Newell, N.D., Rigby, J.K., Fischer, A.G., Whiteman, A.J., Hickox, J.E., and Bradley, J.S., 1953, The Permian reef complex of the Guadalupe Mountains region, Texas and New Mexico: San Francisco, W.H. Freeman and Company, 236 p.

Pingatore, N.E., Jr., 1970, Diagenesis and porosity modification in *Acropora palmata,* Pleistocene of Barbados, West Indies: Journal of Sedimentary Petrology, v. 40, p. 712-721

Plumley, W.J., Risley, G.A., Graves, R.W., Jr., and Kaley, M.E., 1962, Energy index for limestone interpretation and classification,

in Classification of carbonate rocks, W.E. Ham, ed.: American Association of Petroleum Geologists, Mem. 1, p. 85-107

Purdy, E.G., 1963, Recent calcium carbonate facies of the Great Bahama bank, 2. Sedimentary facies: Journal of Geology, v. 71, p. 472-497

Shinn, E.A., 1969, Submarine lithification of Holocene carbonate sediments in the Persian Gulf: Sedimentology, v. 12, p. 109-144

Steinen, R.P., 1974, Phreatic and vadose diagenetic modification of Pleistocene limestone—petrographic observations from subsurface of Barbados, West Indies: American Association of Petroleum Geologists, Bull., v. 58, p. 1,008-1,024

Taylor, J.M.C., and Illing, L.V., 1971, Variation in recent beachrock cements, Qatar, Persian Gulf, *in* Carbonate cements, O.P. Bricker, ed.: Baltimore, Johns Hopkins Press, p. 32-35

Thompson, S., III, Tovar R., J.C., and Conley, J.N., 1978, Oil and gas exploration wells in the Pedregosa Basin: New Mexico Geological Society, Guidebook 29th field conference, p. 331-342 Tissot, B.P., and Welte, D.H., 1978, Petroleum formation and occurrence: Berlin, Springer Verlag, 538 p.

Travis, R.B., 1970, Nomenclature for sedimentary rocks: American Association of Petroleum Geologists, Bull., v. 54, no. 7, p. 1,095-1,107

Wilson, J.L., 1975, Carbonate facies in geologic history: New York, Springer Verlag, 471 p.

Winland, H.D., and Matthews, R.K., 1974, Origin and significance of grapestones, Bahama Islands: Journal of Sedimentary Petrology, v. 44, p. 921-927

Wray, J.L., 1977, Calcareous algae: Amsterdam, Elsevier Scientific Publishing Company, 185 p.

Zeller, R.A., Jr., 1960, Reef and associated facies of Horquilla Limestone, Big Hatchet Mountains area, southwestern New Mexico: Roswell Geological Society, Guidebook for field trip to northern Franklin Mountains and southern San Andres Mountains with emphasis of Pennsylvanian stratigraphy, p. 149-156

, 1965, Stratigraphy of the Big Hatchet Mountains area, New Mexico: New Mexico Bureau of Mines and Mineral Resources, Mem. 16, 128 p.

, 1975, Structural geology of Big Hatchet Peak quadrangle, Hidalgo County, New Mexico: New Mexico Bureau of Mines and Mineral Resources, Circ. 146, 23 p.

Appendices

(1-3)

Appendix 1 Field data

In this appendix, essential details of the field data that were used in construction of the Big Hatchet Peak section are made available to the interested reader. Many of the fundamentals follow the system for measuring and describing columnar stratigraphic sections given by Kottlowski (1965). Because of the many subsequent advances in description of sedimentary units and because of the many variations among different workers, the basic concepts and methods used in this study are specified in the first part of this appendix. Discussion of accessibility and details of traverse data are given in the second part so that this columnar section, or parts of it, can be reconstructed in the field. A list of samples is given in the third part.

Petrographic analyses of the samples are given in appendix 2. A summary graphic plot of the basic data, interpretations, and evaluations of the petroleum source and reservoir units is given in appendix 3.

Field description: basic concepts and methods

Table 4 is an analytical description of the lithostratigraphic map and column units in the Big Hatchet Peak section from the top to the base. Two standard formations, the Horquilla and the Paradise, are recognized as fundamental lithostratigraphic map units. Two informal members, designated upper and lower, are defined within the Horquilla. These members may be separated by a subtle disconformity, but they have not been mapped.

The entire section of 3,308 ft is subdivided into a succession of 78 lithostratigraphic column units. A *column unit* is defined here as an operational lithostratigraphic unit that is used in the construction of a columnar strati-graphic section. Such a unit is determined by selecting an assemblage of strata with distinctive aspects of lithologic properties or sedimentary structures. Preferably, such a unit should be traceable on the surface or in the subsurface with megascopic or 10 x microscopic criteria. Normally, such units are contained within map units (formations or members) but may be determined independently of them. In contrast to map units which are named, column units are numbered as they are measured and described in stratigraphic order from the base upward.

In the description, on each line with the unit number, is a summary of the basic rock types and other megascopic characteristics used to distinguish the unit from the ones below and above. Where possible, unit boundaries were drawn at sharp bedding surfaces that are inferred to represent depositional hiatuses. Thicknesses of the units are given in feet rather than meters so that correlations can be made more easily with other surface and subsurface sections in the area. Each unit is subdivided into descriptive intervals based on smaller scale changes in lithology, sedimentary structure, or outcrop characteristics.

Thicknesses of the units and descriptive intervals were measured with a 5-ft Jacob staff that has an Abney level at the head and a mechanical counter attached below. The clinometer on the Abney level was set with the most reliable dip that could be measured with a Brunton pocket transit in the given unit or in adjacent units. Each increment of thickness was measured in a strike-normal direction, and stratigraphic horizons were traced in short lateral offsets where needed on strike-oblique traverses to keep the line of section along the locus of best exposures. Small percentages of error in cumulative thickness may have been introduced by the lateral offsetting and by rounding off thicknesses of individual units to the nearest foot.

Field analyses were made on a unit-by-unit basis. This procedure is more rational than one based on analysis of an arbitrary thickness interval but is not as rigorous as a bed-by-bed analysis used in detailed sedimentological studies. After the boundaries of a unit were determined, a sample of each rock type was taken near the base, and the lithologic properties were described as completely as possible with a 10 x hand lens, a color chart, a bottle of dilute hydrochloric acid, a percentage chart, and other field guides. The sedimentary structures, topographic expression, quality of exposure, and amount of cover were described for the basal interval represented by the sample. Subsequent intervals within the unit were designated where minor changes were observed megascopically or by spot checks of the lithologic properties. Additional samples were taken if other rock types or significant changes in composition or texture were encountered, or if the unit was over 50 ft thick. The lithologic descriptions of the samples were checked in the laboratory with a 10 x binocular microscope. Redescription of some units, especially the ones studied early in the project when the basic concepts and methods were being developed, was needed to present a more uniform style. Some corrections were made after the petrographic determinations became available.

Descriptive intervals within the units are subdivided into separate paragraphs for each basic rock type, in decreasing order of abundance. Within the paragraphs, for ready reference, are five separate sentences describing in order: 1) basic rock name and color, 2) composition, 3) texture, 4) sedimentary structure, and 5) outcrop characteristics, including topographic expression, quality of exposure, and amount of cover. Lithologic properties are presented in the first three sentences because they are fundamental and are the most useful in correlations between surface and subsurface sections. Observations on sedimentary structures are important but are dependent upon the quality of exposure and are rarely correlated in detail with subsurface data because of the lack of cores. Notes on outcrop characteristics are most useful in surface work; however, a topographic profile can be correlated in a general way with some subsurface logs.

Specific discussions of each of these properties are given in the following subsections:

1) BASIC ROCK NAME AND COLOR—Basic rock names are used as paragraph headings. The names are modified from the classification of Travis (1970), and the determinations are based on standard criteria of composition and texture. In this dominantly carbonate sec-

tion, limestone, dolostone, and chert are most common. Mudstone is rare; this term is used for a general detrital rock type that includes the specific subtypes of siltstone, claystone, shale, and argillite. Percentage of each rock type is based on a field estimate of the ratio of the net thickness of the rock type to the gross thickness of the descriptive interval as measured in the line of section. Estimates were made to the nearest 10 percent. A trace is indicated for a rock type that makes up less than 10 percent of the interval.

Rock colors were described using the standard GSA chart of Goddard and others (1951). The color of the fresh rock is given first, as it appears wet under 10 x magnification, because it corresponds to the color of representative samples of drill cuttings. Only a few differences were noted between the fresh color as it was described by sunlight in the field and as it was checked in the laboratory with a binocular microscope and a standard white-light illuminator. The color name is followed by the Munsell notation in parentheses. Variations are listed in order of decreasing percentages of the surface area occupied by each major color. The color of the weathered rock was determined megascopically in the field on a dry surface.

Using the microcrystalline limestones as a basis for comparison: commonly, the color is light gray (N7) on the weathered surface; medium dark gray (N4) as seen megascopically on the fresh, dry surface; dark brownish gray (5YR3/1) as seen megascopically on the fresh, wet surface; and brownish gray (5YR4/1) ranging to dark yellowish brown (10YR4/2) and to olive gray (5Y4/2) as seen microscopically on the fresh, wet surface. In microcrystalline limestones, a fresh, wet, microscopic color with a lightness-darkness value of N4 or less generally indicates a significant content of organic carbon that is worthy of geochemical analysis for petroleum-source evaluation.

Where appropriate, the fresh color of the dominant matrix is described in the first sentence, and contrasting colors of specific grain types are described in the third sentence as part of the textural analysis. Contrasting colors in alternating layers may be described in the fourth sentence as part of the sedimentary-structure analysis.

2) COMPOSITION—Chemical components were described as calcareous or dolomitic based on a fast or slow reaction with 12.5 percent dilute HCl on the fresh, wet surface. Siliceous components generally were determined by scratching a line on the surface with the point of a rock hammer or a probe and estimating the percentage of the line that is harder than steel as observed with a hand lens or microscope. Minor glauconitic, pyritic, and megascopic carbonaceous components were identified by inspection.

Coarser detrital components of gravel and sand were very rarely observed in this section. Muddy components of silt and probable clay were found in very minor amounts in nearly every carbonate-rock chip that was dissolved in acid, but these components were described only where at least a significant trace was determined. Some of the residue may consist of organic, carbonaceous material such as kerogen or bitumen (dead oil).

Percentage estimates of the components were made to the nearest 10 percent. However, these estimates, especially in the carbonate rocks, are probably the least accurate of the field analyses because of the indirect nature of the tests. Nevertheless, field estimates of composition are important considerations in the selection of samples for petroleum-source analyses.

3) TEXTURE—Types of sedimentary particles, and their size, shape, and arrangement, are fundamental lithologic properties. Moreover, their relationships to porosity and permeability are basic considerations in petroleum-reservoir analyses.

As in many carbonate sections, the limestones have the most diverse textures. Unfortunately, the modern literature on the subject deals mainly with subclassifications of limestones based on petrographic criteria and tends to neglect the fundamental step of describing textural constituents in the field. During this investigation, some of the appropriate features selected from the various schemes were assembled into a system for field analysis that is still being developed. Those parts that were used in the Big Hatchet Peak section are presented in the following paragraphs.

Textural constituents occupy an intermediate position in the conceptual hierarchy of rock properties that lies above mineral components and below sedimentary structures. Textural constituents of limestones include grains, matrix, pores, pore-filling cements, and diagenetic products of recrystallization or replacement.

A *carbonate grain* (modified from Leighton and Pendexter, 1962, p. 35) is a discrete carbonate particle with a higher level of organization than the aggregate of its component crystals. Phaneric grains, which have diameters larger than about 0.03 mm, can be detected in the field with the unaided eye; aphanic grains of smaller size tend to be included in the matrix. With 10 x magnification, grain types can be identified down to diameters of about 0.5 mm or below in some cases.

The two general types of carbonate grains are lithoclasts and allochems. A *lithoclast* (modified from Bissell and Chilingar, 1967, p. 160) is a grain with a fragmental form that was derived from a pre-existing rock. An *allochem* (modified from Folk, 1962, p. 63) is a carbonate grain with a whole or fragmental form produced by biochemical or mechanochemical processes prior to consolidation in a sedimentary rock. Allochems include intraclasts, skeletal grains, peloids, and coated grains such as ooids and grapestone grains. All of these types were recognized during the present investigation.

An *intraclast* (modified from Folk, 1962, p. 63) is an allochemical carbonate grain with a fragmental form that was derived from a penecontemporaneous sediment. The distinction between a lithoclast and an intraclast may be difficult. A lithoclast may be inferred if the color, composition, or texture are significantly different from those of associated allochemical or authichemical material. An intraclast may be inferred if the lithology resembles associated sediments, especially if it is a fragment containing associated allochemical grains. Only a few lithoclastic and intraclastic grains were recognized during the field investigation.

A *skeletal grain* (modified from Leighton and Pendexter, 1962, p. 36) is an allochemical grain with an organic form; it is made of calcareous hard parts secreted by organisms. Skeletal grains may include whole forms of solitary or small colonial organisms, or

fragments of either. A fragment of an individual fossil is classified as skeletal; a fragment containing more than one fossil, especially if associated with other types of grains and embedded in a matrix, is classified as intraclastic or lithoclastic. Specific types of skeletal grains recognized in the present study include fusulinids and other foraminifers, sponges (only spicules), rugose and tabulate corals, bryozoans, brachiopods, gastropods (very rare), crinozoans, and various types of algae (identified from Wray, 1977) ranging from fragments of phylloid types, to encrusting types in oncoids, to individual dasyclad forms, to small types that were indeterminate in the field. Only the fusulinids and some algae were collected for the generic and specific identifications that were made by G.L. Wilde (see table 1). In the petrographic analyses (appendix 2), Jacka has identified many more types of microfossils than were determined under 10 x magnification.

A *peloid* (modified from Bathurst, 1975, p. 84-86; term proposed by E.D. McKee) is a pelletlike allochemical grain composed of homogeneous microcrystalline material. Shape generally varies from spheroidal to prolate (elongate, rodlike). Some may be rounded intraclasts. Small spheroidal ones may be ooids whose internal layering has been obliterated by endolithic algae. Those with irregular shapes may be skeletal grains that have been homogenized by the same process. Ellipsoidal ones up to about 0.15 mm in diameter are probably fecal pellets, but they cannot be recognized with only 10x magnification (Folk, 1962, p. 65). Tightly packed peloids may show a clotted (grumose) texture.

A *coated grain* (modified from Leighton and Pendexter, 1962, p. 59) is an allochemical grain that is wrapped in one or more carbonate layers. An *ooid* (modified from Bathurst, 1975, p. 77-84) is a spheroidal to ellipsoidal coated grain with two or more concentric layers; it may also have a radial internal fabric. An arbitrary upper size limit of 2 mm in diameter has been placed on the concept of an ooid, and the term *pisolite* (or pisolith) has been used for the larger counterpart. However, the latter term has also been used in a different way for vadose concretions that generally have a less regular shape. No pisolites were recognized during the present investigation. A *grapestone grain* (modified from Bathurst, 1975, p. 87; term introduced by L.V. Illing) is a composite grapelike cluster of two or more grains coated by one or more carbonate layers; the exterior generally is lumpy. Some particles encountered in the present investigation were described simply as coated grains where specific types were not recognized, or where the shape was elongate.

An *oncoid* (modified from Wilson, 1975, p. 12) is a carbonate grain with algal encrustations, and where recognized should be classified as skeletal. Also not to be confused with a coated grain is a carbonate grain with a rind produced by boring of endolithic algae and filling with extremely finely crystalline calcite (a "micrite envelope" of Bathurst, 1975, p. 90); although none were recognized in the field study, several were determined in the petrographic analyses.

Specific determinations of some grains could not be made with confidence under 10x magnification because of their small size. Such grains were described as small or very small if their diameters were less than 1 mm or 0.5 mm, respectively.

The *matrix* (modified from Bissell and Chilingar, 1967, p. 160) of a limestone is defined as the relatively finer depositional sediment in which carbonate grains are embedded; the matrix may be the dominant constituent of the rock. In all of the limestones of the present study, the calcareous matrix was determined to be *microcrystalline;* that is, the diameters of individual calcite crystals are less than 1/16 (0.062) mm (modified from Plumley and others, 1962, p. 86). Folk (1962, p. 65-66) defined *micrite as* a contraction of "microcrystalline" calcite, but the size of the crystals was specified as being in his aphanocrystalline (better termed extremely finely crystalline) range, less than 1/256 (0.004) mm. True micrite cannot be determined precisely with only 10 x magnification; however, much of the opaque microcrystalline calcite is probably micrite. Leighton and Pendexter (1962, p. 35) defined *micritic material* (micrite) with an upper size limit of 0.03 mm; this term was used in early stages of the field investigation but was dropped to avoid confusion with a petrographic determination of micrite.

As a field term, matrix has other advantages. Muddy (detrital silt and clay) and other noncarbonate components may be present in minor amounts and can be described under that heading. Micron-sized carbonate grains may be present in which case "micritic" would be misleading. A slight disadvantage is that according to the strict definition of matrix, larger particles must be embedded in it. In some hand-specimen samples of microcrystalline limestone, no such larger particles were seen, but the matrix was described as constituting 100 percent of the rock, implying a broader definition of the term. This alternative is deemed preferable to the introduction of a new term for only a minor distinction. Moreover, a thorough search in each case would probably produce at least a few grains in the same bed.

Dunham (1962, p. 113-117) introduced the concepts of *grain support* in which carbonate grains are in depositional contact, and *mud support* in which carbonate grains are dispersed (floating) in a lime-mud matrix (particles smaller than 0.020 mm). He points out that these textural relationships may generally indicate depositional environments of agitated and quiet water, respectively; however, Dunham also points out many exceptions such that grain and mud support are considered more useful as textural descriptions rather than as environmental indicators. In his discussion and classification, Dunham (1962, p. 117, table I) does not consider the possibility of a limestone containing carbonate grains with some in depositional contact and others dispersed in a matrix.

To include the entire spectrum of such textural relationships, the property of *grain tangency* is defined here as the percentage of grains in depositional contact within a given sample. A grain is in contact with its neighbor if they are touching in at least one point. An elongate grain may be in contact with another along a line or surface. A grain in contact with some adjacent grains but not with others may be counted proportionately. Deformational packing or suturing by pressure solution are discounted.

Ideally, the actual percentage of grains in depositional contact would be determined for each sample with adequate observation of the grain relationships in three dimensions. In practice, general classes of percentages can be described with the following *scale of grain tangency:* none (0 percent, all grains are dispersed in microcrystalline matrix), poor (between 0 and 10 percent), fair (10-50 percent), good (50-90 percent), excellent (90-100 percent), and perfect (100 percent). Dunham's concepts of mud support and grain support correspond to the end members of no grain tangency and perfect grain tangency, respectively. A limestone may attain perfect (100 percent) grain tangency with a 65 percent volume of equidimensional grains or with a much smaller percentage by volume of elongate or irregularly shaped grains (Dunham, 1962, p. 114).

In the present investigation, the scale of grain tangency was based on the examination of the limestone samples with a binocular microscope, although some notes were made in the field. In some samples the grain relationships could be determined with confidence in three dimensions, in others the determination was based on the *apparent grain tangency* observed on one or more two-dimensional surfaces. On no single surface did elongate grains (such as fusulinids) appear to be surrounded by sparry calcite cement, indicating grain support in a right-angle view, as shown by Dunham (1962, p. 121, pl. VIIb).

Dunham (1962, p. 117, table I) presented a classification of limestones based mainly on grain/mud support; this classification has been used widely by carbonate petrographers. His lime *grainstone* may be defined as a limestone with perfect grain tangency and no microcrystalline matrix and his lime *packstone as* a limestone with perfect grain tangency and some microcrystalline matrix. He draws the boundary between no microcrystalline (lime mud) matrix and some at 1 percent (Dunham, 1962, p. 113). Such precision is practicably unattainable with only 10 x magnification and is difficult with a petrographic microscope. His lime *wackestone* may be defined as a generally microcrystalline limestone with 10 percent or more grains and no grain tangency (that is, the grains are mud supported) and his lime *mudstone* as a generally microcrystalline limestone with less than 10 percent grains and no grain tangency. The division at 10 percent grains is reasonable and can be estimated within a few percent using standard charts. His remaining term, lime *boundstone*, is a limestone in which the original components were bound organically during deposition and remained essentially in growth position.

The most serious conceptual problem with Dunham's classification is the wide gap in percentage of grain tangency between his lime packstone (100 percent) and lime wackestone (0 percent). If a whole bed or a hand-specimen sample must meet these requirements, then there are many limestones that cannot be designated with Dunham's classification. Even within the small area of a petrographic thin section the requirement often cannot be met, and a compromise designation of lime wackestone-packstone must be used to indicate the range of grain tangency between microscopic areas of the sample. The compound designation of lime packstone-grainstone indicates overlap across the subtle boundary of 1 percent micritic matrix, and that of lime mudstone-wackestone indicates overlap across the more reasonable boundary of 10 percent grains; these less serious problems are procedural and are not concerned so much with basic concepts.

Because of such problems, Dunham's classification was not used in the field. Description of textural constituents, including percentage estimates of grains and matrix material to the nearest 10 percent and approximations with the scale of grain tangency, was considered more important than a subclassification of limestones. Nevertheless, Dunham's terms are added to the sentence of texture description, based on the study of the samples with a binocular microscope, because carbonate specialists are familiar with them. Geologists who are not so familiar with his admittedly tentative terms (Dunham, 1962, p. 117) may encounter communication problems with their inexplicitness and especially with the ambiguous term "mudstone" that can be confused with the detrital rock type when the "lime" prefix is deleted as commonly is practiced.

Orientation of elongate grains (such as fusulinids) and imbrication of lithoclasts were observed in a few channels. Some grading of skeletal grains was observed in a few beds. No detailed study of grain orientation was made. The degree of induration was not described routinely because all of the Paleozoic limestones in this section are well indurated.

No porosity was observed on the fresh surfaces of the limestones, and only a trace number of small vugs were seen on the weathered surface of one unit (74). Some sparry calcite cement has filled vugs, intraskeletal cavities, and other types of former porosity in many units; however, many relatively young fractures, probably Tertiary in age, are also filled with sparry calcite. Whether some spar was introduced during diagenesis or all of it was deposited during or after the Tertiary fracturing is an important question of reservoir evaluation that is better determined with petrographic evidence.

Evidence of recrystallization and replacement also is best determined petrographically. Nevertheless, in some limestones the matrix appears translucent instead of opaque, and recrystallization to microspar is suspected. In one interval (unit 13, 20-25 ft above the base) some small blebs of sparry calcite have rectangular shapes and may have been molds of anhydrite porphyrotopes (Friedman and Sanders, 1978, p. 569).

Textural constituents of dolostones are similar in many respects to the limestones they have replaced. Ghosts of skeletal grains and some possible intraclasts (unit 49) were recognized in the field study.

Matrix of the dolostones, in contrast to that of the limestones, is generally medium (1/16-1/4 mm) to coarsely (1/4-1 mm) crystalline (Folk, 1962, p. 74, table II). Although the crystals are rhombic, they generally are tightly fitted, probably by overgrowths, into a mosaic texture (Bissell and Chilingar, 1967, p. 161). Only a small amount of sucrosic (intercrystalline) porosity was seen. In imbibition tests, drops of water did not soak into the matrix before 30 seconds, so the permeability is judged to be very low, probably less than 0.1 millidarcies.

Nearly all of the dolostones have small scattered vugs, about 1 mm in diameter, on the fresh surfaces. Larger vugs up to 30 mm in diameter are seen on the weathered surfaces and no doubt are the products of enlargement by superficial solution.

Dunham's subclassification of limestones was used to designate the inferred texture prior to dolomitization. An assumption was made that the rhombic mosaic matrix was originally microcrystalline calcite and that the original grains are preserved as ghosts in the dolostones. If true, most of the dolostones are replacements of lime mudstones or wackestones.

Many of the dolostone units can be traced laterally at least for hundreds or thousands of yards (for example, unit 49) and probably are results of early diagenetic dolomitization. A few show abrupt lateral changes within a few feet from limestone to dolostone as fault zones are approached (for example, the upper part of unit 48); they probably are products of solution of dolostones, possibly by hydrothermal action along Wolfcampian fault zones, and immediate replacement of adjacent limestones.

Textural constituents of cherts are even more similar to the limestones than the dolostones. The matrix is generally microcrystalline (probably extremely finely crystalline) and opaque to translucent. Skeletal and other grains replaced by chert tend to be well preserved. In some cases, the selective process has replaced particular grains and left others with their original calcareous composition. In one interval (unit 31, 10-20 ft above the base), coarse rhombic crystals appear to have been dolomite porphyrotopes that were replaced by chert. Dunham's classification was used to designate the original limestone texture.

Textural constituents of the detrital mudstones were described in standard terms similar to those of the carbonate rocks. Siltstones (unit 4, 12-13 ft) were observed to be nonfissile. Red mudstones (unit 54, 95-97 ft) were observed to be platy and fissile (shaly).

4) SEDIMENTARY STRUCTURE—Descriptions of sedimentary structures include data on lithosomes, beds and bedding surfaces, laminae, and biogenic structures. These data are important in analyses of depositional environments and paleocurrent directions and in projections of reservoir geometry. Unfortunately, fair to good exposures are needed for reliable descriptions of sedimentary structures, so the analyses of these properties cannot be as comprehensive as those of the lithologic properties.

Nearly all lithosomes of limestone and dolostone in this section appear to be horizontal tabular bodies, but they generally are not described because of the laterally limited exposures. In most cases the contacts coincide with bedding surfaces. Dolostone/limestone replacement boundaries are described if they are oblique to bedding surfaces. A lithosome of chert in two-dimensional exposure is described as a *band* if the length/width ratio is 10:1 or greater and as a *nodule* if the ratio is less than 10:1. Orientation of the long axis is generally parallel to bedding unless described otherwise. Some chert nodules are described as *linked* if they are connected laterally, parallel to bedding; others are described as *anastomosed* if they are connected vertically or obliquely to bedding.

The one lithosome of siltstone (unit 4, 12-13 ft) appears to be a horizontal tabular body; the basal contact is covered, and at the top contact the siltstone is gradational with the overlying muddy limestone. Lithosomes of red mudstone (for example, unit 54, 95-97 ft) are restricted laterally by the shapes of ancient cavities that they fill.

Stratification within lithosomes is described in terms of bedding and lamination. The phrase "no discernible stratification" in a fair to good exposure indicates that neither bedding nor lamination are evident in the field and in a poor exposure indicates that such layers are not evident but may be masked by weathering.

Bedding and lamination concepts are modified from the system of Campbell (1967). A *bed* is a principal depositional layer, and a *lamina* is the smallest megascopic layer within a bed. (Some geologists consider laminae as merely thinner counterparts of beds.) Laminasets may be recognized within beds, and beds may be grouped into bedsets.

Beds are inferred to be originally horizontal unless they are recognized as inclined or wavy. Shapes are inferred to be tabular unless described as lenticular. In one case (unit 15, 0-2 ft), beds were seen to lap out downward along the base of the unit. The range of bed thickness and the average are given in centimeters. This procedure is considered simpler and more accurate than describing in terms of bed-thickness classes. Patterns of upward thinning or thickening were seen in a few units.

The phrase "hints of beds" is used if multiple bedding surfaces are barely discernible within a descriptive interval. "Single bed" is used if bedding surfaces are evident only at the base and top of the interval and if the exposure quality is fair to good. "Single bed?" is used if a bedding surface is evident at the base or the top, but part of the interval between is poorly exposed such that other surfaces may be masked. "No discernible bedding" is used if laminae are evident but principal layers are not.

Bedding surfaces are described, especially where exposed at the bases of descriptive intervals, if they are particularly sharp, irregular, or have stylolites along them. Plan views of bedding surfaces were seen only rarely, and no directional features were recognized.

Lamination is described as horizontal, inclined, or rippled. Laminasets were evident in only two units (2 and 43). Thicknesses of individual laminae were not measured routinely, but they generally are less than a few millimeters. Inclinations of laminae were measured where possible, but only general directions of inclination were estimated in two-dimensional exposures. The phrase "hints of lamination" is used if lamination surfaces are barely discernible within a bed. "No discernible lamination" is used if beds are evident but internal layers are not, especially in good exposures.

Some bedding and lamination surfaces coincide with changes in composition or texture. In many cases, the lithology is the same above and below a stratification surface. In a few cases, no stratification surfaces are evident, but lithologic alternations are seen. Some limestone beds consist of dominantly skeletal material or other grains in the lower part and grade upward to dominantly microcrystalline material in the upper part; others show an inverse relationship. In some beds, skeletal grains are concentrated in lenses near the base that

may be channels. In one case (unit 38, 0-4 ft), lenses of concentrated grains weather to a distinctive orange color and appear superficially to be grainy chert nodules.

No megascopic biogenic sedimentary structures were recognized in this section. Some phylloid algal plates form buildups a few feet high, but they are confined to beds or bedsets; no large mounds were seen. Some small corals appear to be in growth position. No burrows or borings were recognized, but they may be masked in fair to poor exposures.

5) TOPOGRAPHIC EXPRESSION, QUALITY OF EXPOSURE, AND AMOUNT OF COVER—Outcrop characteristics are obvious properties of sedimentary units, although they have only minor lithostratigraphic significance. Systematic description of them is of greatest value to field geologists who attempt to reconstruct the columnar section, trace units laterally, or study the better exposed units in more detail.

Topographic relief is the degree to which the rocks of a descriptive interval in a columnar section project above the baseline slope of the traverse. A scale of topographic expression is presented here: *slope,* if any vertical projection (sheerness) is less than 0.3 ft above the baseline; *slight ledge,* if the vertical projection is between 0.3 and 1 ft; *moderate ledge,* if between 1 and 3 ft; *fairly prominent ledge,* if between 3 and 10 ft; *prominent ledge,* if between 10 and 30 ft; *cliff;* if between 30 and 100 ft; and *prominent cliff,* if over 100 ft. Multiples of 3 and 10 were selected as boundaries to provide an approximate geometric scale analogous to those used for bedding and lamination (Campbell, 1967). Instead of using the scale, one may measure the vertical projection for each interval, as is now recommended for bedding and lamination thicknesses; however, the extra time needed to obtain precise measurements of topographic expression may not be justified. Ideally, the topographic profile may be surveyed over the entire traverse.

Horizontal projections also may be important parts of the description. Some cliffs overhang the ledges beneath them; others are recessed from the underlying ledges.

Boundaries of ledges and cliffs tend to coincide with changes of rock types at bedding surfaces. However, the coincidences are fewer in this dominantly carbonate section than in others that have many alternations of mudstone. Moreover, changes from fairly prominent ledges to slopes or to cliffs can be seen as units are traced laterally. Offsets in the line of section to follow the locus of best exposures, or the safest traverse over a cliff, may produce some artificial discontinuities in the composite description.

Quality of exposure is the degree to which the sedimentary features in the rocks of a descriptive interval are discernible on the surface. A scale for quality of exposure is presented here: *good exposure,* if such features as bedding and lamination are discernible, or their absence may be determined with confidence; *fair exposure,* if bedding is discernible but lamination is not; and *poor exposure,* if neither bedding nor lamination are discernible. The degree of fracturing or weathering in a poor exposure may be described.

Amount of cover is the degree that soil, vegetation, or Quaternary deposits conceal the bedrock. If less than half of a descriptive interval is concealed, it is described as *partly covered;* if half or more, it is described as *mostly covered.* If no exposure is seen for over 10 ft of section, a separate *covered interval* may be described, and the probable types of bedrock may be inferred from adjacent exposures or from rubble on the surface. If an interval of a particular rock type is believed to lie beneath the cover between exposures of other rock types, a separate *covered unit* may be designated. Many covered intervals, but no covered units, are described in the Big Hatchet Peak section.

Access and traverse data

ACCESS—The general access to the Big Hatchet Peak section is shown in fig. 2. Most of the section can be worked from Chaney Canyon on the west side of the Big Hatchet Mountains. The upper few hundred feet near the peak is best worked by entering Thompson Canyon on the east side and climbing the trail to the top.

Permission to enter Chaney Canyon on the Heard Ranch was obtained originally from Andy Peterson. Later, Ben H. Ormand, president of Pacific Western Land Company of Gila, New Mexico, the present land owner, gave permission, as did Max Kelley who supervises the area from the Heard Ranch headquarters. Permission to enter Thompson Canyon on the Hatchet Ranch was given by Mahlon T. Everhart. Because the Big Hatchet area is on federal land supervised by the Bureau of Land Management, permission was also obtained from Daniel C.B. Rathbun, Manager of the Las Cruces district. The mountains currently are designated as a wilderness study area and include a state wildlife refuge for bighorn sheep and other animals.

To reach the area from Deming, a main town along I-10, drive west 31 mi to the junction with NM-81 (exit 49), and then south 19 mi to the village of Hachita.

The following road log may be used to reach the Chaney Canyon area:

Checkpoint	Direction	Distance (mi)
Hachita, New Mexico	proceed south on NM-81	20.5
milepost 25	continue south	0.3
after cattle guard	turn left (east) onto ranch road, go around north side of Benton well	0.4
gate	enter state wildlife refuge, curve right (southeast)	0.7
Chaney well	turn left (east) to follow road up gentle grade of alluvial fan	2.5
junction	turn left (east) to follow jeep trail (old logging road)	0.7
west of main arroyo	curve right (south) to go up steep grade of alluvial fan	0.6
end of jeep trail	turn around and park	total 25.7

A four-wheel drive vehicle with good power is needed to reach the base of the section in Chaney Canyon. The nearest motel facilities are in Deming or Lordsburg, and the optimum driving time to the base is over two hours, so camping out is advisable if the section is to be studied in detail. A campsite is present at the end of the jeep trail. Extra food and water should be taken in case an unexpected rain makes the low part of the ranch road too muddy to leave. The worst part, between Benton well and the gate, can remain very muddy for several

weeks after only a brief rain; a detour to the south of that part can be made after a few days of dry weather.

Normally, the best field season is from mid-April through mid-July. Days are too short to justify camping out during the winter months, and snowstorms occasionally cover the outcrops. Strong winds from the southwest during late February, March, and early April are a hazard while working the cliffs. Maximum summertime temperatures are often over 100 °F but are comfortable with a gentle breeze. On the longest summer days, sunrise is at 6:00 a.m. and sunset is at 8:00 p.m. Mountain Daylight Time. During late July and August, rainstorms can be a daily afternoon occurrence, sometimes with lightning crackling all over the mountains. With the rains come gnats, flies, bees, and other desert varmints. A few rattlesnakes may be seen, but generally they are not a problem. Rainstorms are less frequent during September and October; however, they can be just as intense as those during the summer.

TRAVERSE DATA—Table 5 provides details of traverse data. The line of section is shown on the geologic map (fig. 2) and on the panoramic photograph (fig. 5). Unit numbers were painted in red at the lowest exposure of each unit and, where possible, a red line was painted at the base. More permanent metal-tag markers may be placed later.

The thickness of each unit was measured to the nearest 1 ft with the Jacob staff-Abney level combination described earlier. The total cumulative thickness is calculated to be 3,308 ft, and that figure should be within 5 percent of the true total thickness. Strikes and dips of beds used in measuring each unit are shown in the fourth column of table 5. Strikes were measured to the nearest 5 ° using a declination setting of N. 12.5° E., and dips were measured to the nearest 2° with a Brunton pocket transit placed on a masonite board oriented to be coplanar along main bedding surfaces. Where possible, at least one measurement of strike and dip was taken in each unit, but only significant variations are recorded.

An approximate survey of the line of section from unit 1 through unit 72 is given in the fifth through the eighth columns of table 5. The direction from the base to the top of each unit was measured to the nearest 5° with a Brunton pocket transit; however, the slope distance to the nearest yard along the traverse was estimated by pacing over rugged topography and is the least accurate of the measurements given. The difference in elevation from the base to the top of each unit was measured by height-of-eye, using the pocket transit as a hand level. Each increment was measured to the nearest 1 ft. The cumulative difference in elevation from the base of unit 1 to the top of unit 72 is calculated to be + 2,110 ft and should be accurate within 5 percent. The rest of the section, units 73-78, was not surveyed because another pack trip to Big Hatchet Peak would have been necessary. Elevation of the top is approximately 8,120 ft and the base of the section is at about 5,940 ft. The difference of 2,180 ft agrees fairly well with the 2,110 ft measured plus the 100 to 200 ft estimated for the rest of the section.

Notes in the ninth column of table 5 describe the general topographic setting of each unit along the line of section. Units 1-16 were measured in arroyos or on crests of spurs. Units 17-45 were measured on the main spur; the first fairly prominent ledge was encountered in unit 30 and the first prominent ledge in unit 36. Units 46-78 were measured over the nine cliffs and the intervening ledges and slopes.

As indicated, 18 lateral offsets ranging from 10 yards to 615 yards were needed to keep the line of section along the locus of best exposures, to avoid local structural complexities, or to follow the safest traverse3 over the cliffs. Where possible, these offsets were made by tracing marker units to tie the segments of the stratigraphic succession.

FOOT TRAILS—Selected portions of the section from unit 1 through unit 72 may be reached by the following foot-trail logs. To reach the base of the section from the end of the jeep trail, walk west-northwest downhill for 270 yards to the bottom of the arroyo. To reach the point 15 ft above the base of unit 16 (after the offset), walk along the main trail uphill, going southwest for 30 yards, south for 205 yards, and southeast for 85 yards. Continue southeast on the main trail for 70 yards to unit 18. To bypass units 19-21, continue on the main trail south-southwest for 50 yards (to tree), then south-southeast for 65 yards to unit 22. Continue southeast for 75 yards to unit 25. Continue east-southeast for 55 yards and generally southeast for 135 yards to unit 30. Continue generally south over prominent ledges for 75 yards to unit 33, south-southwest for 150 yards to unit 40, and south-southwest for 70 yards to unit 41. At this point, the line of section goes generally southeast to traverse units 41-49; however, the main trail to higher units goes south-southwest downhill for 85 yards to cross the drainage, south-southwest for 180 yards, and southeast for 85 yards to the top of the first cliff. At this point, the line of section goes generally southeast to traverse units 50-53; however, the main trail to higher units goes south-southeast for 70 yards to a main drainage with large talus boulders and then southeast up the drainage for 150 yards to rejoin the section at unit 54.

The prominent drainage notch here is the only breach that was found in this part of the second cliff. The steep 20-ft climb up to the breach, with only a few small footholds in the limestone, is one of the main hazards. A nylon rope was tied to the tree at the top, but the rope should be tested before attempting the climb. The rest of the main trail generally coincides with the line of section, except that the fifth cliff can be climbed with less difficulty at the main drainage notch to the east of where unit 68 was measured. Although ropes were tied to aid in climbing the other cliffs, they also should be tested; all such climbs should be done carefully.

Hiking and climbing time from the end of the jeep trail up 1,000 ft to unit 54, near the breach in the second cliff, is about 1 1/2 hours at a moderate pace with a few brief rest stops, but not stopping to study the strati-graphic sequence. Hiking and climbing time up 2,100 ft to the top of unit 72 is about 4 hours. Although the return trip back down to the end of the jeep trail can be made in half the time or less, it also should be done carefully.

WORK ON BIG HATCHET PEAK—Because of the long climb from the Chaney Canyon base, the upper 363 ft of section, units 73-78, were worked out of a camp on Big Hatchet Peak. Arrangements were made with William J. Everhart at the Hatchet Ranch to transport camping

gear, food, and water by horseback to the peak. He was assisted by David L. Smith and Alvin L. Morris. The best procedure is to drive to Thompson Canyon in the morning, pack the goods to be transported, and climb the trail to the peak. That afternoon meet the riders at the top and make camp. Communications can be made with a portable CB radio. To return, pack the gear to be transported again, go back down the trail, and meet the riders in Thompson Canyon where the horses are unloaded.

The following road log may be used to reach the Thompson Canyon area. Some parts between Rock tank and the end are rough, but the road is passable with a four-wheel drive vehicle or a pickup truck.

Checkpoint	Direction	Distance (mi)
Hachita, New Mexico	proceed south on NM-81	
junction	turn left (south) on ranch road	9.6
Hatchet Ranch	after checking with rancher, continue south	6.9
junction	turn left (southeast)	0.4
junction	go right (southwest)	3.4
Rock tank	continue generally southwest	0.2
gate	continue southwest	1.7
end of road	park on south side of Thompson Canyon	1.8
		total 24.0

As shown on fig. 3, the horse trail starts at the end of the road, goes southwest up the canyon, curves right to go southwest uphill then down and up a fault-controlled valley, then northeast across a saddle on the ridge trending south and southeast from Big Hatchet Peak, continuing northeast toward Sheep tank, and finally northwest up the draw to the peak. The horse trail is about 2 mi long, climbs about 2,600 ft, and can be travelled on foot in about 6 hours at a moderate pace. However, some walking time can be saved by crossing the arroyo north of the end of the road, climbing westward up the limestone-dolostone ridge, going down and following the horse trail northwest up the valley to the saddle, but then going northwest and north along the crest of the ridge to the peak. Either way, no serious hazards are encountered. Other routes may be possible, but those attempted were found to be blocked by hazardous climbs over sheer cliffs or thick vegetation in drainages.

On the peak, at an elevation of 8,356 ft, is a triangulation station of the U.S. Coast and Geodetic Survey and a solar-powered antenna of the U.S. Customs Service. The antenna is checked every few weeks by helicopter. The best campsite is located in a small saddle some yards to the southwest. At the end of the four-day reconnaissance trip in late October 1977, a heavy rain during the last night soaked through a canvas pup tent and drenched all the equipment. Next morning, the clouds hanging over the peak were so thick that visibility was reduced to a few yards, and the climb back down the crest of the ridge was somewhat hazardous. During the five-day period in late April 1978 when the remaining part of the section was measured and described, the winds were so strong at night that a new nylon pup tent was blown down several times, and finally the tabs holding the guy lines were ripped off.

To reach the top of the measured section, begin at the triangulation station, walk northeast along the crest for 100 yards, then east-southeast downhill along the crest for 150 yards, then east-northeast along the crest (covered by soil and vegetation) for 40 yards, and northeast downhill for 50 yards. The stratigraphic position here at the top of unit 78 is approximately the same as that of the beds exposed at the triangulation station. Farther southeast down the dip slope, some younger Horquilla limestone beds are exposed; however, major faults separate these beds from the youngest Horquilla that is in contact with the overlying Earp Formation. R.A. Zeller (personal communication, 1961) estimated that the beds on Big Hatchet Peak are about 200 ft stratigraphically below the base of the Earp.

To reach the base of unit 73, begin at the top of unit 78 and follow the traverse data of table 5 in reverse. As before, climbing over the cliffs is somewhat hazardous. An advantage in climbing down from the top first is that the nylon ropes can be tested and replaced if necessary before going down. Hiking and climbing time from the triangulation station to the base of unit 73 is about 2 hrs at a moderate pace.

Working the upper units from Big Hatchet Peak is definitely easier than working them from the Chaney Canyon base. However, the logistical problems and the time involved should be considered before such work is attempted. No petroleum objectives were found, and an equivalent stratigraphic section is much more accessible in the upper part of the New Well Peak section (Zeller, 1965, p. 84-85).

FIELD TIME—A total of 74 days was spent in the field working alone from June 1976 to July 1979. This project took three years to complete because of the limited field season when camping out is feasible, the many delays caused by unexpected rain or snow, and work on other important projects. Reconnaissance work took 23 days searching for the best exposures, working out structural problems, finding the best places for the offsets, clearing the foot trails, and improving the jeep trail up to the base of the section in Chaney Canyon. Measuring, describing, and sampling the Big Hatchet Peak section took 42 days, but about a quarter of that time was spent in hiking and climbing to and from the higher units. Nine days were spent in concluding field work, checking some earlier descriptions, surveying the line of section from unit 1 through unit 72, and taking photographs of key features. Now that the section is all laid out, a detailed study could be completed in about 10 days under ideal conditions.

Sample collection

Table 6 is a list of the 142 samples that were collected in the Big Hatchet Peak section. The list is in order from the top to the base and follows the descriptions in table 4, the tables presenting results of laboratory analyses, and the summary graphic plot in appendix 3.

Sample notations indicate the name of the section, the unit number, and the footage above the base of the unit. For example, BHP-78-42 indicates 1) the Big Hatchet Peak section, 2) unit 78, and 3) that the collection was from 42 ft above the base of unit 78. This procedure is the simplest and most flexible one that designates samples from a single section in stratigraphic order. Some workers use notations with the cumulative footage

above the base of the section; however, serious problems can arise if subtle structural complications or arithemetical errors are discovered after measurement. Some workers use a consecutive-number series, but intervening samples collected after the initial set cannot be numbered in stratigraphic order.

A few deviations from the usual notation are included. A reconnaissance sample was collected from the limestone bed on top of Big Hatchet Peak that is not in the line of section. Samples representing different rock types from the same footage interval are labelled a and **b.** For example, BHP-19-4a contains limestone, and BHP-19-4b contains chert.

To show the stratigraphic spacing of the samples, the cumulative footage above the base of the section is calculated in the second column of table 6. Samples were collected near the base of each unit to determine the major lithologic changes across unit boundaries. Additional collections were made to show significant minor changes within the units. In units with a thickness greater than 50 ft, additional samples were taken as a check on the vertical extent of lithologic properties.

The basic rock name that characterizes each sample is given in the third column. Complete lithologic descriptions may be found in table 4. Sample notations are given at the end of the specific intervals from which the samples were taken.

Purposes for which the samples were collected are indicated in the fourth through seventh columns. All collections with the same notation were taken from the same block of rock to provide a basis for comparison of analytical results. Samples for different purposes were placed in separate bags. The bags are 4 1/2 x 6 inches in size and are made of protexo® by HUBCO. On one side of each label, the name and address of the collector are stamped; on the other side is a stamp with blanks for basic information including the sample notation, rock type, analytical purpose, location, and date of collection.

The largest number of samples (137) was collected for the petrographic analyses. At least one sample was collected of each rock type making up 10 percent or more of each unit; some samples of rock types making up significant trace amounts were also collected. A hand specimen about 2 x 3 x 4 inches with both fresh and weathered rock was included in each bag. An arrow pointing up stratigraphically was drawn in red with a felt waterproof marker on the weathered surface. Also included was a thin chip of fresh rock, about 1 inch in diameter, that was used to make the lithologic description in the field and the check with the binocular microscope in the laboratory. A few extra pieces of fresh rock were included in some cases. Most of the thin sections were prepared by Thea A. Davidson and Jim P. Dodson, technicians at the New Mexico Bureau of Mines and Mineral Resources (NMBMMR); four supplementary thin sections were prepared by Mike Gower of Standard Petrographic in Lubbock, Texas. Results of the petrographic analyses by Alonzo D. Jacka are given in table 7. Two samples (BHP-4-13, BHP-54-96) were submitted to R.M. North, NMBMMR, for x-ray identification of silt and clay minerals; results are incorporated in table 4.

A moderate number of samples (57) was collected for paleontologic analyses, especially of the fusulinids. While the section was being measured, at least one sample of fusulinids was collected from each unit in which they were observed; additional ones were collected where seen to be abundant or well preserved. Some algae also were collected. After the initial identifications were made, supplementary collections were taken to get closer control on the series boundaries. Results of the taxonomic and age determinations by Garner L. Wilde are given in table 1. Oriented thin sections for critical identifications were prepared by Edolio Yanguas of Houston, Texas (samples BHP-2-1, BHP-13-75, BHP-22-1, BHP-53-3, and BHP-68-4). Especially in the lower part of the Horquilla where fusulinids were too small to be seen in the field with 10 x magnification, some identifications were made from thin sections prepared for petrographic analyses (samples BHP-1-0, BHP-2-1, BHP-3-2, BHP-5-0, BHP-8-1a, BHP-9-5, BHP-9-6, BHP-11-1, BHP-12-1, BHP-13-7, BHP-13-23, BHP-14-3, and BHP-24-1).

The 11 samples for petroleum-source analyses were selected from units with dark limestones to evaluate the intervals that appeared to be the richest in organic carbon. Only a minimum number of surface samples were collected in order to conserve funds for more definitive analyses of subsurface samples of drill cuttings. Results of the analyses by Paul J. Cernock and others at GeoChem Laboratories in Houston, Texas, are given in table 2. Because, as expected, only moderate amounts of organic carbon were determined in these shallow-marine shelf deposits, no additional collections were made.

The 13 samples for petroleum-reservoir analyses were collected from all of the dolostone units in which vuggy porosity was observed. Although few in number, these samples were taken to analyze in moderate detail this major reservoir facies of the upper member of the Horquilla that so far has not been found elsewhere in surface or subsurface sections. Based on preliminary imbibition tests, the matrix permeability of the dolostones and the total effective porosity-permeability of the limestones were inferred to be very low. Results by Konnie W. Andrews and others at Core Laboratories in Dallas, Texas, are given in table 3; they confirm the preliminary observations, but the vuggy porosity could not be evaluated accurately with the plug analyses.

The 218 sample bags have been returned to NMBMMR for storage and contain much rock material that can be used for further analyses. Thin-section blanks are kept separately; they were etched in dilute hydrochloric acid and used in the laboratory check of the lithologic descriptions with a binocular microscope. Thin sections prepared for petrographic analyses are stored in Jacka's collection; those prepared for paleontologic analyses are stored in Wilde's collection.

TABLE 4—DESCRIPTION OF LITHOSTRATIGRAPHIC UNITS, BIG HATCHET PEAK SECTION (E 1/2 SEC. 6, T. 31 S., R. 15 W., HIDALGO COUNTY, NEW MEXICO). Each descriptive interval within a unit is designated by footages above base of unit; each sample is listed at end of description of rock type, notation indicates **BHP** unit number and footage above base of unit.

Unit	Description	Thickness (ft)
	Top is at present erosion surface on Big Hatchet Peak.	
	Horquilla Formation (Pennsylvanian-Permian), highest exposed; total estimated, 3,500 ft; total measured	3,230
	Upper member of Horquilla (Desmoinesian- Wolfcampian), highest exposed, total measured	1,867
78	Limestone, partly covered	45
	38-45 ft Limestone (100%): medium brownish gray (5YR5/1 to N5); weathers light gray (N7) to yellowish gray (5Y7/1), some red iron stain along fractures. Calcareous (100%). Matrix (80%): microcrystalline; skeletal (20%): fusulinids (4 x 6 mm), algae, crinozoans (1-1.5 nun diameter), others; fair grain tangency, some grading; lime wackestone-packstone. Hints of beds 10-30 cm thick, stylolites along some surfaces; no discernible lamination. Fairly prominent ledge; fair to poor exposure, some fractured and weathered. BHP-78-42.	
	23-38 ft Limestone (100%): resembles 0-17 ft. Moderate ledge; poor exposure, deeply weathered (covered laterally).	
	17-23 ft Covered (100%): probably limestone, some rubble. Slope.	
	0-17 ft Limestone (100%): dark brownish gray (5YR3/1) to dark yellowish brown (10YR3/2); weathers medium light gray (N6-N7). Calcareous (100%). Matrix (80%): microcrystalline; skeletal (20%): pale yellowish brown (10YR6/2), fusulinids (4 x 6 mm), algae; generally no grain tangency, some tangent with grading; lime wackestone-packstone. Beds 10-50 cm, average 40 cm thick, stylolites along surfaces; no discernible lamination; concentrations of fusulinids may indicate channels. Prominent ledge; fair to good exposure, some fractured and deeply weathered. BHP-78-4.	
77	Limestone, mostly covered	100
	75-100 ft Covered (100%): probably limestone, much rubble. Slope.	
	68-75 ft Limestone (100%): resembles 40-44 ft. Slight ledge; poor exposure.	
	60-68 ft Covered (100%): probably limestone. Slope.	
	50-60 ft Limestone (100%): resembles 40-44 ft. Slight ledge; poor exposure.	
	44-50 ft Covered (100%): probably limestone. Slope.	
	40-44 ft Limestone (100%): moderate brownish gray (5YR5/1) to pale yellowish brown (10YR5/2); weathers light gray (N7). Calcareous (100%). Matrix (60%): microcrystalline; skeletal (40%), algae, fusulinids (4 mm diameter); poor grain tangency; lime wackestone. No discernible stratification. Moderate ledge; fair to poor exposure. BHP-77-41.	
	24-40 ft Covered (100%): probably limestone. Slope.	
	21-24 ft Limestone (100%): medium brownish gray (5YR5/1); weathers light gray (N7). Calcareous (100%). Skeletal (80%): algae, mostly in small fragments, some oncoids (7 x 10 mm) with irregularly layered encrustations (3 mm thick), rare fusulinids, others; very small grains (10%): some with coats or rinds; matrix (10%): microcrystalline; lime packstone-wackestone. No discernible stratification. Moderate ledge above cliff; poor to fair exposure. BHP-77-22.	
	0-21 ft Covered (100%): probably limestone. Slope.	
76	Limestone, cliff	44
	17-44 ft Limestone (100%): resembles 0-7 ft. Beds 100 cm or more thick; upward thickening. Upper part of cliff; fair exposure.	
	10-17 ft Limestone (100%): resembles 0-7 ft. Beds 50 cm thick. Lower part of cliff; fair exposure.	
	7-10 ft Limestone (100%): dark brownish gray (5YR3/1) to dark yellowish brown (10YR4/2); weathers light gray (N7). Calcareous (100%), muddy (trace). Matrix (80%): microcrystalline calcite, silt, and probable clay; skeletal (20%): pale yellowish brown (10YR6/2), algae forming irregularly layered encrustations (3 mm thick) on oncoids, fusulinids (3 x 5 mm), others; poor grain tangency; lime wackestone. Beds 5-10 cm thick, some slightly wavy surfaces may be result of deformation, slickensides on some surfaces. Slight ledges (cliff laterally); fair exposure. BHP-76-8.	
	0-7 ft Limestone (100%): light brownish gray (5YR6/1) to pale yellowish brown (10YR6/2); weathers medium light gray (N6 to N7). Calcareous (100%). Matrix (90%): microcrystalline; skeletal (10%): algae, fusulinids (2 mm diameter), others; poor grain tangency; lime wackestone. Beds about 30 cm thick, stylolites along some surfaces; no discernible lamination. Fairly prominent ledge (forms lower part of cliff laterally, modern cave 10 ft high to southwest); fair exposure. BHP-76-3.	
75	Limestone, cliff, upper part covered	54
	44-54 ft Covered (100%): probably limestone. Slope.	
	18-44 ft Limestone (100%): resembles 4-15 ft. Fair exposure.	
	15-18 ft Limestone (100%): resembles 0-4 ft. Fair exposure.	
	4-15 ft Limestone (100%): medium brownish gray (5YR5/1); weathers light gray (N7). Calcareous (100%). Skeletal (60%): fusulinids (4 x 6 mm), algae, crinozoans, others; matrix (40%): microcrystalline; good grain tangency; lime wackestone-packstone. Beds 30-100 cm thick, stylolites along surfaces, sharp surface at base; no discernible lamination. In cliff, fair to good exposure. BHP-75-7.	
	0-4 ft Limestone (100%): brownish gray (5YR4/1) to dark yellowish brown (10YR4/2), some black specks; weathers light gray (N7), some yellow and red iron stain. Calcareous (100%), siliceous (trace). Grains (60%): very small, some black; skeletal (30%): algae, biserial foraminifers (1 x2 mm), others; matrix (10%): microcrystalline; excellent grain tangency; lime packstone-wackestone. Beds 5-10 cm thick, some wavy surfaces, sharp surface at base; no discernible lamination. Lower part of cliff; fair exposure, some weathered, nodular. BHP-75-1.	
	Mudstone (trace): moderate red (5R5/4), weathers moderate pink (5R7/4). Muddy (60%), calcareous (40%). Chalky texture, may be weathered or deformed limestone. Irregular seams 3-6 mm thick between limestone beds; some mudstone appears to fill fractures, may be filling ancient cavities.	

TABLE 4 (continued)

Unit	Description	Thickness (ft)
74	Limestone, cliff 54-115 ft Limestone (100%): resembles 35-54 ft. Upper part of cliff, recessed at top. 35-54 ft Limestone (100%): brownish gray (5YR4/1); weathers medium light gray (N6 to N7), some red iron stain. Calcareous (100%), siliceous (trace). Matrix (60%): microcrystalline; skeletal (40%): fusulinids (4 x 6 mm), very small algae?; good grain tangency; lime wackestone-packstone; porosity (trace): small scattered vugs near top on weathered surface. Beds 25 cm thick, sharp surface at base. In cliff; fair exposure. BHP-74-54. 5-35 ft Limestone (100%): brownish gray (5YR4/1); weathers light gray (N7). Calcareous (100%). Matrix (80%): microcrystalline; grains (20%): very small, some coats or rinds; poor grain tangency, lime wackestone. Hints of beds 10-30 cm thick, stylolites along some surfaces. In cliff; fair exposure, some fractured. BHP-74-35. 0-5 ft Limestone (100%): brownish gray (5YR4/1 to N4); weathers light gray (N7), some red iron stain, some very pale orange (10YR8/2), calcareous crust. Calcareous (100%). Grains (70%): very small; skeletal (20%): crinozoans (1-3 mm diameter), rare fusulinids (3-5 mm diameter), others; matrix (10%): microcrystalline; perfect grain tangency; lime packstone-grainstone. Beds 20-30 cm thick in lower part, not discernible in upper part, sharp surface at base; no discernible lamination. Lower part of cliff, recessed from ledges below; fair to good exposure. BHP-74-0.	115
73	Limestone and chert 1-5 ft Limestone (60%): resembles 0-1 ft. Moderate ledge; fair to good exposure. Chert (40%): brownish black (5YR2/1 to N2); weathers same. Siliceous (90%), calcareous (10%). Matrix (90%): microcrystalline, opaque; skeletal (10%): sponge spicules, rare crinozoans (1 mm diameter); poor grain tangency; lime wackestone. Nodules 3 x 6 cm, long axis generally parallel to bedding. **BHP-73-2.** 0-1 ft Limestone (90%): dark grayish brown (5YR3/2); weathers light gray (N7). Calcareous (90%), siliceous (10%). Matrix (70%): microcrystalline; skeletal (30%): very small, sponge spicules (1 mm long), others; poor grain tangency; lime wackestone. Beds 15 cm thick; no discernible lamination. Slight ledges; fair exposure. BHP-73-1. Chert (10%): resembles 1-5 ft.	5
72	Limestone, prominent ledge, slope at top. 35-50 ft Limestone (100%): resembles 0-35 ft. Slight ledges to slopes, partly covered. 0-35 ft Limestone (100%): brownish gray (5YR4/1); weathers light gray (N7). Calcareous (100%). Matrix (90%): microcrystalline; skeletal (10%): pale yellowish brown (10YR6/2), fusulinids (3 x 8 mm); no grain tangency; lime wackestone. Hints of beds about 100 cm thick. Prominent ledge; fair to good exposure. BHP-72-2.	50
71	Limestone, fairly prominent ledge, upper part covered 19-45 ft Covered (100%): probably limestone, may contain chert in upper part. Slope. 0-19 ft Limestone (100%): brownish gray (5YR4/1); weathers light gray (N7), some red iron stain. Calcareous (100%), siliceous (trace). Matrix (100%): microcrystalline; skeletal (trace): pale yellowish brown (10YR6/2), fusulinids (2 x 4 mm), brachiopods, others; no grain tangency; lime mudstone. No discernible stratification. Fairly prominent ledge; poor to fair exposure, some fractured and weathered. BHP-71-2.	45
70	Dolostone, cliff, slope at top. 37-54 ft Dolostone (100%): resembles 0-37 ft. Moderate to slight ledges above cliff, covered slope at top. 0-37 ft Dolostone (100%): light brownish gray (5YR6/1 to N6); weathers very pale orange (10YR8/2). Dolomitic (100%), siliceous (trace). Matrix (100%): medium to coarsely crystalline, rhombic, mosaic; skeletal (trace): ghosts of crinozoans?, others; poor grain tangency; lime mudstone; porosity (trace): vugs 0.5-1 mm diameter on fresh surface, 10-20 mm on weathered surface. No discernible stratification. Upper part of cliff, fair to good exposure. BHP-70-3.	54
69	Limestone, minor chert, cliff 75-87 ft Limestone (100%): medium brownish gray (5YR5/1); weathers medium gray (N6). Calcareous (100%). Matrix (80%): microcrystalline; skeletal (20%): algae, others; poor grain tangency; lime wackestone. Hints of beds 20-30 cm thick. Upper part of cliff; slightly recessed; fair exposure. BHP-69-85. 44-75 ft Limestone (100%): resembles 20-25 ft. Matrix (60%); skeletal (40%): algae, few fusulinids. Beds 10-50 cm thick, stylolites along surfaces. In cliff; fair exposure, some local solution produced pockmarked weathered surface. 25-44 ft Limestone (100%): resembles 20-25 ft. Matrix (100%). Fairly prominent ledges to cliff; fair exposure. 20-25 ft Limestone (100%): brownish gray (5YR4/1); weathers light gray (N7). Calcareous (100%), siliceous (trace). Matrix (70%): microcrystalline; skeletal (30%): pale yellowish brown (10YR6/2), fusulinids (3 x 6 mm); fair grain tangency, no dominant orientation; lime wackestone-packstone. Beds 5-25 cm thick; no discernible lamination. Fairly prominent to moderate ledges (cliff to southwest); fair to good exposure. BHP-69-24. 15-20 ft Limestone (100%): resembles 0-10 ft. 10-15 ft Limestone (90%): dark brownish gray (5YR3/1); weathers light gray (N7). Calcareous (100%). Matrix (100%): microcrystalline; lime mudstone. Beds 10-20 cm thick, sharp surfaces, some deformed. Slightly recessed part of cliff; fair exposure. Chert (10%, absent to east): brownish gray (5YR4/1 to N4); weathers pale yellowish brown (10YR7/2). Siliceous (100%), calcareous (trace). Matrix (90%): microcrystalline, opaque to translucent; skeletal (10%): sponge spicules, others; poor grain tangency; lime wackestone. Nodules 15-25 cm in height, some are linked to form bodies 100 cm long. BHP-69-14. 0-10 ft Limestone (100%): brownish gray (5YR4/1 to N5); weathers light gray (N7). Calcareous (100%). Matrix (80%): microcrystalline; skeletal (20%): pale yellowish brown (10YR6/2 to N6), fusulinids (3 x 4 mm), algae, others; fair grain tangency; lime wackestone-packstone. Beds 10-25 cm thick, stylolites along surfaces; no discernible lamination. Lower part of cliff; fair to good exposure. BHP-69-3.	87

TABLE 4 (continued)

Unit	Description	Thickness (ft)
68	Limestone, cliff, upper part covered 100-120 ft Covered (100%): probably limestone. Talus slope. 70-100 ft Limestone (100%): resembles 35-70 ft. Moderate to slight ledges; poor exposure, partly covered. 35-70 ft Limestone (100%): medium brownish gray (5YR5/1 to N5); weathers light gray (N7 to N6). Calcareous (100%), siliceous (trace). Matrix (90%): microcrystalline, skeletal (10%): fusulinids (3 x 6 mm), crinozoans, algae?, others; poor grain tangency; lime wackestone. No discernible stratification. Upper part of cliff; poor to fair exposure, some fractured and weathered. BHP-68-70. 8-35 ft Limestone (100%): resembles 0-5 ft. 5-8 ft Limestone (100%): resembles 0-5 ft. Skeletal material is concentrated in lower parts of some beds. 0-5 ft Limestone (100%): dark brownish gray (5YR3/1); weathers medium light gray (N6). Calcareous (100%). Matrix (80%): microcrystalline; skeletal (20%): pale yellowish brown (10YR6/2), fusulinids (4 x 6 mm), crinozoans, algae, rare brachiopods; poor grain tangency; lime wackestone. Beds 10-35 cm thick; no discernible lamination. Lower part of cliff; fair to good exposure. BHP-68-4.	120
67	Dolostone, upper part covered 115-148 ft Covered (100%): probably dolostone. Talus slope covered by soil and vegetation. 75-115 ft Dolostone (100%): resembles 15-30 ft. Matrix (100%); skeletal (trace): ghosts of crinozoans, others; no grain tangency; lime mudstone; porosity (trace): vugs 1-2 mm diameter, rarely 5 mm, some on weathered surface. Fairly prominent ledges; fair exposure, partly weathered. BHP-67-114. 55-75 ft Dolostone (100%): resembles 15-30 ft. Vugs 1 mm diameter on fresh surface, more numerous than those of 15-30 ft, less evident on weathered surface. Prominent ledge (forms upper part of cliff to southwest); fair to good exposure. BHP-67-68. 30-55 ft Dolostone (100%): resembles 15-30 ft. Moderate to fairly prominent ledges (forms cliff to southwest); poor to fair exposure, partly covered. 15-30 ft Dolostone (100%): light brownish gray (5YR7/1 to N7): weathers very pale orange (10YR8/2) to pinkish gray (5YR8/1). Dolomitic (100%). Matrix (90%): medium to coarsely crystalline, rhombic, mosaic; lime mudstone; porosity (10%): vugs 1-3 mm diameter on fresh surface, up to 10 mm on weathered surface, some partly filled with yellowish to greenish impure calcite. No discernible stratification. Prominent ledges; fair to good exposure. BHP-67-22. 0-15 ft Dolostone (100%): medium brownish gray (5YR5/1 to N5); weathers pale yellowish brown (10YR6/2). Dolomitic (100%), calcareous (trace). Matrix (100%): medium crystalline, rhombic, mosaic; skeletal (trace): crinozoans (1 mm diameter), not replaced, others; no grain tangency; lime mudstone; porosity (trace): vugs 0.5-1 mm diameter. No discernible stratification. Moderate ledge in lower part to prominent ledge in upper part; fair to good exposure. BHP-67-10.	148
66	Limestone 17-30 ft Limestone (100%): resembles 0-17 ft. Slight ledges; poor exposure, partly covered. Chert (trace): small nodules. 0-17 ft Limestone (100%): brownish gray (5YR5/1 to N5); weathers light gray (N7). Calcareous (100%). Matrix (90%): microcrystalline, opaque to translucent, may be recrystallized; skeletal (10%): fusulinids (2 x 6 mm), others; no grain tangency; lime wackestone. Hints of beds over 100 cm thick; irregular replacement contact with underlying dolostone, I ft relief. Moderate to fairly prominent ledge; fair exposure. BHP-66-9.	30
65	Dolostone 80-97 ft Dolostone (100%): resembles 0-15 ft. Matrix (100%): coarsely to very coarsely crystalline, rhombic, mosaic; lime mudstone; porosity (trace): vugs 1-2 mm diameter. Fairly prominent ledges; fair exposure. BHP-65-94. 40-80 ft Dolostone (100%): resembles 0-15 ft. Matrix (90%); porosity (10%): vugs resemble 15-40 ft. Moderate to slight ledges; poor exposure, partly covered. 15-40 ft Dolostone (100%): resembles 0-15 ft. Matrix (90%); lime mudstone; porosity (10%): vugs 0.5-1 mm diameter on fresh surface, 2-20 mm, average 5 mm diameter, on weathered surface. Fairly prominent ledge; fair exposure. BHP-65-22. 0-15 ft Dolostone (100%): light brownish gray (5YR7/1 to N7); weathers yellowish gray (5Y8/1). Dolomitic (100%). Matrix (100%): medium to coarsely crystalline, rhombic, mosaic; skeletal (trace): ghosts of crinozoans, others; no grain tangency; lime mudstone; porosity (trace): vugs 1 mm diameter. Hints of beds over 100 cm thick, sharp surface at base; dolostone replacement locally extends slightly below the top into underlying limestone. Moderate ledge; fair exposure. BHP-65-2.	97
64	Limestone 0-26 ft Limestone (100%): light brownish gray (5YR7/1 to N7); weathers light gray (N7). Calcareous (100%). Matrix (60%): microcrystalline, may be partly recrystallized; skeletal (40%): phylloid algae, fusulinids (2.5 x 4.5 mm), others; fair grain tangency; lime wackestone-packstone. Hints of beds about 400 cm thick. Fairly prominent ledge; fair exposure. BHP-64-1.	26
63	Dolostone 15-23 ft Dolostone (100%): resembles 0-15 ft. Slight ledges to slopes, poor exposure, partly covered. 0-15 ft Dolostone (100%): light pinkish gray (5YR7/1 to 5YR8/1 to N8); weathers grayish orange (10YR7/4) to pale yellowish brown (10YR6/2), yellow iron stain. Dolomitic (100%). Matrix (90%): coarsely crystalline, minor very coarsely crystalline, rhombic, mosaic, some sucrosic; skeletal (trace): ghosts of crinozoans; no grain tangency; lime mudstone; porosity (10%): vugs 1-2 mm in diameter on fresh surface, trace of intercrystalline porosity, on weathered surface see 30% vuggy porosity with vugs up to 10 mm diameter. Hints of beds about 200 cm thick, sharp surface at base. Fairly prominent ledge (forms cliff to southwest); fair exposure. BHP-63-2.	23

TABLE 4 (continued)

Unit	Description	Thickness (ft)
62	Limestone, thicker beds than below, cliff 75-95 ft Limestone (100%): resembles 0-40 ft. Phylloid algae present. Moderate ledges to slopes above top of cliff; poor exposure, partly covered. 65-75 ft Limestone (100%): resembles 0-40 ft. Phylloid algae present. Single bed? Uppermost part of cliff. 50-65 ft Limestone (100%): resembles 0-40 ft. Matrix (60%); skeletal (40%). No phylloid algae. Beds 10-30 cm thick, sharp surface at base. In cliff, slightly recessed; fair exposure. 40-50 ft Limestone (100%): resembles 0-40 ft. Highly fractured. 0-40 ft Limestone (100%): light brownish gray (5YR7/1 to N7); weathers light gray (N7). Calcareous (100%). Matrix (60%): microcrystalline, may be partly recrystallized; skeletal (40%): phylloid algae (more evident on weathered surface), fusulinids (2 x 3 mm), crinozoans, others; fair grain tangency, lime wackestone-packstone. Hints of beds about 200 cm thick, sharp surface at base. In cliff, fair exposure. BHP-62-5.	95
61	Limestone, thinner beds than above, cliff 10-15 ft Limestone (100%): resembles 0-5 ft. Beds 20-30 cm thick. 5-10 ft Limestone (100%): resembles 0-5 ft. Skeletal (70%): phylloid algae, small algae, crinozoans, others; matrix (30%): microcrystalline; good grain tangency; lime wackestone-packstone. Beds 30-50 cm thick, stylolites along surfaces, sharp stylolitic surface at base with 10 cm relief; no discernible lamination. In cliff, fair to good exposure. 0-5 ft Limestone (100%): medium brownish gray (5YR5/1 to N5); weathers light gray (N7). Calcareous (100%), siliceous (trace). Grains (70%): very small, skeletal (20%): algae, fusulinids (2 x 3 mm), others; matrix (10%): microcrystalline; good grain tangency; lime wackestone-packstone. Beds 15-20 cm thick, stylolites along surfaces, sharp surface at base; no discernible lamination. In cliff, slightly recessed; fair to good exposure. BHP-61-2.	15
60	Limestone, beds thinner upward, cliff 0-23 ft Limestone (100%): light gray (N7), light brownish gray (5YR6/1); weathers medium light gray (N6 to N7). Calcareous (100%), siliceous (trace). Skeletal (100%): abundant crinozoans (1-3 mm diameter), some replaced by chert, others; matrix (trace, increases toward top): microcrystalline; excellent grain tangency; lime packstone. Beds show upward thinning from 50 to 10 cm, sharp surface at base. Lower part of cliff; fair exposure. BHP-60-2. Chert (trace): small nodules.	23
59	Limestone and chert 0-3 ft Limestone (60%): light brownish gray (5YR6/1 to N6); weathers light gray (N7). Calcareous (100%). Matrix (60%): microcrystalline; grains (40%): very small; fair grain tangency; lime wackestone-packstone; partly recrystallized to sparry calcite. Hints of beds 10-30 cm thick, sharp surface at base; no discernible lamination. Fairly prominent ledge (forms cliff to southwest); fair to good exposure. BHP-59-1. Chert (40%): light brownish gray (5YR6/1); weathers light brown (5YR6/4) to light brownish gray (5YR6/1), much red iron stain. Siliceous (80%), calcareous (20%). Matrix (90%): microcrystalline; skeletal (10%): crinozoans (up to 4 mm diameter), others, not replaced; poor grain tangency; lime wackestone. Nodules 10 x 30 cm. BHP-59-2.	3
58	Limestone, fairly prominent ledge 0-22 ft Limestone (100%): light brownish gray (5YR6/1); weathers light gray (N7). Calcareous (100%). Matrix (90%): microcrystalline; skeletal (10%): fusulinids (1.5 x 4 mm), crinozoans, others; poor grain tangency; lime wackestone. Hints of beds 15-20 cm thick. Fairly prominent ledge (forms cliff to southwest); fair exposure. BHP-58-1. Chert (trace): small nodules in upper part.	22
57	Limestone and minor chert 25-65 ft Limestone (100%): resembles 0-15 ft. Slight ledges to slopes; poor exposure, covered at top. 15-25 ft Limestone (100%): resembles 0-15 ft. White skeletal material (algae?) on weathered surface. Stylolites along bedding surfaces. Moderate ledge; poor to fair exposure. BHP-57-23. 0-15 ft Limestone (100%): medium brownish gray (5YR5/1); weathers light gray (N7.). Calcareous (100%). Matrix (60%): microcrystalline; skeletal (40%): algae, crinozoans (coarser at base), rare fusulinids (2 mm diameter); grains (trace): very small; excellent grain tangency; lime packstone-wackestone. Hints of beds 30-50 cm thick, sharp surface at base, slightly undulating. Slight ledge to slope; poor to fair exposure, partly covered in lower part. BHP-57-10. Chert (trace): small nodules.	65
56	Dolostone 90-103 ft Dolostone (100%): light brownish gray (5YR7/1); weathers light pinkish gray (5YR8/1 to 5YR7/1). Dolomitic (100%), siliceous (trace). Matrix (100%): medium to coarsely crystalline; rhombic, mosaic; lime mudstone; porosity (trace): vugs about 1 mm diameter on fresh surface, on weathered surface 10% vuggy porosity seen with vugs 10-30 mm diameter. Hints of beds 20-30 cm thick. Fairly prominent ledge; fair exposure. BHP-56-92. 30-90 ft Dolostone (100%): resembles 0-15 ft. Fairly prominent ledge; fair to poor exposure. Mudstone (trace): red. Fills vertical fracture 1-5 cm wide, at 30-33 ft, trends N. 70° E. 15-30 ft Covered (100%): probably dolostone. Slope. 0-15 ft Dolostone (100%): brownish gray (5YR4/1); weathers light brownish gray (5YR7/1 to N7). Dolomitic (100%). Matrix (90%): medium to coarsely crystalline, rhombic, mosaic; skeletal (10%): ghosts of crinozoans, others; no grain tangency; lime wackestone; porosity (trace): vugs about 1 mm diameter on fresh surface, on weathered surface see 20% vuggy porosity with vugs averaging 2 mm diameter, some up to 15 mm. Hints of beds 50-100 cm thick, fairly sharp surface at base; no discernible lamination. Prominent ledge; fair exposure, some fractured and weathered. BHP-56-7.	103

TABLE 4 (continued)

Unit	Description	Thickness (ft)
55	Limestone and chert, cliff, upper part covered 35-45 ft Covered (100'o): probably limestone and chert. Dip slope on top of cliff. 20-35 ft Limestone (80%): resembles 0-10 ft. Uppermost part of cliff. Chert (20%): resembles 0-10 ft. 10-20 ft Limestone (70%): resembles 0-10 ft. Upper part of cliff, slightly recessed. Chert (30%): resembles 0-10 ft. 0-10 ft Limestone (80%): medium brownish gray (5YR5/1); weathers light gray (N7). Calcareous (100%), siliceous (trace). Matrix (80%): microcrystalline; skeletal (20%): fusulinids (1 x 2 mm), crinozoans, others, some replaced by chert; grains (trace): very small; poor grain tangency; lime wackestone. Hints of beds 30-50 cm thick, fairly sharp surface at base; no discernible lamination. Upper part of cliff; fair to good exposure. BHP-55-2. Chert (20%): light brownish gray (5YR6/1), bluish; weathers pale yellowish brown (10YR6/2) to light brown (5YR6/4). Siliceous (90%), calcareous (10%). Matrix (90%): microcrystalline, translucent to opaque; skeletal (10%): partially replaced by chert, fusulinids (1 mm diameter), algae?, crinozoans, others; no grain tangency; lime wackestone. Nodules up to 10 x 80 cm. BHP-55-3.	45
54	Limestone, minor chert, some ancient-cavity fill, cliff 105-120 ft Limestone (90%): resembles 0-15 ft. Upper part of cliff (10 yards to west is modern cave 10 ft high, 10 ft wide, 30 ft deep, with large sparry calcite crystals and fallen limestone blocks in fill). Chert (10%): resembles 0-15 ft. 97-105 ft Limestone (90%): resembles 0-15 ft. In cliff. Chert (10%): resembles 0-15 ft. Ancient cavity fill (local, in limestone host): red limestone and mudstone resembling 95-97 ft. Contains limestone lithoclasts 3 mm in diameter. Fills ancient cavity 8 ft high, 2 ft wide. 95-97 ft Limestone (90%): resembles 0-15 ft. In cliff. Chert (10%): resembles 0-15 ft. Ancient cavity fill (local, in limestone host): Limestone (70%): moderate reddish brown (10R5/6), weathers light brown (5YR6/6). Calcareous (100%), muddy (trace). Matrix (90%): microcrystalline calcite, silt and probable clay; grains (10%): very small; poor grain tangency, hints of grading; lime wackestone. Fills ancient cavity 2 ft (50 cm) high, 3 ft (80 cm) wide; beds 2-5 mm thick, appear to lap out against wall of cavity; horizontal laminae 1 mm or less thick, some slightly inclined or broad ripple laminae truncated by base of overlying laminaset, some slightly deformed, some convoluted. Recessed in cliff; fair to good exposure. BHP-54-96 (includes mudstone). Mudstone (30%): dusky red (5R3/4) to dark reddish brown (10R3/4), weathers grayish red (5R4/2). Muddy (80%): quartz silt and illite clay (X-ray identification by R.M. North, NMBMMR); calcareous (20%), sandy (trace). Matrix (100%): silt, clay, and microcrystalline calcite; sand grains (trace): very coarse lithoclasts of gray limestone, fine to very fine quartz; poor grain tangency, hints of grading; indurated, platy, fissile (shaly). Interlayered with limestone in ancient cavity fill; beds 1-3 mm thick; hints of horizontal lamination. 15-95 ft Limestone (90%): resembles 0-15 ft. Main part of cliff. Chert (10%): resembles 0-15 ft. 0-15 ft Limestone (90%): dark brownish gray (5YR3/1); weathers medium light gray (N6). Calcareous (100%). Matrix (90%): microcrystalline; skeletal (10%): fusulinids (1 mm diameter), others; no grain tangency; lime wackestone. Hints of beds 30-50 cm thick, fairly sharp surface at base. In lower part of cliff; poor to fair exposure, some fractured and weathered. BHP-54-2. Chert (10%): medium brownish gray (5YR5/1), bluish; weathers light brown (5YR6/4) to pale yellowish brown (10YR6/2). Siliceous (90%), calcareous (10%). Matrix (90%): microcrystalline, opaque to translucent; skeletal (10%): fusulinids (1.5 mm diameter), others; no grain tangency; lime wackestone. Nodules 10 x 20 cm to 10 x 50 cm. BHP-54-4.	120
53	Limestone, fairly prominent ledge 15-23 ft Limestone (100%): resembles 0-15 ft. Chert (trace): scattered small nodules. 0-15 ft Limestone (100%): brownish gray (5YR4/1); weathers light gray (N7). Calcareous (100%). Matrix (90%): microcrystalline; skeletal (10%): crinozoans (1-3 mm diameter), algae, rare fusulinids; ooids? (trace): very small; no grain tangency; lime wackestone. Hints of beds about 50 cm thick. Fairly prominent ledge recessed in lower part of cliff; poor to fair exposure, fractured and weathered. BHP-53-1, BHP-53-3 (fusulinids).	23
52	Limestone and chert, cliff 0-35 ft Limestone (70%): brownish gray (5YR4/1 to N4); weathers light gray (N7). Calcareous (100%). Matrix (90%): microcrystalline; skeletal (10%): crinozoans, fusulinids, some rugose corals and brachiopods on weathered surface; no grain tangency; lime wackestone. Hints of beds 10-50 cm thick. Lower part of cliff; fair to good exposure. BHP-52-2, BHP-52-5 (fusulinids). Chert (30%): brownish gray (5YR4/1); weathers pale yellowish brown (10YR6/2) to light brown (5YR6/4). Siliceous (80%), calcareous (20%), carbonaceous (trace in discontinous laminae less than 1 mm thick). Matrix (100%): microcrystalline; opaque; skeletal (trace): fusulinids (1.5 mm); no grain tangency; lime mudstone. Nodules 5 x 10 cm to 10 x 50 cm, fairly regular shapes with long axes generally parallel to bedding. BHP-52-3.	35

TABLE 4 (continued)

Unit	Description	Thickness (ft)
51	Limestone, minor chert, cliff 4-12 ft Limestone (100%): resembles 0-3 ft. 3-4 ft Limestone (70%): resembles 0-3 ft. Chert (30%): very deeply weathered, reddish brown nodules. Probable replacement of skeletal material. Forms hackly pattern on weathered surface. 0-3 ft Limestone (100%): brownish gray (5YR4/1 to N4); weathers light gray (N7). Calcareous (100%). Matrix (100%): microcrystalline; skeletal (trace): algae? (1 mm wide), white, recrystallized to sparry calcite; no grain tangency; lime mudstone. Single bed?, sharp surface at base. Lower part of cliff; fair to poor exposure, fractured, calcite veins. **BHP-51-2.**	12
50	Limestone, partly covered 30-42 ft Limestone (100%): resembles 0-2 ft. Moderate ledge at base of cliff; poor exposure. 25-30 ft Covered (100%): probably limestone. Slope. 20-25 ft Limestone (100%): resembles 0-2 ft. Slight ledge; poor exposure. 10-20 ft Covered (100%): probably limestone. Slope. 4-10 ft Limestone (100%): resembles 0-2 ft. Slight ledge; poor exposure. 2-4 ft Covered (100%): probably limestone. Slope. 0-2 ft Limestone (100%): light brownish gray (5YR6/1 to N6); weathers light gray (N7). Calcareous (100%). Grains (60%): very small, some coats or rinds; matrix (30%): microcrystalline; skeletal (10%): crinozoans, fusulinids (3 mm diameter), others; partially recrystallized to sparry calcite, translucent to transparent; good grain tangency; lime wackestone-packstone. Single bed?, fairly sharp surface at base, irregular replacement contact with underlying dolostone. Slight ledge, poor to fair exposure. BHP-50-1.	42
49	Dolostone, cliff 50-59 ft Dolostone (100%): resembles 0-9 ft. Moderate ledge to slope above top of cliff; poor exposure. 19-50 ft Dolostone (100%): resembles 0-9 ft. Lichens cover part of weathered surface. No discernible stratification. In upper part of cliff, poor to fair exposure. BHP-49-30, BHP-49-45. 9-19 ft Dolostone (100%): resembles 0-9 ft. Lichens cover part of weathered surface. Where not covered (to east), vugs 10-20 mm diameter average seen, some up to 50-100 mm diameter, forming 30% of weathered surface. Hints of beds about 50 cm thick, fairly sharp surface at base. In cliff, fair exposure. BHP-49-14, BHP-49-19. 0-9 ft Dolostone (100%): light brownish gray (5YR7/1 to N7); weathers pinkish gray (5YR8/1) to yellowish gray (5Y8/1), some dark mottling by lichens. Dolomitic (100%). Matrix (100%): medium to coarsely crystalline, rhombic, mosaic; porosity (trace): few small vugs 1-3 mm diameter on fresh surface; lime mudstone; in basal 0.5 ft are intraclasts? (trace): barely discernible flat pebbles 10-30 mm long and 5-10 mm wide, angular, some imbricated to dip S. 45° W. Beds about 100 cm thick, sharp surface at base; no discernible lamination. In cliff; fair exposure. BHP-49-1, BHP-49-4, BHP-49-9.	59
48	Limestone, laterally equivalent dolostone, cliff 2-5 ft Limestone (100%): brownish gray (5YR4/1); weathers light gray (N7). Calcareous (100%). Matrix (90%): microcrystalline, slightly altered; skeletal (10%): crinozoans (2 mm diameter), fusulinids (1 mm diameter), others. Beds 10-20 cm thick; no discernible lamination. Prominent ledge (slightly recessed from cliff); fair to good exposure. BHP-48-2a. Dolostone (laterally 100%): light brownish gray (5YR7/1 to N7); weathers pinkish gray (5YR8/1) to yellowish gray (5YR8/1). Dolomitic (100%), siliceous (trace). Matrix (100%): medium to coarsely crystalline, rhombic, mosaic; lime mudstone. Replacement boundary with overlying limestone rises to southwest through the entire interval in 2 ft lateral distance; 20 ft from fault zone. BHP-48-2b. 0-2 ft Limestone (100%): medium brownish gray (5YR5/1 to N5); weathers light gray (N7). Calcareous (100%). Matrix (100%): microcrystalline; skeletal (trace): small types, some phylloid algae; no grain tangency; lime mudstone. Beds 10-20 cm thick, stylolites along surfaces, sharp surface at base; no discernible lamination. Prominent ledge (slightly recessed from cliff); fair to good exposure, some fractured. BHP-48-1.	5
47	Limestone and chert, cliff 30-40 ft Limestone (100%): resembles 0-5 ft. Matrix (100%); skeletal (trace): phylloid algae. Some bedding surfaces are irregular, fairly sharp surface at base. Fair to poor exposure, some fractured. 25-30 ft Limestone (100%): resembles 0-5 ft. Slight increase in phylloid algae. Single bed, sharp surface with stylolites at base. Fair to good exposure. 5-25 ft Limestone (100%): resembles 0-5 ft. Clusters of phylloid algae. No discernible stratification. Fair to good exposure. 0-5 ft Limestone (80%): light brownish gray (5YR6/1 to N6); weathers light gray (N7). Calcareous (100%). Matrix (90%): microcrystalline; skeletal (10%): phylloid algae, dasyclad? algae (thalli 2 x 4 mm), other small types; no grain tangency; lime wackestone. Hints of beds 10-50 cm thick. In cliff, fair to good exposure. BHP-47-1. Chen (20%): light brownish gray (5YR6/1), pale red purple (5RP6/2); weathers light brown (5YR5/6). Siliceous (100%). Matrix (100%): microcrystalline, opaque to translucent; skeletal (trace): small types; no grain tangency; lime mudstone. Bands 5 x 70 cm and nodules 5 x 10 cm, fairly regular shapes. BHP-47-2.	40
46	Limestone and dolostone, cliff 16-33 ft Limestone (100%): light brownish gray (5YR6/1 to N6); weathers light gray (N7). Calcareous (100%): locally dolomitic (trace). Matrix (90%): microcrystalline; skeletal (10%): phylloid algae, tabulate corals (up to 4 mm wide); no grain tangency; lime wackestone. Beds 5 cm thick in lower part, not discernible in upper part, sharp surface at base. In cliff; fair exposure, some fractured and slightly weathered. BHP-46-17.	33

TABLE 4 (continued)

Unit	Description	Thickness (ft)
	10-16 ft Limestone (100%): resembles 0-4 ft.	
	4-10 ft Dolostone (100%): light gray (N7) to light brownish gray (5YR7/1); weathers light yellowish gray (5Y8/1) to light pinkish gray (5YR8/1). Dolomitic (100%). Matrix (100%): medium to coarsely crystalline, rhombic, mosaic, no visible porosity; lime mudstone. No discernible stratification. In cliff; fair to good exposure. BHP-46-5.	
	Limestone (laterally 100%): resembles 0-4 ft. Dolostone grades laterally into skeletal limestone a few yards to south-southwest.	
	0-4 ft Limestone (100%): light brownish gray (5YR6/1 to N6); weathers light gray (N7), light olive gray (5Y7/1). Calcareous (100%), siliceous (trace). Skeletal (60%): phylloid algae, form olive hackly pattern on weathered surface, in hand specimen some thalli (1 mm thick) are seen to be selectively replaced by chert; matrix (40%): microcrystalline, some patches up to 2 x 2 cm between algal plates; fair grain tangency; lime wackestone-packstone; cement (trace): sparry calcite fills former cavities. Single bed?, sharp surface at base. Lower part of cliff; fair to good exposure, much fractured and weathered. BHP-46-1.	
45	Limestone and dolostone, partly covered	61
	57-61 ft Limestone (100%): resembles 10-29 ft. Matrix (100%). Basal part of cliff; poor exposure, fractured and weathered.	
	50-57 ft Limestone (100%): resembles 10-29 ft. Matrix (90%); skeletal (10%): phylloid algae. Moderate ledge to slope, moderately weathered.	
	41-50 ft Limestone (100%): resembles 10-29 ft. Moderate ledge; deeply weathered and fractured.	
	36-41 ft Limestone (100%): resembles 10-29 ft.	
	29-36 ft Covered (100%): probably limestone. Slope.	
	10-29 ft Limestone (100%): light brownish gray (5YR6/1 to N6); weathers light gray (N7 to N6). Calcareous (100%). Skeletal (60%): phylloid algae, form olive hackly pattern on weathered surface, in hand specimen some white to pinkish thalli (1 mm wide) are preserved, others are replaced or recrystallized; rare fusulinids; matrix (40%): microcrystalline; fair grain tangency; lime wackestone-packstone; cement (trace): sparry calcite fills former cavities. Hints of beds about 50 cm thick. Slight to moderate ledges; fair exposure, some fractured and weathered. BHP-45-17.	
	3-10 ft Covered (100%): probably limestone. Slope.	
	0-3 ft Limestone (60%): brownish gray (5YR4/1) to olive gray (5Y4/1); weathers light gray (N7). Calcareous (100%). Matrix (60%): microcrystalline; grains (40%): very small, some coats or rinds; skeletal (trace): very small types; fair grain tangency; lime wackestone-packstone. No discernible stratification, fairly sharp bedding surface at base. Slight ledges, poor exposure, partly covered, fractures filled with calcite. BHP-45-2.	
	Dolostone (40%): light brownish gray (5YR6/1 to N6); weathers pinkish gray (5YR8/1). Dolomitic (70%), siliceous (30%). Matrix (90%): finely to medium crystalline, rhombic?, mosaic; skeletal (10%): tabulate corals, including favositids and silicified chaetetids, form distinctive zone at base. Replacement bodies 30-50 cm diameter, some centers are coral colonies, occur in limestone host. BHP-45-1, BHP-45-3 (corals).	
44	Limestone, fairly prominent ledge at base, partly covered	15
	12-15 ft Limestone (100%): brownish gray (5YR4/1); weathers light gray (N7). Calcareous (100%). Matrix (100%): microcrystalline; skeletal? (trace): very small types. Beds 10-20 cm thick. Slight ledges; poor to fair exposure (covered laterally).	
	9-12 ft Covered (100%): probably limestone. Slope.	
	0-9 ft Limestone (100%): light brownish gray (5YR6/1) to light olive gray (5Y6/1); weathers light gray (N7) to very light gray (N8), some mottled. Calcareous (100%). Matrix (100%): microcrystalline; skeletal (trace): brachiopod shells (8 mm diameter), others; no grain tangency; lime mudstone. Cement (trace): sparry calcite (may be secondary). Beds 20-30 cm thick, stylolites with 6 cm relief along some surfaces, sharp surface at base; no discernible lamination. Fairly prominent ledge; fair to good exposure, some fractures filled with calcite. BHP-44-2.	
43	Limestone, irregular laminations	8
	0-8 ft Limestone (100%): light brownish gray (5YR5/1) and interlayered light olive gray (5Y5/1); weathers light gray (N7) and yellowish to greenish gray (5Y8/1 to 5GY8/1) in irregular laminations. Calcareous (80%), dolomitic (20%). Skeletal (70%): brachiopod shells (4 x 7 x 7 mm), crinozoans, others; matrix (30%): microcrystalline calcite and finely to medium crystalline dolomite; cement (trace): former cavities (2 x 4 mm) filled with sparry calcite; good grain tangency; lime packstone-wackestone. Beds 10-30 cm thick, stylolites along surfaces, sharp surface at base; laminasets 30 mm thick; laminae 1 mm thick or less, slightly irregular surfaces, some wispy. Moderate ledge; fair to good exposure. BHP-43-7.	
	Contact may be slightly disconformable	
	Lower member of Horquilla (Morrowan-Desmoinesian)	1,363
42	Limestone and chert	28
	0-28 ft Limestone (70%): brownish gray (5YR4/1 to N4); weathers light gray (N7). Calcareous (100%). Matrix (90%): microcrystalline; skeletal (10%): crinozoans (1-4 mm diameter, some diagonal to bedding), fusulinids (2 x 6 mm); poor grain tangency; lime wackestone. Beds 10-50 cm thick, thicker beds contain larger crinozoan fragments; no discernible lamination. Slight to moderate ledges; fair to good exposure. BHP-42-12.	
	Chert (30%): medium brownish gray (5YR5/1 to N5), some with light bluish tinge; weathers pale yellowish brown (10YR6/2) to light brown (5YR6/4). Siliceous (100%), calcareous (trace), pyritic (trace). Matrix (90%): microcrystalline, opaque to translucent; skeletal (10%): crinozoans (1.5 mm diameter), fusulinids; no grain tangency; lime wackestone. Nodules 5 x 10 cm to 10 x 50 cm, some linked, some anastomosed, few bands 5-10 cm thick. BHP-42-14.	

TABLE 4 (continued)

Unit	Description	Thickness (ft)
41	Limestone, partly covered. 48-64 ft Covered (90%): probably limestone and chert. Slope. Limestone (10%): resembles 20-25 ft. Slight ledges; poor exposure. Chert (trace): resembles 20-25 ft. 45-48 ft Limestone (100%): resembles 20-25 ft. Rare rugose corals. Chert (trace): resembles 20-25 ft. Nodules 3 x 5 cm to 12 x 18 cm. 25-45 ft Covered (90%): probably limestone and chert. Slope. Limestone (10%): resembles 20-25 ft. Slight ledges, poor exposure. Chert (trace): resembles 20-25 ft. Nodules 15 x 40 cm. 20-25 ft Limestone (100%): dark brownish gray (5YR3/1 to N3); weathers light gray (N7). Calcareous (100%), siliceous (trace). Matrix (90%): microcrystalline; skeletal (10%): algae? (1 mm diameter, some 5 mm long, white), partially replaced or filled with silica and calcite, others; grains (trace): very small; no grain tangency; lime wackestone. Hints of beds 10-30 cm thick. Slight ledges to slopes; poor exposure, partly covered. BHP-41-20. Chert (trace): dark brownish gray (5YR3/1); weathers pale yellowish brown (10YR6/2). Siliceous (80%), calcareous (20%). Matrix (100%): microcrystalline; skeletal (trace); no grain tangency; lime mudstone. Nodules 2 x 4 cm to 3 x 30 cm, irregular shapes. 0-20 ft Covered (90%): probably limestone and chert. Slope. Limestone (10%): resembles 20-25 ft. Slight ledges to slope; poor exposure. Chert (trace): resembles 20-25 ft.	64
40	Limestone 0-11 ft Limestone (100%): brownish gray (5YR4/1); weathers light gray (N7 to N6). Calcareous (100%). Grains (80%): small ooids and peloids (less than 1 mm diameter), coated grains, some elongate (0.5 x 2 mm); skeletal (10%): crinozoans, fusulinids, tabulate corals; matrix (10%): microcrystalline; perfect packing; lime packstone-grainstone. Hints of beds 50 cm thick. Moderate ledge; fair exposure. BHP-40-1.	11
39	Limestone, chert in large nodules, partly covered 13-26 ft Covered (90%): probably limestone and chert. Limestone (10%): resembles 0-13 ft. Slight ledges, poor exposure. Chert (trace): resembles 0-13 ft. 0-13 ft Limestone (80%): light brownish gray (5YR6/1 to N6); weathers light gray (N7 to N6). Calcareous (100%). Matrix (70%): microcrystalline to sparry?, some translucent, may be recrystallized; skeletal (30%): crinozoans, fusulinids, others; fair grain tangency; lime wackestone-packstone. Beds 10-50 cm, average 30 cm thick; no discernible lamination. Moderate ledge; fair to good exposure. BHP-39-1. Chert (20%): light brownish gray (5YR6/1), white (N9), slight bluish tinge; weathers pale yellowish brown (10YR6/2) to light brown (5YR6/4). Siliceous (90%), calcareous (10%). Matrix (70%): microcrystalline, opaque to translucent; skeletal (30%): fusulinids, others, some not replaced; fair grain tangency; lime wackestone-packstone. Nodules 6 x 16 cm up to 50 x 60 cm, larger ones have irregular shapes, some smaller ones are linked; band 5 cm thick. BHP-39-4.	26
38	Limestone and chert 70-82 ft Limestone (100%): resembles 10-14 ft. Beds 10-30 cm thick. Slight to moderate ledges; fair exposure, slightly weathered. Chert (trace): resembles 14-35 ft. 50-70 ft Limestone (90%): resembles 10-14 ft. Slight ledges to slope; poor exposure, partly covered. Chert (10%): resembles 14-35 ft. 41-50 ft Limestone (100%): resembles 10-14 ft. Slope to slight ledge; poor to fair exposure. Chen (trace): resembles 14-35 ft. Nodules 8 x 12 cm, 18 x 24 cm. 35-41 ft Limestone (100%): resembles 10-14 ft. Hints of beds 10-30 cm thick. Moderate ledge; fair exposure. Chert (trace): resembles 14-35 ft. Few nodules 30 x 60 cm. 14-35 ft Limestone (70%): resembles 10-14 ft. Slight ledges to slopes; poor exposure, partly covered. Chert (30%): grayish black (N2); weathers dark brownish gray (5YR3/1). Siliceous (100%). Matrix (100%): microcrystalline; lime mudstone. Nodules 3 x 6 cm to 8 x 30 cm, generally parallel to bedding, some linked. 10-14 ft Limestone (90%): dark brownish gray (5YR3/1 to N4); weathers light gray (N7). Calcareous (100%). Matrix (100%): microcrystalline; lime mudstone. Hints of beds 30-50 cm thick. Moderate to slight ledge; fair exposure. Chert (10%): brownish gray (5YR4/1 to N4); weathers light brown (5YR6/4). Siliceous (60%), calcareous (40%). Matrix (60%): microcrystalline, opaque to translucent; ooids (20%): small (0.5 mm diameter); skeletal (20%): crinozoans, others; fair grain tangency; lime wackestone-packstone. Nodules 2 x 6 cm to 30 x 60 cm, some irregular shapes. 4-10 ft Limestone (90%): resembles 10-14 ft. Slight ledges to slope; poor exposure, partly covered. Chert (10%): resembles 10-14 ft. 0-4 ft Limestone (100%): light brownish gray (5YR6/1 to N6); weathers medium light gray (N6). Calcareous (100%), siliceous (trace). Skeletal (90%): abundant crinozoans (1-3 mm diameter), few fusulinids, others; grains (10%): small (1 mm diameter); matrix (trace): microcrystalline; perfect grain tangency; lime packstone-grainstone. Hints of beds 10-30 cm thick; some lenses 3 x 8 cm to 20 x 50 cm of concentrated grains, weathers grayish orange (10YR7/4), with a distinctive grainy surface. Moderate ledge, fair exposure. BHP-38-0 (lens), BHP-38-3.	82
37	Limestone 15-38 ft Limestone (100%): resembles 0-5 ft. Slight ledge to slope; poor exposure, partly covered. 5-15 ft Limestone (100%): resembles 0-5 ft. Slight ledges, poor to fair exposure. 0-5 ft Limestone (100%): medium brownish gray (5YR5/1 to N5); weathers light gray (N7). Calcareous	38

TABLE **4** (continued)

Unit	Description	Thickness (ft)
	(100%), siliceous (trace). Grains (60%): very small; skeletal (20%): crinozoans, others; matrix (20%): microcrystalline; good grain tangency; lime wackestone-packstone. Single bed?, fairly sharp surface at base. Uppermost part of prominent ledge, moderate ledges above; fair to good exposure. BHP-37-0.	
36	Limestone and chert, prominent ledge 18-39 ft Limestone (80%): resembles 0-11 ft. Matrix (100%). Upper part of prominent ledge. Chert (20%): resembles 0-11 ft. Nodules, few bands. 15-18 ft Limestone (70%): resembles 0-11 ft. Fairly sharp bedding surfaces at base and top. Chert (30%): resembles 0-11 ft. Bands 5-10 cm thick, some nodules. 11-15 ft Limestone (100%): resembles 0-11 ft. Skeletal (80%): crinozoans and fusulinids; matrix (20%). Fairly sharp bedding surfaces at base and top. 0-11 ft Limestone (80%): medium brownish gray (5YR5/1 to N5); weathers light gray (N7). Calcareous (100%), siliceous (trace). Matrix (70%): microcrystalline; skeletal (30%): fusulinids (2 x 4 mm), crinozoans (2 mm); fair grain tangency; lime wackestone-packstone. Beds 30-50 cm thick; no discernible lamination. Lower part of prominent ledge; fair to good exposure. BHP-36-2. Chert (20%): brownish gray (5YR5/1); weathers pale yellowish brown (10YR6/2), to light brown (5YR6/4). Siliceous (80%), calcareous (20%). Matrix (100%): microcrystalline, opaque to translucent; skeletal (trace): fusulinids; no grain tangency; lime mudstone. Bands 5-10 cm thick, nodules 3 x 5 cm, some 100-200 cm long, fairly regular shapes. BHP-36-4.	39
35	Limestone and chert, slight ledges 0-22 ft Limestone (80%): brownish gray (5YR4/1 to 5Y4/1 to N4); weathers light gray (N7). Calcareous (100%). Matrix (100%): microcrystalline; skeletal (trace): crinozoans (1 mm diameter); no grain tangency; lime mudstone. Beds 10-30 cm thick. Slight ledges; fair to poor exposure, partly covered. BHP-35-1. Chert (20%): dark brownish gray (5YR3/1 to N4); weathers pale yellowish brown (10YR6/2) to light brown (5YR6/4). Siliceous (100%). Matrix (100%): microcrystalline, opaque to translucent; skeletal (trace): fusulinids, crinozoans; no grain tangency; lime mudstone. Nodules generally 10 x 15 cm, no bands. BHP-35-10.	22
34	Limestone and minor chert, fairly prominent ledge 33-40 ft Limestone (100%): resembles 0-10 ft. Few tabulate corals? (3 cm long). Beds 50-100 cm thick, stylolites along surfaces. Fairly prominent ledge. 10-33 ft Limestone (90%): resembles 0-10 ft. Beds 15-30 cm thick. Slight ledges; poor exposure, partly covered. Chert (10%): resembles 0-10 ft. Nodules have more irregular shapes. 0-10 ft Limestone (100%): brownish gray (5YR4/1); weathers light gray (N7). Calcareous (100%), siliceous (trace). Skeletal (90%): crinozoans, fusulinids, others; matrix (10%): microcrystalline; excellent grain tangency; lime packstone-grainstone. Bed 30 cm thick at base, stylolites along surfaces, no discernible stratification above. Upper part of fairly prominent ledge; fair exposure. BHP-34-6. Chert (trace): brownish gray (5YR4/1 to N4); weathers grayish orange (10YR7/4). Siliceous (80%), calcareous (20%). Matrix (100%): microcrystalline, opaque to translucent; skeletal (trace): crinoids, others; no grain tangency; lime mudstone. Nodules 10 x 15 cm.	40
33	Limestone and chert, fairly prominent to moderate ledges 15-24 ft Limestone (90%): resembles 7-15 ft. Middle part of fairly prominent ledge; fair to good exposure. Chert (10%): resembles 7-15 ft. Nodules more regular in shape. 7-15 ft Limestone (70%): brownish gray (5YR5/1 to N5); weathers light gray (N7). Calcareous (100%). Matrix (80%): microcrystalline; skeletal (20%): fusulinids, few crinozoans; poor grain tangency; lime wackestone. Beds 5-10 cm thick, separated by chert, irregular surfaces. Lower part of fairly prominent ledge; fair to good exposure. Chert (30%): brownish gray (5YR4/1), light gray (N7), bluish; weathers pale yellowish brown (10YR6/2) to light brown (5YR6/4). Siliceous (90%), calcareous (10%). Skeletal (70%): fusulinids (1 x 3 mm), crinozoans, others; matrix (30%): microcrystalline, opaque; fair grain tangency; lime wackestone-packstone. Nodules 5 x 10 cm to 15 x 100 cm; irregular shapes. BHP-33-7. 4-7 ft Limestone (100%): medium brownish gray (5YR5/1), very light gray (N8); weathers light gray (N7). Calcareous (100%). Skeletal (90%): abundant crinozoans (1-4 mm diameter), rare fusulinids; matrix (10%): microcrystalline; grains (trace): very small; good grain tangency; lime packstone-grainstone. Single bed; no discernible lamination. Lowermost part of fairly prominent ledge; fair to good exposure. BHP-33-6. 0-4 ft Limestone (70%): brownish gray (5YR4/1 to N4); weathers light gray (N7). Calcareous (100%). Matrix (70%): microcrystalline; skeletal (30%): crinozoans, brachiopods, rare fusulinids; poor grain tangency; lime wackestone. Beds 5-15 cm thick, irregular surfaces. Slight to moderate ledges; fair to poor exposure. Chert (30%): brownish gray (5YR4/1 to N4); weathers light brownish gray (5YR6/1). Siliceous (80%), calcareous (20%). Matrix (90%): microcrystalline, opaque to translucent; skeletal (10%): crinozoans (2 mm diameter); others. Bands 5 x 100 cm, nodules 10 x 30 cm, slightly irregular shapes.	24
32	Limestone and minor chert 20-35 ft Limestone (90%): resembles 0-10 ft. Slope to slight ledges; poor exposure, partly covered. Chert (10%): resembles 0-10 ft. 10-20 ft Limestone (90%): resembles 0-10 ft. Beds 30-50 cm thick. Moderate to slight ledges. Chert (10%): resembles 0-10 ft. Larger nodules. 0-10 ft Limestone (100%): dark brownish gray (5YR3/1 to N3 to N4); weathers light gray (N7 to 5Y7/1). Calcareous (100%), muddy (trace). Matrix (100%): microcrystalline; skeletal (trace): crinozoans (1 mm diameter); no grain tangency; lime mudstone. Bed at base 50 cm thick, above are hints of beds about 100 cm thick. Fairly prominent ledge; fair exposure. BHP-32-2. Chert (trace): light brownish gray (5YR6/1), slightly bluish; weathers light brown (5YR6/4). Siliceous (100%). Matrix (100%): microcrystalline, opaque; lime mudstone. Nodules up to 10 x 15 cm; very deeply weathered.	35

TABLE 4 (continued)

Unit	Description	Thickness (ft)
31	Limestone and chert 10-20 ft Limestone (80%): dark brownish gray (5YR3/1 to N3); weathers light gray (N7), slightly brownish. Calcareous (90%), muddy (10%), siliceous (trace). Matrix (90%): microcrystalline calcite, silt and probable clay; skeletal (10%): crinozoans (1.5 mm diameter), fusulinids, rugose corals (over 2 cm diameter); grains (trace): very small; poor grain tangency; lime wackestone. Beds 10-30 cm thick, separated by chert. Slight to moderate ledges; fair to poor exposure. BHP-31-10. Chert (20%): dark brownish gray (5YR3/1 to N3); weathers brownish gray (5YR4/1 to N4 to 10YR4/2). Siliceous (100%). Matrix (70%): microcrystalline, opaque; porphyrotopes (30%): coarse crystals (0.5 mm) scattered in matrix, rhombic, may be dolomite; lime mudstone. Nodules up to 10 x 100 cm, irregular shapes at base, more regular above. BHP-31-15. 0-10 ft Covered (100%): probably limestone and chert. Slope.	20
30	Limestone, fairly prominent ledge 0-15 ft Limestone (100%): brownish gray (5YR4/1 to N4); weathers light gray (N7) to light olive gray (5Y6/1). Calcareous (100%). Matrix (90%): microcrystalline; grains (10%): very small; skeletal (trace): small fusulinids; poor grain tangency; lime wackestone. Hints of beds 50-100 cm thick, fairly sharp surface at base. Middle to upper part of fairly prominent ledge; fair exposure. BHP-30-0.	15
29	Limestone and chert, partly covered 21-29 ft Limestone (80%): resembles 0-6 ft. Beds 10-30 cm thick. Moderate ledge to lower part of fairly prominent ledge; fair exposure. Chert (20%): resembles 0-6 ft, decrease in upper part. 10-21 ft Covered (100%): probably limestone and chert. Slope. 6-10 ft Limestone (80%): resembles 0-6 ft. Slight ledges. Chert (20%): resembles 0-6 ft. 0-6 ft Limestone (70%): brownish gray (5YR4/1 to N4); weathers light gray (N7). Calcareous (90%), cherty (10%). Matrix (80%): microcrystalline calcite, some patches of chert replacing calcite; grains (20%): small; poor grain tangency; lime wackestone. Beds 5-15 cm thick, transitional base. Moderate ledge; fair exposure. BHP-29-2. Chert (30%): dark brownish gray (5YR3/1 to N3), medium brownish gray (5YR5/1), some bluish; weathers pale red (5R6/2), light brown (5YR6/4). Siliceous (100%). Matrix (100%): microcrystalline, opaque to translucent; lime mudstone. Nodules 5 x 30 to 10 x 100 cm, irregular shapes. BHP-29-3.	29
28	Limestone and minor chert 0-10 ft Limestone (90%): light brownish gray (5YR6/1 to N6); weathers light gray (N7). Calcareous (100%). Skeletal (100%): abundant crinozoans (1-6 mm diameter), few fusulinids (2.5 mm diameter); matrix (trace): microcrystalline; perfect grain tangency; lime packstone-grainstone. Hints of beds 30 cm thick, sharp surface at base. Slight ledges to slopes; poor exposure, partly covered. BHP-28-5. Chert (10%): medium brownish gray (5YR5/1 to N5), some bluish; weathers light brownish gray (5YR6/1). Siliceous (100%). Matrix (80%): microcrystalline, translucent; skeletal (20%): crinozoans (2 mm diameter), fusulinids, others; poor grain tangency; lime wackestone. Nodules 10 x 30 cm.	**10**
27	Limestone and chert, partly covered 70-75 ft Limestone (80%): resembles 0-4 ft. Slight ledges; poor exposure. Chert (20%): resembles 0-4 ft. Some irregular shapes. 65-70 ft Covered (100%): probably limestone and chert. Slope. 55-65 ft Limestone (70%): resembles 0-4 ft. Slight ledges; poor exposure. Chert (30%): similar to 0-4 ft. Some irregular shapes. 44-55 ft Covered (100%): probably limestone and chert. Slope. 40-44 ft Limestone (90%): resembles 0-4 ft. Slight ledge; poor to fair exposure. Chert (10%): resembles 0-4 ft. Nodules 15 cm diameter. 33-40 ft Limestone (70%): resembles 0-4 ft. Moderate ledges; poor exposure, much rubble. Chert (30%): resembles 0-4 ft. Nodules 1 x 3 cm, more irregular shapes. 25-33 ft Limestone (90%): resembles 0-4 ft. Few brachiopods. Beds up to 50 cm thick. Slight ledges; poor to fair exposure. Chert (10%): resembles 0-4 ft. 5-25 ft Limestone (80%): resembles 0-4 ft. Some horizontal and current-ripple laminae. Slight ledges to slope; poor exposure, partly covered. Chert (20%): resembles 0-4 ft. 4-5 ft Limestone (100%): brownish gray (5YR4/1); weathers light gray (N7). Calcareous (100%). Grains (70%): very small; matrix (30%): microcrystalline; good grain tangency; lime wackestone-packstone. Beds 5-10 cm thick; horizontal and current-ripple laminae. Slight ledge; fair to good exposure. 0-4 ft Limestone (80%): dark brownish gray (5Y3/1); weathers light gray (N7). Calcareous (90%), muddy (10%). Matrix (90%): microcrystalline calcite, silt and probable clay; grains (10%): very small; skeletal (trace): crinozoans, others; poor grain tangency; lime wackestone. Beds 10-20 cm thick. Slight ledges; fair exposure. BHP-27-2. Chert (20%): dark brownish gray (5YR3/1 to N3), slightly bluish; weathers light brownish gray (5YR6/1). Siliceous (90%), calcareous (10%). Matrix (80%): microcrystalline, opaque; skeletal (20%): very small types; poor grain tangency; lime wackestone. Nodules 5 x 30 to **10** x 100 cm, parallel to bedding. BHP-27-3.	75
26	Limestone **0-11** ft Limestone (100%): light brownish gray (5YR5/1 to 5Y5/1 to N5); weathers light gray (N7). Calcareous (90%), muddy (10%). Matrix (70%): microcrystalline calcite, silt and probable clay; grains (30%): very small; skeletal (trace): fusulinids, others?; fair grain tangency; lime wackestone. Hints of beds 20-50 cm thick. Moderate to slight ledges; fair exposure. BHP-26-0. Chert (trace): small nodules near top.	11

TABLE 4 (continued)

Unit	Description	Thickness (ft)
25	Limestone and chert 77-119 ft Limestone (80%): resembles 0-7 ft. Slight ledges to slopes; poor exposure, partly covered. Chert (20%): resembles 0-7 ft. 71-77 ft Limestone (100%): resembles 0-7 ft. Slight ledge. 63-71 ft Limestone (90%): resembles 0-7 ft. Slight ledge. Chert (10%): resembles 0-7 ft. Smaller nodules. 47-63 ft Limestone (80%): resembles 0-7 ft. Slopes to slight ledges; poor to fair exposure, partly covered. Chert (20%): resembles 0-7 ft. 35-47 ft Limestone (70%): resembles 0-7 ft. Moderate ledge; fair to good exposure. Chert (30%): resembles 0-7 ft. 15-35 ft Limestone (90%): resembles 0-7 ft. Slight ledges; fair exposure. Chert (10%): resembles 0-7 ft. Nodules, 5 cm diameter, more regular shapes. 7-15 ft Limestone (70%): resembles 0-7 ft. Slight ledges to slopes; poor exposure, partly covered. Chert (30%): resembles 0-7 ft. 0-7 ft Limestone (70%): dark brownish gray (5YR3/1 to N3); weathers light gray (N7). Calcareous (90%), muddy (trace). Matrix (90%): microcrystalline; skeletal (10%): crinozoans, fusulinids (3 x 4 mm); no grain tangency; lime wackestone. Beds 5-10 cm thick. Moderate ledge; fair exposure. BHP-25-3. Chert (30%): dark brownish gray (5YR3/1), some bluish; weathers grayish orange (10YR7/4), pale red (5R6/2). Siliceous (90%), calcareous (10%). Matrix (90%): microcrystalline; skeletal (10%): crinozoans, fusulinids; no grain tangency; lime wackestone. Nodules 3 x 5 cm to 10 x 50 cm, irregular shapes, some linked, some anastomosed. BHP-25-4.	119
24	Limestone 0-25 ft Limestone (100%): brownish gray (5YR4/1 to N4); weathers light gray (N7). Calcareous (100%). Grains (40%): dark peloids (1 mm diameter), some elongate, others; matrix (30%): microcrystalline; skeletal (30%): rugose and tabulate corals (some may be in growth position), small fusulinids; fair grain tangency; lime wackestone-packstone. Hints of beds 30-50 cm thick. Slight ledge, poor to fair exposure. BHP-24-1.	25
23	Limestone and chert, partly covered 9-25 ft Covered (100%): probably limestone and chert. Slope. 4-9 ft Limestone (100%): resembles 0-4 ft. Slight ledge, deeply weathered, some fractured. 0-4 ft Limestone (70%): brownish gray (5YR4/1); weathers light gray (N7). Calcareous (90%), siliceous (10%). Matrix (70%): microcrystalline; skeletal (30%): very small types; poor grain tangency; lime wackestone. Hints of beds 10-30 cm thick, fairly sharp bedding surface at base. Slight ledge; poor exposure, highly fractured. Chert (30%): light brownish gray (5YR6/1 to N5), light bluish gray (5B7/1); weathers light brownish gray (5YR6/1), to moderate yellowish brown (10YR5/2), some reddish jasperoid streaks in fractures. Siliceous (90%), calcareous (10%). Matrix (100%): microcrystalline, opaque to translucent; skeletal (trace): very small types, replaced; no grain tangency; lime mudstone. Nodules 5 x 10 cm to 10 x 100 cm, generally parallel to bedding, irregular shapes, some linked, some anastomosed. BHP-23-4.	25
22	Limestone 5-30 ft Limestone (100%): resembles 0-2 ft. Some interbeds of crinozoan hash. Fair to poor exposure, covered at top. Chert (trace): resembles 0-2 ft. Deeply weathered brown to dark brown. Nodules up to 5 x 50 cm. 2-5 ft Limestone (100%): brownish gray (5YR4/1 to N4); weathers light gray (N7). Calcareous (100%). Skeletal (100%): nearly all crinozoans (1-2 mm diameter), one interbed 10 cm thick of abundant brachiopod shells; matrix (trace): microcrystalline; excellent grain tangency; lime packstone. Hints of beds 10-30 cm thick, fairly sharp surface at base; hints of horizontal lamination. Moderate to slight ledge; fair exposure. Chert (trace): resembles 0-2 ft. Few nodules. 0-2 ft Limestone (100%): dark brownish gray (5YR3/1 to N3); weathers light gray (N7). Calcareous (90%), muddy (10%). Matrix (60%): microcrystalline calcite, silt and probable clay; grains (30%): very small, some coats or rinds; skeletal (10%): crinozoans, rare fusulinids, algae?; fair grain tangency; lime wackestone-packstone. Beds 10-50 cm thick, sharp erosion surface at base is overlain by 1-2-cm-thick bed of crinozoan hash; no discernible lamination. Slight ledges; fair to good exposure. BHP-22-1. Chert (trace): black (N1); weathers brownish black (5YR2/1). Siliceous (100%), calcareous (trace). Matrix (100%): microcrystalline, opaque; grains (trace): very small; no grain tangency; lime mudstone. Nodules 5 x 10 cm.	30
21	Limestone and chert 1-6 ft Limestone (80%): dark brownish gray (5YR3/1 to N3); weathers light gray (N7). Calcareous (90%), muddy (10%). Matrix (100%): microcrystalline calcite, silt, and probable clay; skeletal (trace): crinozoans, brachiopods; no grain tangency; lime mudstone. Hints of beds 30-50 cm thick. Moderate to slight ledges; fair exposure. BHP-21-2. Chert (20%): brownish black (5YR2/1 to N2); weathers dark brownish gray (5YR3/1). Siliceous (100%). Matrix (100%): microcrystalline, opaque; skeletal (trace): brachipods, others; no grain tangency; lime mudstone. Nodules 5 x 15 cm to 10 x 90 cm. BHP-21-3. 0-1 ft Limestone (100%): dark brownish gray (5YR3/1); weathers light gray (N7). Calcareous (100%). Skeletal (90%): all crinozoans (1-2 mm diameter), medium light gray (N6); matrix (10%): microcrystalline; good grain tangency; lime packstone-grainstone. Single bed, erosion surface at base with 1-2 cm relief; no discernible lamination. Lower part of moderate ledge; fair exposure. Chert (trace): resembles 1-6 ft.	6

TABLE 4 (continued)

Unit	Description	Thickness (ft)
20	Limestone and minor chert 5-17 ft Limestone (90%): resembles 0-5 ft. Moderate to slight ledges, fair to good exposure. Chert (10%): resembles 0-5 ft. Nodules 2 x 3 cm to 14 x 15 cm, some are linked to form bodies 15 x 60 cm. 0-5 ft Limestone (100%): brownish gray (5YR4/1 to N4); weathers light gray (N7). Calcareous (100%). Matrix (70%): microcrystalline; skeletal (30%): foraminifers (1 mm diameter), fusulinids, crinozoans, others; fair grain tangency; lime wackestone-packstone. Hints of beds 30-50 cm thick. Moderate ledge to slope at top; poor exposure, partly covered in upper part. BHP-20-2. Chert (trace): dark brownish gray (5YR3/1 to N3); weathers medium brownish gray (5YR5/1 to N5). Siliceous (70%), calcareous (30%). Matrix (80%): microcrystalline, opaque; grains (20%): very small; skeletal (trace): fusulinids; poor grain tangency; lime wackestone. Nodules 3 x 12 cm to 10 x 16 cm.	17
19	Limestone and minor chert, mostly covered 5-25 ft Covered (100%): probably limestone and chert. Slope. 0-5 ft Limestone (90%): brownish gray (5YR4/1 to N4); weathers light gray (N7). Calcareous (100%). Matrix (60%): microcrystalline; grains (30%): very small; skeletal (10%): crinozoans, rare fusulinids; fair grain tangency; lime wackestone-packstone. Hints of beds 30 cm thick. Slight ledge; poor exposure. BHP-19-4a. Chert (10%): brownish gray (5YR4/1 to N4); weathers light brownish gray (5YR4/1). Siliceous (90%), calcareous (10%). Matrix (80%): microcrystalline, opaque; skeletal (20%): crinozoans (some not replaced), others; poor grain tangency; lime wackestone. Nodules 5 x 30 cm. BHP-19-4b.	25
18	Limestone, partly covered 25-43 ft Limestone (100%): resembles 0-4 ft. Matrix (80%); skeletal (20%). Slight ledge to slope; poor exposure. 5-25 ft Covered (100%): probably limestone. Slope. 4-5 ft Limestone (100%): resembles 0-4 ft. Skeletal (70%): increase in shell fragments; matrix (30%); good grain tangency; lime packstone-wackestone. One channel 20 cm deep, 40 cm wide, with shells and limestone lithoclasts up to 200 x 500 mm. 0-4 ft Limestone (100%): dark brownish gray (5YR3/1 to N3); weathers light gray (N7). Calcareous (100%). Matrix (60%): microcrystalline; skeletal (40%): crinozoans, fusulinids, few brachiopod? shell fragments, some concentrations 1-2 cm thick of silicified skeletal material, weathers brownish gray; fair grain tangency; lime wackestone-packstone. Hints of beds 30 cm thick. Slight ledge; poor to fair exposure. BHP-18-0.	43
17	Limestone and minor chert, upper part covered 34-38 ft Covered (100%): probably limestone. Slope. 20-34 ft Limestone (100%): resembles 0-10 ft. Moderate to slight ledges. Chert (trace): resembles 15-20 ft. Small nodules. 15-20 ft Limestone (90%): resembles 0-10 ft. Chert (10%): dark gray (N3 to N2); weathers pale yellowish brown (10YR6/2 to 10YR6/4). Siliceous (90%), calcareous (10%). Matrix (70%): microcrystalline, opaque; skeletal (20%): crinozoans (some not replaced), others; grains (10%): very small; fair grain tangency; lime wackestone-packstone. Nodules 2 x 4 cm to 25 x 60 cm. BHP-17-17. 10-15 ft Limestone (100%): resembles 0-10 ft. Some rugose corals, not in growth position. Slight ledge to slope; poor exposure, partly covered. 0-10 ft Limestone (100%): brownish gray (5YR4/1 to N4); weathers light gray (N7 to 5Y7/1). Calcareous (100%). Matrix (90%): microcrystalline; skeletal (10%): fusulinids (1.5 x 2.5 mm), some algae? in dark silicified lenses; no grain tangency; lime wackestone. Beds up to 30 cm thick. Slight ledges; fair to poor exposure. BHP-17-4.	38
16	Limestone and chert, upper part covered. 18-45 ft Covered (90%): probably limestone. Slope. Limestone (10%): resembles 4-5 ft. Slope to slight ledges; poor exposure. 15-18 ft Limestone (100%): resembles 4-5 ft. 5-15 ft Limestone (90%): resembles 4-5 ft. Abundant fusulinids. No discernible stratification. Moderate ledge; poor to fair exposure. Chert (10%): light gray, bluish (N7, matrix), brownish gray (5Y4/1, grains); weathers medium brownish gray (5YR5/1). Siliceous (90%), calcareous (10%). Matrix (70%): microcrystalline, opaque to translucent; skeletal (30%): fusulinids (some not replaced), others; fair grain tangency; lime wackestone-packstone. Nodules generally less than 5 cm long, one 10 x 30 cm. BHP-16-10. 4-5 ft Limestone (100%): brownish gray (5YR5/1 to N5); weathers light gray (N7). Calcareous (100%). Skeletal (80%): fusulinids (1 x 2 mm) larger and more abundant, others; matrix (20%): microcrystalline; good grain tangency; lime packstone-wackestone. Single bed, sharp surface at base; hints of horizontal lamination. Slight ledge to slope; poor exposure, covered in upper part. BHP-16-4. 0-4 ft Limestone (80%): brownish gray (5YR4/1); weathers light gray (N7). Calcareous (100%). Skeletal (90%): many crinozoans (some 1-6 mm diameter), other small types; matrix (10%): microcrystalline; good grain tangency; lime packstone. Bed at base is 50 cm thick, those above are 5 cm thick and separated by chert. Slight ledges; poor exposure, deeply weathered. Chert (20%): brownish gray (5YR4/1), bluish; weathers light brown (5YR6/4). Siliceous (100%). Matrix (100%): microcrystalline, translucent; grains (trace): very small; no grain tangency; lime mudstone. Bands 5 cm thick, irregular shapes, nodules 3 x 10 cm.	45

TABLE **4** (continued)

Unit	Description	Thickness (ft)
15	Limestone, partly covered	50
	27-50 ft Limestone (100%): resembles 2-3 ft. Chaetetid corals (5 cm diameter) about 10 ft below top. Slight ledges to slopes; poor exposure, partly covered.	
	15-27 ft Covered (100%): probably limestone. Slope.	
	7-15 ft Limestone (100%): resembles 2-3 ft. Some small fusulinids and conispiral foraminifers. Slight ledge to slope; poor exposure, partly covered.	
	Chert (trace): dark gray. Thin bands and small nodules.	
	3-7 ft Covered (100%): probably limestone. Slope.	
	2-3 ft Limestone (100%): brownish gray (5YR4/1); weathers light gray (N7). Calcareous (100%). Grains (80%): elongate coated grains, peloids, ooids; skeletal (10%): crinozoans, others; matrix (10%): microcrystalline; good grain tangency; lime packstone. Hints of beds 30-40 cm thick. Upper part of slight ledge; poor to fair exposure.	
	0-2 ft Limestone (100%): dark brownish gray (5YR3/1); weathers medium light gray (N6 to N7), some iron stain along fractures. Calcareous (90%), muddy (10%). Matrix (100%): microcrystalline calcite, silt and probable clay; skeletal (trace): very small types; no grain tangency; lime mudstone. Beds 6-30 cm thick, average 20 cm, lapping out downward to northeast, sharp surface at base; hints of horizontal lamination. Slight to moderate ledges; fair to good exposure. BHP-15-2.	
14	Limestone, minor large white chert nodules, partly covered	57
	55-57 ft Limestone (100%): resembles 0-5 ft. No discernible stratification. Slight ledge; poor exposure, deeply weathered.	
	Chert (trace): resembles 0-5 ft. Nodules 30 cm diameter, may be silicified tabulate (chaetetid) corals; some brown nodules 5 x 10 cm. Deeply weathered.	
	45-55 ft Covered (90%): probably limestone, much rubble. Slope.	
	Limestone (10%): resembles 0-5 ft. No discernible stratification. Slight ledges; poor exposure.	
	39-45 ft Limestone (100%): resembles 0-5 ft. Hints of beds 30-50 cm thick. Slight ledges; poor exposure.	
	Chert (trace): resembles 0-5 ft. Round nodules 10 cm diameter.	
	35-39 ft Covered (100%): probably limestone. Slope.	
	29-35 ft Limestone (100%): resembles 0-5 ft. Beds about 50 cm thick; slight ledge; poor to fair exposure.	
	Chert (trace): brownish gray (5YR4/1); weathers medium brownish gray (5YR5/1). Siliceous (100%). Matrix (100%): microcrystalline, translucent; lime mudstone. Single band 10 cm thick.	
	19-29 ft Covered (100%): probably limestone. Slope.	
	13-19 ft Limestone (100%): resembles 0-5 ft. Some deeply weathered.	
	Chert (trace): resembles 0-5 ft. Few small nodules.	
	5-13 ft Covered (100%): probably limestone. Slope.	
	0-5 ft Limestone (90%): medium brownish gray (5YR5/1); weathers light gray (N7). Calcareous (100%). Grains (90%): peloids (1 mm diameter, some elongate), ooids, elongate coated grains, grapestone grains; skeletal (10%): crinozoans, brachiopods, fusulinids, algae?; matrix (trace): microcrystalline, some patches; cement (trace): clear sparry calcite; excellent packing; lime grainstone. Hints of beds 30-50 cm thick. Slight ledge; poor to fair exposure. BHP-14-3.	
	Chert (10%): light bluish gray (5B7/1); weathers very light gray (N8), some with reddish brown ferruginous crust. Siliceous (90%), calcareous (10%), dolomitic (trace). Matrix (50%): microcrystalline, opaque to translucent; skeletal (40%): replaced crinozoans, tabulate (chaetetid?) corals; dolomite porphyrotopes (10%, locally more abundant): coarse crystals; fair grain tangency; lime wackestone-packstone. Nodules 20 x 30 cm. BHP-14-2.	
13	Limestone, minor chert, partly covered	102
	76-102 ft Covered (90%): probably limestone, much rubble. Slope.	
	Limestone (10%): resembles 55-65 ft. Slight ledge; poor exposure.	
	Chert (trace): dark brownish gray (5YR3/1 to N3); weathers medium brownish gray (5YR5/1 to N5). Siliceous (100%). Matrix (90%): microcrystalline, opaque to translucent; grains (10%): very small; no grain tangency; lime wackestone. Nodules 5 x 15 cm to 10 x 50 cm.	
	74-76 ft Limestone (100%): resembles 55-65 ft. Slight ledge; fair exposure. BHP-13-75.	
	65-74 ft Limestone (100%): resembles 55-65 ft. Chaetetid corals (5 cm diameter) in silicified, ferruginous bodies. Slight ledges to slopes; poor exposure, partly covered.	
	55-65 ft Limestone (100%): brownish gray (5Y4/1 to N4); weathers light gray (N7). Calcareous (100%). Grains (90%): peloids (0.5 to 1.0 mm diameter), somewhat clotted; matrix (10%): microcrystalline, some patches; skeletal (trace): fusulinids, others; good grain tangency; lime packstone-wackestone. Hints of beds about 50 cm thick. Slight ledges; poor exposure, partly covered.	
	36-55 ft Covered (100%): probably limestone. Slope.	
	35-36 ft Limestone (100%): resembles 5-12 ft. Grains (70%): peloids (0.5 to 1 mm diameter), ooids; skeletal (20%): fusulinids, crinozoans, brachiopods, chaetetid corals (3 cm long); matrix (10%): microcrystalline; good grain tangency; lime packstone-wackestone. Single bed?, sharp surface at base. Slight ledge; fair exposure.	
	34-35 ft Limestone (90%): brownish gray (5YR4/1 to N4); weathers light gray (N7). Calcareous (100%). Matrix (100%): microcrystalline; skeletal (trace): crinozoans, others, no fusulinids; no grain tangency; lime mudstone. No discernible stratification, fairly sharp surface at base. Slight ledge; poor to fair exposure.	
	Chert (10%): brownish black (5YR2/1 to N2), yellowish gray (5Y8/1), alternating concentric stripes (1-8 mm thick); weathers dark gray (N3), white (N8), distinctive zebralike pattern. Siliceous (70%), calcareous (30%, in light layers). Matrix (90%): microcrystalline, opaque; grains (10%): very small, may be skeletal; generally no grain tangency, some thin layers with excellent grain tangency and grading; lime wackestone-packstone. Nodules 5 x 15 cm to 6 x 30 cm; internal concentric layers, with thicker (4-8 mm) light ones, and thinner (1-4 mm) dark ones; to east, the chert occurs in bands with internal, parallel, light and dark layers. BHP-13-35.	

TABLE 4 (continued)

Unit	Description	Thickness (ft)
	31-34 ft Limestone (100%): resembles 5-12 ft. Grains (60%): peloids, ooids; matrix (30%): microcrystalline; skeletal (10%): fusulinids, others; good grain tangency; lime packstone-wackestone. Slight ledge; poor exposure.	
	29-31 ft Limestone (100%): resembles 5-12 ft. Grains (70%): peloids, ooids (0.5-1 mm diameter); matrix (20%): microcrystalline; skeletal (10%): fusulinids, others; good grain tangency; lime packstone-wackestone. Hints of beds 30 cm thick. Fairly sharp surface at base. Upper part of slight ledge; fair exposure.	
	28-29 ft Limestone (90%): resembles 12-20 ft. Matrix (80%): microcrystalline; skeletal (20%): crinozoans, brachiopods, others, no fusulinids; poor grain tangency; lime wackestone. Hints of beds 30 cm thick. Lower part of slight ledge; fair exposure.	
	Chert (10%): dark brownish gray (5YR3/1 to N3); weathers brownish gray (5YR4/1). Siliceous (80%), calcareous (20%). Matrix (90%): microcrystalline, opaque to translucent; grains (10%): very small; no grain tangency; lime wackestone. Round nodules 7-10 cm diameter, some joined vertically into figure-8 shapes.	
	25-28 ft Covered (90%): probably limestone. Slope.	
	Limestone (10%): resembles 12-20 ft. Slight ledge; poor exposure.	
	20-25 ft Limestone (100%): medium brownish gray (5YR5/1 to N5); weathers light gray (N7). Calcareous (100%), glauconitic? (trace). Matrix (80%): microcrystalline; blebs (10%): appear to be small vugs (less than 1 mm diameter), filled with dark sparry calcite; skeletal (10%): small algae?, rare fusulinids (up to 1 mm diameter); grains of glauconite? (trace); poor grain tangency; lime wackestone. Hints of beds 15-40 cm thick. Slight ledges; poor to fair exposure. BHP-13-23.	
	12-20 ft Covered (80%): probably limestone. Slope.	
	Limestone (20%): dark brownish gray (5YR3/1); weathers light gray (N7). Calcareous (100%). Matrix (80%): microcrystalline; skeletal (20%): small types, fusulinids not seen; poor grain tangency; lime wackestone. Hints of beds about 30 cm thick. Slight ledges; poor exposure.	
	5-12 ft Limestone (100%): brownish gray (5YR4/1 to N4); weathers light gray (N7 to N8). Calcareous (100%). Matrix (80%): microcrystalline; skeletal (20%): fusulinids (less than 1 mm long), others; grains (trace); fair grain tangency; lime wackestone-packstone. Hints of beds about 50 cm thick, sharp surface at base. Moderate ledges; fair exposure. BHP-13-7.	
	Chert (trace): black to dark gray (N1 to N3); weathers dark brownish gray (5YR3/1). Siliceous (100%). Matrix (100%): microcrystalline, opaque; lime mudstone. Nodules 5 x 15 cm average; one nodule 4 x 10 cm of deeply weathered brown chert forms nucleus of black chert nodule 9 x 23 cm.	
	0-5 ft Limestone (100%): dark brownish gray (5YR3/1 to N3); weathers light gray (N7). Calcareous (100%). Matrix (80%): microcrystalline; skeletal (20%): brachiopods, others, not see fusulinids; poor grain tangency; lime wackestone. No discernible stratification. Slight ledge; poor exposure, partly covered.	
12	Limestone	17
	11-17 ft Limestone (100%): resembles 0-3 ft. Few chaetetid corals (10 cm diameter, colonies 30 x 40 cm). Beds average 50 cm thick, sharp surface at base. Moderate ledges; fair exposure.	
	Chert (trace): dark brownish gray (5YR3/1 to N3); weathers light brownish gray (5YR6/1 to N6). Siliceous (100%). Matrix (80%): microcrystalline, opaque; grains (20%): replaced ooids, others; poor grain tangency; lime wackestone. Nodules 5 x 30 cm.	
	10-11 ft Limestone (100%): resembles 3-4 ft. Gradational base; may have horizontal lamination, slightly contorted. Slight ledge; poor to fair exposure.	
	4-10 ft Limestone (100%): brownish gray (5YR4/1 to N5); weathers light gray (N7). Calcareous (90%), glauconitic (10%). Grains (90%): ooids (0.5-1 mm diameter), elongate coated grains (0.5 x 2 mm); matrix (10%): microcrystalline, some patches; skeletal (trace): shell fragments; good grain tangency; lime packstone. Hints of beds 30-50 cm thick, slightly irregular base, may be erosion surface. Moderate ledges; poor to fair exposure.	
	3-4 ft Limestone (100%): brownish black (5YR2/1 to N3); weathers gray (N5). Calcareous (80%), muddy (20%). Matrix (100%): microcrystalline calcite, silt, and probable clay; lime mudstone. No discernible stratification, may have gradational base. Slight ledge to slope; poor exposure.	
	0-3 ft Limestone (100%): brownish gray (5YR4/1 to N5); weathers light gray (N7). Calcareous (100%), glauconitic (trace). Skeletal (60%): crinozoans, brachiopods, bryozoans?, others; matrix (40%): microcrystalline, some patches; grains (trace): very small; glauconite grains (trace): dark, some flakes; fair grain tangency; lime wackestone-packstone. Beds average 20 cm thick, irregular surfaces, erosional truncation at base (60 cm bed below is truncated to 30 cm in 1.5 m laterally to northeast); no discernible lamination. Moderate ledges; fair to good exposure. BHP-12-1.	
11	Limestone, minor chert, partly covered	70
	69-70 ft Limestone (100%): brownish gray (5YR4/1); weathers light gray (N7), some pinkish iron stain. Calcareous (90%), silty (10%). Matrix (90%): microcrystalline; silt grains (10%): dispersed in matrix; lime mudstone. Single bed, sharp surface at base. Slight ledge; fair exposure.	
	59-69 ft Limestone (100%): resembles 0-6 ft. Beds average 40 cm thick, fairly sharp surface at base. Moderate ledges; fair to good exposure.	
	45-59 ft Limestone (100%): resembles 0-6 ft. Hints of beds 100 cm thick, base may be gradational. Moderate ledge; fair exposure.	
	27-45 ft Limestone (100%): resembles 0-6 ft. Matrix (100%): microcrystalline; lime mudstone. Beds 30 cm thick. Moderate to slight ledges; fair to poor exposure, partly covered.	
	20-27 ft Limestone (90%): brownish black (5YR2/1); weathers light gray (N7). Calcareous (90%), muddy (10%). Matrix (90%): microcrystalline calcite, silt and probable clay; skeletal (10%): crinozoans, light gray (N7); no grain tangency; lime wackestone. Beds 7-30 cm thick, average 15 cm. Slight ledge; fair to poor exposure, partly covered.	
	Chert (10%): black (N1); weathers dark gray (N3). Siliceous (100%). Matrix (100%): microcrystalline, opaque; lime mudstone. Nodules 5 x 30 cm.	

TABLE 4 (continued)

Unit	Description	Thickness (ft)
	15-20 ft Limestone (100%): resembles 0-6 ft. Slight ledge; fair exposure, covered at top. 9-15 ft Covered (100%): probably limestone. Slope. 6-9 ft Limestone (100%): resembles 0-6 ft. Grains (60%); matrix (40%); fair grain tangency; lime wackestone-packstone. Hints of beds 50 cm thick, sharp surface at base. Slight ledge; fair exposure. 0-6 ft Limestone (100%): brownish gray (5YR4/1 to 10YR4/2 to 5YR4/1); weathers light gray (N7). Calcareous (100%). Grains (90%): ooids (less than 1 mm diameter), some flattened, elongate coated grains (0.1 x 2 min); matrix (10%): microcrystalline, some patches; skeletal (trace): crinozoans, brachiopods, others; good grain tangency where not separated by patches of matrix, lime packstone-mudstone. Single bed?, sharp surface at base, no discernible lamination. Moderate ledge; fair to good exposure. BHP-11-1.	
10	Limestone and minor chert 4-7 ft Limestone (90%): resembles 0-3 ft. Some brachiopods and other skeletal material occur in lenses. Beds 20-40 cm thick. Moderate ledge; fair exposure. Chert (10%): resembles 0-3 ft. Bands 2 cm thick, small nodules. 3-4 ft Limestone (100%): brownish black (5YR2/1 to 5Y2/1 to N2); weathers light gray (N7). Calcareous (80%); muddy (20%). Matrix (100%): microcrystalline calcite, silt, and probable clay; lime mudstone. Single bed; some interlayering of muddy, fissile (shaly) types and cleaner, nonfissile types. Slight ledge; fair exposure. BHP-10-3. 0-3 ft Limestone (90%): dark brownish gray (5YR3/1); weathers light gray (N7). Calcareous (100%). Matrix (100%): microcrystalline; skeletal (trace): crinozoans, light gray (N7, 1-2 mm diameter); no grain tangency; lime mudstone. Hints of beds 30 cm thick, sharp surface at base. Slight ledges; fair exposure. Chert (10%): dark gray to black (N3 to N1), bluish; weathers brownish black (5YR2/1). Siliceous (90%), calcareous (10%). Matrix (90%): microcrystalline, opaque; skeletal (10%): small types; no grain tangency; lime mudstone. Band 3 cm thick at base, nodules 6 x 20 cm.	7
9	Limestone 0-20 ft Limestone (100%): dark brownish gray (5YR3/1 to 5Y3/1); weathers light gray (N7). Calcareous (100%). Grains (70%): ooids (less thin 1 mm diameter), elongate coated grains (0.1 x 2 mm), rare grapestone grains; skeletal (20%): crinozoans, brachiopods, some shell beds (a distinctive one from 7 to 9 ft above base); matrix (10%, forms 80% of basal 0.1 ft): microcrystalline; good grain tangency; lime packstone-wackestone. Beds 5-80 cm thick, average 60 cm, some beds coincide with alternations of skeletal and coated grains, sharp contact at base; hints of horizontal lamination. Moderate ledges; fair to good exposure. BHP-9-5, BHP-9-6.	20
8	Limestone and chert 0-10 ft Limestone (70%): dark brownish gray (5YR3/1 to 10YR2/2); weathers light gray (N7). Calcareous (100%). Matrix (70%): microcrystalline; skeletal (20%): very small types, some crinozoans; grains (10%): ooids, others; fair grain tangency; lime wackestone-packstone. Beds average 10 cm thick, separated by chert, sharp surface at base. Slight ledges; fair exposure, covered at top. BHP-8-1a. Chert (30%): dark brownish gray (5YR3/1 to 5Y3/1 to N3), weathers light brownish gray (5YR6/1), some iron stain. Siliceous (100%). Matrix (90%): microcrystalline, opaque; grains (10%): ooids, others; skeletal (trace): crinozoans, others; poor grain tangency; lime wackestone. Bands 2-4 cm thick, irregular tops and bases, nodules up to 10 x 45 cm, some linked, some anastomosed. BHP-8-lb.	10
7	Limestone, partly covered 21-23 ft Limestone (100%): brownish gray (5YR4/1 to 10YR4/2 to 5Y3/2); weathers light gray (N7). Calcareous (100%). Grains (70%): ooids (less than 1 mm diameter), grapestone grains (1 x 2 mm); skeletal (20%): crinozoans (1-2 mm diameter), others; matrix (10%): darker, microcrystalline; good grain tangency; lime packstone-wackestone. Single bed? Slight ledge; poor to fair exposure. BHP-7-23. 19-21 ft Covered (100%): probably limestone. Slope. 17-19 ft Limestone (100%): resembles 0-4 ft. Slight ledge, fair exposure. Possible mudcracks on surface at top of bed; filled with sparry calcite. 11-17 ft Covered (100%): probably limestone, much rubble. Slope. 9-11 ft Limestone (100%): resembles 4-6 ft. Matrix (70%); skeletal (30%): disarticulated brachiopod shells, generally convex up. Slight ledge; fair exposure. 6-9 ft Covered (100%): probably limestone, much rubble. Slope. 4-6 ft Limestone (100%): dark brownish gray (5YR3/1 to N4); weathers light gray (N7). Calcareous (100%). Matrix (60%): microcrystalline; skeletal (40%): corals, brachiopods, others weather dark reddish brown; one lens 15 x 60 cm with ooids and other grains; fair grain tangency; lime wackestone-packstone. Hints of beds 30 cm thick, sharp surface at base. Upper part of slight ledge; fair exposure. 0-4 ft Limestone (100%): brownish gray (5YR4/1 to 10YR4/2 to 5Y3/2); weathers light gray (N7). Calcareous (100% siliceous (trace). Matrix (100%): microcrystalline; lime mudstone. Hints of beds 40-60 cm thick; no discernible lamination. Slight ledge; fair exposure. BHP-7-1.	23
6	Limestone and chert, partly covered 35-60 ft Covered (80%): probably limestone and chert. Slope. Limestone (20%): resembles 0-2 ft. Slight ledges; poor exposure. Chert (trace): resembles 0-2 ft. 33-35 ft Limestone (100%): resembles 0-2 ft. Slight ledge; poor to fair exposure. 30-33 ft Limestone (70%): resembles 0-2 ft. Matrix (90%); grains (10%): in lenses. Slight ledge; fair exposure. Chert (30%): resembles 0-2 ft. Bands 2-4 cm thick, some nodules. 14-30 ft Covered (100%): probably limestone and chert. Slope. 12-14 ft Limestone (70%): resembles 0-2 ft. Some tabulate corals. In one 10 cm bed are laminae inclined 15° to N. 45° E. Slight ledge. Chert (30%): resembles 0-2 ft. 10-12 ft Covered (100%): probably limestone. Slope.	60

TABLE 4 (continued)

Unit	Description	Thickness (ft)
	~~9-10 ft Limestone (100%): resembles 0-2 ft. Slight ledge.~~	
	2-9 ft Covered (100%): probably limestone. Slope.	
	0-2 ft Limestone (70%): dark brownish gray (5YR3/1 to N4); weathers light gray (N7). Calcareous (100%), siliceous (trace). Matrix (50%): microcrystalline; grains (50%): very small peloids or skeletal material; fair grain tangency; lime wackestone-packstone. Single bed?, sharp surface at base; no discernible lamination. Upper part of moderate ledge; fair exposure. BHP-6-1a. Chert (30%): dark brownish gray (5YR3/1 to 5Y3/1); weathers dark gray (N4), some yellowish brown iron stain. Siliceous (90%), calcareous (10%). Matrix (60%): microcrystalline, opaque; grains (40%): very small; fair grain tangency; lime wackestone-packstone. Nodules 10 x 20 cm, irregular shapes, long axes parallel to bedding. BHP-6-1b.	
5	Limestone	5
	0-5 ft Limestone (100%): brownish gray (5YR4/1 to 5Y4/1); weathers light gray (N7), some yellowish brown iron stain. Calcareous (100%). Grains (70%): elongate grains (0.1 x 2 mm) with rinds or coats, ooids (average 1 mm diameter); skeletal (30%): crinozoans, brachiopod shells; matrix (trace): microcrystalline; excellent grain tangency; lime packstone-grainstone. Beds 10-30 cm thick, average 20 cm, basal surface is covered but may be sharp; some horizontal to slightly wavy lamination, alternating lighter and darker layers are seen on weathered surface. Moderate ledges; fair to good exposure. BHP-5-0.	
	Contact not exposed, probable disconformity.	
	Paradise Formation (Mississippian/Chesterian), only upper part exposed, total measured	78
4	Limestone, siltstone, lower part covered	14
	13-14 ft Limestone (100%): olive black (5Y2/1); weathers medium gray (N5). Calcareous (60%); dolomitic (20%); silty (20%): quartz, minor feldspar, and no clay (X-ray identification by R.M. North, NMBMMR); organic (10%): black residue, probably kerogen and minor bitumen (soluble in naptha). Matrix (80%): microcrystalline calcite, silt, and disseminated organic material. Porphyroblasts (20%): white dolomite crystals. Horizontal stratification barely discernible; gradational with underlying siltstone. Slight ledge to slope; poor exposure, upper part is covered. BHP-4-13.	
	12-13 ft Siltstone (100%): olive brown (5Y3/4), some yellowish; weathers pale brown (5YR5/2). Silty (80%): quartz; calcareous (20%). Matrix (70%): silt, and microcrystalline calcite; skeletal (30%): chonetid brachiopod shells, disarticulated, silicified; fair grain tangency. Single bed; hints of horizontal lamination. Slight ledge; poor exposure, fractured. BHP-4-12.	
	0-12 ft Covered (100%): probably limestone. Slope. Limestone (trace): resembles 13-14 ft. Poor exposure at top of interval.	
3	Limestone	8
	0-8 ft Limestone (100%): dark yellowish brown (10YR4/2); weathers pale yellowish brown (10YR5/2 to N7). Calcareous (100%), siliceous (trace). Matrix (90%): microcrystalline; skeletal (10%): crinozoans, gastropods, others; lithoclasts (trace): limestone pebbles, imbricated, inclined to northeast; poor grain tangency; lime wackestone. Beds 3-4 cm thick, horizontal, slightly irregular surface; no discernible lamination. Moderate ledge; fair to good exposure, some fractured. BHP-3-2.	
2	Limestone, partly covered	45
	35-45 ft Covered (100%): probably limestone. Slope.	
	33-35 ft Limestone (100%): resembles 1-3 ft. Slight ledge; poor exposure.	
	15-33 ft Covered (100%): probably limestone. Slope.	
	13-15 ft Limestone (100%): resembles 1-3 ft. Horizontal and inclined laminae, troughs plunging about S. 20° E. Slight ledge; fair to good exposure.	
	5-13 ft Covered (100%): probably limestone. Slope.	
	4-5 ft Limestone (100%): resembles 1-3 ft. Horizontal lamination.	
	3-4 ft Limestone (100%): resembles 1-3 ft. No discernible lamination.	
	1-3 ft Limestone (100%): dark yellowish brown (10YR4/2); weathers grayish orange pink (5Y7/2). Calcareous (100%). Skeletal (50%): crinozoans (0.5-1.5 mm diameter); others; grains (40%): ooids (0.5-2 mm diameter), elongate grains with rinds or coats; matrix (10%): microcrystalline; excellent grain tangency; lime packstone. Beds 50 cm thick, sharp surfaces; laminasets 5-10 cm thick, tabular to wedge shapes, with inclined laminae convex up, lapping out downward at bases of sets, striking N. 30 ° E., dipping 45 ° SE., truncated at top by channel 50 cm wide, 5 cm deep, axis aligned N. 10° W.-S. 10° E., filled with horizontal and current-ripple laminae. Moderate ledges, good exposure. BHP-2-1.	
	0-1 ft Limestone (100%): dark yellowish brown (10YR4/2); weathers grayish orange (10YR6/4). Calcareous (80%), muddy (10%), siliceous (10%), carbonaceous (trace). Skeletal (60%): crinozoans, brachiopods, others; grains (20%): very small; matrix (20%): microcrystalline calcite, silt (noncalcareous, may be quartz), probable clay, and carbonaceous material; lithoclasts (trace, locally abundant): pebbles of limestone 2-30 mm diameter, some larger ones are black, carbonaceous to siliceous limestone, no discernible grading, poor sorting, prolate forms, subrounded to subangular, no discernible orientation; fair grain tangency; lime wackestone-packstone. Local channel eroded 30 cm deep into underlying limestone of unit 1, channel is probably a few meters wide, wedging out to east and thinning to west; two beds 10 and 20 cm thick, sharp erosion surface at base; no discernible lamination. Slight ledge; fair exposure. BHP-2-0.	
1	Limestone	11
	0-11 ft Limestone (100%): brownish gray (5YR4/1); weathers grayish orange (10YR7/4) to light gray (N7). Calcareous (100%), muddy (trace). Skeletal (60%): crinozoans (1-2 mm diameter, light gray, N6 to N7), cryptostome bryozoans (100 x 700 mm) with spiral axes and attached fronds *(Archimedes* sp.), other types; grains (30%): ooids (1 mm diameter or smaller), elongate grains with rinds or coats; matrix (10%): microcrystalline calcite, minor silt and probable clay; good grain tangency; lime packstone. Beds 5-25 cm thick, average 20 cm, some surfaces slightly uneven, may be erosional; no discernible lamination. Slight ledges; fair to good exposure. BHP-1-0.	
	Base is covered by Quaternary alluvial-fan and stream deposits, in southern tributary to main Chaney Canyon drainage.	

TABLE 5-TRAVERSE DATA, BIG HATCHET PEAK SECTION, HIDALGO COUNTY, NEW MEXICO.

Unit	Thickness (ft)	Cumulative thickness (ft)	Strike, dip	Direction from base to top	Distance along traverse (yards)	Difference in elevation (ft)	Cumulative difference (ft)	Topography
-Base is in SE 1/4 NW 1/4 NE 1/4 sec. 6, T. 31 S., R. 15 W.; elevation is about 5,940 ft								
1	11	11	N. 50 E., 36 SE.	S. 10 W.	5	+ 3	+3	Arroyo
2	45	56	N. 50 E., 36 SE.	S. 10 W.	26	+19	+ 22	Arroyo
3	8	64	N. 50 E., 36 SE.	S. 10 W.	3	+ 5	+ 27	Arroyo
4	14	78	N. 50 E., 36 SE.	S. 10 W.	11	+ 6	+ 33	Arroyo
5	5	83	N. 50 E., 36 SE.	S. 10 W.	2	+ 5	+ 38	Spur
6	60	143	N. 50 E., 36 SE.	S. 5 E.	40	+23	+ 61	Spur
7	23	166	N. 50 E., 36 SE.	S. 35 E.	13	+11	+ 72	Spur
8	10	176	N. 50 E., 36 SE.	S. 35 E.	3	+ 7	+ 79	Spur
-Offset on top of unit 8, go S. 60 W., 60 yards, cross arroyo to next spur, gain 4 ft in elevation								
9	20	196	N. 50 E., 36 SE.	S. 10 E.	2	+ 6	+ 89	Spur
10	7	203	N. 50 E., 36 SE.	S. 10 E.	7	+ 7	+ 96	Spur
11	70	273	N. 50 E., 36 SE.	S. 30 W.	80	+33	+ 129	Spur
12	17	290	N. 50 E., 36 SE.	S. 40 E.	7	+11	+ 140	Arroyo
13	(35)	-	N. 50 E., 36 SE.	S. 30 E.	12	+16	+ 156	Arroyo
-Offset at 35 ft above base of unit 13, go N. 60 E., 34 yards, to crest of spur, gain about 2 ft in elevation								
13	102	392	N. 50 E., 36 SE.	S. 20 E.	45	+33	+ 191	Spur
14	(5)	-	N. 50 E., 36 SE.	S. 40 E.	2	+ 1	+ 192	Spur
-Offset at 5 ft above base of unit 14, go S. 40 W., 33 yards, to arroyo, lose 1 ft in elevation								
14	57	449	N. 50 E., 36 SE.	S. 35 E.	45	+24	+215	Arroyo
15	50	499	N. 50 E., 36 SE.	S. 40 E.	24	+24	+ 239	Arroyo
16	(15)	-	N. 50 E., 36 SE.	S. 40 E.	5	+10	+ 249	Arroyo
-Offset at 15 ft above base of unit 16, go N. 70 E., 185 yards, to crest of main spur, gain 1 ft in elevation								
16	45	544	N. 50 E., 36 SE.	S. 20 E.	20	+17	+ 267	Spur
17	38	582	N. 50 E., 36 SE.	S. 25 E.	30	+22	+ 289	Spur
18	43	625	N. 50 E., 36 SE.	S. 30 E.	18	+22	+ 311	Spur
19	25	650	N. 50 E., 36 SE.	S. 10 W.	22	+11	+ 322	Spur
20	17	667	N. 50 E., 36 SE.	S. 25 W.	10	+12	+ 334	Spur
21	6	673	N. 50 E., 36 SE.	S. 40 W.	38	+ 5	+ 339	Spur
22	30	703	N. 45 E., 36 SE.	S. 40 E.	9	+17	+ 356	Spur
23	25	728	N. 45 E., 36 SE.	S. 40 E.	12	+13	+ 369	Spur
24	25	753	N. 45 E., 36 SE.	S. 10 W.	23	+15	+ 384	Spur
25	(47)	-	N. 45 E., 36 SE.	due S.	27	+27	+411	Spur
25	119	872	N. 45 E., 36 SE.	S. 60 E.	72	+23	+ 434	Spur
26	11	883	N. 55 E., 34 SE.	S. 20 W.	10	+ 9	+ 443	Spur
27	75	958	N. 50 E., 32 SE.	S. 35 E.	34	+43	+ 486	Spur
28	10	968	N. 50 E., 32 SE.	S. 20 E.	4	+ 5	+ 491	Spur
29	29	997	N. 50 E., 32 SE.	due S.	22	+20	+ 511	Spur
30	15	1,012	N. 50 E., 32 SE.	S. 40 E.	6	+11	+ 522	First fairly prominent ledge
31	**20**	1,032	N. 50 E., 32 SE.	S. 15 W.	12	+17	+ 539	Spur
32	**35**	1,067	N. 50 E., 32 SE.	S. 20 E.	19	+22	+ 561	Spur
33	**24**	1,091	N. 45 E., 34 SE.	S. 5 E.	16	+22	+ 583	Spur
34	**40**	1,131	N. 45 E., 34 SE.	S. 40 E.	20	+22	+ 605	Spur
35	**22**	1,153	N. 45 E., 34 SE.	S. 10 W.	15	+12	+ 617	Spur
36	**39**	1,192	N. 45 E., 34 SE.	S. 30 W.	35	+38	+ 655	First prominent ledge
37	38	1,230	N. 45 E., 34 SE.	S. 5 W.	25	+18	+ 673	Spur
38	82	1,312	N. 45 E., 34 SE.	S. 15 W.	50	+55	+ 728	Spur
39	26	1,338	N. 40 E., 34 SE.	S. 10 E.	14	+16	+ 744	Spur
40	11	1,349	N. 40 E., 34 SE.	S. 30 E.	4	+10	+ 754	Spur
-Offset on top of unit 40, go S. 35 W., 41 yards, to crest of spur, gain 17 ft in elevation								
41	64	1,413	N. 40 E., 34 SE.	S. 35 E.	30	+30	+ 801	Spur
42	28	1,441	N. 30 E., 34 SE.	S. 35 E.	14	+17	+ 818	Spur
43	8	1,449	N. 30 E., 34 SE.	S. 15 E.	2	+ 5	+ 823	Spur
44	15	1,464	N. 35 E., 34 SE.	S. 10 E.	22	+11	+ 834	Spur
45	61	1,525	N. 35 E., 34 SE.	S. 55 E.	36	+42	+ 876	Spur
46	33	1,558	N. 35 E., 34 SE.	S. 5 E.	30	+24	+ 900	First cliff
47	40	1,598	N. 35 E., 34 SE.	S. 5 E.	10	+38	+ 938	First cliff
–Offset on top of unit 47, go N. 50 E., about 30 yards; climb down cliff, trace marker to northeast, cross fault in first cliff; lose 65 ft in elevation								
48	5	1,603	N. 35 E., 25 SE.	S. 30 E.	2	+ 3	+ 876	First cliff
49	59	1,662	N. 35 E., 25 SE.	S. 5 E.	20	+60	+ 936	First cliff
–Offset on top of unit 49, go S. 40 W., about 200 yards; climb down cliff, trace marker to southwest, climb up wide breach in cliff; gain 35 ft in elevation								
50	42	1,704	N. 20 E., 30 SE.	N. 70 E.	28	+ 25	+ 996	
51	12	1,716	N. 20 E., 20 SE.	S. 65 E.	3	+11	+ 1,007	Second cliff
52	35	1,751	N. 20 E., 20 SE.	S. 65 E.	12	+ 39	+ 1,056	Second cliff
53	23	1,774	N. 20 E., 20 SE.	S. 45 E.	7	+ 16	+ 1,072	Second cliff
-Offset on top of unit 53, go S. 20 W., 38 yards, gain 16 ft in elevation								
54	(25)		N. 20 E., 20 SE.	S. 20 W.	20	+ 15	+ 1,103	Second cliff-talus
54	120	1,894	N. 20 E., 20 SE.	S. 15 E.	28	+ 93	+ 1,196	Second cliff-breach

TABLE 5 (continued)

Unit	Thickness (ft)	Cumulative thickness (ft)	Strike, dip	Dip from base to top	Distance along traverse (yards)	Difference in elevation (ft)	Cumulative difference (ft)	Topography
55	45	1,939	N. 10 E., 24 SE.	N. 80 E.	20	+ 32	+ 1,228	Second cliff
56	103	2,042	N. 10 E., 24 SE.	S. 85 E.	33	+ 78	+ 1,306	
57	65	2,107	N. 10 E., 24 SE.	S. 80 E.	28	+ 39	+ 1,345	
58	22	2,129	N. 10 E., 24 SE.	due E.	9	+ 19	+ 1,364	Third cliff
59	3	2,132	N. 10 E., 24 SE.	due E.	1	+ 3	+ 1,367	Third cliff
60	23	2,155	N. 10 E., 24 SE.	N. 20 E.	15	+ 22	+ 1,389	Third cliff
61	15	2,170	N. 10 E., 24 SE.	N. 70 E.	10	+ 11	+ 1,400	Third cliff
62	95	2,265	N. 10 E., 24 SE.	N. 55 E.	60	+ 76	+ 1,476	Third cliff
63	23	2,288	N. 10 E., 24 SE.	S. 5 W.	8	+ 17	+ 1,493	
64	26	2,314	N. 10 E., 24 SE.	S. 75 E.	7	+ 18	+ 1,511	
65	97	2,411	N. 10 E., 24 SE.	S. 50 E.	34	+83	+1,594	
66	30	2,441	N. 10 E., 24 SE.	S. 50 E.	11	+22	+ 1,616	
67	(75)	-	N. 10 E., 24 SE.	S. 20 E.	27	+ 55	+ 1,671	Fourth cliff
67	(115)	-	N. 10 E., 24 SE.	S. 40 E.	20	0	+ 1,671	
-Offset at 115 ft above base of unit 67, go S. 75 W., 350 yards, gain 126 ft in elevation								
67	148	2,589	N. 25 E., 26 SE.	S. 65 E.	15	+ 8	+ 1,805	
68	120	2,709	N. 25 E., 26 SE.	N. 85 E.	40	+ 110	+ 1,915	Fifth cliff
69	87	2,796	N. 15 E., 26 SE.	N. 75 E.	30	+ 80	+ 1,995	Sixth cliff
70	54	2,850	N. 15 E., 26 SE.	S. 40 E.	23	+ 38	+ 2,033	Sixth cliff
71	45	2,895	N. 15 E., 26 SE.	S. 15 E.	18	+ 33	+ 2,066	
72	50	2,945	N. 15 E., 26 SE.	S. 30 E.	20	+ 44	+ 2,110	
-Offset on top of unit 72, go S. 80 E., 615 yards, downhill								
73	5	2,950	N. 26 E., 26 SE.	(did not measure directions, distances, or elevations above)				Seventh cliff
74	(5)	-	N. 26 E., 26 SE.					Seventh cliff
-Offset at 5 ft above base of unit 74, go east-southeast, 50 yards, downhill								
74	(35)	-	N. 26 E., 26 SE.					Seventh cliff
-Offset at 35 ft above base of unit 74, go west, few yards, uphill								
74	115	3,065	N. 26 E., 26 SE.					
-Offset on top of unit 74, go east, 20 yards, downhill								
75	(4)		N. 10 W., 24 NE.					Eighth cliff
–Offset at 4 ft above base of unit 75, go west, 20 yards, uphill; at cleft, trace marker to upthrown side of 10 ft fault, another 15 yards								
75	54	3,119	N. 45 E., 25 SE.					Eighth cliff
76	(10)	-	N. 10 E., 24 SE.					Ninth cliff
-Offset at 10 ft above base of unit 76, go northeast, 15 yards, downhill, along base of main part of cliff								
76	44	3,163	N. 10 E., 24 SE.					Ninth cliff
77	(75)	-						
–Offset at 75 ft above base of unit 77, go west-southwest, 50 yards, uphill, then S. 10 E. toward cliff								
77	100	3,263	N. 10 E., 24 SE.					
–Offset on top of unit 77, go west, about 10 yards, uphill, to fracture, breach in prominent ledge								
78	(17)	-	N. 5 E., 26 SE.					
-Offset at 17 ft above base of unit 78, go west, 160 yards, uphill								
78	45	3,308	N. 5 E., 26 SE.					Highest exposure
–Top is in NE 1/4 SE 1/4 SE 'A sec. 6, T. 31 S., R. 15 W.; elevation is about 8,120 ft; location is about 0.2 mi ENE. of Big Hatchet Peak.								

TABLE 6-SAMPLES COLLECTED FROM THE BIG HATCHET PEAK SECTION. Sample notation indicates BHP unit number and footage above base of unit.

Sample notation (BHP-)	Cumulative ft above base of section	Rock type	Purpose			
			petrography	paleontology	source analysis	reservoir analysis
top peak	-	limestone	x	x		
78-42	3,305	limestone	x	x		
78-4	3,267	limestone	x	x		
77-41	3,204	limestone	x	x		
77-22	3,185	limestone	x			
76-8	3,127	limestone	x	x	x	
76-3	3,122	limestone	x	x		
75-7	3,072	limestone	x	x		
75-1	3,066	limestone	x			
74-54	3,004	limestone	x	x		
74-35	2,985	limestone	x			
74-0	2,950	limestone	x	x		
73-2	2,947	chert	x			
73-1	2,946	limestone	x			
72-2	2,897	limestone	x	x		
71-2	2,852	limestone	x	x	x	

TABLE 6 (continued)

Sample notation (BHP-)	Cumulative ft above base of section	Rock type	Purpose			
			petrography	paleontology	source analysis	reservoir analysis
70-3	2,799	dolostone	x			x
69-85	2,794	limestone	x	x		
69-24	2,733	limestone	x	x		
69-14	2,723	chert	x			
69-3	2,712	limestone	x	x		
68-70	2,659	limestone	x	x		
68-4	2,593	limestone	x	x	x	
67-114	2,555	dolostone	x			
67-68	2,509	dolostone	x			x
67-22	2,463	dolostone	x			x
67-10	2,451	dolostone	x			
66-9	2,420	limestone	x	x	x	
65-94	2,408	dolostone	x			x
65-22	2,336	dolostone	x			x
65-2	2,316	dolostone	x			x
64-1	2,289	limestone	x	x		
63-2	2,267	dolostone	x			x
62-5	2,175	limestone	x	x		
61-2	2,157	limestone	x	x		
60-2	2,134	limestone	x			
59-2	2,131	chert	x			
59-1	2,130	limestone	x			
58-1	2,108	limestone	x	x		
57-23	2,065	limestone		x		
57-10	2,052	limestone	x	x		
56-92	2,031	dolostone	x			x
56-7	1,946	dolostone	x			x
55-3	1,897	chert	x			
55-2	1,896	limestone	x	x		
54-96	1,870	limestone, mudstone	x			
54-4	1,778	chert	x			
54-2	1,776	limestone	x	x		
53-3	1,754	limestone		x		
53-1	1,752	limestone	x			
52-5	1,721	limestone		x		
52-3	1,719	chert	x			
52-2	1,718	limestone	x		x	
51-2	1,706	limestone	x			
50-1	1,663	limestone	x	x		
49-45	1,648	dolostone	x			
49-30	1,633	dolostone	x			
49-19	1,622	dolostone	x			x
49-14	1,617	dolostone	x			x
49-9	1,612	dolostone	x			x
49-4	1,607	dolostone	x			x
49-1	1,604	dolostone	x			
48-2b	1,600	dolostone	x			
48-2a	1,600	limestone	x	x		
48-1	1,599	limestone	x			
47-2	1,560	chert	x			
47-1	1,559	limestone	x			
46-17	1,542	limestone	x			
46-5	1,530	dolostone	x			
46-1	1,526	limestone	x	x		
45-17	1,481	limestone	x	x		
45-3	1,467	dolostone		x		
45-2	1,466	limestone	x			
45-1	1,465	dolostone	x			
44-2	1,451	limestone	x			
43-7	1,448	limestone	x	x		
42-14	1,427	chert	x			
42-12	1,425	limestone	x	x		
41-20	1,369	limestone	x		x	
40-1	1,339	limestone	x	x		
39-4	1,316	chert				
39-1	1,313	limestone		x		
38-3	1,233	limestone	x	x		
38-0	1,230	limestone (lens)	x			
37-0	1,192	limestone	x			

TABLE 6 (continued)

Sample notation (BHP-)	Cumulative ft above base of section	Rock type	Purpose: petrography	Purpose: paleontology	Purpose: source analysis	Purpose: reservoir analysis
36-4	1,157	chert	x			
36-2	1,155	limestone	x			
35-10	1,141	chert	x			
35-1	1,132	limestone	x			
34-6	1,097	limestone	x	x		
33-7	1,074	chert	x			
33-6	1,073	limestone	x	x		
32-2	1,034	limestone	x			
31-15	1,027	chert	x			
31-10	1,022	limestone	x	x	x	
30-0	997	limestone	x	x		
29-3	971	chert	x			
29-2	970	limestone	x			
28-5	963	limestone	x	x		
27-3	886	chert	x			
27-2	885	limestone	x			
26-0	872	limestone	x	x		
25-4	757	chert	x			
25-3	756	limestone	x			
24-1	729	limestone	x			
23-4	707	chert	x			
22-1	674	limestone	x	x		
21-3	670	chert	x			
21-2	669	limestone	x		x	
20-2	652	limestone	x	x		
19-4b	629	chert	x			
19-4a	629	limestone	x			
18-0	582	limestone	x			
17-17	561	chert	x			
17-4	548	limestone	x			
16-10	509	chert	x			
16-4	503	limestone	x	x		
15-2	451	limestone	x		x	
14-3	395	limestone	x			
14-2	394	chert	x			
13-75	365	limestone				
13-35	325	chert	x			
13-23	313	limestone	x	x		
13-7	297	limestone	x			
12-1	274	limetone	x	x		
11-1	204	limestone	x			
10-3	199	limestone	x		x	
9-6	182	limestone	x			
9-5	181	limestone	x			
8-1b	167	chert	x			
8-1a	167	limestone	x			
7-23	166	limestone	x			
7-1	**144**	limestone	x			
6-1b	84	chert	x			
6-1a	84	limestone	x			
5-0	78	limestone	x			
4-13	77	limestone	x			
4-12	76	siltstone	x			
3-2	58	limestone	x			
2-1	12	limestone	x			
2-0	11	limestone	x			
1-0	0	limestone	x			

Appendix 2 Petrographic data

Table 7 is a catalog of 137 petrographic analyses based on examination with a Zeiss polarizing microscope of thin sections cut from samples collected in the Big Hatchet Peak section. The samples are listed in reverse stratigraphic order from youngest to oldest. Samples numbered BHP-top peak to BHP-43-7 are from the upper Horquilla, BHP-42-14 to BHP-5-0 are from the lower Horquilla, and BHP-4-13 to BHP-1-0 are from the Paradise Formation.

Each description consists of three parts—the general and specific rock names, a list of allochem and detrital grains in order of decreasing abundance, and a discussion of diagenetic features in order of occurrence. This information is plotted graphically with respect to the stratigraphic column in appendix 3. Selected thin sections are discussed in the main text section on petrography and are illustrated in the plates of photomicrographs.

Rock names

General rock names at the head of each description include limestone, dolostone, chert, and siltstone. The minority of mixed rock types include dolomitic, silty, or sandy limestone, limy or cherty dolostone, and silty or sandy chert.

Specific carbonate-rock names in boldface are combinations of prefixes denoting allochem grains based on the classification of Folk (1962) and of root terms denoting depositional textures based on the classification of Dunham (1962). An example is **oobiopelgrainstone.**

The prefix oo- refers to ooids, which are spheroidal carbonate grains less than 2 mm in diameter that have concentrically laminated coatings. The prefix **pel-** refers to peloids, which are spheroidal, micritic, internally structureless grains; these may be fecal pellets or micritized skeletal grains that have been rounded during transport. The prefix **bio-** refers to whole skeletal forms or bioclasts produced by organic or inorganic fragmentation. The prefix **intra-** refers to intraclasts, which are derived by local erosion of penecontemporaneously lithified material; the material may have been lithified by exposure within a supratidal zone or by intertidal or submarine cementation. The term **grapestone** refers to a composite grain of ooids, peloids, bioclasts, or intraclasts, commonly with a micrite binding and/or one or more carbonate coatings. The prefixes are not arranged in order of increasing or decreasing abundance; they are selected to form the most euphonious combination. For instance, oobiopelgrainstone sounds better than pelbi000grainstone.

The root term **mudstone** in the Dunham classification is a lime-mud supported rock with less than 10 percent carbonate grains (allochems). **Wackestone** is a lime-mud supported rock with more than 10 percent carbonate grains. **Packstone** is a grain-supported rock with original lime-mud material occupying spaces between grains; no cement is present. **Grainstone** is a grain-supported rock whose original (primary) intergranular pores may have been filled entirely by cement, or to varying degrees by vadose internal sediment. These root terms indicate the predominant fabric; however, in many instances, the area of one thin section will contain two distinct fabrics. In such instances, the rock type is designated as a wackestone-packstone or packstone-grainstone.

Grain types

The grains identified in the thin sections are allochems or detrital grains. Allochems are grains of carbonate sediment that have been transported only short distances from their sites of precipitation; they include the ooids, peloids, bioclasts, intraclasts, and grapestone grains defined in the previous section. Bioclasts are classified in general terms or by genus where possible. Detrital grains are derived from pre-existing rocks and may be transported long distances. The only ones seen in this section are composed of quartz or carbonaceous material.

Diagenetic features

Diagenetic features consist of postdepositional processes and products of stabilization (of original minerals), recrystallization, replacement, solution, fracturing, internal sedimentation, cementation, and the resulting porosity relationships. Preservation of porosity in carbonate rocks normally is more dependent on the diagenetic history than on the types of original grains or depositional fabric.

In the descriptions of table 7, diagenetic features are listed in order of occurrence where possible. Events taking place in the original marine environment are listed first. Subsequent events taking place in vadose or phreatic environments, with the diagenetic fluids being fresh or saline ground waters, are listed afterward. Times of silicification or recrystallization generally are difficult to place precisely within the sequence of diagenetic events, and these are listed arbitrarily last in many cases. For brevity, many of the features are described in single words or phrases instead of complete sentences.

Key terms used in the descriptions are defined within the following general groups of early marine, fresh-water, and saline diagenetic features. Where diagenetic history was relatively simple, the carbonate sediment may have been subjected to early marine diagenesis and subsequently stabilized to limestone in fresh-water or to dolostone in saline (to hypersaline) fluids. Where the history was more complex, a carbonate sediment may have been subjected to alternating fresh and saline ground waters, such that features from those two groups may be preserved in one rock.

Carbonate sediments may show the following early diagenetic features if they remain exposed to the marine environment on stable surfaces for sufficient time:

beachrock cement—gravitational, microstalactitic, acicular cement crusts precipitated interstitially in lime sands subjected to marine-vadose (intertidal) diagenesis after deposition and before burial. These cements originally consist of aragonite or high-magnesium calcite.

submarine cement—isopachous crusts of original acicular aragonite or high-magnesium calcite precipi-

tated interstitially in lime sands subjected to marinephreatic (subtidal) diagenesis.

micritization—destruction of original texture of shells (or ooids) by boring, endolithic, blue-green algae that overgrow dead shells on the sea floor. The filamentous borings become backfilled by micritic cement. Thin shells may become thoroughly micritized.

micrite envelopes—thin micritic rinds formed on the exterior of relatively thick shells (or bioclasts) by boring endolithic algae that do not penetrate the entire shell. They are distinguished from micritic rim cements that generally coat and bound all grains in lime sands. True micrite envelopes may occur only on isolated grains or on all grains.

algal coated grains—relatively thick, accretionary coatings formed by algae (or encrusting foraminifers) on grains during marine-phreatic diagenesis. The coatings are micritic but generally are much thicker than micrite envelopes or micritic rim cements.

Limestones stabilized during fresh-water diagenesis may show the following features:

calcitization—replacement of aragonite by calcite.

recrystallization—a process of fresh-water diagenesis in which the original lime-mud matrix commonly is recrystallized to microspar (crystal diameters range from 5 to 30 microns) or pseudospar (crystals greater than 30 microns). During recrystallization, syntaxial rims commonly form on monocrystalline crinozoan components.

aragonitic shells dissolved—selective fresh-water dissolution of aragonitic shells, with no dissolution of calcitic shells.

hollow micrite envelopes—voids produced by selective fresh-water dissolution of crystalline aragonitic cores within micrite envelopes. Such aragonitic cores generally were bioclasts (mollusk shells or phylloid algae) or ooids.

non tectonic fractures—crumbly fractures commonly produced during fresh-water diagenesis by partial collapse of aragonitic shell molds. These fractures result from dissolution of such shells before the matrix has been thoroughly lithified. They may also develop in association with collapse breccias or differential lithification of matrix.

compaction wisps—feathery concentrations of impurities, such as organic material or dead oil, produced as stringers of solution residues during compaction of unlithified carbonate sediments; these features are absent in limestone that are lithified early.

stylolites—diagenetic features formed commonly along bedding surfaces in limestones that resemble sutures or tracings of a stylus; they apparently are formed after some lithification by solution fronts migrating along the surfaces. Impurities such as organic material, dead oil, or clastic material may be concentrated in the stylolitic seams.

vadose internal sediment—micritic, pelloidal, or fine-clastic material deposited within cavities of limestones; this material may be washed in during an early transgression of the marine environment, or during subaerial exposure and subsequent fresh-water incursion from the terrestrial environment. Such internal sediment normally fills only the floor of a cavity, with cement filling the rest, and can be used as a geopetal (up/down) criterion.

microstalactitic gravitational cement—calcite cement formed in small voids within vadose environments in much the same manner as stalactites form in caves. Such cements are geopetal features as they exhibit pendulous downward elongation from upper surfaces of voids.

epitaxial cement—calcite cement formed by optically continuous overgrowths on pre-existing shells or bioclasts. This cement is most strikingly manifested on monocrystalline crinozoan components; it commonly forms large aureoles that poikilotopically enclose neighboring grains.

blocky-equant cement—calcite cement in relatively large voids that forms a mosaic of equidimensional, blocklike crystals.

drusy cement—calcite cement in relatively large voids that forms a mosaic of crystals with increasingly larger diameters toward the center of the cavity. The initial lining of the void may be a thin crust of scalenohedral calcite crystals.

silicification—a process occurring during fresh-water diagenesis of a newly deposited carbonate in which silica (chert) commonly nucleates in organic-rich materials, such as shells, ooids, peloids, burrows, or stromatolites. Initially the silica invades and replaces the surrounding matrix to form small nodules. If the process continues for a sufficiently long time, the nodules grow to become massively silicified bodies or layers. Micrite matrix, micritic peloids, and stromatolites generally are replaced by microquartz. Crystalline shells and ooids normally are replaced by megaquartz or fibrous chalcedony (length-slow or length-fast). Voids commonly are filled by chalcedony or megaquartz cements.

exsolved dolomite rhombs—dolomite porphyroblasts occurring in siliceous limestone or chert; they exsolve from magnesium calcite during silicification. These phenomena probably result from ionic mobilization that occurs among expanding silica-replacement fronts. The magnesium predominantly is derived locally from shell material.

Dolostones stabilized during saline (to hypersaline) diagenesis may show the following features:

neomorphic dolomitization—a process in which dolomite has directly replaced aragonitic lime mud or shells, and a new texture of euhedral to subhedral rhombic crystals is formed;

paramorphic dolomitization—a process in which dolomite has directly replaced calcitic materials, and the original calcitic texture has been preserved;

dedolomitization—a process in which neomorphic, rhombic-crystal dolomite has been paramorphically replaced by calcite, and the original dolomitic fabric is perfectly preserved;

intercrystalline porosity—secondary porosity in tiny voids among rhombic faces of dolomite crystals; it is found only in dolostones and dedolostones (dolomite replaced by calcite) where compromise boundaries have not been formed between adjacent crystal faces;

anhydritization—emplacement of anhydrite porphyroblasts (or nodules) by hypersaline ground water in dolostone (or limestone). In many cases, the anhydrite is dissolved during subsequent fresh-water diagenesis, but

the distinctive stair-step outlines of the porphyroblastic crystals are preserved around the edges of molds; and

anhydrite-mold porosity—tertiary (third-stage) moldic porosity formed by dissolution of anhydrite porphyroblasts or nodules.

Identification of carbonate minerals

All thin sections were stained with a combination of potassium ferricyanide and alizarin red-S, according to the method of Lindholm and Finkelman (1972). This stain discriminates nonferroan calcite and dolomite from ferroan calcite and dolomite that contain ferrous iron. Nonferroan calcite is stained red, and nonferroan dolomite is not stained. Ferroan calcite is stained purple, and ferroan dolomite is stained blue.

Ferroan calcite or dolomite cements are precipitated in reducing, phreatic environments. Nonferroan calcite or dolomite cements are precipitated in oxidizing or reducing, vadose or phreatic environments, in the absence of ferrous iron. Zoned crystals of ferroan and nonferroan calcite or dolomite probably are precipitated in alternating oxidizing and reducing environments.

TABLE 7—PETROGRAPHIC DESCRIPTIONS OF THIN SECTIONS FROM THE BIG HATCHET PEAK SECTION. Sample notation indicates **BHP** unit number and footage above base of unit.

Sample notation (BHP-)	Description
top peak	Limestone; **biopelwackestone.** Crinozoans, bryozoans, small foraminifers, peloids, fusulinids, *Tubiphytes,* and brachiopods. Micritization. Some recrystallization of matrix. Quartz porphyroblasts have formed by partial replacement of micritized shells and matrix. Most intrabiotic cavities are lined by thin crusts of scalenohedral calcite cement and are filled by coarse, equant crystals of ferroan calcite. In some large fusulinids the following sequence of cements occurs: 1) thin crust of calcite scalenohedra, 2) siderite (or ankerite), and 3) ferroan calcite. Nontectonic fractures formed; they are filled by ferroan calcite. Some recrystallized matrix also consists of ferroan calcite.
78-42	Limestone; **biowackestone.** Crinozoans, phylloid algae, small foraminifers, bryozoans, pelecypods, brachiopods, ostracods, and *Tubiphytes.* Micritization. Aragonitic shells dissolved and nontectonic fractures formed; molds and fractures filled by calcite cement. Silicification of some shells.
78-4	Limestone; **biowackestone.** Fusulinids, bryozoans, crinozoans, small foraminifers, phylloid algae, *Tubiphytes,* brachiopods, and ostracods. Micritization. Aragonitic shells dissolved and nontectonic fractures formed; molds and fractures are filled by calcite (first generation). Silicification of some shells.
77-41	Limestone; **biowackestone.** *Tubiphytes,* crinozoans, phylloid algae, small foraminifers, pelecypods, brachiopods, bryozoans, fusulinids, and ostracods. Micritization and micrite envelopes. Aragonitic shells dissolved and hollow micrite envelopes formed. All voids were filled by calcite cement. Largest voids contain a first generation of calcite and a second generation of ferroan calcite that completely filled the pores.
77-22	Limestone; **biograpestone grainstone-packstone.** Crinozoans, grapestone grains, *Tubiphytes,* phylloid algae, brachiopods, pelecypods, and small foraminifers. Micritization, micrite envelopes, and algal coated grains. Aragonitic shells dissolved and hollow micrite envelopes and nontectonic fractures formed; all voids became filled by calcite cement.
76-8	Limestone; **biowackestone.** *Tubiphytes,* crinozoans, fusulinids, small foraminifers, pelecypods, gastropods, phylloid algae, bryozoans, and crustose red algae. Rhabdoliths of intergrown phylloid algae and *Tubiphytes.* Micritization and micrite envelopes. Aragonitic shells dissolved and hollow micrite envelopes formed; both molds were filled by calcite cement. Recrystallization of matrix.
76-3	Limestone; **biowackestone.** *Tubiphytes,* small foraminifers, bryozoans, gastropods, pelecypods, and ostracods. Micritization. Aragonitic shells dissolved to form molds, vugs, and nontectonic fractures. Larger vugs contain layered, micritic, vadose internal sediment. All voids filled by calcite cement. Recrystallization of matrix.
75-7	Limestone; **biopelwackestone.** *Tubiphytes,* peloids, bryozoans, fusulinids, pelecypods, small foraminifers, and *Girvanella* borings. Micritization. Aragonitic shells dissolved and nontectonic fractures formed; both molds and fractures filled by calcite cement. Silicification of some shells.
75-1	Limestone; **oobiopackstone.** Ooids, *Tubiphytes,* phylloid algae, bryozoans, crinozoans, gastropods, pelecypods, ostracods, small foraminifers, and fusulinids. Micritization and micrite envelopes. Aragonitic shells dissolved and hollow micrite envelopes and nontectonic fractures formed; all voids were filled by calcite cement.
74-54	Limestone; **biowackestone.** Fusulinids, ostracods, pelecypods, and bryozoans. Micritization. Aragonitic shells dissolved and nontectonic fractures formed; molds and fractures were filled by calcite cement. Anhydrite porphyroblasts were emplaced and dissolved; molds were filled by dolomite cement.
74-35	Limestone; **oobiopelgrainstone.** Bryozoans, peloids, *Tubiphytes,* small foraminifers, ooids, and pelecypods. Micritization and micrite envelopes. Aragonitic shells and ooids dissolved and hollow micrite envelopes and nontectonic fractures formed. All primary and secondary voids filled by calcite cement.
74-0	Limestone; **biopackstone.** Crinozoans, bryozoans, pelecypods, *Tubiphytes,* ostracods, trilobites, and small foraminifers. Micritization. Aragonitic shells dissolved and nontectonic fractures were formed; both filled by calcite cement. Recrystallization of matrix.
73-2	Chert; **biopelwackestone.** Siliceous sponge spicules, crinozoans, and peloids. Microquartz replaced matrix and contains dolomite inclusions. No dolomite porphyroblasts occur in unreplaced limestone. Crinozoans are replaced by mega-quartz.
73-1	Limestone; **biopelwackestone.** Crinozoans, bryozoans, peloids, pelecypods, brachiopods, ostracods, *Tubiphytes,* and small foraminifers. Aragonitic shells dissolved and nontectonic fractures formed; both molds and fractures are filled by calcite cement. Recrystallization of matrix; some quartz porphyroblasts in matrix.
72-2	Limestone; **biowackestone.** Fusulinids, crinozoans, pelecypods, *Tubiphytes,* ostracods, and small foraminifers. Aragonitic shells dissolved; molds filled by calcite cement. Recrystallization of matrix.
71-2	Limestone; **biowackestone.** Bryozoans, *Tubiphytes,* phylloid algae, crinozoans, brachiopods, and ostracods. Aragonitic shells dissolved; molds filled by calcite cement.
70-3	Dolostone; **biowackestone.** Only recognizable bioclasts are crinozoans. Medium to very coarse neomorphic dolomitization of matrix (up to 1.5 mm) and paramorphic dolomitization of crinozoans. Good preservation of intercrystalline porosity.

TABLE 7 (continued)

Sample notation (BHP-)	Description
69-85	Limestone; **oobiowackestone.** *Tubiphytes*, phylloid algae, ooids, crinozoans, and brachiopods. Micritization, micrite envelopes, and algal coated grains. Aragonitic shells and ooids dissolved, and hollow micrite envelopes formed; molds filled by calcite cement.
69-24	Limestone; **biopelwackestone.** Peloids, fusulinids, crinozoans, bryozoans, *Tubiphytes*, small foraminifers, brachiopods, and pelecypods. Aragonitic shells dissolved and nontectonic fractures formed by collapse of shell molds and fusulinid walls. All primary and secondary molds were filled by calcite cement. Some recrystallization of matrix occurred; some bioclasts were partially silicified.
69-14	Chert; **biowackestone.** Siliceous sponge spicules and crinozoans. Matrix replaced by microquartz and contains some dolomite porphyroblasts. Shells replaced by chalcedonite and megaquartz. Fractures are filled by calcite cement.
69-3	Limestone; **biowackestone.** *Tubiphytes*, bryozoans, phylloid algae, crinozoans, fusulinids, small foraminifers, and ostracods. Aragonitic shells dissolved, nontectonic fractures formed; all voids were filled by calcite cement. Recrystallization of matrix.
68-70	Limestone; **biopelwackestone.** *Tubiphytes*, crinozoans, ostracods, phylloid algae, peloids, brachiopods, and small foraminifers Micritization, micrite envelopes, and algal coated grains. Aragonitic shells dissolved and hollow micrite envelopes formed; voids were filled by calcite cement.
68-4	Limestone; **oobiopelwackestone.** *Tubiphytes*, phylloid algae, crinozoans, fusulinids, peloids, small foraminifers, ostracods, and ooids. Micritization and algal coated grains. Some dolomite porphyroblasts and some calcitic shells partially paramorphically dolomitized. Aragonitic shells dissolved; molds filled by calcite and dolomite cements.
67-114	Dolostone; **biowackestone.** Crinozoans are only recognizable fossils. Coarse neomorphic dolomitization of matrix (up to 0.6 mm). Paramorphic dolomitization of crinozoans. Anhydrite porphyroblasts emplaced and dissolved to form tertiary molds. Fair intercrystalline porosity preserved along with anhydrite molds. Small amounts of microstalactitic, gravitational calcite cements in anhydrite molds.
67-68	Dolostone; **biowackestone.** Crinozoans are only identifiable fossils. Coarse neomorphic dolomitization of matrix (up to 0.5 mm). Crinozoans paramorphically dolomitized. Small anhydrite porphyroblasts emplaced and then dissolved. Fair preservation of intercrystalline porosity. Some microstalactitic calcite cement in anhydrite molds.
67-22	Dolostone; **biowackestone.** Crinozoans are only recognizable bioclasts. Coarse to very coarse neomorphic dolomitization of matrix (1.2 mm). Crinozoans paramorphically dolomitized. Anhydrite porphyroblasts emplaced and dissolved. Many voids contain microstalactitic gravitational calcite cement. Outer portions of some microstalactites have been paramorphically dolomitized. Good intercrystalline porosity preserved along with anhydrite molds.
67-10	Dolostone; **biowackestone.** Crinozoans are only recognizable fossils. Medium neomorphic dolomitization of matrix; crystals range in diameter up to 0.120 mm. Crinoid columnals paramorphically dolomitized. Anhydrite porphyroblasts emplaced and dissolved. Fair intercrystalline porosity preserved along with anhydrite molds.
66-9	Limestone; **biowackestone.** Fusulinids, *Tubiphytes*, crinozoans, small foraminifers, phylloid algae, brachiopods, and ostracods. Large dolomite porphyroblasts in matrix. Aragonitic shells dissolved and molds filled by calcite cement.
65-94	Dolostone; **biowackestone.** Only recognizable bioclasts are crinozoans. Very coarse neomorphic dolomitization of matrix, with crystals ranging in size up to 2 mm. Paramorphic dolomitization of crinozoans. Anhydrite porphyroblasts emplaced and dissolved. Intercrystalline voids and fractures partly filled by microstalactitic gravitational calcite cement. Good porosity preserved.
65-22	Dolostone; **biowackestone.** Only recognizable bioclasts are crinozoans. Coarse neomorphic dolomitization of matrix with crystals ranging up to 0.610 mm in diameter. Paramorphic dolomitization of crinozoans. Anhydrite porphyroblasts emplaced and dissolved. Many large intercrystalline voids and anhydrite molds are still open and are partly filled by gravitational dripstone cement. Good preservation of porosity.
65-2	Dolostone; **biowackestone.** Only recognizable bioclasts are crinozoans. Medium neomorphic dolomitization of matrix (crystals range in diameter up to 0.20 mm). Paramorphic dolomitization of crinozoans. Fair preservation of intercrystalline porosity.
64-1	Limestone, dolomitic; **oobiowackestone.** Phylloid algae, crinozoans, fusulinids, bryozoans, pelecypods, *Tubiphytes*, and ooids. Aragonitic shells dissolved; molds filled by calcite and dolomite cements. Recrystallization of matrix, and emplacement of quartz porphyroblasts. Large anhydrite porphyroblasts were emplaced and dissolved; stairstep molds filled by coarse dolomite cement crystals that have replaced much surrounding calcite matrix. Recrystallized calcite matrix and shells have been neomorphically replaced by medium to very coarsely crystalline dolomite porphyroblasts, which completely destroyed the previous fabric. No porosity preserved.
63-2	Dolostone; **biowackestone.** Recognizable bioclasts include crinozoans. Coarse and very coarse neomorphic dolomitization of matrix. Crystals range up to 1.4 mm in diameter. Many intercrystalline voids filled by coarse calcite cement. Some possible anhydrite molds contain coarse dolomite cement and calcitic, gravitational, dripstone cement. Good preservation of intercrystalline and moldic porosity.
62-5	Limestone; **biowackestone.** Crinozoans, bryozoans, fusulinids, brachiopods, phylloid algae, pelecypods, small foraminifers, trilobites, and *Tubiphytes.* Aragonitic shells dissolved and nontectonic fractures formed; both molds and fractures became filled by calcite cement. Quartz porphyroblasts emplaced in matrix. Recrystallization of matrix. Dead oil and neomorphic dolomitization along stylolite. No porosity preserved.
61-2	Limestone; **biopelwackestone.** Peloids, phylloid algae, crinozoans, fusulinids, small foraminifers, brachiopods, and *Tubiphytes.* Micritization and micrite envelopes. Aragonitic shells dissolved and hollow micrite envelopes formed. Nontectonic fractures and other voids filled by calcite cement; possible anhydrite molds are filled by calcite cement.
60-2	Limestone; **biopackstone.** Crinozoans, bryozoans, fusulinids, brachiopods, and small foraminifers Micritization. Partial silicification of some shells.
59-2	Chert; **biowackestone.** Crinozoans, siliceous sponge spicules, bryozoans, and brachiopods. Matrix replaced by microquartz which contains some dolomite inclusions. Shells replaced by megaquartz and chalcedonite. Some crinozoans only partly replaced by silica. Fractures filled by calcite cement.
59-1	Limestone; **biopelwackestone.** Peloids, crinozoans, ostracods, brachiopods, small foraminifers, bryozoans, and *Tubiphytes.* Recrystallization of matrix.
58-1	Limestone; **biowackestone.** Crinozoans, phylloid algae, *Tubiphytes*, bryozoans, pelecypods, brachiopods, ostracods, and small foraminifers Aragonitic shells dissolved; molds filled by calcite cement. Some recrystallization; some quartz porphyroblasts emplaced.

TABLE 7 (continued)

Sample notation (BHP-)	Description
57-10	Limestone; **biopelpackstone.** Crinozoans, small foraminifers, *Tubiphytes*, bryozoans, peloids, ostracods, brachiopods, and echinoids. Micritization. Syntaxial rims on some crinozoans. Silicification of some shells; small fractures filled by calcite cement.
56-92	Dolostone; **biowackestone.** Only recognizable bioclasts are paramorphically dolomitized crinozoans. Coarse neomorphic dolomitization of matrix; crystals range in diameter up to 0.90 mm. Paramorphic dolomitization of crinozoans. Emplacement and solution of anhydrite; fair intercrystalline porosity has been preserved along with anhydrite molds.
56-7	Dolostone; **biowackestone.** Only recognizable bioclasts are crinozoans. Coarse neomorphic dolomitization of matrix; crystals range in diameter up to 0.6 mm. Paramorphic dolomitization of crinozoans. Very little intercrystalline porosity has been preserved.
55-3	Chert; **biowackestone.** Crinozoans, fusulinids, bryozoans, and siliceous sponge spicules. Matrix replaced by microquartz and contains dolomite inclusions. Shells replaced by megaquartz and chalcedonite. Dedolomitization of many porphyroblasts in chert.
55-2	Limestone; **biopelgrapestone packstone.** Peloids, small foraminifers, crinozoans, grapestone grains, fusulinids, brachiopods, ostracods, and bryozoans. Some large grapestone grains (1.5 mm diameter). Micritization. Recrystallization of matrix; silicification of some shells. Fractures filled by calcite cement.
54-96	Limestone; laminated, red internal sediment. Contains some peloids and tiny, unidentifiable bioclasts. Much of sediment was neomorphically dolomitized. Extensive replacement of the sediment by anhydrite. Cores of many dolomite crystals were selectively replaced by anhydrite. Subsequently, anhydrite became partly dissolved, and some anhydrite was replaced directly by calcite; voids were filled by calcite cement. Some highly corroded dolomite crystals still remain. Later, intensive dedolomitization and coarse recrystallization took place. The red color is due to oxidation of tiny pyrite crystals which are disseminated throughout.
54-4	Chert; **biowackestone.** Bryozoans, crinozoans, ostracods, brachiopods, and small foraminifers. Some crinozoans are unsilicified. Matrix replaced by microquartz which contains countless dolomite inclusions. Shells are replaced by megaquartz and chalcedonite. Dolomite cement was precipitated in intrabiotic cavities prior to silicification. Dedolomitization of all dolomite cement crystals and many matrix crystals has occurred. Intersecting fractures are filled by calcite cement.
54-2	Limestone; **biopelwackestone.** Peloids, *Tubiphytes*, fusulinids, bryozoans, crinozoans, brachiopods, ostracods, and phylloid algae. Aragonitic shells dissolved and nontectonic fractures formed; these became enlarged to form vugs and solution channels that are filled by calcite cement. One large solution channel contains microstalactitic gravitational cement (radial fibrous dripstone). Recrystallization of matrix; silicification of some shells.
53-1	Limestone; **biowackestone.** Crinozoans, bryozoans, *Tubiphytes*, brachiopods, ostracods, phylloid algae(?), and small foraminifers. Aragonitic shells dissolved and nontectonic fractures formed. All secondary voids are filled by calcite cement. Recrystallization of matrix; quartz porphyroblasts emplaced. Anhydrite porphyroblasts were emplaced and subsequently dissolved; molds were filled by dolomite cement.
52-3	Chert; **biowackestone.** Bryozoans, crinozoans, siliceous sponge spicules, brachiopods, and ostracods. Matrix replaced by microquartz which contains abundant inclusions of dolomite. Shells are replaced by megaquartz and chalcedonite. Silicification postdated filling of bryozoans' chambers by rhombic dolomite cement which was later dedolomitized. Two generations of fractures are filled by calcite cement.
52-2	Limestone; **biowackestone.** Bryozoans, crinozoans, pelecypods, *Tubiphytes*, ostracods, and brachiopods. Micritization and micrite envelopes. Aragonitic shells dissolved and hollow micrite envelopes formed; both were filled by calcite cement. Recrystallization. Silicification of many shells.
51-2	Limestone; **biopelwackestone.** Peloids, bryozoans, pelecypods, small foraminifers, crinozoans, phylloid algae, and ostracods. Algal coated grains. Micritization. Aragonitic shells dissolved and nontectonic fractures formed. All voids filled by calcite cement.
50-1	Limestone; **biopelwackestone-packstone.** Bryozoans, crinozoans, *Tubiphytes*, peloids, phylloid algae, small foraminifers, and brachiopods. Micritization and formation of micrite envelopes. Aragonitic shells dissolved, hollow micrite envelopes formed; nontectonic fractures were formed by partial collapse of molds. Recrystallization of matrix; all voids were filled by calcite cement.
49-45	Dolostone; **biowackestone.** Crinozoan components are only recognizable bioclasts. Fine to very coarse neomorphic dolomitization of matrix (crystals range up to 2 mm in diameter) and paramorphic dolomitization of crinozoan components. Anhydrite porphyroblasts were emplaced and then dissolved; third order stairstep molds were formed and preserved along with secondary intercrystalline voids. Good porosity.
49-30	Dolostone; **biowackestone.** Crinozoan components and possible trilobite fragments are the only recognizable bioclasts. Fine to extremely coarse neomorphic dolomitization of matrix (up to 4.5 mm) and paramorphic dolomitization of crinozoans. Anhydrite porphyroblasts were emplaced and then dissolved; molds later became partially filled by calcitic gravitational cement. Good preserved porosity includes secondary intercrystalline voids and tertiary anhydrite molds.
49-19	Dolostone; **biowackestone.** Crinozoans are only recognizable fossils. Fine to very coarse neomorphic dolomitization of matrix (up to 3.5 mm) and paramorphic dolomitization of crinozoans. Anhydrite porphyroblasts were emplaced and dissolved. Gravitational calcite cement precipitated in some anhydrite molds. Fair preservation of secondary inter-crystalline voids and tertiary anhydrite molds.
49-14	Dolostone; **biowackestone.** The only recognizable bioclasts are crinozoan components. Fine to very coarse neomorphic dolomitization of matrix (up to 3.5 mm) and paramorphic dolomitization of crinozoan components. Anhydrite porphyroblasts were emplaced and dissolved; molds became partially filled by calcitic gravitational cement. Good porosity consists of intercrystalline voids and anhydrite molds.
49-9	Dolostone; **biowackestone.** Crinozoans are the only recognizable fossils. Fine to very coarse neomorphic dolomitization of matrix (up to 3.3 mm) and paramorphic dolomitization of crinozoans. Anhydrite porphyroblasts were emplaced and dissolved. Some sparry calcite cement was precipitated in intercrystalline voids. Good porosity consists of intercrystalline voids and anhydrite molds.
49-4	Dolostone; **biowackestone.** Crinozoans are the only recognizable bioclasts. Fine to extremely coarse neomorphic dolomitization of matrix (up to 4.7 mm) and paramorphic dolomitization of crinozoan components. Anhydrite porphyroblasts were emplaced and dissolved; molds were partially filled by calcitic gravitational cement. Good porosity consists of intercrystalline voids and anhydrite molds.

TABLE 7 (continued)

Sample notation (BHP-)	Description
49-1	Dolostone; **biowackestone.** Only recognizable bioclasts are crinozoans. Fine to coarse neomorphic dolomitization of matrix and paramorphic dolomitization of crinozoans. Anhydrite porphyroblasts were emplaced and then dissolved. Third order anhydrite molds and fractures were partially filled by micritic internal sediment. Micritic internal sediment became dolomitized; coarse dolomite cement was precipitated in anhydrite molds. Some calcitic gravitational cement was precipitated within anhydrite molds on dolomite cement crystals and dolomitized internal sediment. Outer periphery of calcitic dripstone cement became partially dolomitized. Good preservation of tiny intercrystalline voids and partially filled anhydrite molds.
48-2b	Dolostone; **biowackestone.** Crinozoans are the only recognizable bioclasts. Coarse and very coarse neomorphic dolomitization of matrix, with crystals ranging up to 2.5 mm in diameter. Paramorphic dolomitization of crinozoans. Fractures were filled by calcite cement; poor preservation of intercrystalline porosity.
48-2a	Limestone; **oobiopelpackstone-grainstone.** Crinozoans, small foraminifers, bryozoans, peloids, brachiopods, ooids, fusulinids, trilobites, and pelecypods. Micritization and micrite envelopes. Aragonitic shells dissolved, and hollow micrite envelopes and nontectonic fractures formed. Primary voids, molds, and fractures became filled by calcite cement.
48-1	Limestone; **biopelwackestone.** Peloids, crinozoans, *Tubiphytes*, bryozoans, phylloid algae, brachiopods, ostracods, and trilobites. Micritization. Aragonitic shells dissolved; molds and nontectonic fractures formed; both were filled by calcite cement. Much coarse recrystallization of matrix; some silicification. Stylolites cut fractures and vugs which were filled by calcite cement.
47-2	Chert; **biowackestone.** Siliceous sponge spicules, crinozoans, and bryozoans. Everything is silicified except some crinozoan components. Dolomite porphyroblasts occur within silica; fractures are filled by calcite cement.
47-1	Limestone; **biowackestone.** Crinozoans, bryozoans, *Tubiphytes*, phylloid algae, and brachiopods. Aragonitic shells dissolved; solution molds and vugs were filled by calcite cement. Two generations of fractures are now filled by calcite cement. Some crinozoans and brachiopods were silicified.
46-17	Limestone; **biowackestone.** Crinozoans, bryozoans, *Tubiphytes*, brachiopods, phylloid algae, pelecypods, and ostracods. Aragonitic shells dissolved; molds were enlarged into vugs and solution channels; these were filled by calcite cement. The matrix is recrystallized. Two generations of fractures were filled by calcite cement. Anhydrite porphyroblasts were emplaced and dissolved; molds were filled by calcite cement.
46-5	Dolostone; **biowackestone.** Only recognizable bioclasts are crinozoans. Matrix exhibits very coarse neomorphic dolomitization with crystals ranging in diameter up to 3 mm. Monocrystalline crinozoans were paramorphically dolomitized. Some intercrystalline porosity is preserved. Calcitic gravitational dripstone cement partially fills small fractures.
46-1	Limestone; **biopelwackestone.** Peloids, *Tubiphytes*, small foraminifers, phylloid algae, and ostracods. Aragonitic shells dissolved and nontectonic fractures formed. Fractures and molds became filled by meteoric calcite cement. Recrystallization of matrix and emplacement of quartz porphyroblasts. Sparry anhydrite porphyroblasts were emplaced and dissolved; tertiary molds were filled by extremely coarse dolomite cement which also extends outward as replacement of surrounding calcite matrix and engulfs quartz porphyroblasts.
45-17	Limestone; **biopelwackestone.** Peloids, *Tubiphytes*, small foraminifers, bryozoans, phylloid algae, pelecypods, crinozoans, and ostracods. Micritization. Aragonitic shells dissolved; molds were filled by equant calcite cement. Recrystallization of matrix and syntaxial rims formed on many crinoid columnals. Sparry anhydrite porphyroblasts were emplaced and then dissolved; tertiary stairstep molds were filled by dolomite cement.
45-2	Limestone; **intrabiograpestone packstone.** Phylloid algae, grapestone grains, crinozoans, intraclasts, fusulinids, small foraminifers, and ostracods. Micritization and micrite envelopes. Aragonitic shells dissolved and hollow micrite envelopes formed; both were filled by calcite and quartz cement. Much recrystallization of micrite matrix. Quartz porphyroblasts have partially replaced many micritized shells.
45-1	Dolostone; **biowackestone.** Crinozoans are only recognizable bioclasts. Fine to medium neomorphic dolomitization of matrix; paramorphic dolomitization of crinozoans. Sparry anhydrite porphyroblasts were emplaced and were partially replaced by calcite. The remaining anhydrite was dissolved, and molds became filled by coarse dolomite cement. First generation fractures are filled by dolomite cement; second generation fractures cut first fractures and are filled by calcite cement.
44-2	Limestone; **biopackstone.** Bryozoans, crinozoans, *Tubiphytes*, phylloid algae, brachiopods, and ostracods. Micritization. Aragonitic shells were dissolved, and some microbrecciation and fracturing took place. All voids were filled by calcite cement. Silicification of some crinozoans and brachiopod shells.
43-7	Dolostone, limy; **biopackstone.** Crinozoans, bryozoans, brachiopods, pelecypods, and small foraminifers. Micritization. Micrite matrix was dolomitized, and some shells were dissolved. Some partial paramorphic dolomitization of calcitic shells. Intrabiotic cavities filled by calcite cement; secondary voids filled by dolomite cement. Silicification; some silica appears to have replaced anhydrite.
42-14	Chert; **biopackstone.** Crinozoans, bryozoans, and brachiopods. Matrix replaced by microquartz which contains abundant dolomite inclusions. Fossils were replaced by length-fast chalcedony and megaquartz. Many crinozoans were paramorphically dolomitized.
42-12	Limestone; **biopelpackstone.** Peloids, crinozoans, bryozoans, small foraminifers, brachiopods, pelecypods, and *Tubiphytes*. Micritization. Aragonitic shells dissolved; molds and crumbly fractures are filled by calcite cement. Recrystallization of matrix. Some late dolomite cement in molds and fractures.
41-20	Limestone; **biograpestone grainstone.** Grapestone grains, small foraminifers, bryozoans, *Tubiphytes*, pelecypods, brachiopods, and ostracods. Micritization and micrite envelopes. Aragonitic shells dissolved and hollow micrite envelopes formed. Nontectonic fractures, hollow micrite envelopes, shell molds, and primary voids were filled by calcite cement. Anhydrite porphyroblasts were emplaced; subsequently, they were partially replaced by silica (length-slow chalcedony) and partially dissolved.
40-1	Limestone; **oobiopelgrapestone grainstone.** Ooids, peloids, grapestone grains, crinozoans, bryozoans, pelecypods, small foraminifers, and brachiopods. Superficial oolitic coatings on many bioclasts. Micritization and micrite envelopes. Aragonitic shells dissolved; shell molds and hollow micrite envelopes filled by calcite cement. Silicification. Large nontectonic fractures contain micritic, vadose internal sediment and calcite cement.
39-4	Chert; **biograinstone.** *Komia* (stromatoporoid or alga) and crinozoans. All *Komia* replaced by megaquartz. All crinozoans replaced by megaquartz, flamboyant quartz, and paramorphic dolomite. Primary voids filled by drusy mega-quartz. Dolomite was first precipitated as cement in fractures and then partially replaced adjacent chert matrix.

New Mexico Bureau of Mines and Mineral Resources

Circular 176

"Pennsylvanian stratigraphy, petrography, and petroleum geology of Big Hatchet Peak section Hidalgo County, New Mexico"

by Sam Thompson III and Alonzo D. Jacka

First printing, 1981

Errata

p. 20, rig. 30: Overlay slipped upward 1 mm. Boundaries of units are shown too high.

p. 20, Fig. 32: Overlay slipped upward 3 mm. Boundary between units 54 and 55 is shown too high. Deleted r (label for climbing ropes) in lower right corner.

p. 21, Fig. 38: Overlay slipped downward 1 mm. Boundary between units 75 and 76 is shown too low; boundary between units 76 and 77 is ok.

TABLE 7 (continued)

Sample notation (BHP-)	Description
39-1	Limestone; **oobiograinstone.** *Komia*, ooids, bryozoans, crinozoans, fusulinids, and brachiopods. Primary voids filled by calcite cement. Coarse epitaxial cements on monocrystalline crinozoans. Stylolites well developed.
38-3	Limestone; **oobiograinstone.** Crinozoans, *Komia*, bryozoans, and fusulinids. Micritization. Primary voids filled by calcite cement. Large aureoles of epitaxial cement on crinozoans. Silicification of many shells.
38-0	Limestone; **biograinstone.** Crinozoans, bryozoans, and fusulinids. Large aureoles of epitaxial cement on crinozoans. Partial paramorphic dolomitization of many crinozoans. Silicification of many shells. Primary voids not filled by calcite cement were completely filled by quartz cement.
37-0	Limestone; **oobiopelpackstone.** Ooids, peloids, crinozoans, bryozoans, phylloid algae, small foraminifers, pelecypods, brachiopods, and ostracods. Micritization and micrite envelopes. Aragonitic shells and ooids dissolved, and hollow micrite envelopes formed; all voids were filled by calcite cement. Many tiny quartz porphyroblasts emplaced.
36-4	Chert; **biowackestone.** Crinozoans, fusulinids, and bryozoans. Micrite matrix replaced by microquartz, which contains much rhombic dolomite as inclusions. Fossils replaced by length-fast chalcedony (chalcedonite). Intrabiotic cavities filled by: 1) dolomite cement and 2) chalcedonite. Many crinozoans were paramorphically dolomitized.
36-2	Limestone; **biopackstone.** Crinozoans, bryozoans, fusulinids, and small foraminifers. Micritization. Silicification of shells. Fusulinid chambers and first generation fractures were filled by ferroan calcite cement. Second generation fractures were filled by calcite cement.
35-10	Chert; **biowackestone.** Crinozoans, bryozoans, and siliceous sponge spicules. Silicification probably followed calcitization. Many dolomite porphyroblasts formed within chert; crinozoan components were paramorphically dolomitized. Fractures contain coarse dolomite cement and paramorphically dolomitized dripstone cement.
35-1	Limestone; **biowackestone.** Crinozoans, bryozoans, phylloid algae, small foraminifers, and brachiopods. Micritization. Aragonitic shells dissolved and nontectonic fractures formed; both molds and fractures were filled by calcite cement. Silicification of many shells.
34-6	Limestone; **biopelgrainstone.** Crinozoans, bryozoans, peloids, small foraminifers, and brachiopods. Micritization and micrite envelopes. Some micritic, vadose internal sediment. Coarse epitaxial cement on crinozoans. Fractures filled by calcite cement. Silicification of many shells.
33-7	Chert; **biowackestone.** Crinozoans, fusulinids, and brachiopods. Carbonate stabilized to limestone prior to silicification. Most crinozoan columnals consist predominantly of calcite. Some have been partially paramorphically dolomitized and silicified; many also have discrete, satellite crystals of dolomite that are syntaxial with monocrystalline calcitic components. In fusulinid chambers, dolomite cement had been precipitated and dedolomitized before silicification; chambers are predominantly filled by length-fast chalcedony (chalcedonite). Dolomite porphyroblasts in chert matrix were also dedolomitized. Fractures are filled by calcite cement.
33-6	Limestone; **biograinstone.** Crinozoans, fusulinids, bryozoans, brachiopods, small foraminifers, and ostracods. Micritization. Micritic, vadose internal sediment deposited in many large voids. Coarse epitaxial cement formed on crinozoans. Silicification of many shells.
32-2	Limestone; **biopelwackestone.** Peloids, small foraminifers, crinozoans, phylloid algae, fusulinids, and *Girvanella* (boring alga) traces. Micritization. Aragonitic shells dissolved and nontectonic fractures formed; both molds and fractures were filled by calcite cement.
31-15	Chert; **biowackestone.** Siliceous sponge spicules and crinozoan components. Large, slightly ferroan dolomite porphyroblasts formed during silicification. The dolomite porphyroblasts transect siliceous sponge spicules; ghosts of the spicules are manifested by engulfment of organic matter. Monocrystalline crinozoan components have been paramorphically dolomitized. Fractures are filled by slightly ferroan dolomite cement, which is epitaxial on fractured dolomite crystals. Dolomite porphyroblasts range up to 500 microns in diameter.
31-10	Limestone; **oobiopackstone.** Ooids, bryozoans, crinozoans, brachiopods, ostracods, and trilobites. Micritization. Silicification of many shells.
30-0	Limestone; **biopelwackestone.** Peloids, small foraminifers, bryozoans, phylloid algae, pelecypods, ostracods, crinozoans, brachiopods, and trilobites. Micritization and micrite envelopes. Aragonitic shells dissolved, hollow micrite envelopes and nontectonic fractures formed; all voids became filled by calcite cement. Silicification of many shells. Hematite pseudomorphs of pyrite occur within many silicified fields.
29-3	Chert; **biowackestone.** Siliceous sponge spicules, crinozoans, bryozoans, and pelecypods. Carbonate was converted to limestone, and aragonitic shells were dissolved. Recrystallization of micrite matrix and filling of molds by calcite cement, followed by silicification. Some siliceous spicules were replaced by calcite. Dolomite porphyroblasts occur within chert. Postsilicification fractures were filled by calcite cement.
29-2	Limestone; **biopelwackestone.** Peloids, bryozoans, crinozoans, pelecypods, small foraminifers, and brachiopods. Micritization and formation of algal-coated grains. Aragonitic shells dissolved; molds were filled by calcite cement. Coarse recrystallization of matrix.
28-5	Limestone; **oobiograinstone.** Crinozoans, bryozoans, ooids, small foraminifers, fusulinids, and brachiopods. Micritization. Large aureoles of epitaxial cement on crinozoans. Silicification occurred after cementation because silica extends outward from shells to replace cement crystals.
27-3	Chert; **biopelpackstone.** Crinozoans, peloids, siliceous sponge spicules, bryozoans, and brachiopods. Calcitization was followed by silicification. Silica appears to have nucleated on siliceous spicules because silicification is densest where spicules are concentrated.
27-2	Limestone; **biopelwackestone.** Peloids, bryozoans, brachiopods, crinozoans, pelecypods, and small foraminifers. Micritization. Aragonitic shells dissolved; molds were filled by calcite cement. Coarse recrystallization of matrix.
26-0	Limestone; **biopelgrapestone packstone.** Peloids, crinozoans, bryozoans, pelecypods, brachiopods, and small foraminifers. Micritization. Aragonitic shells dissolved and nontectonic fractures formed. Both molds and fractures were filled by calcite cement.
25-4	Chert; **biowackestone.** Crinozoans, siliceous sponge spicules, and pelecypods. Calcitization and dissolution of aragonitic shells was followed by silicification. Aragonitic shell molds have been filled by: 1) ferroan dolomite, 2) calcite, and 3) chalcedonite. Fractures are filled by calcite and zoned crystals of ferroan and nonferroan calcite.
25-3	Limestone; **biowackestone.** Crinozoans, bryozoans, brachiopods, phylloid algae, fusulinids, and ostracods. Aragonitic shells dissolved; molds were filled by calcite cement. Two generations of fractures are recorded; the first cuts compaction wisps, the second transects the first and was followed by silicification of shells. All fractures filled by calcite cement.
24-1	Limestone; **oobiograpestone grainstone.** *Komia*, crinozoans, ooids, and small foraminifers. Micritic, pelletoidal, vadose internal sediment forms a geopetal fabric in many voids. All voids filled by coarse calcite cement.

TABLE 7 (continued)

Sample notation (BHP-)	Description
23-4	Chert; **biopelwackestone.** Peloids, crinozoans, bryozoans, and brachiopods. Calcitization was followed by silicification. Dolomite porphyroblasts occur within silicified areas. Some crinozoans only partly replaced by silica, while brachiopods and peloids are completely replaced.
22-1	Limestone; **biograpestone grainstone.** Crinozoans, bryozoans, grapestone grains, small foraminifers, brachiopods, and pelecypods. Micritization and micrite envelopes. Aragonitic shells dissolved to form molds and hollow micrite envelopes. All primary and secondary voids later became filled by calcite cement. Poikilotopic epitaxial cement formed on crinozoans. Silicification of many bioclasts.
21-3	Chert; **biopelwackestone.** Peloids, crinozoans, bryozoans, siliceous spicules, and brachiopods. Nearly all skeletal grains (except some crinozoans) are completely replaced by silica. Calcitization was followed by silicification; dolomite porphyroblasts occur within silicified matrix.
21-2	Limestone, dolomitic and limy dolostone; **biopackstone-wackestone.** Crinozoans, brachiopods, echinoids, bryozoans, ostracods, phylloid algae, and small foraminifers. Both dolomitic limestone and limy dolostone occur in layers. Only micrite matrix was dolomitized. Aragonitic shells dissolved and molds filled by calcite cement. Silicification of some shells. No porosity preserved.
20-2	Limestone; **biopelwackestone.** Bryozoans, crinozoans, peloids, *Tubiphytes*, brachiopods, small foraminifers, phylloid algae, and ostracods. Micritization. Encrustation of large bioclasts by *Tubiphytes*. Aragonitic shells dissolved; original matrix was recrystallized. Some shells were partially silicified. All voids were filled by calcite cement.
19-4b	Chert; **oobiopelwackestone.** Peloids, crinozoans, bryozoans, ooids, brachiopods, and phylloid algae. Calcitization and dissolution of aragonitic shells, followed by silicification. Biomolds are filled by length-slow chalcedony. Dolomite porphyroblasts occur within silicified areas, and many became dedolomitized. First generation fractures were filled by dolomite cement which later became dedolomitized. Second generation fractures are filled by calcite cement.
19-4a	Limestone; **biopackstone.** Crinozoans, brachiopods, bryozoans, and phylloid algae. Aragonitic shells dissolved; molds filled by calcite cement. Two generations of fractures; the first is filled by calcite cement and the second by dolomite.
18-0	Limestone; **biograinstone.** Bryozoans, crinozoans, small foraminifers, brachiopods, fusulinids, and phylloid algae. Aragonitic shells dissolved; molds filled by calcite cement. Silicification of some shells.
17-17	Chert; **oobiopelwackestone.** Crinozoans, fusulinids, ooids, peloids, bryozoans, brachiopods, and pelecypods. Calcitization and dissolution of aragonitic shells, followed by silicification. The only shells which escaped silicification are crinozoan columnals.
17-4	Limestone; **biowackestone.** Bryozoans, crinozoans, phylloid algae, small foraminifers, and brachiopods. Aragonitic shells dissolved; molds filled by calcite cement. Silicification of some shells.
16-10	Chert, silty; **biopackstone.** Quartz grains, fusulinids, bryozoans, crinozoans, and siliceous sponge spicules. Calcitization preceded silicification. Most of calcite matrix and all fusulinids and bryozoans completely replaced, but many crinozoans are only partially replaced. The silicified matrix contains abundant dolomite porphyroblasts. Original micrite matrix has been recrystallized to coarse pseudospar in unsilicified areas. Fractures in chert contain dolomite, which occurs as both cement and replacement, and drusy megaquartz.
16-4	Limestone; **biopackstone.** Fusulinids, crinozoans, phylloid algae, small foraminifers, and brachiopods. Aragonitic shells dissolved; molds were filled by calcite cement. Silicification of some shells. Exsolved dolomite crystals occur within silicified portions of crinozoans.
15-2	Limestone, silty; **biopelpackstone.** Peloids, brachiopods, small foraminifers, and ostracods are abundantly represented; very few quartzose silt grains. Intersecting sets of crumbly, nontectonic fractures formed and became filled by calcite cements.
14-3	Limestone; **biograpestone grainstone.** Bryozoans, crinozoans, grapestone grains, phylloid algae, brachiopods, and trilobites. Micritization, micrite envelopes, and algal-coated grains abundant. Micritic vadose internal sedimentation was followed by dissolution of aragonitic shells to form molds and hollow micrite envelopes. All voids were filled by calcite cement. Silicification of many shells.
14-2	Dolostone, cherty; **biowackestone.** Only recognizable bioclasts are crinozoans. Coarse neomorphic dolomitization; crystal diameters range up to 900 microns. Paramorphic dolomitization of crinozoans. Dolomite is slightly ferroan. Silica occurs predominantly as cement in intercrystalline voids as length-fast chalcedony and drusy quartz. Silica has replaced some undolomitized crinozoans. No porosity preserved.
13-35	Chert (zebra pattern); **biowackestone.** Crinozoans, bryozoans, brachiopods, and ostracods. The zebra pattern represents alternating thin layers of silica and carbonate. The siliceous layers contain many dolomite inclusions, some partially replaced calcitic fossils, and dedolomite. The carbonate-rich layers consist predominantly of dedolomite and some silicified fossils. Fractures formed after silicification are filled by calcite cement. Dolomite was first emplaced through these fractures as replacement of the surrounding chert, and it subsequently became dedolomitized before calcite cement filled the fractures.
13-23	Limestone; **biopackstone.** Phylloid algae, *Tubiphytes*, bryozoans, and crinozoans. Micritization. Aragonitic shells dissolved and nontectonic fractures formed; both molds and fractures were filled by calcite cement.
13-7	Limestone; **biopelpackstone.** Crinozoans, bryozoans, peloids, small foraminifers, pelecypods (or phylloid algae?), brachiopods, and ostracods. Aragonitic shells dissolved and nontectonic fractures formed; both types of voids were filled by calcite cement.
12-1	Limestone; **oobiowackestone-packstone.** Brachiopods, bryozoans, crinozoans, ooids, ostracods, and trilobites. Silicification of many fossils.
11-1	Limestone; **oobiopelpackstone-grainstone.** Peloids, ooids, crinozoans, bryozoans, brachiopods, pelecypods, trilobites, small foraminifers, and ostracods. Micritization. Aragonitic shells dissolved; molds filled by calcite cement. Sample contains a layer of packstone and a layer of grainstone.
10-3	Limestone; **biowackestone.** Crinozoans and brachiopods. Fine neomorphic dolomitization of matrix was followed by dedolomitization. Calcitic shells were not dolomitized. Dead oil occurs along compaction wisps and in intercrystalline voids. No preserved porosity.
9-6	Limestone; **oobiograpestone grainstone.** Ooids, crinozoans, small foraminifers, pelecypods, grapestones, and brachiopods. Micritization. Aragonitic shells dissolved and nontectonic fractures formed. All voids filled by calcite cement. Crinozoan components were selectively silicified.

TABLE 7 (continued)

Sample notation (BHP-)	Description
9-5	Limestone; **oobiograpestone grainstone.** Ooids, bryozoans, crinozoans, grapestones, brachiopods, and pelecypods. Micritization and formation of algal coated grains. Aragonitic shells dissolved and molds filled by calcite cement. Large aureoles of epitaxial cement were precipitated on crinozoan components; the aureoles poikilotopically enclose neighboring grains. Silicification of many shells.
8-1b	Chert; **oobiowackestone.** Crinozoans, ooids, pelecypods, and brachiopods. Calcitization and dissolution of aragonitic shells. Silicification. Fractures formed, then filled by calcite cement.
8-1a	Limestone; **oobiopelgrapestone wackestone-packstone.** Ooids, bryozoans, crinozoans, brachiopods, small foraminifers, peloids, grapestones, pelecypods, and trilobites. Micritization. Aragonitic shells dissolved; molds filled by calcite cement. Silicification of some shells. Sample transects a layer of wackestone and one of packstone.
7-23	Limestone; **oobiopelgrapestone grainstone.** Ooids, crinozoans, grapestones, peloids, bryozoans, brachiopods, and pelecypods. Micritization and micrite envelopes. Micritic, vadose internal sediment was deposited in primary voids. Aragonitic shells dissolved and hollow micrite envelopes formed. Pelecypod molds were filled by calcite cement, while hollow micrite envelopes were filled later by ferroan calcite cement. Silicification of some shells.
7-1	Limestone; **intrabiopelpackstone-wackestone.** Peloids, algal calcispheres, intraclasts, and tiny unrecognizable bioclasts. This rock may represent an algal stromatolite; it has very thin interlaminations of packstone and wackestone.
6-1b	Chert, sandy, silty; **biopelwackestone.** Peloids, quartzose silt grains, crinozoans, bryozoans, siliceous sponge spicules, and brachiopods. Silica has replaced both matrix and most shells, but some crinozoan components are only partially replaced. Dolomite porphyroblasts are abundant in chert and many have been dedolomitized. Straight fractures have formed after silicification; they became filled by ferroan calcite cement, which has replaced silica matrix outward from the fractures.
6-la	Limestone; **biopelpackstone.** Peloids, crinozoans, and brachiopods. Recrystallization of matrix.
5-0	Limestone; **oobiograinstone.** Crinozoans, brachiopods, bryozoans, ooids, and pelecypods. Micritization and micrite envelopes. Micritic internal sediment was deposited in many voids and was followed by precipitation of beachrock cement rims on grains. Aragonitic shells were dissolved, and hollow micrite envelopes were formed. These primary and secondary voids became filled by meteoric calcite cements.
4-13	Limestone, dolomitic; **biowackestone.** Crinozoans, brachiopods, ostracods, and quartz silt grains. Dolomite rhombs constitute 30-50%. Recrystallization of calcite matrix followed partial neomorphic dolomitization. Abundant dead oil; forms film around dolomite rhombs. No porosity preserved.
4-12	Siltstone. Large and small brachiopod bioclasts occur within a quartzose siltstone matrix. Siltstone contains carbonaceous clasts and some dead oil along laminae, and is cemented by ferroan calcite.
3-2	Limestone; **biopelpackstone.** Peloids, crinozoans, and pelecypods. Peloids exhibit a bimodal size distribution (50-90 microns, and 300-800 microns). Aragonitic shells dissolved and nontectonic fractures formed; both were filled by calcite and pyrite (now oxidized). Pyrite and dead oil are concentrated along a stylolite.
2-1	Limestone; **oobiograpestone grainstone.** Ooids, crinozoans, bryozoans, pelecypods, grapestones, brachiopods, and ostracods. Ooids all represent superficial coatings on bioclasts and exhibit a bimodal size distribution (50-90 microns, and 300-900 microns). Micrite envelopes formed on many grains, and thick algal coatings formed on others. Hollow micrite envelopes were formed. All porosity occluded by blocky, equant meteoric calcite cements.
2-0	Limestone, sandy, silty; **oobiowackestone.** Quartz grains, ooids, bryozoans, crinozoans, and brachiopods. The rock is mottled and has been subjected to very complex diagenesis. Thick algal coatings formed around many bryozoans, and tiny pyrite crystals formed within them. Pyrite also formed within the stereome of crinozoan components and in portions of the matrix; all pyrite became oxidized. Ferroan calcite cement occurs within bryozoan zooecia. Much of the matrix has been recrystallized to microspar and pseudospar, which is now ferroan calcite; many dolomite rhombs have been replaced by ferroan calcite. Some clay has been emplaced (by replacement?). Pyrite has also been formed along stylolites and subsequently oxidized.
1-0	Limestone; **biograinstone.** Ooids, crinozoans, and bryozoans. Micritization and micrite envelopes abundant. Thick algal coatings formed around many grains. Micritic, vadose internal sediment was deposited in large primary voids to form a packstone-like fabric. Aragonitic shells dissolved and nontectonic fractures were formed by partial collapse of molds. All primary and secondary voids were filled by coarse epitaxial (on crinozoans) and drusy calcite cements.

Appendix 3 Columnar stratigraphic section

Fig. 42 is a graphic summary of the stratigraphy, petrography, and petroleum geology of the Big Hatchet Peak section. This columnar stratigraphic section is plotted vertically on the standard exploration scale of 1 inch:100 ft and includes selected data from the main text and the two previous appendices. Each full page covers a stratigraphic interval of 1,000 ft plotted from the youngest unit at the top to the oldest unit at the base. The pages may be reproduced and spliced together if desired. A generalized one-page summary is given in fig. 4.

The format is designed to be useful in correlation with other surface or subsurface sections, in sedimentologic analyses of depositional and diagenetic features, and in evaluation of petroleum source and reservoir units. As with any graphic plot, this one is intended as a supplement to, rather than a replacement of, the written documentation.

Columns are numbered from left to right for ease of reference between this explanatory text and the information plotted on the stratigraphic section. We suggest that the reader follow this text and become familiar with the information in each vertical column before attempting to follow a particular unit or sample horizontally across the pages.

For basic items in several columns, conventional methods of plotting are followed. Selected variables that were observed or interpreted somewhat continuously over the entire section are plotted as bar graphs. Others that were determined at discrete positions in units or samples are plotted in separate columns with one-to-four-letter mnemonic abbreviations. This system is considered easier to devise, plot, and comprehend than those of some geologists in which diverse sets of intricate graphic symbols are used and commonly crammed into one column. Also, this mnemonic system can be adapted more readily for computer processing.

Columns 1-19 on each left page include information on stratigraphy and depositional features. Columns 20-34 on each right page include information on diagenetic features and petroleum evaluation.

Columns 1-4 indicate the major stratigraphic units in decreasing order of rank: system, series, formation, and member. On the right side of column 2, the biostratigraphic control is plotted from table 2; it is based mainly on fusulinid identifications by G. L. Wilde. Columns 5 and 6 show the vertical scale based on cumulative thickness in meters and feet above the base of the section. Column 7 shows the plotted thickness of the lithostratigraphic column units, which form the basic framework of the section. Details of traverse directions and thickness measurements of each unit are given in table 5. Although several offsets were made in the line of section to follow the locus of best workable exposures, the net horizontal distance covered is less than 0.7 mi, so units appear to be stacked within the same outer-shelf facies belt.

Column 8 is a generalized plot of the major rock types that is derived from the field description of lithostratigraphic column units in table 4. Each symbol in this lithologic column is designed to represent a stratigraphic-interval thickness of 10 ft. Some irregular intervals of 5-15 ft are plotted at unit boundaries to keep the cumulative thickness in this column within 5 ft of that shown in column 6. Standard graphic symbols are used for the three basic rock types: limestone, dolostone, and chert (the latter occurs only within limestone host rocks). Disconformities are inferred at the bases of the upper and the lower Horquilla.

Column 9 is a plot of the topographic relief encountered in the line of section. As defined in appendix 1, the relief is expressed in terms denoting the vertical projection (sheerness) above the baseline slope of the traverse: slope (less than 0.3 ft), slight ledge (0.3-1 ft), moderate ledge (1-3 ft), fairly prominent ledge (3-10 ft), prominent ledge (10-30 ft), and cliff (30-100 ft); no prominent cliffs (over 100 ft) were encountered. For those intervals in which a range of relief was described, the maximum is plotted. Column 10 is a plot of the quality of exposure: covered, if the bedrock is buried by soil, vegetation, or recent sediment; poor, if the rock type is discernible; fair, if bedding within the rock type is discernible; and good, if lamination (or its absence) within the bedding is discernible. Where a range of exposure was described, the best is plotted. These columns should be helpful to geologists who wish to follow the line of section in the field and concentrate on more detailed studies in better exposed intervals. Both columns are plotted to the nearest 5 ft of section.

Column 11 shows bedding, lamination, and other primary sedimentary structures that are plotted as near as possible to their true stratigraphic position within each unit. Only measurable thicknesses of beds are indicated. Some intervals may contain beds several meters thick, but they are too poorly exposed to be plotted with confidence. Where a range of bed thicknesses was determined, the maximum is plotted. At the base of each unit, bedding and other features were described as completely as possible in the first interval, and generally only changes were described in remaining intervals. Thus the maximum thickness given at the base is representative of the other intervals unless a different value is plotted at a higher position in that unit. Patterns of upward thinning or thickening, suggesting aggradation or progradation, are indicated where obvious in a single exposure; however, a detailed study of bed thicknesses may uncover many more such patterns. Nearly all beds appear to have been deposited with a horizontal attitude; the few beds with initial inclination are plotted. All exposed beds were observed to have sharp, planar surfaces, but those with especially sharp surfaces (and normally with minor erosional relief) are plotted to indicate significant hiatuses in the depositional record. Some such diastems are plotted even if the thicknesses of the beds were not measurable. A few channels with moderate erosional relief were observed, and all are plotted. All observed lamination and imbrication are plotted, but they are described in considerably more detail in table 4. One possible indication of a mud-cracked bedding surface is shown (unit 7). Secondary structures, such as the geometry of chert nodules, were described but not plotted.

Column 12 indicates the depositional environment as

determined at the base of each unit, and any observed changes are shown in the intervals above. The shallow-marine aspect of the carbonate rock types and the biota and the generally horizontal stratification indicate that most of the section was deposited in a subtidal environment. Associated intervals with trough, inclined (planar base and top), and current-ripple laminasets are assumed to be intertidal deposits; however, no bipolar cross laminasets were observed. Column 13 shows the determinations of paleocurrent directions based on the sedimentary structures, with consideration given to the depositional environment.

Column 14 shows each sample number plotted with a leader to the stratigraphic position. For each sample, the cumulative footage above the base of the section, the rock type, and the purpose for which it was taken are listed in table 6. Data on samples that were analyzed petrographically are plotted as near as possible to the stratigraphic positions of the samples. Columns 15 and 16 indicate the basic rock type and the dominant color of the fresh, wet rock as described in the field (table **4).**

Columns 17, 18, 19, 21, 22, and 30 present information based on petrographic analyses, which are described more completely in table 7. Column 17 shows that most of the section is lacking in detrital components. Column 18 shows the Dunham class of carbonate texture, indicating grain support (grainstone, packstone) or mud support (wackestone). For a sample in which two classes were described, the dominant one is plotted. Column 19 lists the allochem grains in order of decreasing abundance, as determined for each thin section. In some cases a semicolon is placed at the end of the series, and algal coated grains (described with micritization) or additional fossils seen in the field are noted. Some environmentally or stratigraphically significant fossils seen in the field are placed in position within this column but outside of the sample-data rows.

Column 20, on the right page, is a repeat of the sample notations (given in column 14). It provides a bridge for the continuation of the sample-data rows.

Column 21 is an attempt to plot on a stratigraphic section the essential diagenetic features in their general order of occurrence. The abbreviations are grouped into three classes: 1) diagenetic processes, indicated by two upper-case letters and lower-case subscripts, 2) mineral composition, indicated by one upper-case letter and lower-case subscripts, and 3) mineral texture indicated by only lower-case letters. Combinations are joined by hyphens; for example, **RPm-(Ar)-Do-nm-vc** indicates replacement of the matrix (inferred to be aragonite) by dolomite with a neomorphic texture consisting of very coarse crystals. Approximately contemporaneous processes, minerals, or textures are separated by commas; for example, **CEm,f-Cc** indicates cementation in molds and fractures by calcite. Succeeding processes are separated by semicolons, although some may have occurred in relatively rapid succession. Some features of silicification, **RP-Qz,** are placed arbitrarily at the end because their position in the paragenetic sequence was indeterminate.

Although the number of features plotted make this the most complex column on the section, the processes or mineral compositions can be found readily by scanning for double or single upper-case letters, respectively. Diagenetic developments of porosity are indicated by solution (SL), fracturing **(FR),** neomorphic dolomitization **(RP-Do-nm),** and dedolomitization **(RP-(Do)Cc-pm),** the paramorphic replacement of dolomite by calcite. Occlusion of porosity is indicated by internal sedimentation **(IS)** and cementation **(CE).** Only partial occlusion was observed where voids contained microstalactitic, gravitational, calcite cements **(CE-Cc-mg).**

Column 22 summarizes the petrographic analyses of the preserved porosity. All primary porosity, such as intergranular voids in grainstones or intrabiotic cavities, has been occluded. Secondary porosity in limestones, such as solution molds of aragonitic shells, ooids, porphyroblasts, hollow micrite envelopes, or nontectonic fractures resulting from collapse of the molds, has been occluded, normally by calcite cement. Secondary porosity in dolostones, such as intercrystalline voids in neomorphic textures or open space in fractures, is preserved or has been partially to completely occluded. The only tertiary porosity was developed by the dissolution of anhydrite porphyroblasts or nodules, commonly in dolostones, and normally is preserved or only partially occluded. The semiquantitative estimate of preserved porosity based on petrographic observation is plotted in column 30 alongside other data used in the evaluation of the reservoir rocks.

Columns 23-28 summarize the evaluations of petroleum source rocks. Column 23 shows the preliminary field estimate, based mainly on the darkness of the rock color, that was made for each sample submitted for laboratory analysis. Columns 24, 25, and 26 show determinations by GeoChem Laboratories, Inc. of percent organic carbon, kerogen types (two most dominant), and the thermal-alteration index (most significant) taken directly from table 2.

Columns 27 and 28 are plots of the source quality for oil and gas, starting with the laboratory analyses and extrapolating with the lightness value (next to last number in the GSA notation) of the rock colors described in table 4 (see also column 16). Both columns are plotted to the nearest 5 ft of section. In this set of samples, and generally in other sets analyzed in this region, a very poor source with less than 0.10 percent organic carbon tends to have a lightness value of 6 or greater, a poor source with 0.10-0.25 percent has a value of 5 to 4, and a fair source with 0.25-1.00 percent has a value of 3 to 1. No good source with over 1.00 percent organic carbon was actually determined in this section, but the best one with 0.71 percent and a value of 3 (BHP-10-3) was tentatively rated good. Because no algal or amorphous kerogens were found, the source quality for oil was plotted only as poor (value less than 6) or none (6 or greater). Degraded (partially amorphous) herbaceous kerogen, the dominant type, may have been a source for oil, but the thermal-alteration index of 3 or higher indicates a paleotemperature range above 150° C where oil tends to be altered by cracking processes to gas. Woody kerogen, in secondary amounts, would have added to the gas source. The rating of the gas source was based on the percentage of organic carbon and the rock color. This procedure was the best that could be devised with the limited number of samples from this section; it probably provides only a gross approximation and no doubt will be revised (or abandoned) with

additional control, especially with analyses of drill cuttings from key exploration wells.

Columns 29-33 summarize the evaluations of reservoir rocks. Column 29 shows the field evaluation of all samples submitted for petrographic and plug analyses and includes some plots outside the sample-data rows where porosity was observed. Field estimates range from none (N) where no vuggy porosity was observed, to poor (P) with a trace of porosity (less than 10 percent), to fair (F) with 10-20 percent, to good (G) with over 20 percent. In many cases, the estimate of vuggy porosity based on the fresh surface is at least one grade less than if based only on the weathered surface (notations in the form Pv,w). In a few cases, vuggy porosity was seen only on the weathered surface (Pw,v) and is regarded as none in the evaluation. No matrix porosity **(Pm)** was seen definitely with a hand lens, and none was indicated with the water-imbibition test made on each sample.

Column 30 records the observations of porosity noted in the petrographic descriptions (table 7). The scale of none, poor, fair, and good generally corresponds to the same porosity ranges used in the field scale. However, both matrix porosity and the vuggy type (notations **Pm,v)** were recognized in many thin sections (and are illustrated in the plates of photomicrographs). Matrix porosity consists normally of secondary intercrystalline voids in neomorphic dolostones; some of these voids have been enlarged slightly by solution. Vuggy porosity consists normally of tertiary molds of dissolved anhydrite porphyroblasts. A minor amount of preserved fracture porosity **(Pf)** is recorded in two samples (BHP-65-94 and BHP-46-5).

Columns 31 and 32 list all the measurements of porosity (percent) and permeability (millidarcies) made on samples submitted to Core Laboratories, Inc., and the results are taken directly from table 3. Because of the small size of the plugs cut from surface samples, these measurements generally are only of the matrix porosity and permeability, both of which are low. However, one plug cut into a solution channel has a permeability of 42 and (BHP-56-7) and shows that such interconnected vuggy porosity may constitute a good reservoir.

Column 33 is a summary of the reservoir quality, analogous to those for source quality (columns 27 and 28), and is based on the field and petrographic estimates and the few laboratory measurements. Some permeability is assumed; however, most intervals with good porosity are rated fair in reservoir quality based on the conservative assumption that a substantial part of the porosity may not be interconnected. Nevertheless, several significantly thick reservoir units are shown on the graphic plot, and some occur above or below favorable source units. A total of 470 net ft of intervals with poor-to-good reservoir quality is calculated from this column plotted to the nearest 5 ft of section and compares favorably with the 484 net ft actually measured in the field.

Column 34 is a plot of the few shows of hydrocarbons found in this section. Dead oil **(DO)** was described in five thin sections along laminae, compaction wisps, stylolites, fractures, and in some intercrystalline voids. Dead oil appears as dark, opaque material, but the amounts generally are too small to be extracted megascopically for spectrographic analyses. Nevertheless, these indications of oil in this surface section offer additional encouragement to exploration for subsurface objectives.

Figure 42

(columnar stratigraphic section)

Explanation of abbreviations and graphic symbols (by column number):

Column 2
- ▶ = age determination
- ▷ = age indeterminate

Column 8
- limestone
- limestone with chert / zebra chert
- dolostone
- unconformity

Column 9
- cliff
- prominent ledge
- fairly prom. ledge
- moderate ledge
- slight ledge
- slope

Column 10
- good exposure
- fair exposure
- poor exposure
- covered

Column 11
- B-30 = bed 30cm thick
- B∧ = upward thinning
- B∨ = upward thickening

Column 11 (continued)
- Bin = inclined bed
- B = sharp base of bed
- C-20 = channel 20cm deep
- Imb = imbrication of clasts
- Lcr = laminae, current-ripple
- Lhr = laminae, horizontal
- Lin = laminae, inclined
- Lir = laminae, irregular
- Ltr = laminae, trough
- Lwv = laminae, wavy
- Mc = mudcracks

Column 12
- It = intertidal
- St = subtidal

Column 13
- ↘ = paleocurrent to SE

Column 15
- Ch = chert
- Ds = dolostone
- Ls = limestone
- Zs = siltstone

Column 16
- 5YR3/1 = dark brownish gray (GSA no.)

Column 17
- Q = quartz
- Cb = carbonaceous grains

Column 18
- Gr = grainstone
- Pk = packstone
- Wk = wackestone

Column 19
- Acg = algal coated grain
- Acs = algal calcisphere
- Arc = *Archimedes* sp.
- Brc = brachiopod
- Bry = bryozoan
- Cha = chaetetid coral
- Cra = crustose red algae
- Crz = crinozoan
- Ech = echinoid
- Fav = favositid coral
- For = foraminifer, small
- Fus = fusulinid

Column 19 (continued)
- Gir = *Girvanella* sp.
- Grp = grapestone grain
- Gst = gastropod
- Int = intraclast
- Kom = *Komia* sp.
- Ood = ooid
- Ost = ostracod
- Pel = peloid
- Phl = phylloid algae
- Plc = pelecypod
- Rug = rugose coral
- Spc = sponge spicule
- Tab = tabulate coral
- Trl = trilobite
- Tub = *Tubiphytes* sp.

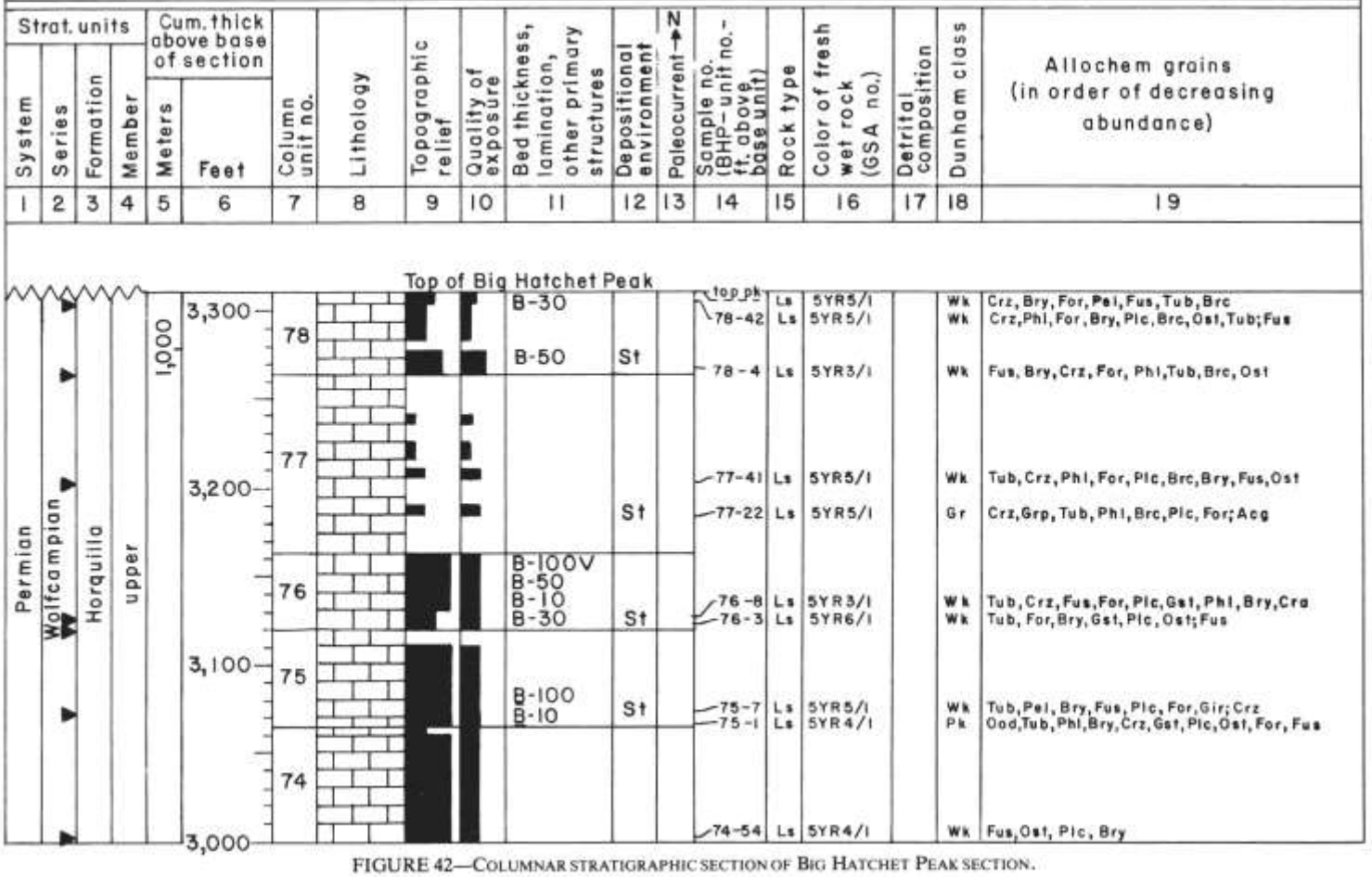

FIGURE 42—COLUMNAR STRATIGRAPHIC SECTION OF BIG HATCHET PEAK SECTION.

Explanation of abbreviations and graphic symbols (continued)

Column 21

1) Process:

MZ = micritization
MZe = " producing micrite envelopes

RX = recrystallization
RXm = " of matrix
RXms = " to microspar
RXps = " to pseudospar
RXsr = " producing syntaxial rims

RP = replacement
RPm = " of matrix
RPg = " " grains
RPsh = " " shells
RPpb = " " porphyroblasts
RPce = " " cement
RPpk = ", poikilotopic

SL = solution
SLsh = " of shells
SLoo = " " ooids
SLpb = " " porphyroblasts
SLhe = " producing hollow micrite envelopes
SLvg = " producing vugs
SLch = " " sol. channels
SLst = " " stylolites

CP = compaction
CPw = " prod. wisps

FR = fracturing
FRn = ", nontectonic
FRt = ", tectonic

IS = internal sedimentation
ISv = " in vadose cavities
ISvm = " " by micrite
ISvg = " " " grains

Column 21 (continued)

ISf = internal sedimentation in fractures

CE = cementation
CEb = " in intrabiotic cavities
CEg = " " intergranular voids
CEx = " " intercrystalline voids
CEm = " " molds
CEsm = " " shell molds
CEom = " " ooid molds
CEpm = " " porphyroblast molds
CEhe = " " hollow micrite envelopes
CEf = " " fractures
CEst = " " stylolites
CEep = ", epitaxial
CEpk = ", poikilotopic
CErm = ", with replacement of matrix

2) Mineral composition:

Cc = calcite
Ccf = " , ferroan
Ccn = " , nonferroan
Ccz = " , zoned

Do = dolomite
Dof = " , ferroan
Don = " , nonferroan
Doz = " , zoned

An = anhydrite

Ar = aragonite

Qz = quartz
Qg = megaquartz

Column 21 (continued)

Qm = microquartz
Qc = chalcedonic quartz

Py = pyrite

Cl = clay

Oil = dead oil

3) Mineral texture:

RX-Cc - ms = microspar
- ps = pseudospar
- sr = syntaxial rims

Do - nm = neomorphic
- f = fine
- m = medium
- c = coarse
- v = very
- e = extremely
- pm = paramorphic
- pb = porphyroblastic

CE-Cc - br = beachrock
- mg = microstalactitic, gravitational
- dr = drusy
- be = blocky, equant

Column 22

P = primary

S = secondary

T = tertiary

Column 23

P = poor
F = fair
G = good

Column 25

H = herbaceous
W = woody

Column 27, 28, 33

good
fair
poor
none

Column 29, 30

N = none
P = poor
F = fair
G = good

Pm = poor matrix porosity
Pv = " vuggy "
Pf = " fracture "

Pv,w = poor vuggy porosity, enhanced on weathered surface
(Pw,v) = poor vuggy porosity, confined to weathered surface

Column 34

DO = dead oil

Sample no. (BHP-unit no. - ft above base unit)	Petrographic analysis: Diagenetic features (in general order of occurrence)	Preserved porosity	Petroleum source evaluation: Field eval.	Organic carbon, %	Kerogen	Alteration index	Oil source	Gas source	Reservoir evaluation: Field observ. of porosity	Petrographic observ. of porosity	Matrix por.,%	Matrix perm., millidarcies	Reservoir quality	Shows of oil, gas
20	21	22	23	24	25	26	27	28	29	30	31	32	33	34
Top peak	MZ; RXm; RP-Qz-pb; CEb-Ccf-be; FRn; CEf-Ccf								N	N				
78-42	MZ; SLsh; FRn; CEm, f-Cc; RPsh-Qz								N	N				
78-4	MZ; SLsh; FRn; CEm, f-Cc; RPsh-Qz								N	N				
77-41	MZ, MZe; SLsh, he; CE-Ccn, Ccf								N	N				
77-22	MZ, MZe; SLsh, he; FRn; CE-Cc								N	N				
76-8	MZ, MZe; SLsh, he; CE-Cc; RXm		P-F	0.24	H, W	3			N	N				
76-3	MZ; SLsh; FRn; ISvm; CE-Cc; RXm								N	N				
75-7	MZ; SLsh; FRn; CE-Cc; RPsh-Qz								N	N				
75-1	MZ, MZe; SLsh, he; FRn; CE-Cc								N	N				
74-54	MZ; SLsh; FRn; CEm, f-Cc; RP-An-pb; SLpb; CEpm-Do								(Pw,v)	N				

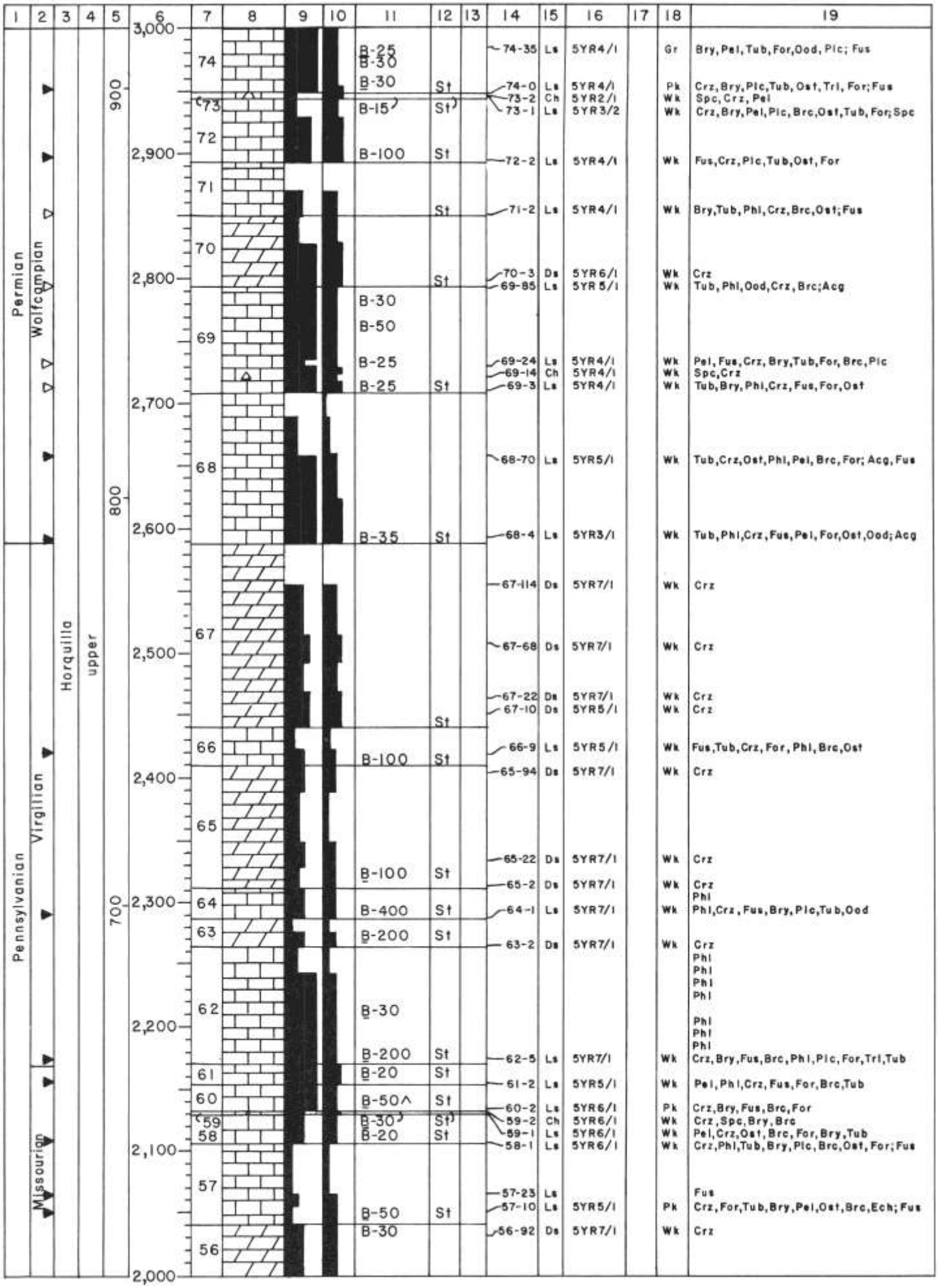
1 2 3 4 5 6 7 8 9 10 11 12 13 14 15 16 17 18 19
Permian
Wolfcampian
Pennsylvanian
Virgilian
Missourian
Horquilla
upper
900
800
700
3,000
2,900
2,800
2,700
2,600
2,500
2,400
2,300
2,200
2,100
2,000
74
73
72
71
70
69
68
67
66
65
64
63
62
61
60
59
58
57
56
B-25
B-30
B-30
St
B-15
St
B-100
St
St
B-30
B-50
B-25
B-25
St
B-35
St
B-100
St
B-100
St
B-400
St
B-200
St
B-30
B-200
St
B-20
St
B-50
St
B-30
St
B-20
St
B-50
St
B-30
74-35 Ls 5YR4/1 Gr Bry,Pel,Tub,For,Ood,Plc; Fus
74-0 Ls 5YR4/1 Pk Crz,Bry,Plc,Tub,Ost,Trl,For;Fus
73-2 Ch 5YR2/1 Wk Spc,Crz,Pel
73-1 Ls 5YR3/2 Wk Crz,Bry,Pel,Plc,Brc,Ost,Tub,For;Spc
72-2 Ls 5YR4/1 Wk Fus,Crz,Plc,Tub,Ost,For
71-2 Ls 5YR4/1 Wk Bry,Tub,Phl,Crz,Brc,Ost;Fus
70-3 Ds 5YR6/1 Wk Crz
69-85 Ls 5YR5/1 Wk Tub,Phl,Ood,Crz,Brc;Acg
69-24 Ls 5YR4/1 Wk Pel,Fus,Crz,Bry,Tub,For,Brc,Plc
69-14 Ch 5YR4/1 Wk Spc,Crz
69-3 Ls 5YR4/1 Wk Tub,Bry,Phl,Crz,Fus,For,Ost
68-70 Ls 5YR5/1 Wk Tub,Crz,Ost,Phl,Pel,Brc,For;Acg,Fus
68-4 Ls 5YR3/1 Wk Tub,Phl,Crz,Fus,Pel,For,Ost,Ood;Acg
67-114 Ds 5YR7/1 Wk Crz
67-68 Ds 5YR7/1 Wk Crz
67-22 Ds 5YR7/1 Wk Crz
67-10 Ds 5YR5/1 Wk Crz
66-9 Ls 5YR5/1 Wk Fus,Tub,Crz,For,Phl,Brc,Ost
65-94 Ds 5YR7/1 Wk Crz
65-22 Ds 5YR7/1 Wk Crz
65-2 Ds 5YR7/1 Wk Crz
Phl
64-1 Ls 5YR7/1 Wk Phl,Crz,Fus,Bry,Plc,Tub,Ood
63-2 Ds 5YR7/1 Wk Crz
Phl
Phl
Phl
Phl
Phl
Phl
Phl
62-5 Ls 5YR7/1 Wk Crz,Bry,Fus,Brc,Phl,Plc,For,Trl,Tub
61-2 Ls 5YR5/1 Wk Pel,Phl,Crz,Fus,For,Brc,Tub
60-2 Ls 5YR6/1 Pk Crz,Bry,Fus,Brc,For
59-2 Ch 5YR6/1 Wk Crz,Spc,Bry,Brc
59-1 Ls 5YR6/1 Wk Pel,Crz,Ost,Brc,For,Bry,Tub
58-1 Ls 5YR6/1 Wk Crz,Phl,Tub,Bry,Plc,Brc,Ost,For;Fus
57-23 Ls Fus
57-10 Ls 5YR5/1 Pk Crz,For,Tub,Bry,Pel,Ost,Brc,Ech;Fus
56-92 Ds 5YR7/1 Wk Crz

20	21	22	23	24	25	26	27	28	29	30	31	32	33	34
74-35	MZ,MZe;SLsh,oo,he;FRn;CE-Cc								N	N				
74-0	MZ;SLsh;FRn;CE-Cc;RXm								N	N				
73-2	RPm-Qm,Do-pb;Rp(Crz)-Qg								N	N				
73-1	SLsh;FRn;CE-Cc;RXm;RP-Qz-pb								N	N				
72-2	SLsh;CEm-Cc;RXm								N	N				
71-2	SLsh;CEm-Cc		P-F	0.35	H,W	3			N	N				
									Pv,w					
									Pv,w					
									Pv,w					
									Pv,w					
70-3	RPm-Do-nm-vc,pm(Crz)	S							Pv,w	Gm	2.7	0.07		
69-85	MZ,MZe;SLsh,oo,he;CEm-Cc								N	N				
									(Pw,v)					
69-24	SLsh;FRn;CE-Cc,RXm;RPsh-Qz								N	N				
69-14	RPm-Qm,Do-pb;RPsh-Qc,Qg;FR;CEf-Cc								N	N				
69-3	SLsh;FRn,CE-Cc;RXm								N	N				
68-70	MZ,MZe;SLsh,he;CE-Cc								N	N				
68-4	MZ;RPm-Do-pb,RPsh-Do;SLsh;CE-Cc,Do		P-F	0.53	H,W	3			N	N				
67-114	RPm-Do-nm-c,pm(Crz);RP-An-pb;SLpb;CEpm-Cc-mg	ST							Pv	Fm,v				
									Pv					
									Pv					
									Pv					
									Pv					
67-68	RPm-Do-nm-c,pm(Crz);RP-An-pb;SLpb;CEpm-Cc-mg	ST							Fv	Fm,v	2.7	0.12		
									Fv,w					
									Fv,w					
									Fv,w					
67-22	RPm-Do-nm-vc,pm(Crz);RP-An-pb;SLpb;CEpm-Cc-mg;RPce-Do-pm	ST							Fv,w	Gm,v	1.1	0.16		
67-10	RPm-Do-nm-m,pm(Crz);RP-An-pb;SLpb	ST							Fv,w	Fm,v				
									Pv					
									N					
66-9	RP-Do-pb;SLsh;CEm-Cc		P	0.48	H,W	3			N					
									N					
65-94	RPm-Do-nm-vc,pm(Crz);RP-An-pb;SLpb;FR;CE-Cc-mg	ST							Pv	Gm,v,f	4.4	0.46		
									Pv					
									Fv,w					
									Fv,w					
									Fv,w					
									Fv,w					
									Fv,w					
65-22	RPm-Do-nm-c,pm(Crz);RP-An-pb;SLpb;CE-Cc-mg	ST							Fv,w	Gm,v	4.0	0.03		
65-2	RPm-Do-nm-m,pm(Crz)	S							Pv	Fm				
64-1	SLsh;CE-Cc,Do;RXm;RP-Qz-pb;RP-An-pb;SLpb;CEm,rm-Do;RP-Do-pb								N	N				
									Fv,w					
									Fv,w					
63-2	RPm-Do-nm-vc;CEx-Cc;RP-An-pb;CEpm-Do,Cc-mg	ST							Fv,w	Gm,v	5.1	0.18		
									N					
62-5	SLsh;FRn;CE-Cc;RP-Qz-pb;RXm;SLst;CEst-Do-nm;Oil								N	N				DO
61-2	MZ,MZe;SLsh,he;FRn;CE-Cc;RP-An-pb;SLpb;CEpm-Cc								N	N				
60-2	MZ;RPsh-Qz								N	N				
59-2	RPm-Qm,Do-pb;RPsh-Qg,Qc;FR;CEf-Cc								N	N				
59-1	RXm								N	N				
58-1	SLsh;CEsm-Cc;RX;RP-Qz-pb								N	N				
57-10	MZ;RXsr(Crz);RPsh-Qz;FR;CEf-Cc								N	N				
									N	N				
56-92	RP-Do-nm-c,pm(Crz);RP-An-pb;SLpb	ST							Pv,w	Fm,v	1.1	0.05		
									Pv,w					
									Pv,w					
									Pv,w					

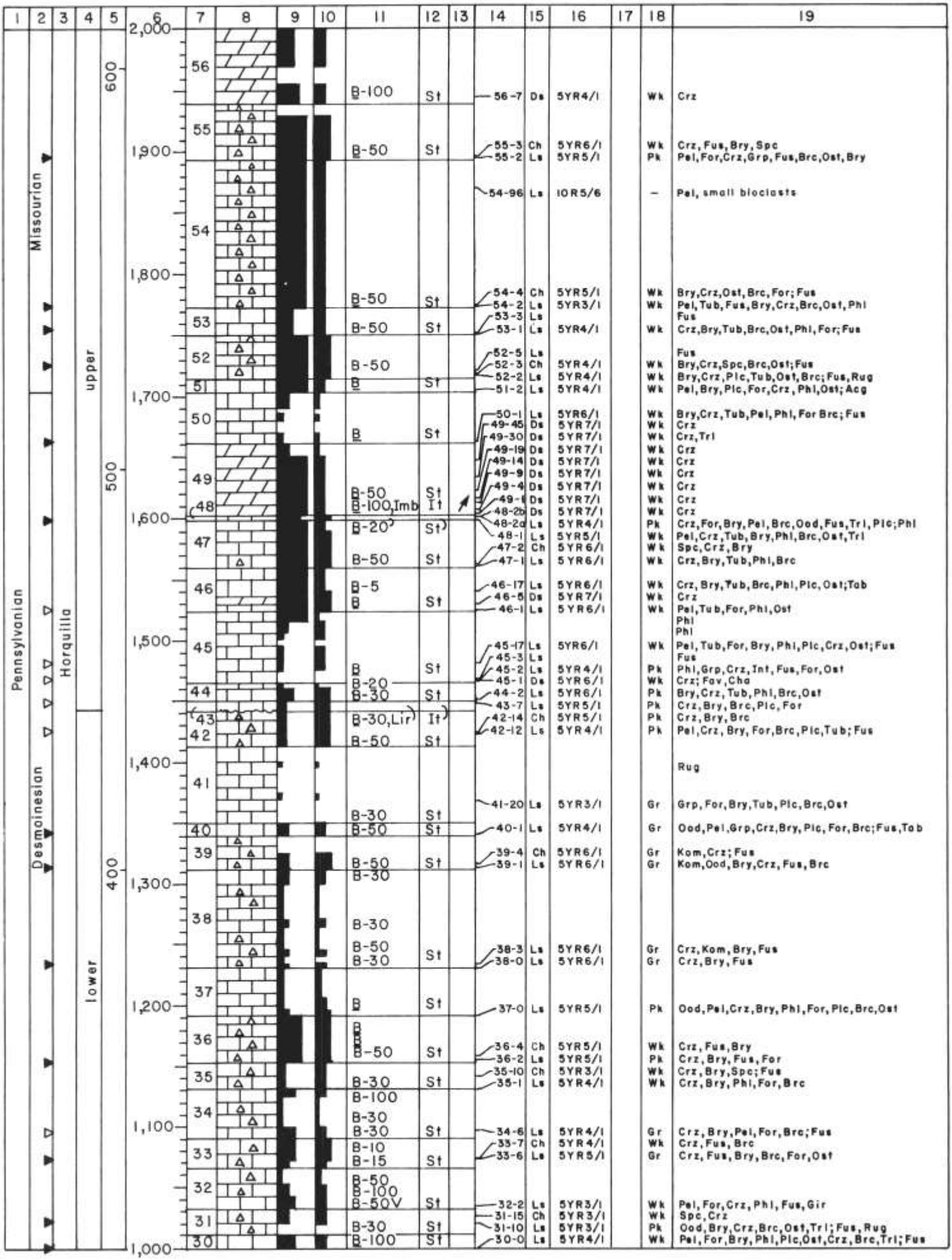
1
2
3
4
5
6
7
8
9
10
11
12
13
14
15
16
17
18
19
Pennsylvanian
Missourian
Desmoinesian
Horquilla
upper
lower
600
500
400
2,000
1,900
1,800
1,700
1,600
1,500
1,400
1,300
1,200
1,100
1,000
56
55
54
53
52
51
50
49
48
47
46
45
44
43
42
41
40
39
38
37
36
35
34
33
32
31
30
B-100
B-50
B-50
B-50
B
B
B-50
B-100,Imb
B-20
B-50
B-5
B
B
B-20
B-30
B-30,Lir
B-50
B-30
B-50
B-50
B-30
B-30
B-50
B-30
B-30
B-100
B-30
B-10
B-15
B-50
B-100
B-50V
B-30
B-100
St
St
St
St
St
St
St
It
St
St
St
St
St
It
St
St
St
St
St
St
St
St
St
St
St
St
St
St
St
It
St
56-7 Ds 5YR4/1 Wk Crz
55-3 Ch 5YR6/1 Wk Crz, Fus, Bry, Spc
55-2 Ls 5YR5/1 Pk Pel, For, Crz, Grp, Fus, Brc, Ost, Bry
54-96 Ls 10R5/6 – Pel, small bioclasts
54-4 Ch 5YR5/1 Wk Bry, Crz, Ost, Brc, For; Fus
54-2 Ls 5YR3/1 Wk Pel, Tub, Fus, Bry, Crz, Brc, Ost, Phl
53-3 Ls Fus
53-1 Ls 5YR4/1 Wk Crz, Bry, Tub, Brc, Ost, Phl, For; Fus
52-5 Ls Fus
52-3 Ch 5YR4/1 Wk Bry, Crz, Spc, Brc, Ost; Fus
52-2 Ls 5YR4/1 Wk Bry, Crz, Plc, Tub, Ost, Brc; Fus, Rug
51-2 Ls 5YR4/1 Wk Pel, Bry, Plc, For, Crz, Phl, Ost; Acg
50-1 Ls 5YR6/1 Wk Bry, Crz, Tub, Pel, Phl, For Brc; Fus
49-45 Ds 5YR7/1 Wk Crz
49-30 Ds 5YR7/1 Wk Crz, Trl
49-19 Ds 5YR7/1 Wk Crz
49-14 Ds 5YR7/1 Wk Crz
49-9 Ds 5YR7/1 Wk Crz
49-4 Ds 5YR7/1 Wk Crz
49-1 Ds 5YR7/1 Wk Crz
48-2b Ds 5YR7/1 Wk Crz
48-2a Ls 5YR4/1 Pk Crz, For, Bry, Pel, Brc, Ood, Fus, Trl, Plc; Phl
48-1 Ls 5YR5/1 Wk Pel, Crz, Tub, Bry, Phl, Brc, Ost, Trl
47-2 Ch 5YR6/1 Wk Spc, Crz, Bry
47-1 Ls 5YR6/1 Wk Crz, Bry, Tub, Phl, Brc
46-17 Ls 5YR6/1 Wk Crz, Bry, Tub, Brc, Phl, Plc, Ost; Tob
46-5 Ds 5YR7/1 Wk Crz
46-1 Ls 5YR6/1 Wk Pel, Tub, For, Phl, Ost
Phl
Phl
45-17 Ls 5YR6/1 Wk Pel, Tub, For, Bry, Phl, Plc, Crz, Ost; Fus
45-3 Ls Fus
45-2 Ls 5YR4/1 Pk Phl, Grp, Crz, Int, Fus, For, Ost
45-1 Ds 5YR6/1 Wk Crz; Fav, Cha
44-2 Ls 5YR6/1 Pk Bry, Crz, Tub, Phl, Brc, Ost
43-7 Ls 5YR5/1 Pk Crz, Bry, Brc, Plc, For
42-14 Ch 5YR5/1 Pk Crz, Bry, Brc
42-12 Ls 5YR4/1 Pk Pel, Crz, Bry, For, Brc, Plc, Tub; Fus
Rug
41-20 Ls 5YR3/1 Gr Grp, For, Bry, Tub, Plc, Brc, Ost
40-1 Ls 5YR4/1 Gr Ood, Pel, Grp, Crz, Bry, Plc, For, Brc; Fus, Tob
39-4 Ch 5YR6/1 Gr Kom, Crz; Fus
39-1 Ls 5YR6/1 Gr Kom, Ood, Bry, Crz, Fus, Brc
38-3 Ls 5YR6/1 Gr Crz, Kom, Bry, Fus
38-0 Ls 5YR6/1 Gr Crz, Bry, Fus
37-0 Ls 5YR5/1 Pk Ood, Pel, Crz, Bry, Phl, For, Plc, Brc, Ost
36-4 Ch 5YR5/1 Wk Crz, Fus, Bry
36-2 Ls 5YR5/1 Pk Crz, Bry, Fus, For
35-10 Ch 5YR3/1 Wk Crz, Bry, Spc; Fus
35-1 Ls 5YR4/1 Wk Crz, Bry, Phl, For, Brc
34-6 Ls 5YR4/1 Gr Crz, Bry, Pel, For, Brc; Fus
33-7 Ch 5YR4/1 Wk Crz, Fus, Brc
33-6 Ls 5YR5/1 Gr Crz, Fus, Bry, Brc, For, Ost
32-2 Ls 5YR3/1 Wk Pel, For, Crz, Phl, Fus, Gir
31-15 Ch 5YR3/1 Wk Spc, Crz
31-10 Ls 5YR3/1 Pk Ood, Bry, Crz, Brc, Ost, Trl; Fus, Rug
30-0 Ls 5YR4/1 Wk Pel, For, Bry, Phl, Plc, Ost, Crz, Brc, Trl; Fus

20	21	22	23	24	25	26	27	28	29	30	31	32	33	34
									Pv,w					
									Pv,w					
									Pv,w					
									Pv,w					
56-7	RPm-Do-nm-c,pm(Crz)	S							Pv,w	Pm	4.9	42		
									N					
									N					
									N					
55-3	RPm-Qm,Do-pb;RPsh-Qg,Qc;RP(Do)pb-Cc								N	N				
55-2	MZ;RXm;RPsh-Qz;FR;CEf-Cc								N	N				
54-96	ISvm,g;RP-Do-nm;RP-An-pb;SLpb;CE-Cc;RP(Do)-Cc;RP-Py-pb								N	N				
54-4	RPm-Qm,Do-pb;CEb-Do;RPsh-Qg,Qc;RP(Do)-Cc;FR;CEf-Cc								N	N				
54-2	SLsh;FRn;SLvg,ch;CE-Cc-be,mg;RXm;RPsh-Qz								N	N				
53-1	SLsh;FRn;CE-Cc;RXm;RP-Qz-pb;RP-An-pb;SLpb;CEpm-Do								N	N				
52-3	RPm-Qm,Do-pb;CEb-Do;RPsh-Qg,Qc;RP(Do)-Cc;FR;FR;CEf-Cc								N	N				
52-2	MZ,MZe;SLsh,he;CEm-Cc;RX,RPsh-Qz		P	0.15	H,W	3			N	N				
51-2	MZ,SLsh;FRn;CE-Cc								N	N				
50-1	MZ,MZe;SLsh,he;FRn;RXm;CE-Cc								N	N				
49-45	RP-Do-nm-vc,pm(Crz);RP-An-pb;SLpb	ST							Pv	Gm,v				
49-30	RP-Do-nm-ec,pm(Crz);RP-An-pb;SLpb,CEpm-Cc-mg	ST							Pv	Gm,v				
49-19	RP-Do-nm-vc,pm(Crz);RP-An-pb;SLpb,CEpm-Cc-mg	ST							Pv	Fm,v	2.4	0.78		
49-14	RP-Do-nm-vc,pm(Crz);RP-An-pb;SLpb,CEpm-Cc-mg	ST							Gv,w	Gm,v	2.9	0.06		
49-9	RP-Do-nm-vc,pm(Crz);RP-An-pb,SLpb,CEx-Cc-be	ST							Gv,w	Gm,v	1.9	0.09		
49-4	RP-Do-nm-ec,pm(Crz);RP-An-pb,SLpb;CEpm-Cc-mg	ST							Pv	Gm,v	5.5	0.31		
49-1	RP-Do-nm-c,pm(Crz);RP-An-pb,SLpb;FR;ISm;RP-Do,CEpm-Do;CEpm-Cc;RP-Do	ST							Pv	Gm,v				
48-2b	RP-Do-nm-vc,pm(Crz);FR;CEf-Cc	S							N	Pm				
48-2a	MZ,MZe;SLsh,he;FRn;CE-Cc								N	N				
48-1	MZ,SLsh;FRn;CE-Cc;RXps;RP-Qz;SLvg;FR;CE-Cc;SLst								N	N				
47-2	RP-Qz,Do-pb;FR;CEf-Cc								N	N				
47-1	SLsh,vg;CE-Cc;FR;FR;CEf-Cc;RPsh-Qz								N	N				
46-17	SLsh,vg,ch;CE-Cc;RXm;FR;FR;CEf-Cc;RP-An-pb;SLpb,CEpm-Cc								N	N				
46-5	RP-Do-nm-vc,pm(Crz);FR;CEf-Cc-mg	S							N	Pm,f				
46-1	SLsh;FRn,CE-Cc;RXm;RP-Qz-pb;RP-An-pb;SLpb,CEpm,rm-Do								N	N				
45-17	MZ;SLsh;CEsm-Cc-be;RXm,sr;RP-An-pb,SLpb;CEpm-Do								N	N				
45-2	MZ,MZe;SLsh,he;CEm-Cc,Qz,RXm;RPsh-Qz-pb								N	N				
45-1	RP-Do-nm-m,pm(Crz);RP-An-pb;RPpb-Cc,SLpb,CEm-Do;FR;CEf-Do;FR;CEf-Cl								N	N				
44-2	MZ;SLsh;FR;CE-Cc;RPsh-Qz								N	N				
43-7	MZ;RPm-Do;SLsh;RPsh-Do-pm;CEb-Cc;CE-Do;RP-Qz								N	N				
42-14	RPm-Qm,Do-pb;RPsh-Qc,Qg;RP-Do-pm(Crz)								N	N				
42-12	MZ;SLsh;FRn;CE-Cc;RXm;CEm,f-Do								N	N				
41-20	MZ,MZe;SLsh,he;FRn;CE-Cc;RP-An-pb;RPpb-Qz;SLpb		F	0.24	H	3			N	N				
40-1	MZ,MZe;SLsh,he;CE-Cc;RP-Qz,FRn;ISfm;CEf-Cc								N	N				
39-4	RPsh-Qz,Do-pm;CEg-Qg-dr;FR;CEf,rm-Do								N	N				
39-1	CEg,ep-Cc;SLst								N	N				
38-3	MZ;CEg,ep-Cc;RPsh-Qz								N	N				
38-0	CEep-Cc,RP-Do-pm(Crz);RPsh-Qz;CEg-Cc,Qz								N	N				
37-0	MZ;MZe;SLsh,oo,he;CE-Cc;RP-Qz-pb								N	N				
36-4	RPm-Qm,Do-pb;RPsh-Qc;CEb-Do,Qc;RP-Do-pm(Crz)								N	N				
36-2	MZ;RPsh-Qz;FR;CEb,f-Ccf;FR;CEf-Cc								N	N				
35-10	RP(Ar)-Cc;RP-Qz,Do-po,pm(Crz);FR;CEf-Do,Cc-mg;RPce-Do-pm								N	N				
35-1	MZ,SLsh;FRn;CEcc;RPsh-Qz								N	N				
34-6	MZ,MZe;ISvm;CEep-Cc;FR;CEf-Cc;RPsh-Qz									N				
33-7	RP(Ar)-Cc;CEb-Do;RP(Do)-Cc;RP-Do-pm(Crz),Qz;FR;CEf-Cc								N	N				
33-6	MZ;SLvg;ISvm;CEep-Cc;RPsh-Qz								N	N				
32-2	MZ;SLsh;FRn;CE-Cc								N	N				
31-15	RP-Qz,Dof-pb,pm(Crz);FR;CEf-Dof								N	N				
31-10	MZ;RPsh-Qz		F	0.23	H-W	3			N	N				
30-0	MZ,MZe;SLsh,he;FRn;CE-Cc;RPsh-Qz;RP-Py								N	N				

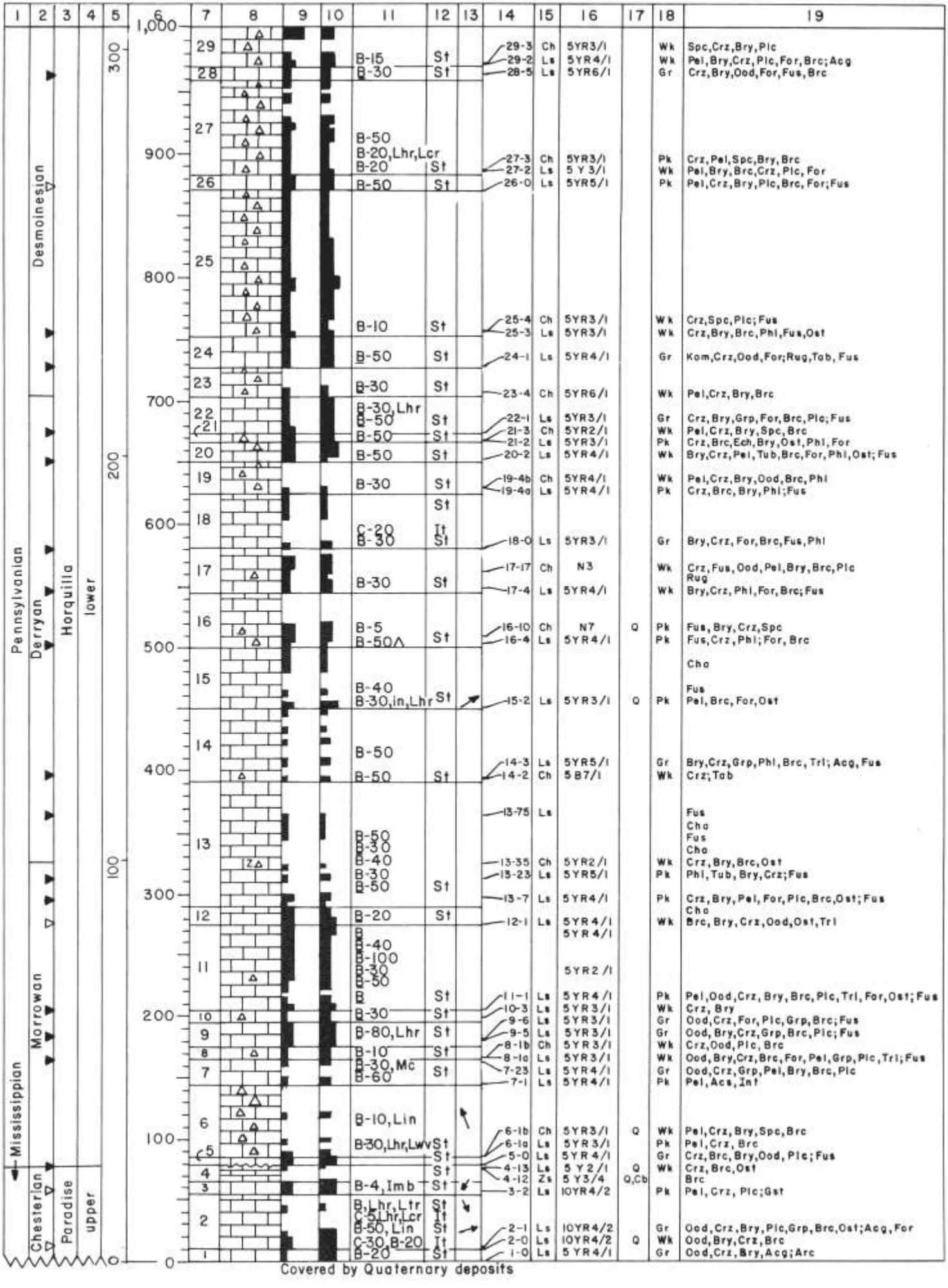
1 2 3 4 5 6 7 8 9 10 11 12 13 14 15 16 17 18 19
Pennsylvanian
Mississippian
Desmoinesian
Derryan
Morrowan
Chesterian
Horquilla
Paradise
lower
upper
1,000
900
800
700
600
500
400
300
200
100
0
300
200
100
0
B-15
B-30
B-50
B-20,Lhr,Lcr
B-20
B-50
B-10
B-50
B-30
B-30,Lhr
B-50
B-50
B-50
B-30
C-20
B-30
B-30
B-5
B-50△
B-40
B-30,in,Lhr
B-50
B-50
B-50
B-40
B-30
B-50
B-20
B
B-40
B-100
B-30
B-50
B
B-30
B-80,Lhr
B-10
B-30,Mc
B-60
B-10,Lin
B-30,Lhr,Lwv
B-4,Imb
B,Lhr,Ltr
C-5,Lhr,Lcr
B-50,Lin
C-30,B-20
B-20
Covered by Quaternary deposits

20	21	22	23	24	25	26	27	28	29	30	31	32	33	34
29-3	RP(Ar)-Cc;SLsh;RXm;CEm-Cc;RP-Qz,Do-pb;FR;CEf-Cc								N	N				
29-2	MZ;SLsh;CEm-Cc;RXps								N	N				
28-5	MZ,CEep-Cc;RPsh,ce-Qz								N	N				
27-3	RP(Ar)-Cc;RP-Qz								N	N				
27-2	MZ;SLsh;CEm-Cc;RXps								N	N				
26-0	MZ;SLsh,FRn;CE-Cc								N	N				
25-4	RP(Ar)-Cc;SLsh;CEsm-Dof,Cc,Qc;RP-Qz;FR;CEf-Cc,z								N	N				
25-3	SLsh;CEm-Cc,CPw;FR;FR;RPsh-Qz;CEf-Cc								N	N				
24-1	ISm,g;CE-Cc								N	N				
23-4	RP(Ar)-Cc;RP-Qz,Do-pb								N	N				
22-1	MZ;MZe;SLsh,he;CE-Cc;CEep,pk-Cc;RPsh-Qz								N	N				
21-3	RP(Ar)-Cc;RP-Qz,Do-pb								N	N				
21-2	RPm-Do;SLsh;CEm-Cc;RPsh-Qz		F	0.51	H,W	3+			N	N				
20-2	MZ;SLsh;RXm;RPsh-Qz;CE-Cc								N	N				
19-4b	RP(Ar)-Cc;SLsh;RP-Qz,Do-pb;FR;CEf-Do;RP(Do)-Cc;FR;CEf-Cc								N	N				
19-4a	SLsh;CE-Cc;FR;CEf-Cc;FR;CEf-Do								N	N				
18-0	SLsh;CE-Cc;RPsh-Qz								N	N				
17-17	RP(Ar)-Cc;SLsh;RP-Qz								N	N				
17-4	SLsh;CE-Cc;RPsh-Qz								N	N				
16-10	RP(Ar)-Cc;RP-Qz,Do-pb;RXps;FR;CEf,rm-Do,Qg								N	N				
16-4	SLsh;CE-Cc;RPsh-Qz,Do-pb								N	N				
15-2	FRn;FRn;CE-Cc		F	0.54	H,W	2+			N	N				
14-3	MZ,MZe;ISvm;SLsh,he;CE-Cc;RPsh-Qz								N	N				
14-2	RP-Dof-nm-c,pm(Crz);CE-Qc,Qz-dr;RPsh-Qz								N	N				
13-35	RP-Qz;FR;CEf,rm-Do-pb;RP(Do)-Cc;CEf-Cc								N	N				
13-23	MZ;SLsh;FRn;CE-Cc								N	N				
13-7	SLsh;FRn;CE-Cc								N	N				
12-1	RPsh-Qz								N	N				
11-1	MZ;SLsh;CE-Cc								N	N				
10-3	RPm-Do-n-f;RP(Do)-Cc;CPw-Oil		G	0.71	H,W	3+			N	N				DO
9-6	MZ;SLsh;FRn;CE-Cc;RPsh-Qz								N	N				
9-5	MZ;SLsh;CEm,ep,pk-Cc;RPsh-Qz								N	N				
8-1b	RP(Ar)-Cc;SLsh;RP-Qz;FR;CEf-Cc								N	N				
8-1a	MZ;SLsh;CE-Cc;RPsh-Qz								N	N				
7-23	MZ,MZe;ISvm;SLsh,he;CEsm-Ccn;CEhe-Ccf;RPsh-Qz								N	N				
7-1	—		F	0.12	H,W	4-			N	N				
6-1b	RP-Qz,Do-pb;RP(Do)-Cc;FRt;CEf,rm-Ccf								N	N				
6-1a	RXm								N	N				
5-0	MZ,MZe;ISm;CEbr-Cc;SLsh,he;CE-Cc								N	N				
4-13	RXm;RPm-Do-nm;Oil								N	N				DO
4-12	Oil(laminae);CE-Ccf								N	N				DO
3-2	SLsh;FRn;CE-Cc,Py;SLst-Py,Oil								N	N				DO
2-1	MZe;SLhe;CE-Cc-be								N	N				
2-0	CEb,rm-Py,Ccf;RXms,ps;RPm-Ccf;RP(Do-pb)-Ccf;RP-Cl								N	N				
1-0	MZ,MZe;ISvm;SLsh;FRn;CE-Cc-dr;CEep-Cc								N	N				

Type faces: Text in 10-pt. English Times, leaded one point
References in 8-pt. English Times, leaded one point
Display heads in 24-pt. English Times

Presswork: Miehle Single Color Offset
Harris Single Color Offset

Binding: Smyth sewn with softbound cover

Paper: Cover on 80-1b. Artone
Text on 70-lb. white matte

Ink: Cover—PMS 288
Text—Black

Quantity: 1000